University of Southampton

Faculty of Environmental and Life Sciences

Ocean and Earth Science

Using optical tools to improve understanding of dissolved organic carbon fluxes along the land-ocean aquatic continuum

by

Stacey Louise Felgate

ORCID ID: 0000-0002-9955-4948

Thesis for the degree of Doctor of Philosophy

June 2022

University of Southampton

Abstract

Faculty of Environmental and Life Sciences

Ocean and Earth Science

Doctor of Philosophy

Using optical tools to improve understanding of dissolved organic carbon fluxes along the land-ocean aquatic continuum

by

Stacey Louise Felgate

The transport of terrigenous dissolved organic matter (tDOM) from land to sea is a significant and changing component of the global carbon cycle. This thesis uses optical tools (absorbance and fluorescence spectrometry) to investigate the composition and fate of tDOM across a range of aquatic settings.

Results show that agricultural expansion within the Belize River Watershed has increased tDOM overlying an adjacent portion of the world's second largest barrier reef system, with the potential for deleterious effects. A substantial decoupling of 'coloured' DOM (cDOM) and dissolved organic carbon (DOC) is identified, likley the result of a sizeable optically 'invisible' DOC fraction (iDOC). In the same watershed, iDOC was found to represent 52 % of the total DOC pool. The molecular properties which render iDOC optically invisible should, in theory, render it more bioavailable than cDOC, but cDOC was positively correlated with bioavailable DOC (BDOC) and biodegradation rate (k) whereas iDOC was positively correlated with refractory DOC (RDOC). This suggests that it is cDOC rather than iDOC which drives biodegradation rates in this system.

A new method is proposed with which to further partition the cDOC fraction according to its fluorescent properties. This method is demonstrated within the Belize River Watershed, where a traditional approach whereby changes in cDOM fluorescence were extrapolated to the DOC pool was deemed appropriate for the qualitative assessment of relative concentration shifts, but yielded unrealistic results in terms of the contribution of each fraction to the DOC pool.

In Great Britain (GB), iDOC accounted for 21 % of the annual riverine flux (0.23 Tg C yr^{-1}) and was primarily explained by rainfall, base flow index, and dairy cattle density. These results were placed in a wider context using a collated data set of ~ 3,000 samples obtained from a wide range of aquatic, geographic, and climatic settings across five continents where, on average, iDOC represented 26 % of the DOC pool (range = 0 – 97%). cDOC and iDOC were estimated across 12 GB estuaries at quarterly intervals (n = 60 transects) to investigate the influence of each fraction on estuarine DOC export, and cDOC transport was almost universally conservative whereas iDOC transport was almost universally non-conservative. Shifts in iDOC concentration therefore appear to be the dominant control over bulk DOC behaviour within these estuaries.

The overarching conclusion of this thesis is that iDOC is a globally significant carbon pool, the broad-scale importance of which has yet to be studied in earnest. Large uncertainties exist with regards the source, behaviour, and fate of iDOC. It is critical that these uncertainties are addressed in order to better constrain the land-ocean carbon flux and, more broadly, the global carbon cycle.

Table of Contents

Table of Tables

Table of Figures

Research Thesis: Declaration of Authorship

Print name: STACEY LOUISE FELGATE

Title of thesis: Using optical tools to improve understanding of dissolved organic carbon fluxes along the land-ocean aquatic continuum

I declare that this thesis and the work presented in it are my own and has been generated by me as the result of my own original research.

I confirm that:

1. This work was done wholly or mainly while in candidature for a research degree at this University;
2. Where any part of this thesis has previously been submitted for a degree or any other qualification at this University or any other institution, this has been clearly stated;
3. Where I have consulted the published work of others, this is always clearly attributed;
4. Where I have quoted from the work of others, the source is always given. With the exception of such quotations, this thesis is entirely my own work;
5. I have acknowledged all main sources of help;
6. Where the thesis is based on work done by myself jointly with others, I have made clear exactly what was done by others and what I have contributed myself;
7. Parts of this work have been published as:

Felgate, Stacey L., et al. “Requirements for the monitoring of land-ocean carbon fluxes at pan-European Scale (RINGO Deliverable 1.4)”. https://bit.ly/3yBmmfn.

Felgate, Stacey L., et al. "Conversion of forest to agriculture increases colored dissolved organic matter in a sub-tropical catchment and adjacent coastal environment." Journal of Geophysical Research: Biogeosciences (2021): e2021JG006295. DOI: 10.1029/2021jg006295.

Signature: ..... Date:.....

Acknowledgements

To Dan Mayor, for never going easy on me and for always having my back. All PhD students deserve a supervisor like you. To Richard Sanders, for unfailing enthusiasm, uncommon faith, and a propensity to say yes. To Chris Evans, for being a voice of reason and an invaluable source of knowledge, experience, and wit. To Chris Barry, for raising the bar. Gentlemen, it has been a privilege.

To my panel members, Jasmin Godbold, Barry Thornton, and Duncan Purdie, whose advice helped set my course. To colleagues at UK CEH who took pity on an ignorant marine scientist, particularly Jenny Williamson and Alice Fitch. One day I'll learn to make my own maps, I promise! And to rest of the LOCATE team, who welcomed me, put up with me, and continue to be a source of knowledge, support, and inspiration.

To the people of Belize who hosted, shared knowledge, and granted access to their beautiful country, especially Abel Carrias, Joaquin Urbina, Josue Ake, Jair Valladarez, Arlene Young, Chantelle Samuels, Samir Rosado, Gilbert Andrews, and Ellis Requena.

To past teachers for lessons you won't find in any text book: Miss Moan, the primary school teacher who lit a tiny fire; Mr Smith, the maths teacher who kept me honest; Mr MacArthur, for paying attention; and Natalie Hicks, the undergraduate supervisor who told me that I could.

To the PhD friends who kept my self-belief intact, my ego in-check, and who never let me forget the importance of having fun: Cassidy Camilla, Maarten Heijnen, Africa Gomez, Nathan Hubot, Pablo Trucco, Dave Price, Millie Goddard Dwyer, Cael, and Anna Lichtschlag. To old friends who still answer the phone, even when I'm being a self-involved nightmare: Joni Anfield, Gregor Clunie, Dawud Duncan, Ross Flannigan, and David Ross. Never underestimate the importance of knowing you that you are (still!) there.

To my mumma, Joan, who is the source, the solution, and the only place that ever felt like home. To my daddy, Colin, for things I don't quite know how to put words to. I have everything I could ever need. Thank you. To my baby brother Scott and his beautiful, inspiring family who keep my heart full. Kiddies, if I teach you one thing let it be that you can do whatever you set your mind to.

This thesis was funded by the Natural Environment Research Council (NERC) SPITFIRE DTP (grant no. NE/L002531/1). Additional funding was provided by the NERC Land-OCean CArbon TransfEr (LOCATE) program (grant no. NE/N018087/1) and the UK Government through the Commonwealth Marine Economies Programme (CMEP)

Chapter 1 Introduction

Sections of this text are based on a report which has been published as:

Felgate, Stacey L. et al., "Requirements for the monitoring of land-ocean carbon fluxes at pan-European scale" ICOS (2020). Full report available here.

1.1 The global carbon cycle

The global carbon (C) cycle distributes C between the lithological, terrestrial, oceanic, and atmospheric reservoirs (Figure 1-1) and can be conceptualised as having two components: the 'fast' biological cycle and the 'slow' geological cycle.

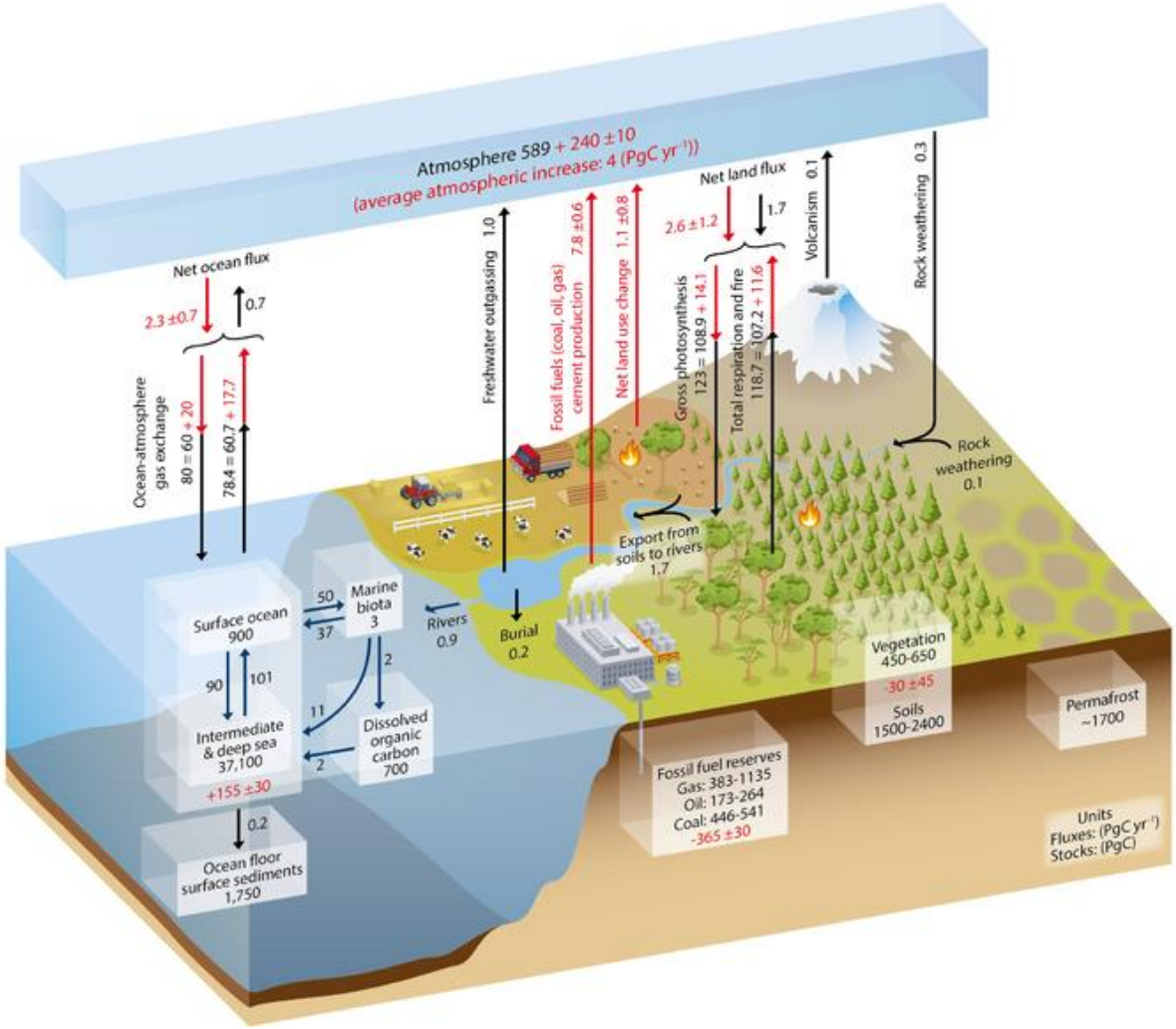

Figure 1-1. Diagram of the global C cycle. Black numbers and arrows indicate pre-industrial 'natural' stocks (boxes) and fluxes (arrows). Red stocks represent cumulative changes during the

Industrial Period (1970 – 2011). Red fluxes represent anthropogenic perturbation (averaged between 2000 and 2009). Uncertainties are reported as 90% confidence intervals. Note that these values represent best estimates at time of publication and have since been updated. Values quoted in the text may therefore differ from those shown. Figure taken from (Stocker et al., 2013).

The geological cycle operates at millennial time scales and processes between 0.1 and 1.0 Pg C yr^{-1} (Friedlingstein et al., 2020), most of which is inorganic (non-biological). When CO_2 dissolves in water (H_20) it forms carbonic acid (H_2CO_3), which rapidly dissociates into HCO_3^- and a hydrogen ion (H^+). If conditions are favourable, further dissociation produces a carbonate (CO_3^{2-}) ion and a second H^+ (Equation 1-1). These ions exist in equilibria, their speciation determined by environmental variables including pH, alkalinity, and water temperature (Doney et al., 2009).

$$CO_2 + H_2O \longleftrightarrow H_2CO_3 \longleftrightarrow HCO_3^- + H^+ \longleftrightarrow CO_3^{-2} + 2H^+ \qquad \boldsymbol{Eqn.1-1}$$

When this reaction occurs in the atmosphere, it produces rain which is acidic enough to induce chemical weathering of carbonate and silicate rocks. This produces bicarbonate (HCO_3^-) and calcium (Ca^{2+}) ions (Equation 1-2), which are typically washed into aquatic systems via surface runoff.

$$2\,CO_2 + H_2O + CaSiO_3 \longrightarrow Ca^{2+} + 2\,HCO_3^- + SiO \qquad \boldsymbol{Eqn.1-2}$$

Much of the Ca^{2+} produced via chemical weathering is then transformed into carbonate ($CaCO_3$) (Equation 1-3), a critical building block for a range of calcifying organisms including corals, foraminifera, cocolithophores, and molluscs. When these organisms die, their calcified structures either undergo dissolution back into the ion pool or are sedimented out for eventual lithification and storage on millennial time scales.

$$Ca^{2+} + 2\,HCO_3^- \longleftrightarrow CaCO_3 + CO_2 + H_2O \qquad \boldsymbol{Eqn.1-3}$$

The biological cycle operates at sub-centennial time scales and processes between 100 and 1000 Pg organic (biological) C yr^{-1} (Friedlingstein et al., 2020). Photosynthesising organisms (i.e. plants and phytoplankton) draw CO_2 from the atmosphere and combine it with water to produce carbohydrates ($(CH_20)_n$) and oxygen (O_2) (Equation1-4):

$$CO_2 + H_2O \xrightarrow{light\ energy} (CH_2O)_n + O_2 \qquad \boldsymbol{Eqn.1-4}$$

The C stored within these carbohydrate molecules supports growth and the formation of more complex organic molecules. The majority of these molecules will be broken down by the plant or a consumer species to produce energy, decomposed upon death, or consumed by fire, whether

naturally or as a fuel source. When this happens, the organic C is converted into inorganic C via remineralisation, much of which will return to the atmosphere as CO_2 (Equation 1-5):

$$(CH_2O)_n + O_2 \longrightarrow CO_2 + H_2O + Energy \qquad \boldsymbol{Eqn.\,1-5}$$

A small organic C fraction avoids this fate, typically because supply exceeds demand, or because decomposition is retarded by ambient environmental conditions such as those found in the wet, anoxic sediments of peat bogs, coastal wetlands, and lake and marine environments. Such material undergoes sedimentation, compaction, and eventual lithification to produce e.g. shale or fossil fuels as part of the geological cycle.

Since the industrial revolution, humans have emitted an extra ~ 460 Pg C into the atmosphere as CO_2, ~ 50 % of which remains there today (Friedlingstein et al., 2019). The rate of emission is increasing: last year's anthropogenic CO_2 emissions were estimated at 37.4 ± 2.9 Pg, equivalent to 10.2 Pg C yr^{-1} (Friedlingstein et al., 2020).

CO_2 is a greenhouse gas (GHG), meaning that its presence in the atmosphere has a warming effect on the planet's surface. It is not the most potent GHG: methane and nitrous oxide both have a greater warming effect per mole; but its abundance and the fact that it can persist for 1000s of years makes it the most climate-relevant greenhouse gas (GHG) on Earth (Lacis et al., 2010). Increasing atmospheric CO_2 emissions have been linked to increasing global temperatures and climate instability, with wide ranging social (Sofuoğlu and Ay, 2020), economic (Albu and Albu, 2020; Hall and Behl, 2006), and environmental consequences (Parry et al., 2008). Our ability to predict and/or mitigate those consequences is hampered by knowledge gaps and large uncertainties in the global C budget (Stocker et al., 2013). We must therefore improve our understanding of the C cycle, including the wide range of complex processes and feedback mechanisms within it, as a matter of urgency.

1.2 The land-ocean carbon flux

Freshwater systems are linked to the ocean via the land ocean aquatic continuum (LOAC), a complex fluid network which links aquatic environments of every kind, and provides a conduit through which C is transported laterally (Cole et al., 2007; Drake et al., 2018; Regnier et al., 2013). It includes headwater streams, groundwaters, rivers, lakes, wetlands, transitional waters (i.e. estuaries, fjords, deltas, lagoons, and coastal waters), constructed water bodies (i.e. ponds, reservoirs, and ditches), shelf seas, and the open ocean. The flux of terrigenous C via the LOAC consists of three components, where 'aquatic' covers the full spectrum of observed salinities. These are:

1. Lateral C fluxes (land – aquatic)

2. Vertical C fluxes (aquatic – atmosphere)

3. Vertical C fluxes (aquatic – sediment)

These fluxes are comprised of a number of different C species, including: dissolved organic C (DOC); particulate organic C (POC); dissolved inorganic C (DIC), which itself consists of: aqueous CO_2 ($CO_{2\,(aq)}$); carbonic acid (H_2CO_3), carbonate (HCO_3^-) and bicarbonate (CO_3^{2-}) ions; particulate inorganic C (PIC); and gasses (carbon dioxide ($CO_{2\,(g)}$); and methane ($CH_{4\,(g)}$), a GHG with ~28 fold higher global warming potential than CO_2 (Myhre et al., 2013). In this thesis, CO_2 and CH_4 are discussed in gaseous form unless otherwise stated.

1.2.1 Inorganic carbon fluxes

Terrigenous inorganic C (IC) has two possible sources. It can be produced during the geological C cycle via the chemical and/or physical weathering of carbonate rocks and mineral soils, or during the biological C cycle via root and soil respiration. The fate of IC within the LOAC is not notably different from IC derived from other sources (i.e. atmospheric or biogenic IC). It is determined by the local carbonate cycle (Figure 1-2) and by the environmental conditions which control it, particularly pH, hydrology, weather, water temperature, and the balance of respiration vs. photosynthesis.

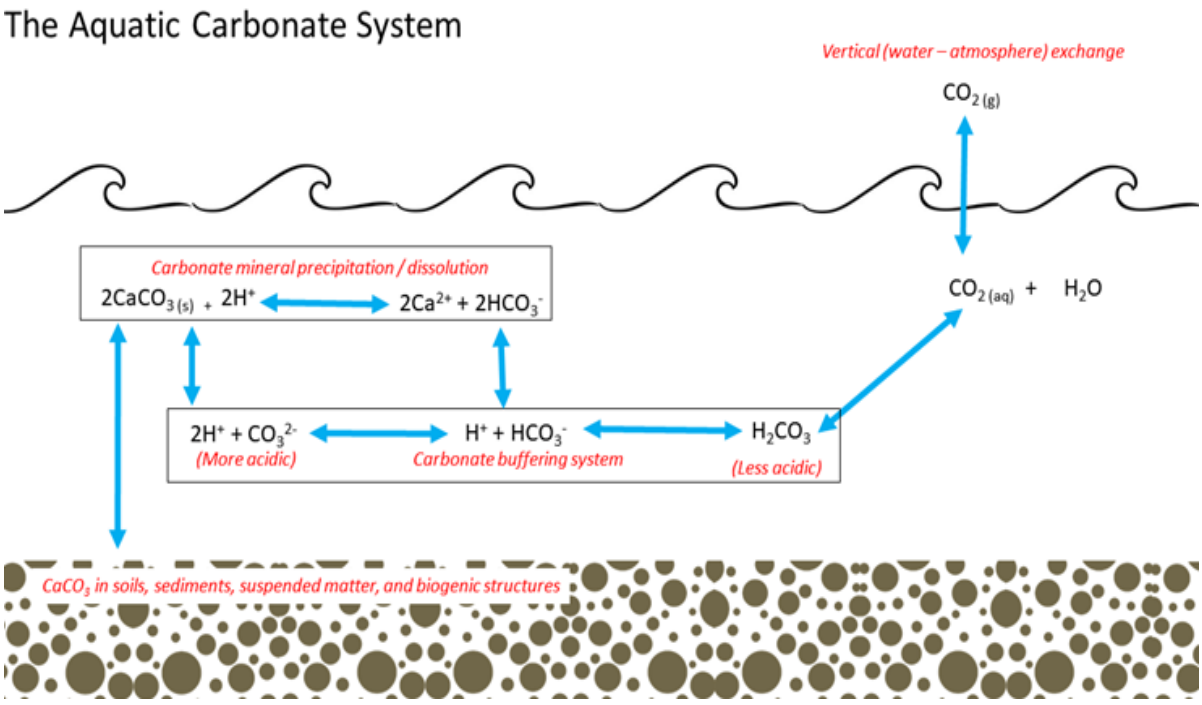

Figure 1-2. Diagrammatic representation of the aquatic carbonate cycle. Figure taken from Felgate et al. (2021a).

1.2.2 Organic carbon fluxes

The size of the terrigenous OC flux is largely controlled by the balance of gross photosynthesis (GPP) and total ecosystem respiration (RECO), which presents as the difference between net primary production (NPP; the amount of C assimilated by plants during photosynthesis) and net ecosystem production (NEP; net C exchange between the ecosystem and the atmosphere) (Figure 1-3).

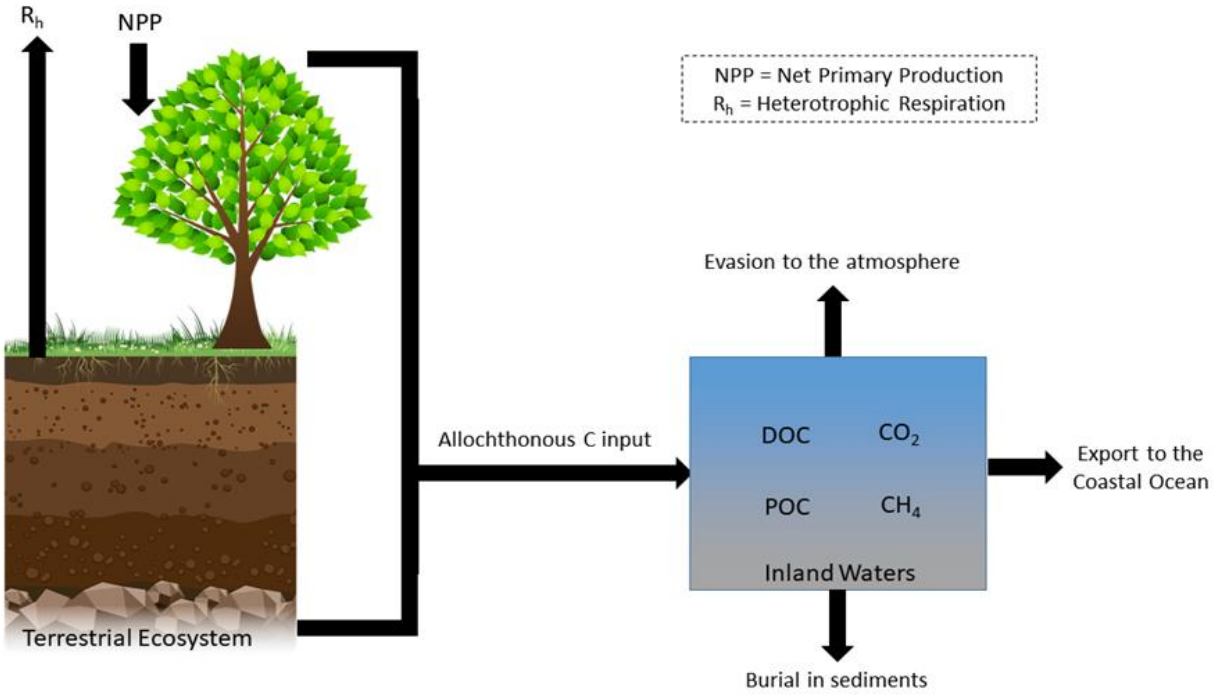

Figure 1-3. Diagrammatic representation of the transport of terrigenous OC along the land-ocean aquatic continuum (LOAC). Figure taken from Felgate et al, (2021a).

In low-latitude regions, increased DOC export is thought to be linked to high rates of NPP, which makes the total amount of terrestrial OC available for entrainment and delivery to aquatic systems greater than in other global biomes (e.g. high latitudes; Li et al. (2019)). In Boreal systems, 3 % - 5 % of terrestrial NPP is transported into the aquatic continuum (Hastie et al., 2018). Conversely, in some high latitude regions NPP is significantly lower and high DOC export is sustained by much higher soil organic carbon (SOC) stores, particularly in peatland and permafrost environments where decomposition rates are constrained by waterlogging or freezing, so that NEP rather than NPP controls export. A similar imbalance between NPP and decomposition also occurs in tropical peatlands, which generate some of the highest DOC export fluxes in the world (e.g. Moore et al., (2013). In human-influenced systems, additional organic C (OC) results from anthropogenic sources, typically from animal faeces and sewage outflows. As this terrigenous OC moves along the LOAC, the majority will undergo aggregation/flocculation and burial within lacustrine and fluvial sediments

(Kirschbaum et al., 2019) or remineralisation, which may stimulate the flux of CO_2 or CH_4 to the atmosphere (Sawakuchi et al., 2017).

Heterotrophic metabolism results in the remineralisation of both DOC and POC and the evasion of C into the atmosphere as CO_2, along with CH_4 produced by the breakdown and/or fermentation of organic substrates, in particular detrital POC. A proportion of DOC is converted into the POC pool by flocculation, some of which is incorporated into sediments following sinking (Sholkovitz 1976). Photodegradation acts upon the coloured fraction of DOC, breaking up larger molecules and often resulting in transformations to the gaseous form (either chemically or via enhanced remineralisation). Each of these processes is influenced by a range of factors including temperature, the concentration and bio-lability of the organic substrate, microbial community activity, water residence time, salinity, and light attenuation (Soares and Berggren, 2019; Vähätalo and Wetzel, 2004).

1.2.3 Anthropogenic perturbation

The flow of terrigenous C into the LOAC is thought to have increased by ~ 1.0 Pg C yr^{-1} since the start of the industrial revolution, almost all of which has occurred as OC. This is mostly the result of increased soil export following land use change (0.9 Pg C yr^{-1}), with sewage and wastewaters also contributing significantly (0.1 Pg C yr^{-1}) (Regnier et al., 2013). As well as an increase in the quantity of terrigenous OC entering the LOAC, its molecular composition has also changed due to anthropogenic perturbations, including changing land use (Chapter 2) and climate (Briones et al., 2010; Rousk et al., 2016). These shifts in the quantity and composition of the terrigenous OC flux can have wide-ranging biogeochemical and ecological effects. Alterations in OC concentrations have been shown to influence the physical, photochemical, biochemical, and biological processes that control the metabolism and functioning of aquatic environments (Queimaliños et al., 2019). Increased allochthonous (externally produced) OC inputs can lead to increased light attenuation and altered thermal structure, which can inhibit primary production (Sandberg et al., 2004), increased benthic OM loadings, which can both stimulate and smother benthic communities (Frouin, 2000), and alter the composition of microbial communities (Lindh et al., 2015). More broadly, changes to the organic matter (OM) within which OC is typically bound (both in terms of concentration or composition) can alter aquatic nutrient dynamics with wide-ranging knock-on effects for ecosystem function (Heinz et al., 2015; Stutter et al., 2018). The consequences of increased terrigenous nutrient input can be eutrophication, algal and microbial blooms, and deoxygenation resulting from increased remineralisation of the associated autochthonous OM (Dagg et al., 2008). Such degradation leads to

an increase in IC as respiring microorganisms produce CO_2. When biodegradation rates are high, this can amplify the effect of increasing atmospheric CO_2 uptake in many aquatic systems, which can be compounded by underlying geology. Ocean acidification is thought to contribute towards the declining resilience and health of coastal ecosystems (Bates et al., 2014; Carstensen and Duarte, 2019; Doney et al., 2009, 2009; Sabine and Feely, 2004), and this can be compounded by river outflows. Additional but less significant IC inputs are also likely to occur due to the dissolution of biogenic structures and/or suspended matter. Combined, these local factors determine aquatic CO_2 concentrations and drive a vertical flux, the direction of which varies in space and time. What is not evaded to the atmosphere as CO_2 will become entrained within local carbonate structures or undergo downstream transport.

The cumulative effect of downstream movement of fresh waters can exert a negative influence in transitional and coastal waters, where pollution from upstream human activities (i.e. agricultural runoff and untreated sewage) via riverine discharge is recognised as a major driver of change (Regnier et al., 2013). Each of these effects has the potential to dramatically restructure the local ecosystem, and each is intrinsically linked to the flow of terrigenous C from land to sea. Changing land-ocean C fluxes can also have significant social, economic, and human-health implications. For example, over the last 50 years headwater DOC concentrations across Northern Europe and Northeast America have increased significantly (Monteith et al., 2007). Evidence also points towards an increase in DOC concentrations in larger rivers (Kritzberg and Ekström, 2012). This has made the extraction of potable water more expensive, increased greenhouse gas (GHG) emissions associated with water treatment plants, and resulted in potentially deleterious human health impacts as a result of carcinogenic by-products of DOC removal from drinking water (Jones et al., 2016; Lavonen et al., 2013). Increases in the amount of POC flowing down major rivers has been linked to a shallowing of estuaries and an increased financial burden in terms of maintaining shipping routes. Acidification driven by increasing aquatic DIC concentrations has been linked to decreasing yields from freshwater and coastal fisheries, resulting in increased fish and shellfish mortality, decreased livelihoods, and increasing consumer cost (Fernandes et al., 2017).

Despite these and myriad other biogeochemical, ecological, social, economic, and human health implications associated with changing land-ocean C fluxes, we currently lack understanding of the spatio-temporal variability associated with the input, processing, and removal of terrigenous C across the LOAC. As a result, we cannot adequately predict how changes to land-ocean C fluxes will influence aquatic C cycling or atmospheric CO_2 levels. Quantifying these fluxes is made particularly

difficult by the degree of variability observed across the varied environments that compose the LOAC, a description of which follows.

1.2.4 Environments of the land-ocean aquatic continuum

1.2.4.1 Soil water and groundwater

The transfer of C from land to sea begins with subsurface soil and groundwater flows. These flows occur along a residence time continuum which operate at a variety of temporal and spatial scales, determined by a range of hydrogeological processes (Tóth, 1963). This can be generalised in terms of deep, intermediate, and shallow flow paths (Figure 1-4).

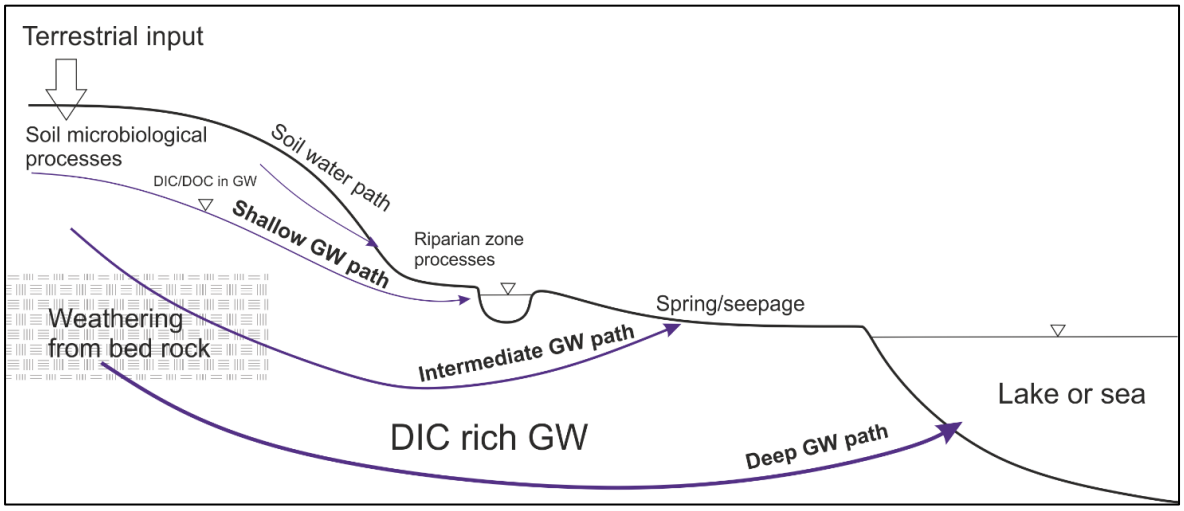

Figure 1-4. Shallow, intermediate, and deep groundwater (GW) flow baths bring C to fluvial systems on differing temporal and spatial scales. This excludes the short-circuiting effects of groundwater withdrawals. Figure taken from (Felgate et al., 2021a).

Deep and intermediate flows operate at regional to continental scales and exhibit residence times ranging from decades to millennial (Lapworth et al., 2018). Shallow flow paths operate at hillslope or smaller resolution and exhibit much shorter residence times, typically in the order of days to years (Gooddy et al., 2006; Laudon and Sponseller, 2018). These shallow flows generally pick up DOC as they pass through organic soils and sub-surface deposits, and that DOC undergoes transformation via oxidation, microbial utilization, adsorption and metal co-precipitation (Shen et al., 2015; Wassenaara et al., 1991), partitioning into a relatively labile DOC pool which is rapidly remineralized, and a relatively recalcitrant DOC pool (including humic and fulvic acids; Regan et al., 2017) which persists in the organic soil, but is prone to precipitation and adsorption as it passes through the mineral soils and porous bedrock associated with deeper flows. As a result, most DOC input to surface waters derives from shallow subsurface flow through organic soils, whereas DIC tends to be

transported via deeper groundwater flow. The more dominant DIC species in groundwater are geologically mediated via bedrock weathering, and soil-mediated via heterotrophic activity and root respiration, which elevates soil pCO_2 and produces dissolved (bi)carbonate ions (Winterdahl et al., 2016). Deirmendjian et al. (2018) found that approximately 75% of the DIC exported into streams in this manner degassed rapidly as CO_2, providing the pathway for a groundwater mediated vertical land-aquatic-atmosphere flux.

Subsurface inflows contribute relatively persistent inputs of dissolved C to surface waters and control CO_2 evasion patterns, but episodic events (i.e. heavy rainfall/drought) can move flow paths between mineral and organic soil layers, generating occasional large pulses of DOC input (Lupon et al., 2019; Rawlins et al., 2014). An added complication is the significant anthropogenic use of groundwater e.g. for drinking water and irrigation (Evans, 2007). Through this process a significant amount of C held as DIC and DOC in groundwaters is redistributed to the surface, where it can enter the fluvial water system. Global groundwater withdrawals are estimated to be ~ 980 km^3 yr^{-1} (Margat and Gun, 2013; Siebert et al., 2010), and in the UK this is estimated to account for a small but significant 0.05 % of all CH_4 emissions (Gooddy and Darling, 2005), yet groundwater withdrawals are never accounted for in C budget and flux estimates.

Groundwater also transfers DOC and DIC directly to surface water bodies such as lakes, wetlands and oceans (Downing and Striegl, 2018). This can be particularly relevant in areas such as the Mediterranean Sea, where submarine groundwater discharge is a major source of dissolved inorganic nutrients, comparable to riverine and atmospheric inputs (Rodellas et al., 2015). Submarine springs can be a significant source of nutrients for the ocean (Slomp and Van Cappellen, 2004), but DIC and DOC fluxes are currently unknown. Groundwater therefore represents a potentially significant factor in the regional C balance, and excluding it from land-ocean C budgets (as is common practice) almost certainly biases balance estimates.

1.2.4.2 Lakes

Lakes are strongly influenced by the surrounding catchment, and inputs from land are often considerably larger than internal lake production via photosynthesis (Cole et al., 1994). Lake sediments accrue at an estimated 0.6 Pg C yr^{-1} globally (Kortelainen et al., 2004; Stallard, 1998; Tranvik et al., 2009), and this store is relatively stable, being protected from fire and subject to limited disturbance. Lakes modify the flux and composition of DOC. The dominant removal process is usually bacterial remineralisation (Berggren et al., 2017; Koehler et al., 2012), but photochemical breakdown can be important within the upper photic zone, where the highly coloured humic

fraction of the DOC pool may be preferentially degraded (Osburn et al., 2011). Rates of DOC processing tend to decrease over time as the more biologically labile and photochemically reactive fractions become depleted (Catalán et al., 2016; Evans et al., 2017). As a result, rates of removal will tend to be highest in lower-residence time lakes receiving fresh inputs from their catchments. However, this general decline in removal rates is counterbalanced by very long residence times in some lakes (years, decades, or even centuries in the largest waterbodies) which allow a very high fraction of the total input to be remineralized. The importance of internal processing in lakes was recently highlighted by a land-ocean modelling study which found that the inclusion of an 'average' UK lake (residence time = 109 days) reduced the amount of DOC that reaches the ocean from 5 to 3 % (Anderson et al., 2019).

Estimates of GHG emissions from lakes range from 0.3 – 1.2 Pg C yr^{-1} (Raymond et al., 2013; Tranvik et al., 2009), although some discrepancy exists as to the inclusion (or otherwise) of reservoirs in these figures. Approximately ~ 75 Tg C yr^{-1} of the upward vertical lake flux occurs as CH_4 (Bastviken et al., 2011), much of which originates from sediment ebullition (bubbling). This is regulated by e.g. water depth and the amount of organic substrates supplied by the surrounding catchment, with the presence of labile OC favouring CH_4 production (Duc et al., 2010). Due to the depth dependency, regions near the shore and mostly in wind shadow can account for ~ 50 % of the total lake CH_4 fluxes (Natchimuthu et al., 2016). Any CO_2 and CH_4 not emitted from the lake will follow the outflowing water into the fluvial system.

1.2.4.3 Modified (constructed) water bodies

Modified or 'constructed' water bodies, defined as *"water bodies where human activities have changed the hydrology of existing natural water bodies thereby altering water residence times and/or sedimentation rates… and water bodies that have been created by excavation, such as canals, ditches, and ponds"* (Lovelock et al., 2019), have been shown to make significant contributions to land-ocean C processing. Any emissions from such water bodies must be considered to be, at least partly, anthropogenic in origin. Their inclusion in lateral and vertical C flux calculations is therefore important for C and GHG accounting, especially as these systems are disproportionately large sources of CH_4 (Bastviken et al., 2011).

Globally, reservoirs are reported to bury ~60 Tg C yr^{-1} (Mendonça et al., 2017). This storage is greatest in tropical and subtropical regions, but it is also likely to be significant across Europe. However, these large water bodies are also estimated to produce 770 Tg CO_2 *eq* yr^{-1}, with CH_4 being the prime contributor to this flux (18 Tg CH_4 yr^{-1} / 504 Tg CO_2 *eq* yr^{-1}; (Deemer et al., 2016) using CO_2

eq value from (Myhre et al., 2013). The nutrient status of reservoirs has been suggested as the main driver of CH_4 emissions (Deemer et al., 2016; DelSontro et al., 2018) although latitudinal patterns also exist in the GHG emissions from these environments (Barros et al., 2011; Deemer et al., 2016). It should be noted that untangling the full C/GHG budget of reservoirs requires extensive monitoring. This is because of potentially high emissions from outflowing rivers, turbines, and spillways which arise as a result of elevated GHG concentrations in discharging reservoir hypolimnion waters (Guérin et al., 2006).

Compared to reservoirs, significantly less research has been conducted on constructed ponds, although similar patterns of biogeochemistry have been found for these small waterbodies. Specifically, diffusive emissions of CH_4 and CO_2 can be considerable (Holgerson and Raymond, 2016; Ollivier et al., 2019; Peacock et al., 2019; Webb et al., 2019), but ebullitive emissions of CH_4 tend to be larger still (Grinham et al., 2018; Natchimuthu et al., 2016; Panneer Selvam et al., 2014; van Bergen et al., 2019). Like reservoirs, C burial in these systems can also be sizeable (Taylor et al., 2019), but it is likely that burial is not large enough to offset their C/GHG emissions (van Bergen et al., 2019). Recent work has demonstrated that the combination of high C fluxes and cumulatively large surface area can result in constructed ponds being significant sources of GHGs on a national scale (Grinham et al., 2018; Ollivier et al., 2019). Globally, the area occupied by constructed ponds is similar to that occupied by large reservoirs (Downing, 2010; Saunois et al., 2019) and a coarse estimate of global CH_4 emissions from ponds is 3 - 8 Tg yr^{-1} / 84 – 224 Tg CO_2 *eq* yr^{-1} (Saunois et al., 2019) Numerous studies have measured GHG emissions from ditches, although the majority of studies have focused on ditches in organic soils (Evans et al., 2016). Synthesised data suggests that ditch CH_4 emissions are larger than those from ponds and that, as for reservoirs and ponds, CH_4 is the largest contributor to climatic warming from these systems (Lovelock et al., 2019). Additionally, ditches can have impacts on fluvial OC dynamics; fluxes and concentrations of DOC and POC have, in some cases, been shown to increase following drainage of organic soils (Evans et al., 2016) and the effect of this increase has been observed downstream in large rivers (Asmala et al., 2019). In some heavily drained countries (e.g. The Netherlands, Finland, the UK) the total length of ditches can exceed that of natural watercourses (Brown et al., 2006; Verdonschot et al., 2011), suggesting that the contribution of ditches to C and GHG cycling could be extensive.

1.2.4.4 Fluvial waters

Headwaters are the first part of the LOAC to receive C inputs from the surrounding land, giving them a unique association with the terrestrial surface environment. As a result, allochthonous (externally supplied), terrigenous material dominates OC cycling in these upstream environments (Royer and

David, 2005). Further downstream, this allochthonous OC combines with various autochthonous (locally produced) forms, resulting from algae, submerged vegetation, as well as other allochthonous inputs from anthropogenic sources such as sewage and agricultural runoff. As OC moves downstream, the proportion of relatively recalcitrant material increases as labile material is preferentially utilised (Catalán et al., 2016). Some evidence exists of the so-called 'priming effect' whereby the local microorganism community are able to metabolise highly recalcitrant OC in the presence of specific labile compounds (e.g. agricultural associated compounds; marine DOC), and so rivers have the potential to act as hotspots for the remineralisation of terrigenous OM (Blanchet et al., 2017). Increased concentrations of autochthonous C may lead to an increase in aquatic respiration and photolysis, whilst increasing residence time with distance downstream promotes the photooxidation of allochthonous C, both of which produce CO_2. Coupled with DIC inputs from groundwater sources, streams are typically supersaturated with CO_2 and the associated degassing represents a significant fraction of catchment scale CO_2 losses (Butman and Raymond, 2011). Indeed, fluvial waters are disproportionately large sources of both CO_2 and CH_4 to the atmosphere given their area, and global emissions have been estimated at 3.9 Pg C yr^{-1} (Drake et al., 2018).

River floodplains often behave similarly to wetlands during flood periods, exporting significant amounts of OC as surface soil C and vegetation contribute to aquatic DOC concentrations (Abril and Borges, 2019; Raymond and Spencer, 2015). Similarly, intermittent (seasonal or episodic) wetting imposes physical disturbance and alters the biogeochemistry (i.e. oxic status) of soils with knock-on effects on C cycling. Ephemeral events can have disproportionate influence on C export to the LOAC (Raymond et al., 2016; von Schiller et al., 2019, 2017) are rarely captured during monitoring activities.

1.2.4.5 Transitional waters

Fluvial waters can strongly influence the coastal zone, transferring large amounts of dissolved and particulate C across a range of environments known collectively as 'transitional waters' (i.e. estuaries, fjords, deltas, lagoons, coastal waters) and the vegetated habitats which surround them.

Estuaries are thought to act as 'dynamic filters', exchanging material and energy with the ocean to varying degrees according to physical, hydrological, and biogeochemical conditions. They tend to be net heterotrophic (Heip et al., 1995), and can be strong sources of CO_2 and CH_4 to the atmosphere. The atmospheric flux of CO_2 from European estuaries is thought to represent a sum equal to 5 – 10 % of Western Europe's anthropogenic emissions (Frankignoulle et al., 1998). However, a great deal of uncertainty surrounds degassing rates as they vary in space and time, with the relative

abundance of pelagic (i.e. phytoplankton dominated) versus benthic (i.e. seagrass or benthic algal dominated) production, both of which are influenced by land-ocean OM flows, playing a major role. Organic matter inputs from catchments (Raymond and Bauer, 2001) and/or adjacent tidal wetlands (Bauer et al., 2013; Wang and Cai, 2004) vary from system to system, and the processing of these inputs determines the trophic balance in estuarine waters.

Estuaries can also serve as significant long-term organic C sinks through sedimentation of terrestrial inputs and, where present, the burial of vegetation, particularly seagrass and saltmarsh organic matter originating from coastal wetlands (Duarte et al., 2004; McLeod et al., 2011; Nellemann et al., 2009). Coastal wetland environments themselves represent only a small fraction of the global coastline (<1%) but are amongst the world's most intense C sink habitats per unit area (Duarte et al., 2005; Luisetti et al., 2019; Nellemann et al., 2009). Their small total area means that these vegetated habitats make small contributions to global C budgets, but their inclusion in land-ocean C budgeting is appropriate given their potential to sequester significant portions of C from incoming fluvial and/or estuarine waters, and their tendency to export significant fractions of their above-ground biomass beyond the immediate environment (e.g. seagrass, ~ 50 %). The extent of European saltmarsh and seagrass has been estimated at 330 thousand and 2.5 million ha, respectively (Luisetti et al., 2013), with global sequestration and burial values generally used in lieu of regional ones.

Coastal inlets such as fjords are recognised as globally important sites for C burial, and their proximity to the terrestrial environment renders them effective 'traps' for terrigenous matter before it can reach the ocean. A study of the fjordic Loch Sunart in Scotland found that 42 % of sediment OC was terrigenous, making it a more effective C store per unit area than the surrounding catchment (Smeaton and Austin, 2017). The mud-flat sediments characteristic of deltaic and lagoon systems are also very effective C storage environments, but can also be intense sites of C processing (Mayor et al., 2018). Little or no CO_2 flux data are available for fjords, deltas, or coastal lagoons, and so these environments represent an important knowledge gap. Other coastal inlets, such as the Rias Baixas on the west coast of the Iberian Peninsula, are influenced by seasonal near-shore upwelling of nutrient-rich deep-waters. This pulse input of nutrients fuels high levels of primary production and the sedimentation of organic matter. In turn, this drives respiration and methanogenesis in sediments with substantial efflux of CH_4 to the atmosphere through diffusion and direct ebullition (de Carlos et al., 2017; Kitidis et al., 2007).

Evidence suggests that the delivery of terrigenous C to these transitional waters (and beyond) via the LOAC is a significant term, with approximately 30 % of terrigenous OC thought to survive to the shelf, contributing ~ 30 % of oceanic sedimentary burial (Burdige, 2007; Kandasamy and Nagender

Nath, 2016). However, the transfer efficiency of OC through these systems is highly variable (Dürr et al., 2011). Whilst estuaries tend to be net CO_2 sources and shelf seas tend to be net CO_2 sinks, it has been suggested that riverine OC might effectively bypass the estuarine zone in some cases (Cai, 2011). In such instances, greater riverine OC inputs would therefore mean greater marine rather than estuarine CO_2 emissions. This may explain variability observed between regional estimates of terrigenous OC export. For example, a study of the North Sea found little evidence of terrigenous material beyond coastal waters (Painter et al., 2018), whilst a study of the Celtic Sea found that up to 30 % of the DOC at the shelf edge is terrigenous (Carr et al., 2019) and on the Western Adriatic shelf, OC burial is equivalent to ~60 % of the associated terrigenous OC inputs (Tesi et al., 2013). Legge et al. (2020) estimated that rivers deliver approximately 60 % of the total C input onto the North West European Shelf (NWES), but Kitidis et al. (2019) found that the majority of terrigenous OC entering the NWES is microbially and photochemically transformed to CO_2 before reaching the shelf, as with the North American shelf (Fennel et al., 2019).

1.2.5 Factors controlling land-ocean carbon transport

The quantity and composition of terrigenous C entering the LOAC is driven by a diversity of factors including regional climate, soil type, hydrology, geology, vegetation, and human activities, and its behaviour and fate therein controlled by a range of intrinsic (molecular) and extrinsic (environmental) factors including water chemistry, light attenuation, temperature, and the composition of the local microbiome (Hansen et al., 2016; Nebbioso and Piccolo, 2013; Raymond and Spencer, 2015; Wagner et al., 2020).

1.2.5.1 Physical catchment characteristics

A number of physical attributes have been shown to strongly influence land-ocean C fluxes. Geology is an important consideration, with some rock forms being more prone to weathering than others, and more permeable and calcareous geology resulting in higher concentrations of DIC in surrounding waterbodies (Shin et al., 2011). This is particularly true in intermediate and deep GW flows where water flows through bedrock before resurfacing supersaturated with DIC picked up in transit. Catchment scale has an effect on regional C budgets, with larger catchments producing larger fluxes of dissolved and particulate matter (Laudon and Sponseller, 2018). Mean catchment slope has been identified as a potential driver of global land to ocean C fluxes (Ludwig et al., 1996; Raymond and Spencer, 2015). Slope is inversely related to DOC flux, as catchments with steeper morphologies are suggested to have a higher proportion of surface runoff where water contact time with soil horizons is restricted (Ludwig et al., 1996), as well as tending to have thinner and less organic-rich soils.

Leaching of organic material from soils enriches runoff with DOC, therefore water leaving catchments with shallower slopes and a higher proportion of through flow relative to surface runoff will to be more concentrated in DOC, all other factors being equal. Shallower slopes also allow for more extensive wetlands and riparian zones, which can influence OC export (Mulholland, 2003). Physical catchment characteristics are relatively stable (i.e. not subject to ongoing, large scale, rapid change).

1.2.5.2 Hydrology and residence time

Hydrology influences the source of aquatic OC, with higher discharge resulting in a greater portion of terrigenous material being transferred into the LOAC (Li et al., 2019). This is because periods of higher discharge typically co-occur with periods of increased surface runoff and/or increased leaching of organic-rich soil horizons and surface litter (Raymond et al., 2016; Raymond and Spencer, 2015). On the other hand, during periods of lower discharge the water flowing through the LOAC typically contains more geogenic (rock-derived) IC and experiences longer flow paths and/or residence times which increase the potential for active biogeochemical cycling of what OM is present.

Residence time (the length of time C spends within a given environment or, more broadly, the LOAC), provides a powerful control on C processing. Headwater streams generally have short residence times. Water moves quickly through them into larger streams and rivers. Hence, whilst they receive large volumes of organic material directly from the catchment, there may be limited potential for biogeochemical processing to occur. The increasing residence time of downstream aquatic systems, as streams drain into rivers, lacustrine, and coastal environments, may mean that C cycling becomes a more important control on overall C budgets with distance downstream. Conversely, the extent to which the material has already been degraded in the upstream aquatic environment may mean that further processing is limited (Catalán et al., 2016). The construction of water bodies (i.e. reservoirs, ponds, and ditches) increases the residence time of water in the LOAC, resulting in downstream OC contributions that are older and, as a result of prior processing, more recalcitrant. This can have significant spatio-temporal implications for C processing (Evans et al., 2017; Müller et al., 2013).

As described in Section 1.2.4.1, groundwater C influx to surface waters via baseflow contributes a significant amount of C with long residence times. The composition of the resultant C has been modified due to subsurface processes and has different reactivity compared to surface and in-situ derived C in surface water bodies (Lapworth et al., 2009; Tye and Lapworth, 2016).

1.2.5.3 Land use and land use change

Changing land use and land cover is a primary driver of changing fluvial organic C exports to the coastal ocean (Bauer et al., 2013), influencing soil OC stocks (Li et al., 2019) and the age, composition and bio-lability of exported DOC (Butman et al., 2015; Parr et al., 2015; Wilson and Xenopoulos, 2009). Natural forested watersheds typically export aromatic, structurally complex DOC that is biologically recalcitrant compared to DOC exported from anthropogenically modified agricultural watersheds that is characterised by reduced structural complexity and increased microbial degradation (Butman et al., 2015). However, this aromatic DOM also tends to be highly coloured, and susceptible to photodegradation, to the extent that overall rates of reactivity may be similar between these contrasting DOM pools (Anderson et al., 2019).

Globally, deforestation and agricultural expansion are major factors influencing LULC change (Chapter 2). Expansion of cropland and pasture continues to be the principle driver of deforestation in the developing world (Houghton, 2003; Song et al., 2018), and between 1980 and 2000, ~80 % of all new agricultural land originated from the world's tropical and subtropical forests (Gibbs et al., 2010). This agricultural expansion has been associated with declines in water quality, including those related to shifts in the composition of the DOM pool such as reduced water clarity, eutrophication, and deoxygenation (Mello et al., 2018; Singh et al., 2017; Yang et al., 2012). However, much of the developed world is undergoing afforestation. A number of European studies have linked the presence of forestry with higher DOC concentrations in freshwaters. Sobek et al. (2007) found that conifer boreal forest positively related to lake DOC concentrations in a study of 7,500 global lakes. In a 75-year data set collected from a river in Sweden, long-term change in water colour was partly explained by an increased presence of Norway spruce (*Picea abies*) in the catchment (Škerlep et al., 2019). A study of fluvial DOC fluxes in North America found that export was higher in forests than in pasture or cropland, and that fluxes were greatest from coniferous forest relative to broadleaf (Lauerwald et al., 2012), whilst another found a significant positive correlation between CO_2 in boreal lakes and the percentage of needle-leaved evergreen trees (Hastie et al., 2018). Drainage of peatland also appears to contribute to the mobilisation of higher (and typically older) DOC fluxes from deeper horizons (Moore et al., 2013). In headwater streams in the blanket bog of the Flow Country, Northern Scotland, DOC concentrations were 30 % higher in drained afforested catchments relative to both drained and undrained controls (*unpublished data*). The driving mechanism(s) behind this relationship remain unclear, although it is now largely established that planting coniferous forestry on organic-rich soils, particularly peatlands, can precipitate a destabilisation of the soil C store (Williamson et al., 2021).

Large-scale expansion of tree planting is not anticipated in areas with historically stable forest cover such as Fenno-Scandia, yet other countries in Europe are increasing tree planting in line with national scale C reduction and climate change mitigation strategies. To broaden our mechanistic understanding of forestry-related DOC increases, more extensive monitoring is required. Conversely, we have no reason to expect mass-deforestation at a pan-European scale, however where it does occur it will likely lead to increased delivery of OC to the LOAC, increased stream metabolism, and higher rates of CO_2 evasion to the atmosphere, at least in the short-term due to soil disturbance.

Other human activities also have an effect on land-ocean C fluxes, for example dam construction has decreased sediment and OC delivery to the LOAC, whilst fertiliser use has increased nutrient fluxes, leading to an increase in autochthonous DOM production (Bianchi and Allison, 2009; Galloway et al., 2008). A long-term (1970 – 2015) study of the Seine River found that in-stream CO_2 was closely related to urban water pollution (Marescaux et al., 2018). The overall effect of these changes may be a moderate increase in CO_2 emissions across the LOAC, and a possible decrease in OC delivery to the coastal ocean, but much uncertainty surrounds this assessment. Land use change is an ongoing process, operating at global scale according to human needs (e.g. requirement for farmland and urban housing) and values (e.g. desire for conservation), and acts in concert with other drivers, including climate change, making prediction of future trajectories challenging.

1.2.5.4 Climate and climate change

1.2.5.4.1 Temperature

Increasing temperatures have the potential to drive myriad effects in relation to the LOAC. This includes decreased GHG drawdown, for example the world's oceans have absorbed ~ 41 % of all anthropogenic C emitted as a result of fossil fuel burning and cement manufacture (Khatiwala et al., 2009), but an increase in sea surface temperature and eventual CO_2 saturation of surface waters may reduce the efficiency of the ocean sink (McKinley et al., 2016). In the medium to long term, this uptake is limited by changes in the overturning circulation which entrains C into deep waters with residence times in the order of hundreds to thousands of years. In the shorter term, however, models predict enhanced thermal stratification of the upper layers of the ocean, including continental shelf waters (Gröger et al., 2013; Holt et al., 2012). This would increase the residence time of terrestrial OC in the sunlit surface mixed layer, promoting enhanced photolysis in coastal and shelf waterspotentially reducing the amount of C entering the longer term deep water sink and increasing oceanic CO_2 emissions.

1.2.5.4.2 Precipitation

The duration, intensity, and frequency of rainfall influence the transfer of terrigenous C into the LOAC. Short periods of rainfall are usually absorbed by soils and vegetation, whilst long (or particularly intense) periods of rainfall can lead to saturated soils and increased runoff. When seasonality leads to dry and wet periods, soil surfaces can become baked hard and lose the capacity to absorb rains, thus the first rains of the season can also cause enhanced runoff. When runoff is high, a greater volume of terrigenous C is carried into the LOAC. In some cases, precipitation is the major explanatory variable for DOC export (Pumpanen et al., 2014).

Precipitation can also influence the supply of DIC into the LOAC. Acid rain enhances carbonate rock weathering, and as atmospheric C concentrations continue to increase, the transport of DIC into the LOAC is also increasing. Increased precipitation also increases GW flows, which can strengthen and dissipate in response to variations in precipitation patterns (Laudon and Sponseller, 2018). For example, elevated DIC concentrations are associated with base flow conditions when surficial water flow paths are inactive (Wallin et al., 2010), or in winter when precipitation is highest and flows are therefore maximal, driving DIC exchange between these deep flows and overlying streams/rivers (Lyon et al., 2010). In lake systems, upwelling of C rich deep water is precipitation-driven and coupled with associated seasonal increases in lateral OC inputs (Denfeld et al., 2015) and a resultant increase in remineralisation and surface CO_2 concentrations. In boreal systems, these seasonal emission peaks generally occur in spring and autumn when rains are maximal. However, Nydahl et al. (2017) found either a negative or no relationship between CO_2 and precipitation in boreal lakes over a 17-year period in Sweden, and suggested that this may be due to the dilution of CO_2 rich groundwater by increased surface water runoff, demonstrating the mitigation potential of prevailing environmental conditions. For example, a recent study (McDonough et al., 2020) found that global changes in groundwater DOC are in part driven by changes in climate, including temperature and precipitation, as well as urbanisation. Flooding can temporarily convert flood plains and surrounding land into what are essentially wetland systems, increasing the wetted area and therefore contributing additional terrigenous OC to the LOAC during episodic events. Conversely, a lack of precipitation can lead to drought conditions which lead to elevated OC concentrations and fluxes in subsequent years (Lepistö et al., 2014).

1.2.5.4.3 Wildfire

Incidences of wildfire have been shown to influence aquatic C cycling, and are linked to a preceding lack of precipitation/drought spell. Due to the dynamic and unpredictable nature of wildfire, there

are limited before-after data sets to assess the potential influence on aquatic C concentrations and export, and there remains a lack of consensus as to the directional effect of wildfire on DOC. A study of a wild fire in Northern Ireland found that DOC concentrations were considerably lower after a fire which had caused increased acidity of the soil (Evans et al., 2017). Increased prevalence of wildfire may facilitate further study of this soil acidity affect. A substantial proportion of the biomass C is converted into pyrogenic C (charcoal) during wildfires which is resistant to degradation over centuries-millennia (Kuhlbusch and Crutzen, 1995; Santín et al., 2015). Therefore, pyrogenic C represents a substantial long-term sink for C in terrestrial ecosystems and the LOAC, accounting for 12 % of direct emission to the atmosphere globally (Jones et al., 2019). Recently a 3 year time-series from the Flow Country measured peatland DOC quantity and composition in rivers during a drought-wildfire-recovery cycle. DOC did not increase significantly post-fire, although it is of note that no samples were taken in the 2 months immediately following the fire due. However, the aromaticity and humification of peatland OC exported into nearby rivers increased at sites which had been classed as 'degraded' prior to the fire (unpublished data). Recent work has highlighted aerial transport of nutrients from wildfires as a potential trigger of significant phytoplankton blooms in the ocean (Tang et al., 2021).

1.2.6 A changing perspective on land-ocean carbon transport

Historical depictions of the C cycle considered the two biologically active reservoirs, land and ocean, as being connected via gas exchanges with the atmosphere (Figure 1-5a). A significant flux between land and the ocean was not introduced until the 1970's, as a way to balance the C budget in the face of rapidly increasing anthropogenic CO_2 emissions. Since the start of the industrial revolution, CO_2 emissions have increased, mainly as a result of fossil fuel combustion, but atmospheric levels have not kept pace. Some authors postulated that the terrestrial C sink must have increased to account for this (Broecker et al., 1979) whilst others suggested that human activities had transformed the terrestrial C sink into a net source of CO_2 to the atmosphere (Woodwell et al., 1978).

A significant lateral flux of C from land to the ocean was proposed as a way to balance the contemporary carbon budget. Initially, the environments which comprise the LOAC were seen as 'passive pipelines' which transported material from land to sea without significant alteration or loss (Figure 1-5a), and so estimates of the land-ocean C flux focussed on riverine export (Equation 1-6):

$$Terrigenous\ input = Riverine\ export \qquad \boldsymbol{Eqn.1-6}$$

Almost 30 years later, an alternative model was proposed in which inland waters were viewed as 'active conduits' rather than 'passive pipes' (Cole et al., 2007), conceptualising them as dynamic sites

of transformation which could lose carbon to sediments and the atmosphere (Figure 1-5b) (Equation 1-7):

$$Terrigenous\ input = Outgassing + Storage + Riverine\ Export \qquad \boldsymbol{Eqn.\ 1-7}$$

The riverine export flux proposed in earlier studies (0.9 Pg C yr^{-1}) was retained, and new estimates of outgassing and sedimentation were applied which accounted for an additional 1 Pg C yr^{-1} anthropogenic emissions. The estimate of terrigenous export therefore increased from 0.9 to 1.9 Pg C yr^{-1} (Table 1-1).

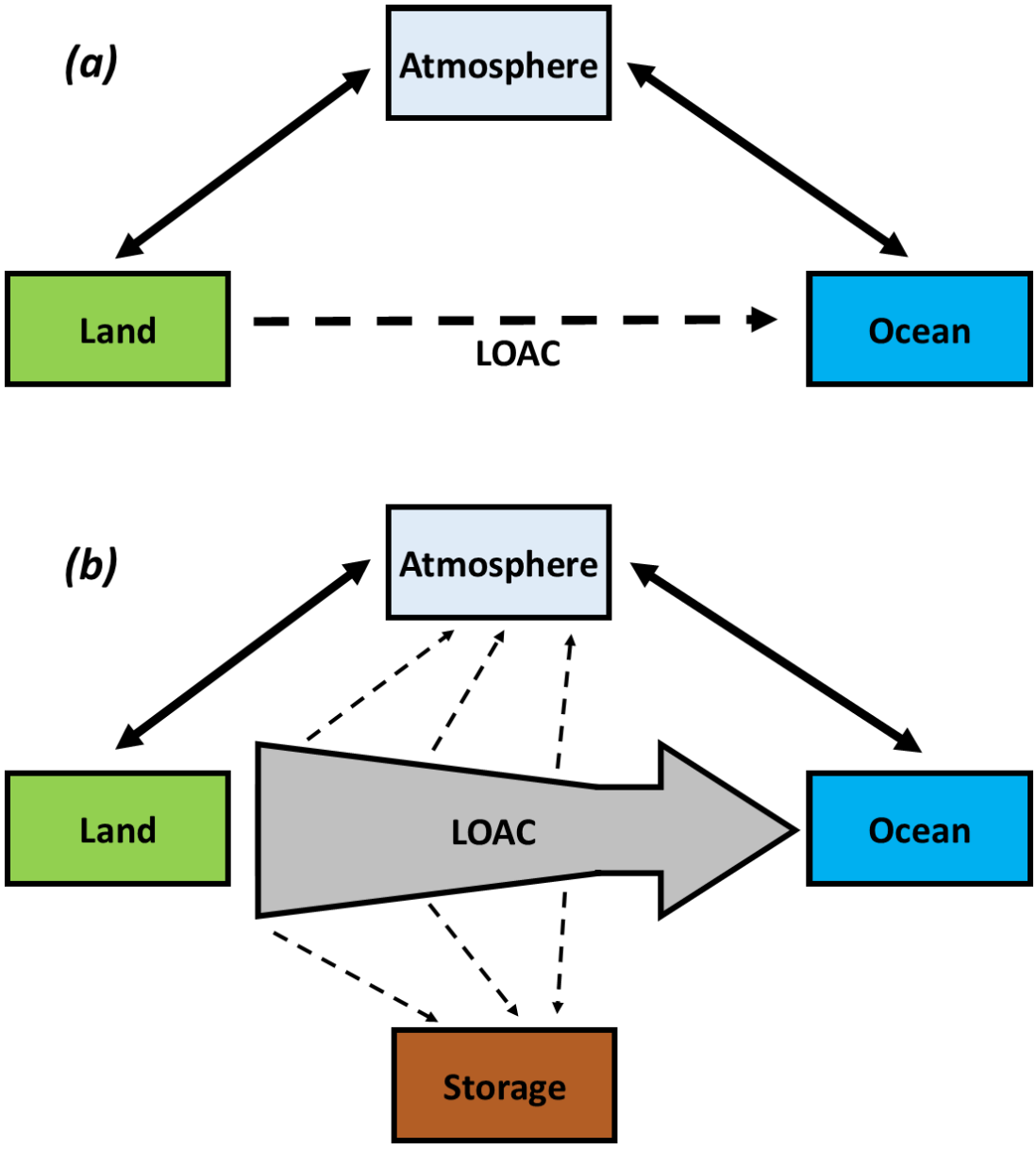

Figure 1-5. Schematic representation of (a) the passive aquatic pipeline vs. (b) the 'active' aquatic conduit. Image adapted from Drake et al. (2018).

Table 1-1. Inland water fluxes, as calculated by Cole et al. (2007). Input from land is calculated as the sum outgassing, storage in sediments, and export to the coastal ocean.

	Organic Carbon (Pg C yr^{-1})				Inorganic Carbon (Pg C yr^{-1})			
	Outgassed	**Stored**	**Exported**	**Input**	**Outgassed**	**Stored**	**Exported**	**Input**
Lakes	0	0.05	0	0.05	0.11	*NA*	0	0.11
Reservoirs	0	0.18	0	0.18	0.28	*NA*	0	0.28
Rivers	0	*NA*	0.45	0.45	0.23	*NA*	0.26	0.49
Estuaries	0	*NA*	*NA*	*NA*	0.12	*NA*	0.19	0.31
Groundwater	0	0	0	0	0.01	0	0	0.01
Total	**0**	**0.33**	**0.45**	**0.78**	**0.75**	**0**	**0.45**	**1.20**

Cole et al. (2007) explicitly stated that this was likely an underestimate with large uncertainties. For example, the study lacked any data from small streams and did not account for organic carbon storage within riverine and estuarine sediments. They also highlighted a great deal of uncertainty around the outgassing flux, primarily due to a lack of data from underrepresented regions. A decade later, Drake et al. (2018) were able to reassess this flux in light of improved outgassing estimates. Using the estimate from Cole et al. (2007) as a starting point, they applied a similar mass balance approach (Equation 1-8; Table 1-2):

$$Terrigenous\ input = Outgassing + Storage + Riverine\ Export\ + Production \qquad \boldsymbol{Eqn.1-8}$$

Table 1-2. Estimates of aquatic carbon fluxes (Pg) as compiled by Drake et al. (2018). Black text indicates independent estimates. Grey italic text indicates values taken from other studies.

	Outgassed to atmosphere	**Stored in sediments**	**Exported to ocean**	**Photosynthetic Production**	**Terrigenous Input**
Cole et al. (2007)	0.8	0.2	0.9	*0.3*	1.6
Battin et al. (2009)	1.2	0.6	0.9	*0.3*	2.4
Tranvik et al. (2009)	1.4	0.6	0.9	*0.3*	2.6
Bastviken et al. (2011)	1.5	*0.6*	*0.9*	*0.3*	2.7
Regnier et al. (2013)	1.2	0.6	1.0	0.3	2.5
Raymond et al. (2013)	2.2	*0.6*	*1.0*	*0.3*	3.4
Borges et al. (2015)	2.8	*0.6*	*1.0*	*0.3*	4.0
Holgerson and Raymond (2016)	3.1	*0.6*	*1.0*	*0.3*	4.3
Sawakuchi et al. (2017)	3.9	*0.6*	*1.0*	*0.3*	5.1

Whilst this reassessment reached a considerably higher estimate of 5.1 Pg C yr^{-1}, it is important to note that this does not represent an increase in the flux itself, but a decreased uncertainty around CO_2 and CH_4 outgassing due to the addition of data from historically underrepresented regions

including Africa (Borges et al., 2015) and the Amazon (Sawakuchi et al., 2017). Additionally, an increase in the estimated global lake area and the identification of high burial rates in small impoundments increased the sedimentation estimate from 0.2 Pg C yr^{-1} (Cole et al., 2007) to 0.6 Pg C yr^{-1} (Regnier et al., 2013; Tranvik et al., 2009) but did not reflect an actual increase and still carries a high level of uncertainty (range = 0.2 to 1.6 Pg C yr^{-1}; Regnier et al., 2013), rendering it poorly constrained.

The riverine export flux, on the other hand, increased by just 0.1 Pg C yr^{-1} and is generally accepted as being well constrained. Our estimate of this term has not varied substantially (0.9 – 1.0 Pg C yr^{-1}) since Kempe (1979) and Schlesinger and Melack (1981) estimated the inorganic and organic components at 0.45 Pg C yr^{-1} and 0.37 – 0.41 Pg C yr^{-1}, respectively (~ 0.9 Pg C yr^{-1} in total). Drake et al. (2018) attribute this to reliable discharge measurements, high stability of fluxes over time, and robust modelling in major rivers. However, the foundational papers used by Cole et al. (2007) rely heavily upon estimates which draw upon the same core data set: either SCOPE-CARBON[1] or data obtained from the large rivers which comprise that study set (Table 1-3).

Table 1-3. Key foundational papers which underpin the contemporary estimate of riverine export of organic carbon to the ocean alongside estimates of DOC, POC, and/or TOC (Pg C yr^{-1}), and the main data source used.

		DOC	POC	TOC	Main data source
Schlesinger and Melack (1981)	1	*NA*	*NA*	0.37 - 0.41	Literature review
Meybeck (1982)	2	0.22	0.18	0.40	Literature review
Ittekkot (1988)	3	*NA*	0.23	*NA*	SCOPE-CARBON
Degens et al. (1991)	4	*NA*	*NA*	0.38	SCOPE-CARBON
Spitzy and Leenheer (1991)	5	0.22	*NA*	*NA*	SCOPE-CARBON
Sarmiento and Sundquist (1992)	6	0.20	0.25	0.40	Synthesis of 1 – 5
Meybeck (1993)	7	0.20	0.02	0.22	SCOPE-CARBON
Meybeck (1993b)	8	0.21	0.17	0.38	SCOPE-CARBON
Meybeck and Ragu (1996)	9	0.22	0.18	0.38	SCOPE-CARBON
Ludwig et al. (1996)	10	0.21	0.17	0.38	SCOPE-CARBON
Stallard (1998)	11	0.23	0.30	0.53	Literature review
Aitkenhead and McDowell (2000)	12	0.36	*NA*	*NA*	Literature review

It is noteworthy that the DOC flux proposed by Aitkenhead and McDowell (2000) is almost double previous estimates, the main difference being the inclusion of data from a broad range of systems, including many smaller rivers not previously considered (0.36 Pg C yr^{-1} vs. 0.20 – 0.23 Pg C yr^{-1}).

[1] SCOPE-CARBON was part of a United Nations funded effort to construct a budget of riverine nutrient fluxes at global scale (SCOPE-UNEP).

Stallard (1998)'s review of POC export was also higher than previous values, and this was again based on a much broader range of rivers.

Almost all of the studies listed in Table 1-3 refer to a sub-set of data which were explicitly excluded because they did not fit with the overriding pattern. Excluded samples were most commonly associated with anthropogenic influence (e.g. eutrophication, damming, and land use change). For example:

"I have chosen not to use some data from the Colombia and Indus rivers because of extensive damming; the Rhine and Seine rivers, because of eutrophication; and other rivers, because of organic pollution" (Meybeck, 1993)"

and

"The most striking exceptions to this trend are the Indus and the Changjiang Rivers. Both have high average DOC concentrations but the soil carbon values are low to medium... This is the reason we did not include them" (Ludwig et al., 1996).

With this in mind, it is unsurprising that estimates of the riverine export flux have remained broadly similar. It may not be the global land-ocean carbon flux that is well constrained as much as it our ability to derive similar estimates from similar data. At best then, our estimate of the riverine C flux is well constrained for a specific sub-set of rivers which are large, drain near-natural catchments, and are absent significant anthropogenic influence.

1.2.7 Data bias, sampling issues, and knowledge gaps

Geographical biases exist across a range of scales. There is a literature focus on large rivers (Dai et al., 2012), despite the fact that smaller rivers and headwater streams draining mountainous catchments and organic-rich soils can be important conduits for fluvial C export (Milliman and Syvitski, 1992; Worrall et al., 2012), and may make a disproportionately large contribution to land-ocean C fluxes (Williamson et al., 2021). The majority of relevant research has been conducted in North America and Central / Northern Europe; areas which have historically been strongly influenced by industrialisation, land use change, and acid deposition. There is a notable absence of studies involving the quantification of groundwater C stores and fluxes in large-scale C flux estimates, or the impact of anthropogenic use and redistribution of groundwater at the surface. Temporal bias also exists, with sampling occurring more frequently in fair-weather (i.e. spring/summer). This is particularly notable in high latitude systems where ice-cover makes aquatic systems inaccessible during the winter months and where storms make seagoing more treacherous,

but is also observed in low latitude systems where rainfall and flooding can render some aquatic systems inaccessible during peak wet season months.

As well as large-scale geographical and seasonal biases, there are also problems relating to sampling frequency. Long-term, high-frequency measurements of C concentration and water discharge are now possible and provide valuable insights into fine-scale C dynamics (Kirchner, 2003; Kyung Yoon et al., 2016) but can be very expensive and are thus typically beyond the budget of, and/or precluded by the 3 - 5 year funding model typically used to support academic studies. This reduces capacity to adequately account for changes over time, especially during storm events when failing to account for changes to organic C dynamics can lead to both under- and over-estimation of annual exports (Clark et al., 2007; Dhillon and Inamdar, 2014, 2013).

There are further issues arising from divergences in analytical methods, such as varying pore sizes being used for filtering water samples between different research disciplines (e.g. marine vs. fresh water), different analytical methods for quantifying C, and the use of indirect rather than direct measurement techniques (Abril et al., 2015; Karanfil et al., 2002; Sugimura and Suzuki, 1988; Vodacek et al., 1995). The traditional use of 0.45 µm as a filter pore size for DOC analysis has resulted in a significant fraction of colloidal OC (COC) being classified as DOC (Yan et al., 2018). DOC has a key role in binding and transporting harmful trace metals (Dai et al., 1995), and the form of OC directly affects its reactivity (Attermeyer et al., 2018). Thus, accurate quantification of OC form is necessary for modelling C degradation and effects on aquatic ecosystem health. Similarly, issues exist around sample preservation, with different disciplines preferring e.g. acidification or freezing over chilling of samples, despite evidence that freezing significantly alters measured DOC concentrations in some systems (e.g. Peacock et al., 2015). Divergence across disciplines can make comparison of data problematic. In the case of this thesis, a single sample collection, preservation, and analysis methodology was selected to avoid these issues. Details of decision making in this regard are given in Appendix A.

Finally, issues arise from the divergent paradigms adopted by different research communities (Kothawala et al., 2020; Marín-Spiotta et al., 2014). Studying the land-ocean export of terrestrial C necessitates collaboration across the disciplines of soil, freshwater and marine sciences. This is made fundamentally more difficult because the different research communities favour different understandings of OC processing (Figure 1-6). The contemporary paradigm in soil science is that environmental and biological controls mediate OC stability (Schmidt et al., 2011), although this is not yet reflected in many soil carbon models, which typically define turnover rates based on organic matter bio-lability. For aquatic systems, molecular composition is considered key (Kellerman et al.,

2015). Thus, separate communities have used different methods to investigate similar questions. Furthermore, the diversity of aquatic environmental typologies around the world has resulted in the development and implementation of a range of strategies for aquatic C flux monitoring. Understanding and integrating data generated via different methodologies in different components of this continuum represents a major challenge for generating land-ocean C flux budgets at every scale (i.e. local, regional, continental, and global).

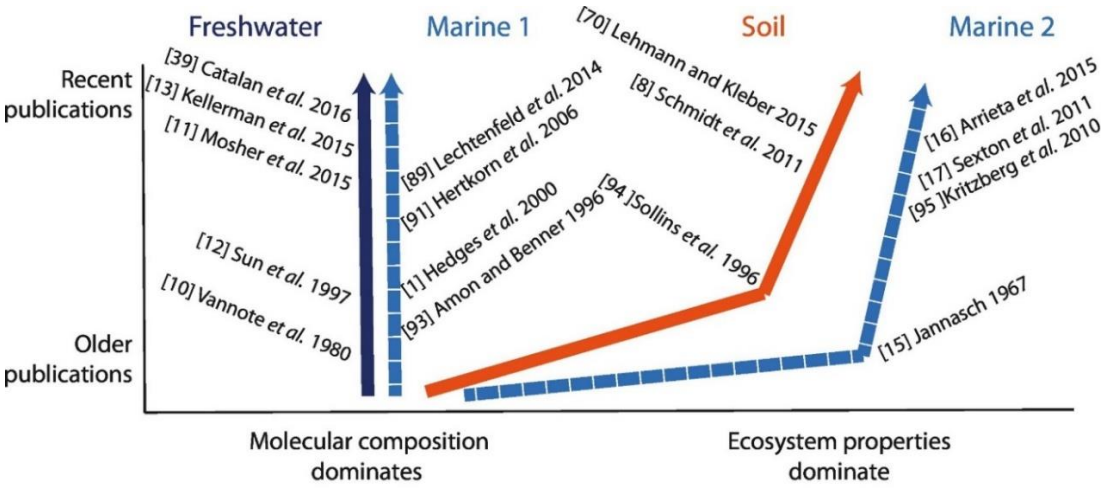

Figure 1-6. Illustration of how our conceptualisation of the dominant controls on organic matter degradation has developed across the freshwater, soil, and marine literature. Examples of studies driving these diverging conceptualisations are given. Figure taken from Kothawala et al. (2020).

The cumulative effect of all these issues is that estimates of the land-ocean C flux carry large uncertainties, the scale of which varies depending on which component part is being quantified and/or discussed. The estimated transfer of C from the LOAC to the open ocean, ~ 1.0 Pg C yr^{-1}; henceforth referred to as the marine flux, has not varied significantly in > 40 years and is considered to carry low uncertainty. On the other hand, estimates of the transfer of C from land into the LOAC, ~ 5.1 Pg C yr^{-1}; henceforth referred to as the terrigenous C flux, have steadily increased over the last decade (Table 1-1. Inland water fluxes, as calculated by Cole et al. (2007). Input from land is calculated as the sum outgassing, storage in sediments, and export to the coastal ocean.Table 1-1). This does not reflect a change in real terms, but instead reflects the high degree of uncertainty around this estimate, and the incorporation of data from regions for which there none was previously available. In light of this uncertainty, the Intergovernmental Panel on Climate Change (IPCC) have highlighted the importance of better constraining the land-ocean C flux, particularly in the context of the Earth System Models (ESMs) which underpin our understanding of the C cycle: *"many of the key processes relevant to decomposition of [terrigenous] OM are missing in models…*

despite their vulnerability to warming and land use change" (IPCC, 2013). For example, the UK ESM contains a land surface module (JULES) which does not transfer terrigenous C to the ocean, and a marine ecosystem module (MEDUSA) which does not cycle the dissolved organic carbon (DOC) which makes up ~ 50 % of the land-ocean flux (Nakhavali et al., 2018; Yool et al., 2013). Thus, if we are to quantify the fate of terrigenous C flux in global biogeochemical models, we must improve our understanding of the processes which act upon it.

1.3 Dissolved organic matter (DOM)

DOM is a complex mixture of thousands if not millions of compounds and the predominant source of organic macronutrients to aquatic systems, including C, nitrogen (N), and phosphorous (P). As a result, its concentration and composition have implications for a range of critical parameters including in-stream metabolism, ecological and biological function, and C cycling (Nebbioso and Piccolo, 2013). It is therefore critical that we have the means and understanding with which to adequately quantify and characterise it.

1.3.1 Coloured and non-coloured DOM

DOM can be classified as either 'coloured' (cDOM) or optically 'invisible' (iDOM), depending on whether or not it absorbs light in the visible (400 – 700 nm) range. Broadly speaking, cDOM tends to be more dominant in freshwaters, whereas iDOM tends to be more dominant in the marine environment. The wavelength range that a DOM molecule can absorb is determined by the amount of energy required to excite one of its electrons to a higher energy level (Figure 1-7). The lowest amount of energy required to do this is equal to the difference in energy (ΔE) between the highest occupied molecular orbital (HOMO) and the lowest unoccupied molecular orbital (LUMO), otherwise known as the HOMO-LUMO gap. The less energy required, the longer the wavelength of light that can be absorbed. Exciting electrons in a single sigma (σ) bond requires the most energy and so single bonded molecules typically have a large HOMO-LUMO gap. Exciting an electron within a double or triple pi (π) bond requires less energy, decreasing the HOMO-LUMO gap. The π bond effect is cumulative and the wavelength range a molecule can absorb increases each additional conjugation (Figure 1-8). Carbonyl groups (C to O double bonds) also increase the wavelength a molecule is capable of absorbing when electron pairs held within non-bonding (n) orbitals are excited to π or σ orbitals. A molecule becomes coloured when it is sufficiently conjugated and/or contains enough carbonyl groups to lower the HOMO-LUMO gap enough that low energy, visible light can be absorbed. As a result, molecules with a simpler structure only absorb light in the ultraviolet (UV)

range (10 – 400 nm) and appear invisible to the naked eye, whilst complex molecules absorb in the visible range and appear coloured.

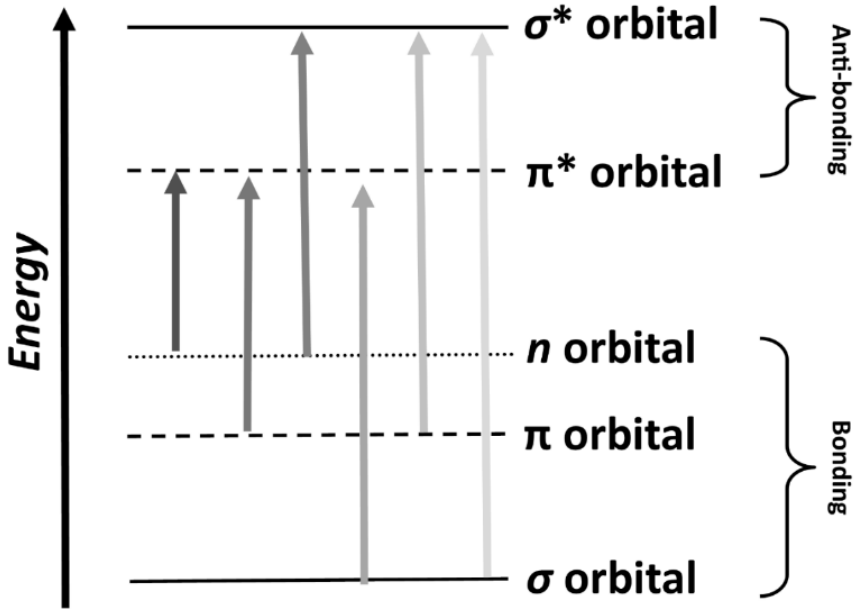

Figure 1-7. Diagram showing all possible electron transitions within a molecule. Electron transitions occur between bonding and anti-bonding orbitals. Arrows show the energy required to excite an electron from one orbital to another.

1.3.1 DOM absorbance

DOM absorbance is measured in decadic units with respect to transmission via the common logarithm (log 10), and presented per cm (cm^{-1}) or per m (m^{-1}). Measurements are made using a spectrophotometer which measures the absorbance of a sample across the UV and visible portion of the light spectrum. This typically produces absorbance values at a range of pre-programmed wavelengths, the number of which varies according to (a) the capability of the instrument and (b) the aims of the study. Where sufficient wavelengths are captured, an absorbance spectra is produced (Figure 1-9). It is important to note that absorbance in natural samples refers to the total absorbance of the sample, rather than any specific molecule with it; DOM absorbance is a net result.

Decadic absorbance is sometimes converted into Napierian units with respect to transmission via the natural logarithm (ln), with no change to the units used. Naperian absorption coefficients (*α)* are derived from decadic absorbance according to Equation 1-9:

$$\alpha = \frac{2.303\, a}{l} \qquad \boldsymbol{Eqn.\,1-9}$$

where α = Naperian absorbance (cm^{-1}), *a* = decadic absorbance (cm^{-1}), and *l* = the path length of the measurement cuvette (m).

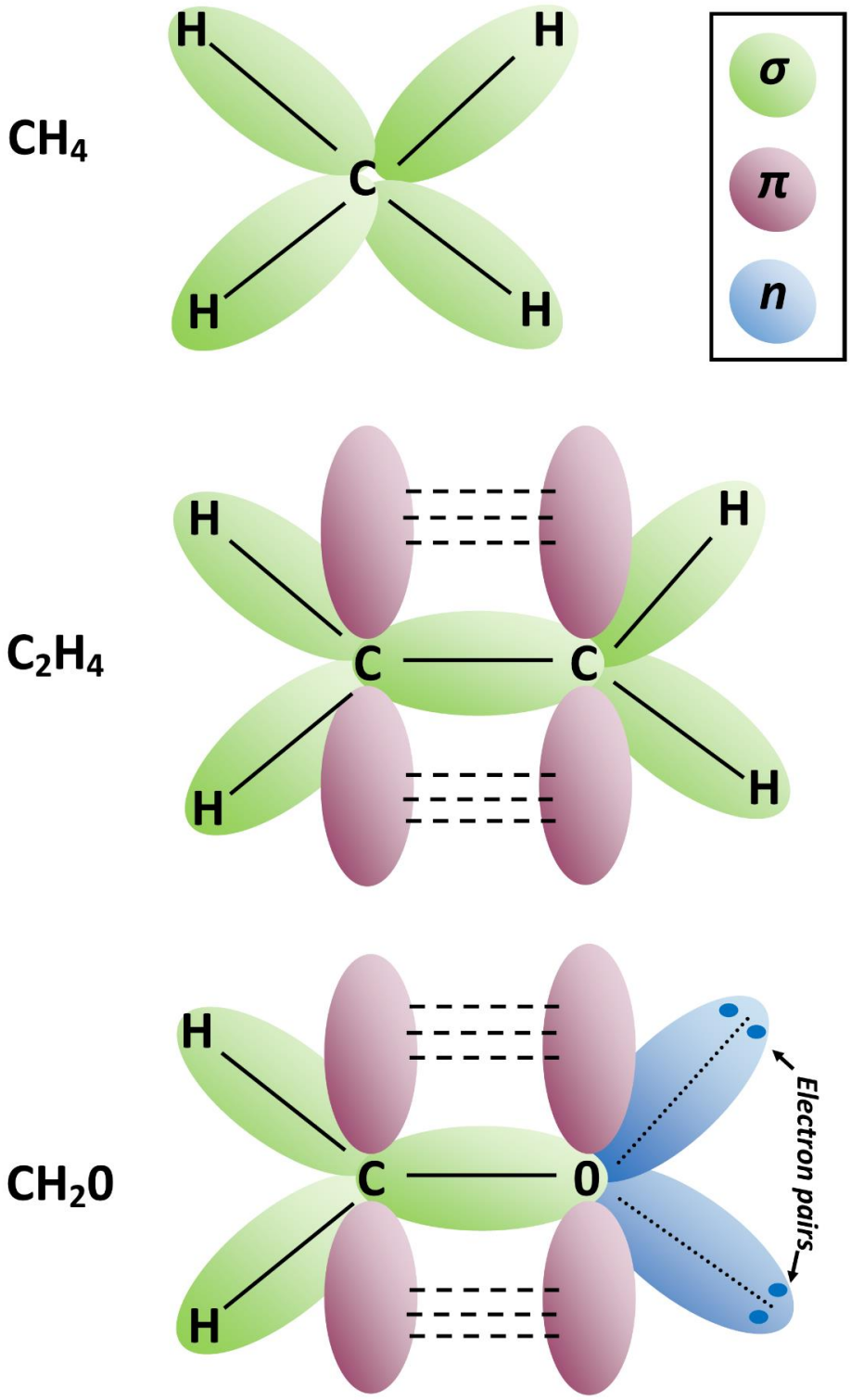

Figure 1-8. Diagram of CH_4, C_2H_4, and CH_20 molecules, which contain bonds between sigma (σ), pi (π), and non-bonding (n) orbitals. The wavelength range at which each molecule absorbs increases with complexity.

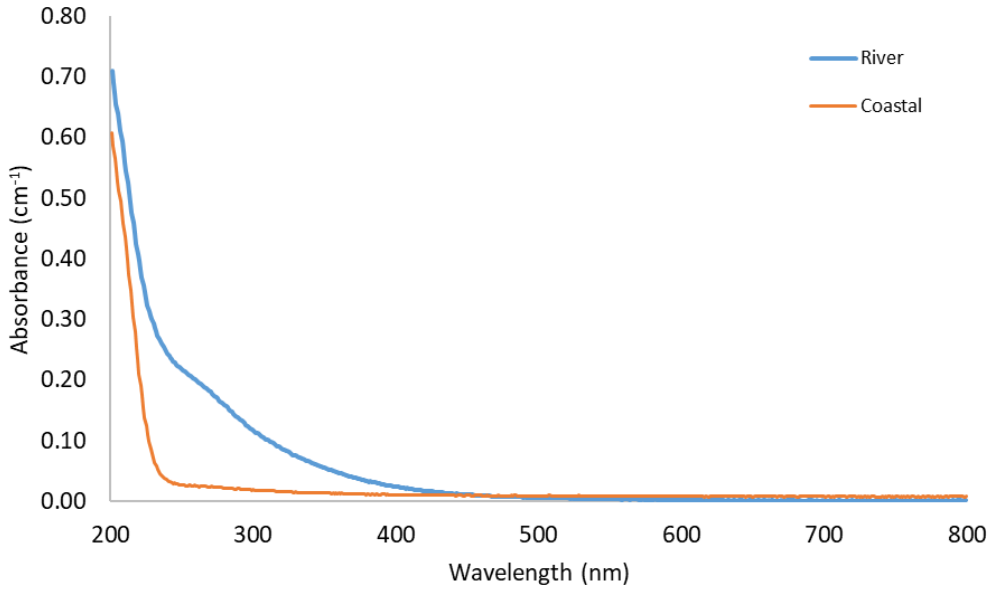

Figure 1-9. Two absorbance spectra produced from samples collected in the Belize River and coastal zone, measured at 1 nm intervals. These example spectra are typical of those expected in such environments.

1.3.2 DOM fluorescence

Whilst absorbance measures the amount of light absorbed by a molecule, fluorescence measures emission of light in response to that absorbance. This occurs when incident light energy is absorbed and then reemitted, often at a different wavelength, as the molecule returns to its ground state. DOM fluorescence is measured in terms of its intensity. This is typically expressed as standardised Raman Units (RU), but can also be expressed relative to a quinine sulphate standard as Quinine Sulphate Units (QSU). Fluorescence measurements carry more specificity and sensitivity than absorbance measurements do, and fluorescent DOM (fDOM) accounts for a high proportion of cDOM. Thus, fDOM is often used to further interrogate the cDOM pool.

An excitation-emission matrix (EEM) is a three-dimensional (3D) image produced via fluorescence spectrophotometry, where absorbance or 'excitation wavelength' (Ex), emission wavelength (Em), and fluorescence intensity are plotted simultaneously (Figure 1-10). Each fluorescence scan contains a huge amount of information which can be difficult to interpret. EEMs can provide a relatively simple way with which to visually assess the composition of the scanned pool. Broad classes of compounds (e.g. humic-like vs. protein-like) exhibit characteristic peaks in specific areas (i.e. Coble Peaks (Coble 1996; Table 1-4). EEMs also form the basis of Parallel Factor (PARAFAC) analysis, a tool commonly used to decompose the DOM pool according to its fluorescent properties (Stedmon et al., 2003a).

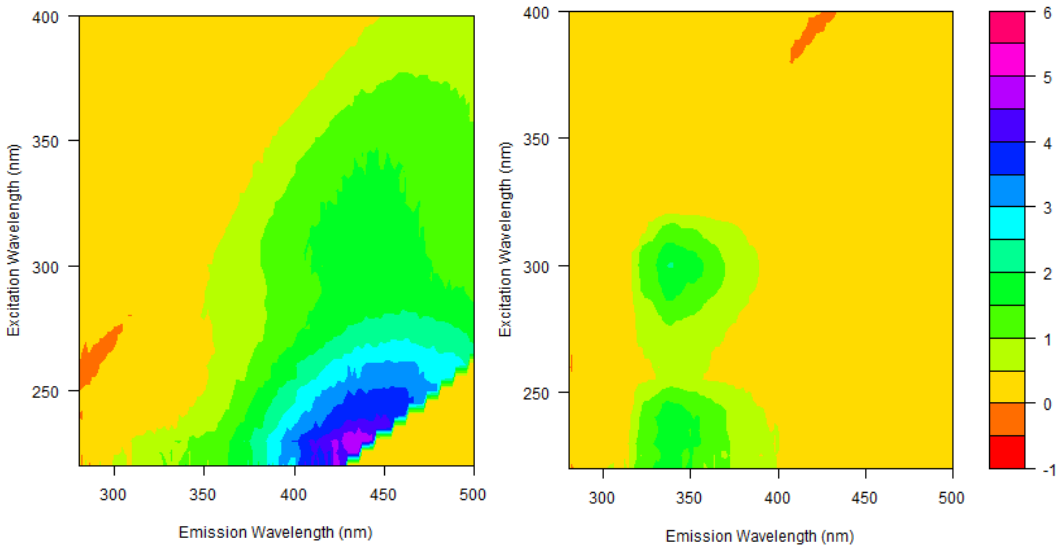

Figure 1-10. Fluorescence excitation-emission matrix (EEM) obtained from the Belize River (left) and coastal zone (right) during field work for Chapter 2, being dominated by humic-like and protein-like fluorescence, respectively. Colour bar indicates fluorescence signal intensity in Raman Units (RU).

Table 1-4. Excitation and emission peaks associated with major fluorescence components present in seawater, as identified by Coble (1996) and commonly referred to as 'Coble Peaks'.

Peak	Ex (nm)	Em (nm)	Characterisation
B	275	310	Tyrosine-like (Protein)
T	275	340	Tryptophan-like (Protein)
A	260	380 - 460	Humic-like
M	312	380 - 420	Marine humic-like
C	350	420 - 480	Humic-like

1.3.3 DOM degradation

The degradation of DOM can be conceptualized as being driven by molecular and/or environmental conditions (Figure 1-6), with the balance of these drivers varying in space and time. At a more basic level, however, DOM degradation is driven by two processes: biodegradation (alteration via the microbial community) and photodegradation (alteration via light; Figure 1-11).

Biodegradation occurs when microorganisms alter the molecular structure of a DOM molecule (Lucas et al., 2008). Photodegradation occurs when incoming light photons alter the molecular structure of a DOM molecule (Kaplan and Cory, 2016). Photodegradation mostly affects cDOM due to its much greater absorption of light, but iDOM can also be altered, being oxidised directly by high-

energy UV light or indirectly by the by-products of cDOM oxidation (Cory et al., 2010a, 2010b; Goldstone et al., 2002; Pullin et al., 2004; Scully et al., 2004).

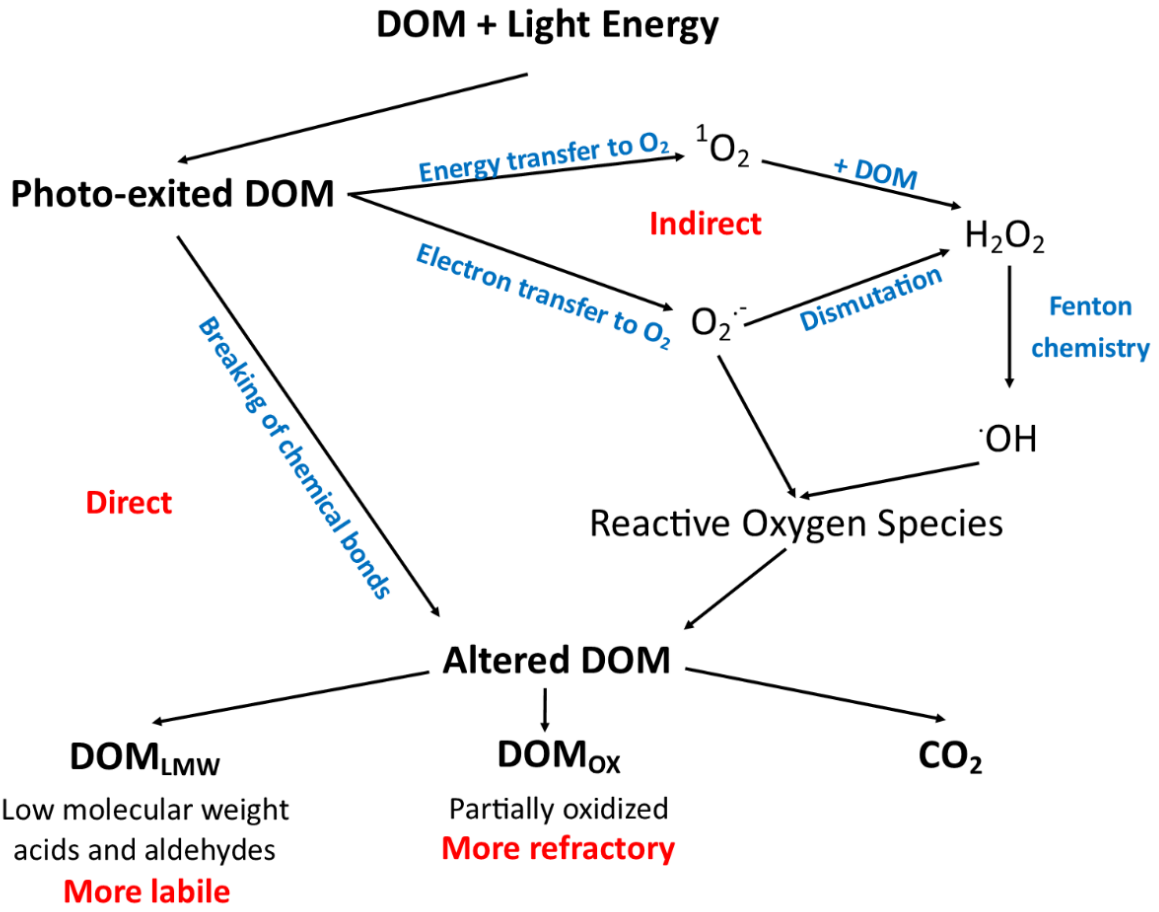

Figure 1-11. Diagram showing the photochemical degradation of DOM through direct and indirect pathways. Image based on Kaplan and Cory (2016).

Additionally, there are interactions between photodegradation and biodegradation which must be understood. How do light exposure, water residence time, and DOM residence time interact? How and on what time scales are photo-products utilised by the microbial community? Does photodegradation rate influence biodegradation rate? (Cory and Kling, 2018). For example, some studies find biodegradation to be the dominant form of DOM removal in aquatic systems, with microbes removing e.g. 6 to 14 % of the available DOC pool whilst light exposure has little or no significant effect, whilst other studies find that photochemical degradation to be dominant (see Wiegner and Seitzinger, 2001 and references therein). Photodegradation appears to be particularly influential in humic waters where up to 50 % of DOC can be removed under natural light conditions whilst non-coloured OM such as sugars exuded by algae tend to exhibit much lower rates of photodegradation (0.2 %) (Wiegner and Seitzinger, 2001).

1.4 Dissolved organic carbon (DOC)

DOC is an intrinsic part the DOM pool, contributing ~ 50 % DOM by molecular weight. As a result, DOC and DOM are often studied in parallel. DOC is operationally defined as the OC which passes through a specific filter pore size, typically in the 0.22 – 0.70 µm range, and in this thesis a definition of 0.45 um is used. DOM is the primary food source underpinning aquatic food webs, and its remineralisation produces DIC, contributing to acidification in low alkalinity, poorly buffered systems, and to CO_2 and CH_4 outgassing in saturated and/or highly turbulent systems. Recent C budgets do not partition the terrigenous C flux into its component parts, but if we assume that DOC accounts for ~ 25 % of terrigenous C entering aquatic systems (OC = ~ 50 % C flux; DOC = ~ 50 % OC flux) and use Drake et al. (2018)'s total C flux estimate of 5.1 Pg C yr^{-1}, the land-freshwater DOC export can be estimated at ~ 1.3 Pg yr^{-1}. Downstream, an estimated ~ 0.45 Pg DOC yr^{-1} is exported out of rivers and into the coastal ocean each year (Cole et al., 2007).

1.4.1 Direct DOC quantification

A number of different DOC quantification methods exist, the most common of which are the automated quantification of DOC as either non-purgeable organic carbon (NPOC) or total organic carbon (TOC). Both methods operate on the principle of separating total carbon (TC) into its inorganic (IC) and organic (OC) fractions via acidification and/or catalytic oxidation into CO_2, which can then be quantified via infrared gas analysis (IRGA) (Figure 1-12).

The NPOC method is analogous to wet oxidation methods whereby IC is converted into CO_2 via acidification and then sparged into the atmosphere. Catalytic oxidation converts the remaining (non-purgeable) OC into CO_2, which is quantified via IRGA. Using the TOC method, one aliquot of sample water is acidified to convert IC to CO_2, and another is subjected to subsequent catalytic oxidation and acidification to convert OC + IC (TC) into CO_2. The CO_2 produced in each step is sparged into a closed system, allowing IC and TC to be quantified via IRGA and OC to be derived as TC – IC.

Neither method is without caveat: TOC analysis is prone to DOC overestimation due to incomplete sparging in high DIC samples, whereas NPOC analysis, which is insensitive to DIC concentration, is prone to DOC underestimation due to the loss of weakly acidic DOC compounds via flocculation, and of volatile organic carbon (VOC) species (Findlay et al., 2010). VOCs are a potentially important part of the DOC pool (Dachs et al., 2005), comprised of low molecular weight, hydrophobic molecules including small hydrocarbons and alkanes, which typically account for < 10 % of the DOC pool (Urbansky, 2001; Wangersky, 1993). Aquatic VOCs are predominantly anthropogenic in origin and

VOC concentrations tend to be highest in urbanized and/or polluted systems (Liu et al., 2008). This thesis required the analysis of DOC samples from fresh and saline waters spanning a wide range of DIC concentrations, none of which were from heavily urbanized or polluted systems, and so the NPOC method was selected.

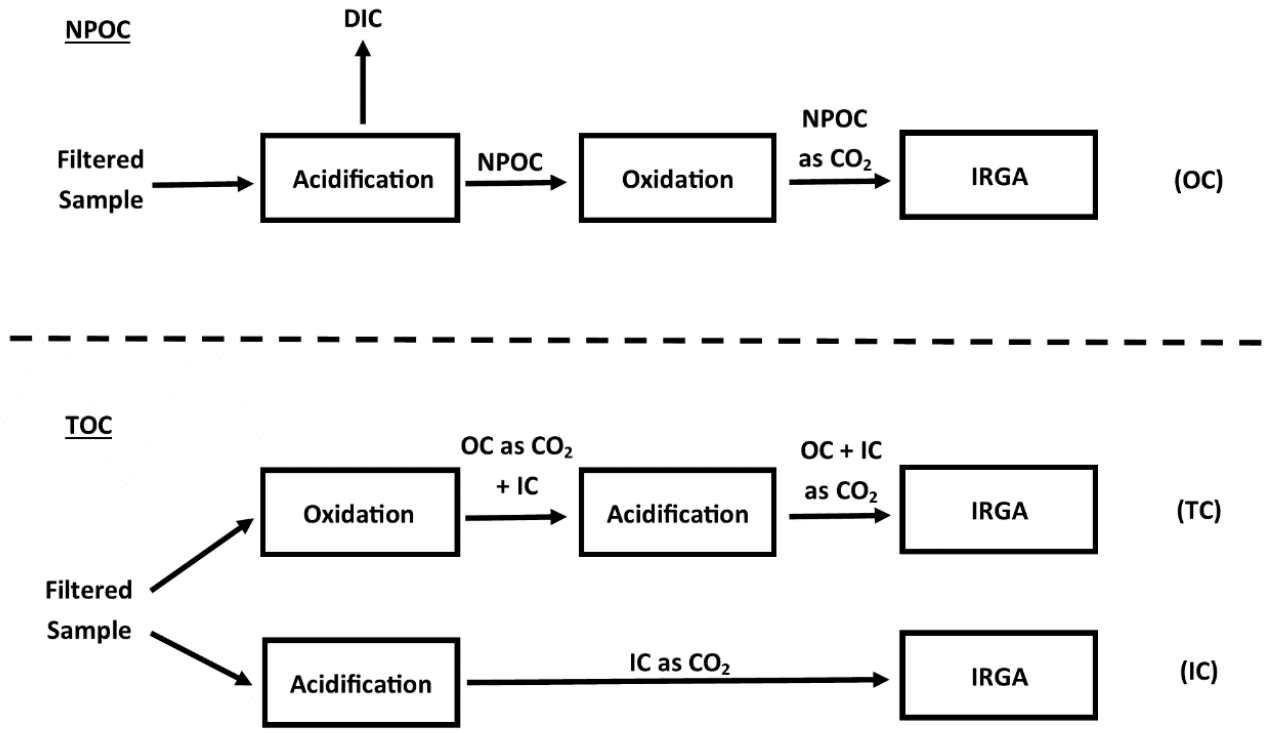

Figure 1-12. Typical analytical scheme for quantification of DOC via NPOC and TOC methods, adapted from Findlay et al. (2010). OC = organic carbon; IC = inorganic carbon; TC = total carbon; IRGA = infrared gas analysis.

1.4.2 Indirect DOC quantification

Indirect quantification of DOC is an integral part of this thesis, and so a greater level of detail is given in this section.

DOC concentrations can also be inferred from DOM absorbance. For more than 50 years, researchers have been proposing methods by which a relationship between cDOM absorbance and DOC might be used to provide an inexpensive alternative to direct analytical quantification of DOC. Initially, these methods used a linear regression approach and absorbance at a single wavelength (λ; Equation 1-10):

$$[DOC] = (b * a_{\lambda} + c) \qquad \boldsymbol{Eqn. 1-10}$$

where *[DOC]* is the DOC concentration, a_λ is absorbance at the wavelength in question, *b* is the model coefficient, and *c* is the y axis intercept. Variations on this method remain popular (Table 1-5).

Table 1-5. Examples of studies which derive a relationship between cDOM absorbance at a single wavelength and DOC concentration. Environment, wavelength (λ; nm), number of samples (n), and the R2 value of the best-fit linear regression model are given.

Source	Environment	λ	R^2
Forsberg (1967)	Lake	420	0.80
Dobbs et al. (1972)	Waste water	254	0.85
Banoub (1973)	Lake	260	0.55
Lewis and Canfield (1977)	River	360	0.69
De Haan (1977)	Lake	250	0.80
Moore (1985)	Peat water	330	0.96
Timperley (1985)	River	270	0.79
Grieve (1986)	Stream	360	0.92
Collier (1987)	Stream	360	0.94
Moore (1987)	River, Soils, Stemflow	330	0.75
Osburn et al. (2011)	Marine	300	0.78
Asmala et al. (2012)	Estuaries	375	0.90
Spencer et al. (2012)	River	254, 350, 440	0.89, 0.81, 0.61
Brezonik et al. (2015)	Inland waters	440	0.93
Massicotte et al. (2017)	Land-ocean continuum	350	0.92
Song et al. (2017)	Inland waters	275	0.85
Griffin et al. (2018)	Lakes	440	0.81

However, single wavelength predictions of DOC are only reliable where the composition of the DOM pool is relatively consistent, and can exhibit a high degree of spatiotemporal variability, and the majority of studies listed in Table 1-5 show data for specific systems and/or occasions where the headline relationship does not hold. For example, Spencer et al. (2012) found significantly weaker relationships in four of their study rivers: the Colorado, Colombia, Rio Grande, and St Lawrence; noting that these are atypical systems which exhibited evidence of autochthonous or anthropogenic sources, or photochemically degraded allochthonous DOM. Song et al. (2017) highlighted the fact that samples from urban settings exhibited highly variable R^2 and slope values due to complex inputs and processing of sewage and nutrients. Asmala et al. (2012) found that the relationship between DOC and cDOM absorbance was strongest in autumn (R^2 = 0.98) and weakest in summer (R^2 = 0.36). The fact that so many studies find instances where the relationship between cDOM absorbance and DOC concentration is weaker than expected is not wholly surprising: variations in cDOM composition

are routinely characterised using the ratio of absorbance at a specific wavelength (e.g. 254 nm) to DOC (as DOC specific absorbance or $SUVA_{254}$; Weishaar et al. (2003)). Site- and season-specific calibrations are therefore required, and no 'global' model exists with which to predict DOC from absorbance using a single wavelength. Recognising this, Fichot and Benner (2011) proposed the addition of a second wavelength term, deriving log-linearized DOC via regression against log-linearized absorbance at 275 and 295 nm (a_{275} and a_{295}; Equation 1-11):

$$\ln[DOC] = \left(a * (\ln a_{275})\right) + \left(b * (\ln a_{295})\right) \qquad \boldsymbol{Eqn.\,1-11}$$

This approach yielded predictive relationships which were less sensitive to seasonal variation than those produced via single wavelength regression (Figure 1-13).

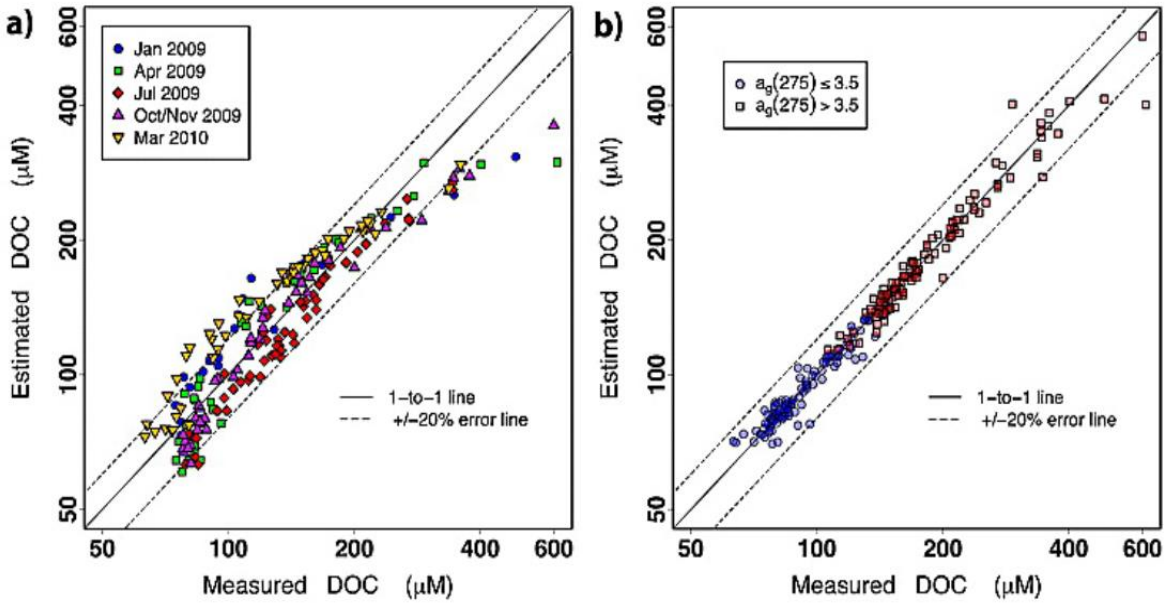

Figure 1-13. DOC concentrations estimated using (a) a single wavelength approach using a355 and (b) a two-wavelength approach using a275 and a295. In both cases, all data were log-transformed prior to regression. Figure taken from Asmala et al. (2012)

However, collinearity across a narrow wavelength range calls the appropriateness of this method into question. More complex regressions which avoid this issue are available, but these do not typically produce better results. For example, Downing et al. (2009) applied a least squares regression analysis to wetland DOC concentrations against 17 optical parameters, including absorbance at multiple wavelengths, to produce a more complex model with an R^2 of 0.90. Tipping et al. (2009) took an entirely different approach, splitting DOC into two components: one strongly absorbing (DOC_A) and one weakly absorbing (DOC_B), based upon their DOC specific absorbance at a

given wavelength, otherwise known as their extinction coefficient, E_λ. First, the relative contribution of each component to total DOC was established via Equations 1-13 and 1-14:

$$[DOC] = f_A + f_B = f_A + (1 - f_A) \qquad \textbf{Eqn. 1 - 13}$$

$$f_A = \frac{\left(E_{\lambda 1,B} - R * E_{\lambda 2,B}\right)}{R\left(E_{\lambda 2,A} - E_{\lambda 2,B}\right) - \left(E_{\lambda 1,A} - E_{\lambda 1,B}\right)} \qquad \textbf{Eqn. 1 - 14}$$

where f_A and f_B are the fractions of components A and B which are present in the sample, $E_{\lambda 1,A}$, $E_{\lambda 2,A}$, $E_{\lambda 1,B}$, and $E_{\lambda 2,B}$ are the extinction coefficients of components A and B at wavelengths λ1 and λ2, and R is the ratio of absorbance at λ1 and λ2. Extinction coefficients were obtained via Equation 1-15:

$$E_\lambda = f_A E_{\lambda,A} + f_B E_{\lambda,B} = f_A E_{\lambda,A} + (1 - F_A) E_{\lambda,B} \qquad \textbf{Eqn. 1 - 15}$$

which was parameterised for 23 different E_λ values defined in Thacker et al. (2008), with all other parameters allowed to vary in order to minimize the sum of squares. Derived extinction coefficients for a_{254} and a_{340} were selected. F_A was calculated using Equation 14 and substituted into Equation 15 in order to calculate E_{254} or E_{340}, either of which could be divided by the associated absorbance (a_{254} or a_{340}) in order to calculate DOC. This produced DOC estimates with an R^2 of 0.99 and a root-mean-squared-deviation (RMSD) of 0.7 mg L^{-1}, which was less than half that produced using a single wavelength approach (a_{254}; RMSD = 1.86 mg L^{-1}; R^2 = 0.96).

Tipping's model was based on a limited number of samples (n = 48) from an apparently broad range of environments (streams, rivers, lakes, groundwaters in the UK and North America), but each system drained an unmodified or lightly modified landscape in a temperate setting. When applied to a highly populated industrial catchment, under-prediction of DOC occurred which was attributed to a non-absorbing DOM pool of anthropogenic pollutant origin. Carter et al. (2012) attempted to account for this by adding a small, fixed residual term to the Tipping model (Equation 1-16):

$$[DOC] = f_A + f_B + 0.8\, mg\, L^{-1} \qquad \textbf{Eqn. 1 - 16}$$

Using a much larger dataset of c. 1700 samples from across the UK and North America, this model used a_{270} and a_{340} to produce predictions of DOC with an R^2 = 0.98 and an RMSD = 1.1 mg L^{-1}, which was superior to the equivalent single wavelength models for a_{270} (R^2 = 0.96; RMSD = 1.9 mg L^{-1}) and a_{350} (R^2 = 0.93; RMSD = 2.6 mg L^{-1}). The extinction coefficients derived in Carter et al. (2012) were used as 'global coefficients' and tested against a selection of published single wavelength studies and independent data sets. The uncalibrated global models consistently produced fits which were just as good if not better than calibrated single wavelength models, demonstrating the superiority of the Carter model. Still, the addition of a fixed residual did not and could not account for variable

model fits, and the model still performed poorly in a minority of cases. This included shallow-bottom lakes exhibiting extinction coefficients > half of those reported for lightly-absorbing algal DOM.

1.4.3 Estimating iDOC from cDOM absorbance

Many of the aforementioned studies report instances of DOC under-prediction associated with human activities, for example land-use modification, water course modification, and eutrophication, whilst others find under-prediction in more natural settings, for example in long-residence time lakes. Almost all of these studies acknowledge the probable role of iDOM in this. Still, the broad acceptance of *"…the predominant role of cDOM in DOC"* (Zhang et al., 2021) persists, and only a handful of studies have attempted to quantify or investigate iDOC itself.

Forsberg, (1967) used a standard single wavelength approach (a_{420}) to estimate DOC in a selection of Swedish lakes and then took the y-intercept as an estimate of iDOC, placing it at between 4 – 6 mg L^{-1}. DOC in that study ranged from 5.5 – 14.3 mg L^{-1}, meaning that iDOC was between 40 – 100 % of the total DOC pool. The author suggested that this variation related to in situ processes. However, the use of such a high wavelength may have biased the results: extinction coefficients are often zero above 400 nm in clear waters, where a lower wavelength would have produced a positive absorbance value and therefore, a non-zero cDOC estimate for the same concentration. Asmala et al. (2012) took a very similar approach in studying several Finnish estuaries, using a lower wavelength ($a_{250\text{-}270}$) and dividing the y-intercept by the average DOC concentration to get mean iDOC as a proportion of DOC. Acknowledging that this provided an indication of iDOC contribution rather than a quantitative measure of it, they reported a mean iDOC fraction of 32 % (range = 18 – 59 %), with the highest values recorded in summer and in the most agricultural catchment whilst the lowest values were recorded in autumn and in the most peated catchment.

A quantitative method with which to estimate iDOC came from Pereira et al. (2014) who modified the Carter model to estimate iDOC concentrations from an absorbance-based estimate of cDOC and a laboratory determined quantification of DOC (Equation 1-17).

$$[iDOC] = [DOC] - [cDOC] = [DOC] - (fA + fB) \qquad \boldsymbol{Eqn.\,1-17}$$

From this, they estimated iDOC concentrations in a tropical headwater stream ranging from 4 – 89 %, with the highest contributions occurring during periods of enhanced surface runoff. Stable isotopes indicated that iDOC originated from surface-soil runoff and leaf-litter leachates, and size exclusion chromatography (SEC) revealed that it was predominantly composed of mono- and polysaccharides and amino- and aliphatic acids. Adams et al., (2018) applied the same model

(Equation 17) to a series of eutrophic lakes in the UK and found that iDOC accounted for 0 - 100 % DOC and was likely of algal origin. Algal exudates are typically composed of similar compound classes to those identified by Pereira et al. (2014) (e.g. saccharides and aliphatic acids). Adams et al., (2018) also derived extinction coefficients for algal exudates to parameterise a third cDOM component (f_C). Their reformulation of the model for three components revealed that ~ 80 % of their initial iDOC fraction was not truly colourless, but instead absorbed light very weakly. This demonstrates that iDOC is a subjective classification, with its definition defined by the wavelengths and model structure selected. DOM presents a spectrum of chemical formulae and structures and we conceptualise its behaviour in relative rather than absolute terms. It follows that the subtle increases in molecular complexity which are required to shift DOM from truly colourless to very weakly coloured as per Adams et al., (2018) are unlikely to lead to dramatically different fates. Thus, whilst the addition of a third component was undoubtedly informative, this thesis will consider iDOC as a singular component as per Pereira et al. (2014).

1.5 Aims and objectives

The overarching objective of this thesis was to improve our understanding of the land-ocean DOC flux. Specifically, this thesis aimed to investigate:

1. The effect of land use on the quantity and composition of terrigenous DOC export (Chapter 2 and 4);

2. The behaviour, source, and prevalence of iDOC in multiple settings and at multiple scales (catchment; land-mass; global) (Chapters 3, 4, and 5); and

3. The importance of including iDOC quantification in absorbance-based investigations of DOC (Chapters 4 and 5).

1.6 Thesis summary

This thesis consists of four data papers which focus on terrigenous DOM in tropical (Belize; Chapters 2 and 3) and temperate (Great Britain; Chapters 4 and 5) LOACs, and a short general discussion (Chapter 6).

1.6.1 Chapters 2, 3, and 4 (Belize)

The Belize River Watershed drains a substantial fraction of the Mesoamerican rainforest, a global biodiversity hotspot undergoing rapid rates of degradation, and enters the coastal environment directly adjacent to the Belize Barrier Reef, an integral portion of the world's second largest coral reef system.

Chapter 2 uses absorbance and fluorescence spectrophotometry to investigate the effect of deforestation and agricultural expansion on the quantity and type of cDOM entering the LOAC and, ultimately, reaching the reef. Results indicate that ongoing land-use change in the mid-catchment has increased the amount of terrigenous soil-derived cDOM in the receiving waterbodies, and that this material persists downstream into the coastal environment. Hydrodynamic modelling suggests that this material reaches the reef system, where it may have a deleterious effect on various economically and environmentally valuable habitats. Chapter 2 also identified a substantial decoupling of cDOM absorbance and DOC concentration which was indicative of a large and variable iDOC fraction.

Chapter 3 investigates this decoupling using the Pereira (2014) model described in Section 1.4.3, and find that iDOC accounted for ~ 60 % of the riverine DOC pool. I also investigate the bioavailability of iDOC and cDOC using dark bioassays, and find that biodegradation rates were positively correlated to cDOC concentration rather than iDOC concentration, whilst iDOC concentrations were positively correlated with the refractory (non-bioavailable) DOC fraction. This suggests that it is cDOC rather than iDOC which fuels biodegradation in the Belize River, which is indicative of environmental controls being dominant, rather than molecular ones.

Chapter 4 builds upon Chapters 2 and 3 to propose a new absorbance and fluorescence-based method with which to quantify DOC associated with different cDOC fractions. Whilst this technique requires further laboratory validation, it offers a low-resource method with which to translate the qualitative findings of fluorescence-based DOM characterisation into quantitative estimates of the DOC concentrations associated with different cDOM pools (e.g. humic-like vs. protein-like DOM).

1.6.2 Chapters 5 and 6 (Great Britain)

Chapters 5 and 6 focus on a selection of rivers (Chapter 5) and estuaries (Chapter 6) within Great Britain (GB; Scotland, England, and Wales) which were selected to be representative of land-use, geology, and climate at land-mass scale.

Chapter 5 shows that iDOC accounts for ~ 3 % of the DOC pool in a near-natural catchment (Conwy Catchment, North Wales), ~ 56 % of the DOC pool in a modified catchment (Tamar Catchment, South England), and ~ 22 % of the annual GB DOC flux. Regression modelling revealed that cDOC concentrations and fluxes were driven by landscape drivers including % forest cover, % peat soils, mean altitude, and rainfall, whereas iDOC concentration appeared to be mostly explained by dairy cattle density. These results are placed in context using a compiled 'global' dataset of ~ 3,000 paired absorbance and DOC samples obtained from > 20 studies spanning a range of geo-climatic settings across five continents. On average, iDOC accounted for ~ 26 % of the global DOC pool.

Chapter 6 investigates estuarine DOC transport through the lens of cDOC and iDOC concentrations. Within 12 GB estuaries, cDOC behaviour was almost universally conservative whilst iDOC behaviour was almost universally non-conservative. Thus, estuarine DOC transport is broadly conservative were cDOC is dominant and iDOC contributions are minimal, and non-conservative where iDOC contributions are substantial. Variable non-conservative iDOC behaviour suggests that iDOC from different sources (e.g. primary production; wastewater; agriculture; *in situ* photo- and bio-degradation) may have different labilities.

1.6.3 Chapter 7 (General discussion)

Chapter 7 provides a short synthesis of Chapters 2 – 6 and highlights significant findings, lessons learned, and knowledge gaps. Several research questions are proposed which directly build upon the work presented in this thesis.

Chapter 2 Conversion of forest to agriculture increases coloured dissolved organic matter in a sub-tropical catchment and adjacent coastal environment

S. Felgate led all aspects of this project, including logistics, field work, data analysis, and manuscript preparation. Full detail of author contributions is provided at the end of the chapter.

Stacey L. Felgate[1,2], Christopher D. G. Barry[3], Daniel J. Mayor[2], Richard Sanders[2,4], Abel Carrias[5], Arlene Young[6], Alice Fitch[3], Claudia G. Mayorga-Adame[7], Gilbert Andrews[6], Hannah Brittain[2], Sarah E. Cryer[1], Chris D. Evans[3], Millie Goddard-Dwyer[2], Jason Holt[7], Bethany K. Hughes[8], Dan Lapworth[9], Adam Pinder[3], Dave M. Price[1], Samir Rosado[6], and Claire Evans[2].

[1]Ocean and Earth Sciences, University of Southampton, Southampton, SO14 3ZH, UK.
[2]Ocean Biogeosciences, National Oceanography Centre, Southampton, SO14 3ZH, UK.
[3]UK Centre for Ecology and Hydrology, Bangor, LL57 2UW, UK.
[4]Norwegian Research Centre, Bjerknes Centre for Climate Research, Bergen, 5008, Norway.
[5]Faculty of Science and Technology, University of Belize, Belmopan, Belize.
[6]Coastal Zone Management Authority and Institute, Belize City, Belize.
[7]Marine Systems Modelling, National Oceanography Centre, Liverpool, L3 5DAUK.
[8]Natural Sciences, University of Southampton, Southampton, SO17 1BJ, UK.
[9]British Geological Survey, Wallingford, OX10 8BB, UK.

A version of this chapter has been published in JGR Biogeosciences as:

Felgate, Stacey L., et al. "Conversion of forest to agriculture increases colored dissolved organic matter in a sub-tropical catchment and adjacent coastal environment." Journal of Geophysical Research: Biogeosciences (2021): e2021JG006295. DOI: 10.1029/2021jg006295.

Supplamentary material has been incorporated into the main text.

2.1 Key points

- A shift from broadleaf forest to agri-urban land increased colored dissolved organic matter in the Belize River watershed

- Humic-like material increased in transit downstream and behaved conservatively in coastal waters, indicative of its recalcitrance
- Land-use change has increased terrigenous dissolved organic matter concentrations overlying Belize's coral reefs

2.2 Abstract

Land-ocean dissolved organic matter (DOM) transport is a significant and changing term in global biogeochemical cycles which is increasing as a result of human perturbation, including land-use change. Knowledge of the behaviour and fate of transported DOM is lacking, particularly in the tropics and subtropics where land-use change is occurring rapidly. We used Parallel Factor (PARAFAC) Analysis to investigate how land-use influenced the composition of the DOM pool along a sub-tropical land use gradient (from near-pristine broadleaf forest to agri-urban settings) in Belize, Central America. Three humic-like and two protein-like components were identified, each of which were present across land uses and environments. Land use mapping identified a strong (R^2 = 0.81) negative correlation between broadleaf forest and agri-urban land. All PARAFAC components were positively associated with agri-urban land use classes (cropland, grassland, and/or urban land), indicating that land-use change from forested to agri-urban exerts influence on the composition of the DOM pool. Humic-like DOM exhibited linear accumulation with distance downstream and behaved conservatively in the coastal zone whilst protein-like DOM exhibited non-linear accumulation within the main river and non-conservative mixing in coastal waters, indicative of differences in reactivity. We used a hydrodynamic model to explore the potential of conservative humics to reach the regions environmentally and economically valuable coral reefs. We find that offshore corals experience short exposures (10 ± 11 days yr^{-1}) to large (~ 120 %) terrigenous DOM increases, whilst nearshore corals experience prolonged exposure (113 ± 24 days yr^{-1}) to relatively small (~ 30 %) terrigenous DOM increases.

2.3 Plain language summary

The transport of land-derived dissolved organic matter into the oceans plays a substantial and important role in the global carbon and nutrient cycles. Land-use change can alter the type and amount of material being transported, with widespread implications for downstream ecosystems. This is particularly true in the tropics and subtropics where land-use change is occurring most rapidly, and where research into its effects is often lacking. We investigated whether land-use had an effect of the type and amount of land-derived material found in a sub-tropical river system which

is experiencing rapid conversion from forest to agricultural land-use and found that streams draining agricultural land contained more land-derived material than those draining forests, and a substantial fraction of this material reached the coastal environment. We estimated the frequency with which this land-derived material reached local environmentally and economically valuable coral reefs, and suggest that land-use derived material reaches nearshore corals often and offshore corals rarely.

2.4 Introduction

The land-ocean aquatic continuum is a complex network of environments which include streams, lakes, reservoirs, wetlands, estuaries, and coastal seas. The lateral transport of terrigenous dissolved organic matter (DOM) through this continuum is a significant and changing biogeochemical term with widespread implications for global carbon and nutrient cycling (Drake et al., 2018). Anthropogenic perturbations including climate change and land-use change are major contributors to altered terrigenous DOM transport, and are estimated to have doubled the amount of land-derived carbon entering the continuum since the start of the industrial revolution, increasing it by ~ 1 Pg (Regnier et al., 2013). Despite this scale of change, we know relatively little about what happens to terrigenous DOM in transit, how much of it reaches the open ocean, or what effects it has therein. This lack of understanding hinders our ability to quantify the role of aquatic DOM in global biogeochemical cycles, including the potential contribution of land-use change derived DOM to anthropogenic CO_2 emissions.

Studies of terrigenous DOM in tropical and sub-tropical catchments are sparse, yet climate change effects are disproportionately high in these regions and they are commonly subject to high rates of land-use change resulting from ongoing development. Between 1980 and 2000, ~ 80 % of new agricultural land originated from the world's tropical and subtropical forests (Gibbs et al., 2010), and the expansion of cropland and pasture continues to be the principal driver of deforestation in the developing world (Houghton, 2007; Song et al., 2018). Agricultural expansion has been associated with declines in water quality, including those related to shifts in the composition of the DOM pool such as reduced water clarity, eutrophication, and deoxygenation (Mello et al., 2018; Singh et al., 2017; Yang et al., 2012). Shifts in DOM composition are commonly investigated using optical tools (absorbance and fluorescence spectrophotometry; Murphy et al., 2010; Stedmon et al., 2003) which target the chromophoric or 'colored' fraction (cDOM). cDOM can also provide a qualitative measure of DOM quantity, with absorbance typically correlating strongly with DOC concentration in terrestrially influenced systems (e.g. Carter et al., 2012). Much of the cDOM pool is also fluorescent

(fDOM), and methods by which fluorescent properties can be used to investigate cDOM character have been well established (Murphy et al., 2010; Stedmon et al., 2003).

Forests typically accrue relatively aromatic, recalcitrant soil organic matter (SOM) in their surface soils (Inamdar et al., 2012) which is highly colored. Deforestation results in reduced soil stability, leading to increased export of this material which peaks post-felling and reduces gradually over time (West et al., 2004). Conversion of deforested land to agriculture can further enhance SOM export as a result of physical disturbance (tillage), hydrological modification (irrigation), and over grazing (Condron et al., 2014; Graeber et al., 2015; Klumpp et al., 2009). As a result, agricultural soils are up to 60 times as erosive as forest soils (Renard et al., 2017). Recent work suggests that older, less aromatic, less highly colored DOM may be released as deeper soil horizons become destabilized. This material is more bio-labile and thus, undergoes more rapid remineralization than surface SOM (Drake et al., 2019). At the same time, overuse of fertilizers can increase the export of aliphatic and low-aromacity, low-colored DOM forms that are also bio-labile (Gücker et al., 2016) whilst anthropogenic DOM of a similar character has been shown to increase in urban settings (Arango et al., 2017; Smith and Kaushal, 2015). This is particularly relevant in areas where sanitation is poor (e.g. Mostofa et al., 2010). Thus, land-use can be the primary explanator of variance in the DOM pool where anthropogenic influence is high (Roebuck et al., 2019), and land-use change from forested to agri-urban can have profound implications for the quantity and composition of DOM entering the land ocean aquatic continuum. Our understanding of forest SOM cycling is dominated by temperate studies (Kalbitz et al., 2000), but previous research has shown that tropical and sub-tropical forest soils may exhibit higher turnover rates and contain lower SOM stocks than temperate forest soils do (Trumbore, 1993) and that they may also contain a substantial pool of less recalcitrant DOM which undergoes relatively rapid remineralization once mobilized (Gmach et al., 2020).

Once in the land-ocean continuum, terrigenous DOM undergoes a range of bio- and photo-mediated transformations, driven by a range of biotic and abiotic processes which vary by geographical and climatic setting, water residence time, environmental conditions and the molecular properties of the DOM (Anderson et al., 2019; Kothawala et al., 2020). Catchment land-use can modify these transformations by altering the environmental conditions, water residence time and/or DOM composition. For example, inorganic nutrient export from agri-urban settings can promote the in-situ growth of microorganisms, resulting in an increase in the amount of autochthonous DOM present (e.g. algal exudates and protein-like material; Evans et al., 2017; Williams et al., 2016) and have been linked with increased DOM diversity (Kamjunke et al., 2019). Altered hydrological conditions and increased residence times associated with watercourse modification (e.g.

hydroelectric dams and reservoirs) can enhance autochthonous production and the opportunities for bio- and photo-degradation (Mayorga et al., 2010; Winemiller et al., 2016). The net effect of such transformations across the continuum determines the quantity and composition of DOM exported to the ocean.

Land-ocean DOM fluxes constitute organic carbon subsidies and inputs of bioavailable dissolved organic nutrients into the coastal ocean which influence, for example, microbial community composition and net ecosystem metabolism, carbonate equilibria, and gaseous carbon fluxes, with implications for water quality, productivity, biodiversity, and the global carbon cycle (Lønborg et al., 2020; St. Pierre et al., 2020). While the economic impacts of nutrient and sediment fluxes on coastal ecosystems are well recognized (Fichot and Benner, 2014; Molotoks et al., 2018), increased DOM inputs can also negatively impact ecosystem health and the marine economy, notably through impacts on coral reefs (Butler et al., 2013; Devlin and Schaffelke, 2012; Sharp et al., 2014). This link between land and sea means that the effective co-management of terrestrial and marine ecosystems and the economies which rely upon them requires an understanding of terrigenous DOM transport and transformation within the aquatic continuum.

In this study we investigate the character and behaviour of terrigenous DOM in a subtropical watershed which has been subject to significant deforestation and agricultural expansion, and which drains into an economically and environmentally valuable coastal zone, focusing on the colored and fluorescent fraction Belize is the most forested country in Central America, but recent estimates place mature forest cover at just 59 % compared to 76 % in 1980, a 25 % loss over 40 years (Cherrington et al., 2010; Voight et al., 2019). Agriculture supports ~ 9 % of Belize's gross domestic product (GDP), and is expanding (Prouty et al., 2008; Statistical Institute of Belize, 2019). Belize is also home to the Belize Barrier Reef which is a global biodiversity hotspot (Young, 2008) and supports ~ 30 % of the country's GDP via tourism and fisheries related activities (Prouty et al., 2008; Statistical Institute of Belize, 2019).

We studied cDOM character in Belize's largest catchment, the Belize River Watershed. We investigated (1) the influence of land-use change on cDOM character using a forested to agri-urban land-use gradient, and (2) the behaviour of land-use change mediated DOM as it moves from land to sea. Finally, we employed a hydrodynamic model to investigate connectivity between terrigenous cDOM and the environmentally and economically important coral reefs of the Belize Barrier Reef. We hypothesized that (1) sub-catchments draining agri-urban land will contain more cDOM than sub-catchments draining forested land; (2) humic-like cDOM will be transported downstream and

into the coastal environment, whilst protein-like cDOM will be rapidly remineralized; and (3) humic-like cDOM will persist within the Belize River plume, and reach the Belize Barrier Reef.

2.5 Methods

2.5.1 Regional setting

The Belize River watershed covers an area of 8542 km^2. Air temperatures range from 25 to 38°C in the wet season (c. May – November), and 16 to 28°C in the dry season (c. December – April). Annual precipitation ranges from ~ 2500 mm in upland regions to ~ 1600 mm in lowland regions, ~ 80 % of which occurs during the wet season, between October and April. Annual actual evapotranspiration is 56 – 75 % precipitation, such that annual runoff in sub-catchments ranges from 400 to 1100 mm. The Maya Mountains (Figure 2-1) comprise Palaeozoic metamorphic and volcanic rocks with granitic intrusions; soils are siliceous, acid, and highly erodible. Surrounding these to the north and west are karstic hill systems where Cretaceous limestones and dolomites underlie calcareous soils with better agricultural stability. Coastal plains account for ~ 50 km of the downstream length of the Belize River and are comprised of Pleistocene alluvium deposits. Agriculture is predominantly banana, sugar, and citrus crops, with grazing livestock (Statistical Institute of Belize, 2019; Young, 2008). More detailed descriptions of Belize's physiogeography, soils, geology, land suitability for agriculture and hydrological characteristics are provided elsewhere (Baillie et al., 1993; Esselman and Boles, 2001; Hartshorn et al., 1984; Heyman and Kjerfve, 1999; King et al., 1993).

The Belize River has two principal sub-catchments: the Macal River (1466 km^2) and the Mopan River (3690 km^2) (Figure 2-1). Both drain from relatively pristine forested landscapes above 400m elevation within the Maya Mountains, but much of the Mopan catchment lies within the Western Uplands region of Guatemala which has been subject to severe deforestation (Karper and Boles, 2004). The main river stem of the Mopan flows ~ 50 km northeast through agricultural land at ~ 150 m elevation, before re-entering Belize at the border near Benque. The Macal drains north and passes through a series of three hydroelectric dams (henceforth termed 'the dam complex'), which are also intended to serve flood control purposes: the Chalillo (capacity = 120 million m^3; build completed 2005, ~ 380 m elevation), Mollejon (1.7 million m^3, completed 1995, ~ 280 m elevation), and Vaca (0.12 million m^3, completed 2010, ~ 130 m elevation) dams. Physicochemical and ecological impacts of these dams are described elsewhere (Lanza, 2019). The Mopan and Macal merge ~ 33 km downstream of the border to form the Belize River at an elevation of 60 m. The Belize River then continues ~ 120 km north-east, gradually declining in elevation towards the coast at Belize City. It is

flanked by mandated riparian forest strips and flows through a predominantly agricultural setting, with inputs from agricultural dominated catchments to the north, and less modified, primarily forested sub-catchments to the south. The coastal environment to which the Belize River discharges supports a considerable tourism sector, diverse fisheries, and mangrove cayes (Young, 2008). Notably, the Belize Barrier Reef, a substantial part of the world's second largest barrier reef system (the Mesoamerican Barrier Reef), lies ~ 20 km offshore, with some nearshore coral formations as close as ~5 km offshore. Studies have found elevated levels of trace metals, which are indicators of landscape derived sediments, in nearby corals influenced by neighbouring catchments which have been subject to significant soil erosion due to forest clearance combined with high slope and runoff (Heyman and Kjerfve, 1999; Prouty et al., 2008).

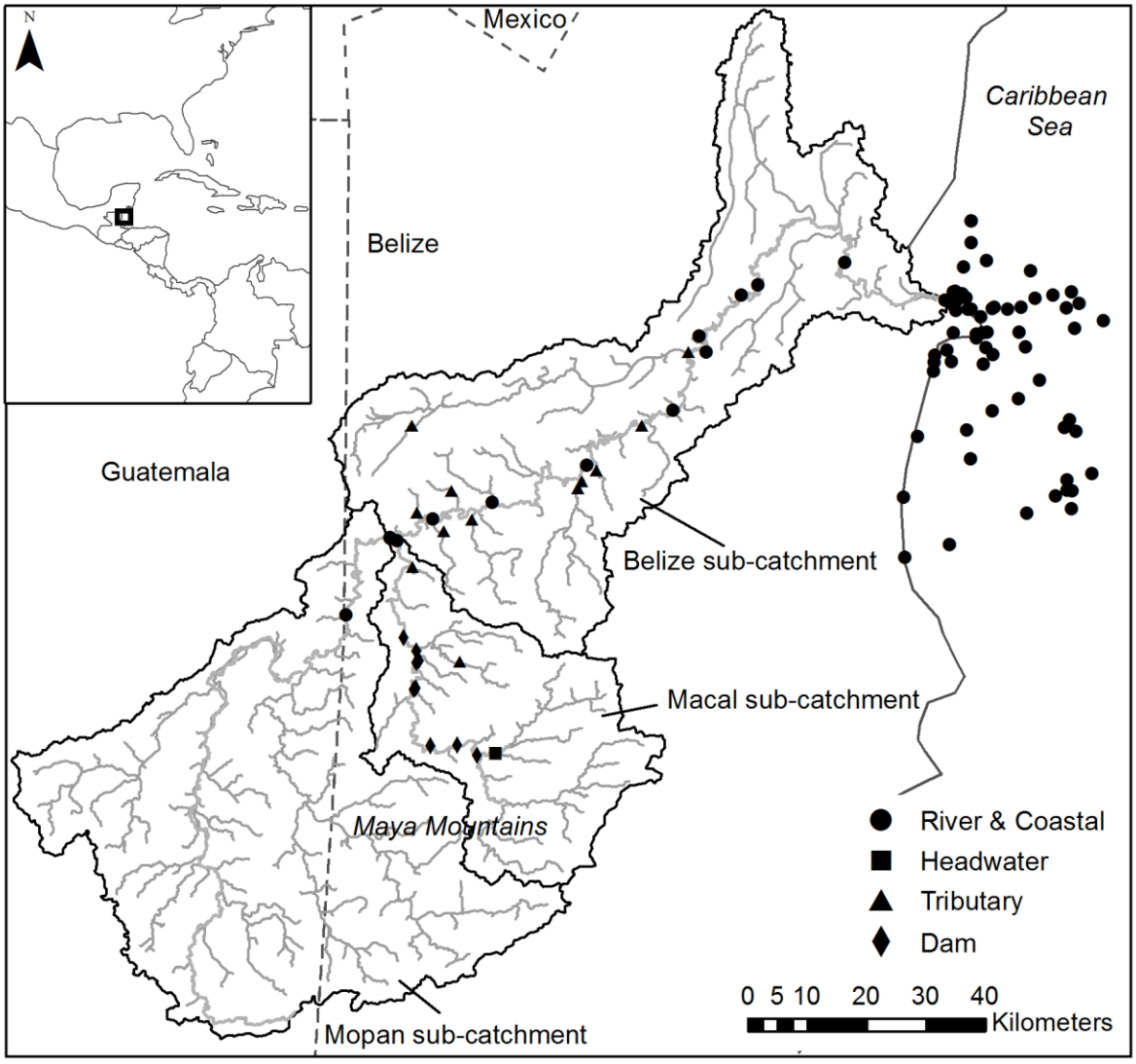

Figure 2-1. Map of the Belize River watershed, with sampling locations shown. The Mopan and Macal sub-catchments are also shown.

2.5.2 Land-use mapping

Land-use within the Belize River watershed was derived from random forest classification in R (R Core Team, 2019a) on composited Sentinel-1 and Sentinel-2 level 2A images captured between November 2018 and February 2019 along with a digital elevation model (DEM) (Lehner et al., 2008). Model validation data were collected in February 2019 using catchment-wide in-person surveys, guided by an existing, coarser resolution country level land cover map (Meerman, 2015). Sub-watersheds were generated for each sampling location using a DEM and the ArcHydro toolbox. Classification errors were < 1% (Table 2-1). Land-use classes were extracted for each sub-watershed as a percentage using zonal statistics. (Table 2-2).

Table 2-1. Confusion matrix, showing actual vs. predicted classifications for each LULC class, along with the associated % classification error. Classification errors were all < 1%. The largest misclassification occurred between lowland and Submontaine broadleaf, highlighted in <u>bold</u>.

		Predicted												
		Broadleaf Savannah	Submontaine Broadleaf	Urban	Water	Wetland	Cropland	Lowland Broadleaf	Mangrove	Grassland	Pine Savannah	Plantation	Shrub	**% Classification Error**
Actual	Broadleaf Savannah	318	7	3	2	23	11	13	4	2	49	13	7	**0.364**
	Submontaine Broadleaf	2	392	0	0	2	4	**<u>91</u>**	3	0	1	5	0	**0.216**
	Urban	1	0	432	0	0	36	0	0	7	3	6	0	**0.136**
	Water	0	0	0	489	10	0	0	0	1	0	0	0	**0.022**
	Wetland	40	3	0	3	417	1	3	2	17	7	4	1	**0.166**
	Cropland	14	1	20	0	0	380	1	2	17	8	26	9	**0.24**
	Lowland Broadleaf	3	**<u>103</u>**	0	0	0	8	353	7	1	3	6	16	**0.294**
	Mangrove	2	0	0	2	5	4	4	477	0	1	1	4	**0.046**
	Grassland	0	5	2	0	0	11	5	0	442	4	23	7	**0.116**
	Pine Savannah	43	29	5	0	4	27	11	1	5	306	29	4	**0.388**
	Plantation	3	0	3	0	1	28	9	1	48	11	393	3	**0.214**
	Shrub	2	0	0	0	2	3	8	35	2	0	6	442	**0.116**

Table 2-2 (next page). Land use data as a percentage cover for each sub-catchment, and for the

catchment as a whole (simulated point BR_DD). The difference between land-use for the whole catchment vs. the tributaries data set is given, demonstrating that this dataset is representative of the wider Belize River Watershed.

	% Broadleaf Savannah	% Submontaine Broadleaf	% Urban	% Water	% Wetland	% Cropland	% Lowland Broadleaf	% Mangrove	% Grassland	% Pine Savannah	% Plantation	% Shrub
	Tributaries											
BC1	1.88	1.03	1.30	0.02	0.57	3.89	55.74	0.00	7.82	11.47	12.04	4.24
CD1	1.79	50.97	0.84	0.52	1.09	2.69	25.65	0.00	1.21	7.13	5.71	2.40
CR1	1.46	0.00	0.74	0.00	0.16	3.95	62.20	0.00	6.35	8.47	12.67	4.01
GV1	1.88	0.01	0.90	0.01	0.42	3.80	63.46	0.00	5.50	11.90	9.09	3.04
KW1	2.20	0.00	8.90	0.00	0.15	9.81	43.73	0.00	4.22	4.71	19.69	6.60
LC1	4.61	0.00	4.22	0.26	0.68	18.18	38.65	0.00	7.06	5.53	13.25	7.55
MC1_BR	3.24	32.50	1.49	0.51	1.05	3.63	31.13	0.00	2.49	14.29	7.16	2.51
MC2_BR	3.24	32.46	1.50	0.51	1.05	3.66	31.10	0.00	2.51	14.28	7.18	2.52
MP1_BR	1.54	19.82	3.10	0.02	0.28	9.24	24.04	0.00	18.15	9.43	12.03	2.35
MP2_BR	1.50	18.87	3.15	0.03	0.28	9.07	24.86	0.00	18.29	9.19	12.29	2.47
MT1	7.50	0.00	1.54	0.02	2.36	11.18	34.33	0.00	2.71	4.63	24.36	11.38
MtP1	1.48	0.00	0.35	0.00	0.08	4.09	65.07	0.00	2.39	2.86	15.01	8.66
MtP2	1.86	0.00	7.96	0.00	0.14	7.34	51.54	0.00	3.35	4.04	16.80	6.97
RC1	4.86	5.71	1.71	0.05	1.84	7.13	49.21	0.00	3.64	8.85	11.61	5.38
RC2	7.58	10.03	0.75	0.12	2.58	3.82	43.78	0.00	1.58	16.82	8.11	4.84
RN1	9.24	6.32	2.84	0.00	1.28	7.60	3.76	0.00	3.61	50.33	13.28	1.75
SP1	1.19	0.00	11.65	0.21	0.17	13.24	3.42	0.00	51.42	3.32	12.59	2.78
SP2	2.40	0.00	3.65	0.00	0.07	12.63	18.05	0.00	35.19	5.87	15.73	6.42
SP3	1.01	0.00	0.32	0.01	0.05	4.13	43.14	0.00	10.68	4.95	15.98	19.72
SP4	1.57	0.00	3.17	0.28	0.22	9.76	44.75	0.00	21.72	3.85	11.14	3.53
Averages	**3.10**	**8.89**	**3.00**	**0.13**	**0.73**	**7.44**	**37.88**	**0.00**	**10.49**	**10.10**	**12.79**	**5.46**
	Whole Catchment											
BR_DD	5.39	13.95	2.72	0.51	1.55	8.77	31.71	0.10	10.71	9.46	11.26	3.86
Difference	**2.29**	**5.06**	**-0.28**	**0.38**	**0.82**	**1.33**	**-6.17**	**0.10**	**0.22**	**-0.64**	**-1.53**	**-1.60**
	Main River											
BR_BR1	1.98	22.30	2.71	0.17	0.49	7.60	26.60	0.00	14.08	10.54	10.98	2.55
BR_BR2	1.97	21.10	2.72	0.17	0.50	7.65	27.56	0.00	14.15	10.50	11.06	2.63
BR_BR3	2.11	19.32	2.79	0.16	0.55	7.94	28.97	0.00	13.61	10.15	11.48	2.92
BR_BR4	2.12	18.93	2.87	0.16	0.55	8.40	28.98	0.00	13.42	10.02	11.57	2.99
BR_BR5	2.20	18.41	2.87	0.16	0.56	8.78	29.23	0.00	13.13	9.88	11.73	3.07
BR_BR6	2.24	18.13	2.84	0.16	0.56	8.75	29.88	0.00	12.94	9.77	11.64	3.11
BR_BR8	2.45	16.51	2.96	0.17	0.57	9.58	30.68	0.00	12.41	9.39	11.78	3.52
BR_BR9	2.44	16.47	2.95	0.17	0.57	9.56	30.76	0.00	12.38	9.37	11.76	3.56

BR_BR10	2.55	16.32	2.94	0.17	0.60	9.52	30.81	0.00	12.31	9.38	11.77	3.62
BR_BR11	2.55	16.29	2.93	0.17	0.61	9.51	30.85	0.00	12.31	9.37	11.77	3.64
BR_BR12	4.86	14.27	2.65	0.50	1.37	8.77	31.99	0.00	10.94	9.44	11.38	3.83
Averages	**2.50**	**18.00**	**2.84**	**0.20**	**0.63**	**8.73**	**29.66**	**0.00**	**12.88**	**9.80**	**11.54**	**3.22**

Eleven distinct classes were identified: submontaine broadleaf forest, lowland broadleaf forest, plantation, urban, grassland, cropland, wetland, inland waters, pine savanna, broadleaf savanna, and shrub. Land-use varied significantly (ANOVA; $p = < 0.05$) between tributary sampling locations, and a strong negative correlation ($R^2 = 0.81$) was observed between % broadleaf forest (lowland and submontaine) and % agri-urban (cropland, grassland, plantation, and urban) land-use (Figure 2-2). Land-use did not vary significantly along the length of the main river (ANOVA; $p > 0.42$; Figure 2-3), and so was excluded as an explanatory variable within the main river dataset. A land cover map of the watershed is given in Figure 2-4.

2.5.3 Water sample collection

Water samples were collected during 3 visits between October 2018 and October 2019 at locations shown in Figure 2-1 (split by sampling visit in Figure 2-5). The dam complex (October, 2019) and tributaries (November 2018, January, 2019, and October, 2019) were sampled from the riverbank using a plastic bucket. A rigid inflatable boat was used to conduct a sampling transect of the main river trunk (November 2018), and a small research vessel was used in coastal waters (November 2018, October 2019). Specific conductance, salinity, pH, and water temperature were recorded at each sampling location using a Hach-Lange® handheld Multimeter probe (Hach, USA). Sampling of the main river trunk operated as a single transect from the Belize-Guatemala western border to the limit of the freshwater extent, near Belize City, and water was collected at intervals selected to approximately equidistant whilst avoiding sampling directly from incoming tributaries. Coastal sampling was conducted as three distinct transects adjacent to the Belize River outflow, covering the inshore region, the mid-section, and the adjacent portion of the Belize Barrier Reef, with samples taken across the full range of observed salinities (0 – 38 ppt). The boat was allowed to deviate from the planned transect lines to locate and sample the freshwater plume, which was identified according to salinity.

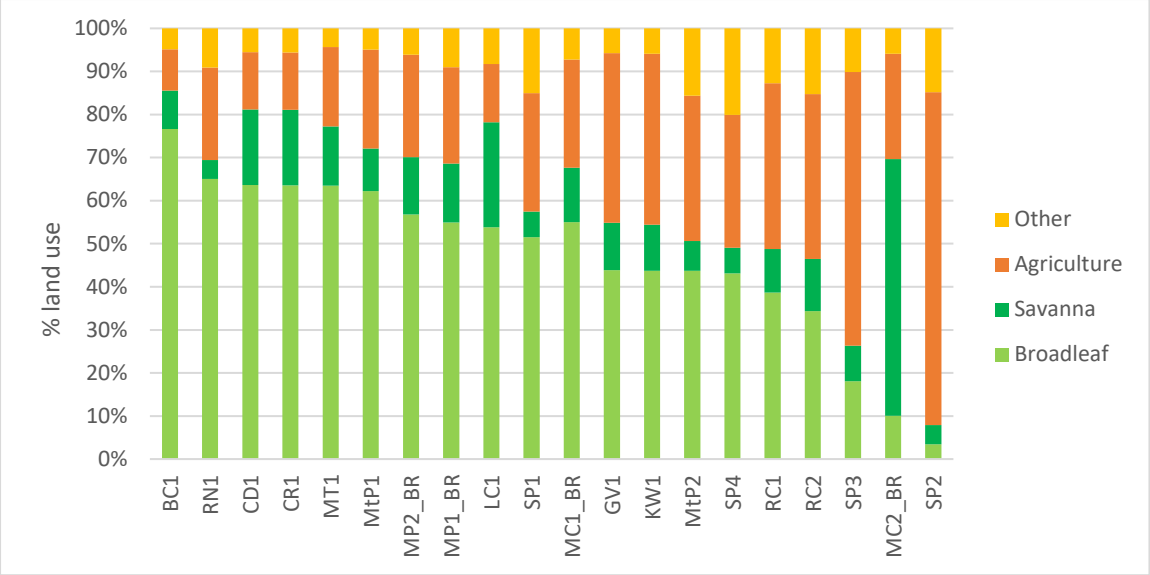

Figure 2-2. Land use data for the tributaries sampling points, presented as a bar chart. Categories have been simplified for plotting: Broadleaf = submontaine and lowland broadleaf; Savanna = pine and broadleaf savanna; Agriculture = cropland, grassland, plantation, and urban; other = wetland, inland water, and shrub. A land-use gradient from broadleaf dominated to agri-dominated exists.

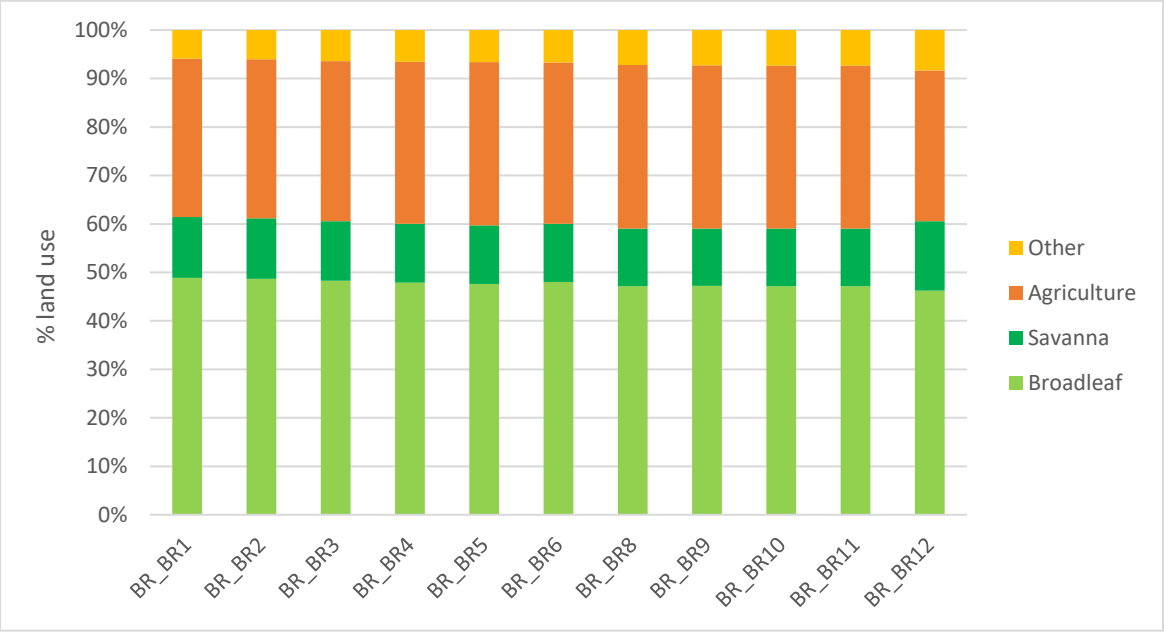

Figure 2-3. Land use data for the main river sampling points. Category groupings are as Figure 2-2. A high degree of similarity in land use was observed along the river transect, from BR_BR1 at the Guatemala-Belize border to BR_BR12 close to the freshwater limit of the Belize River.

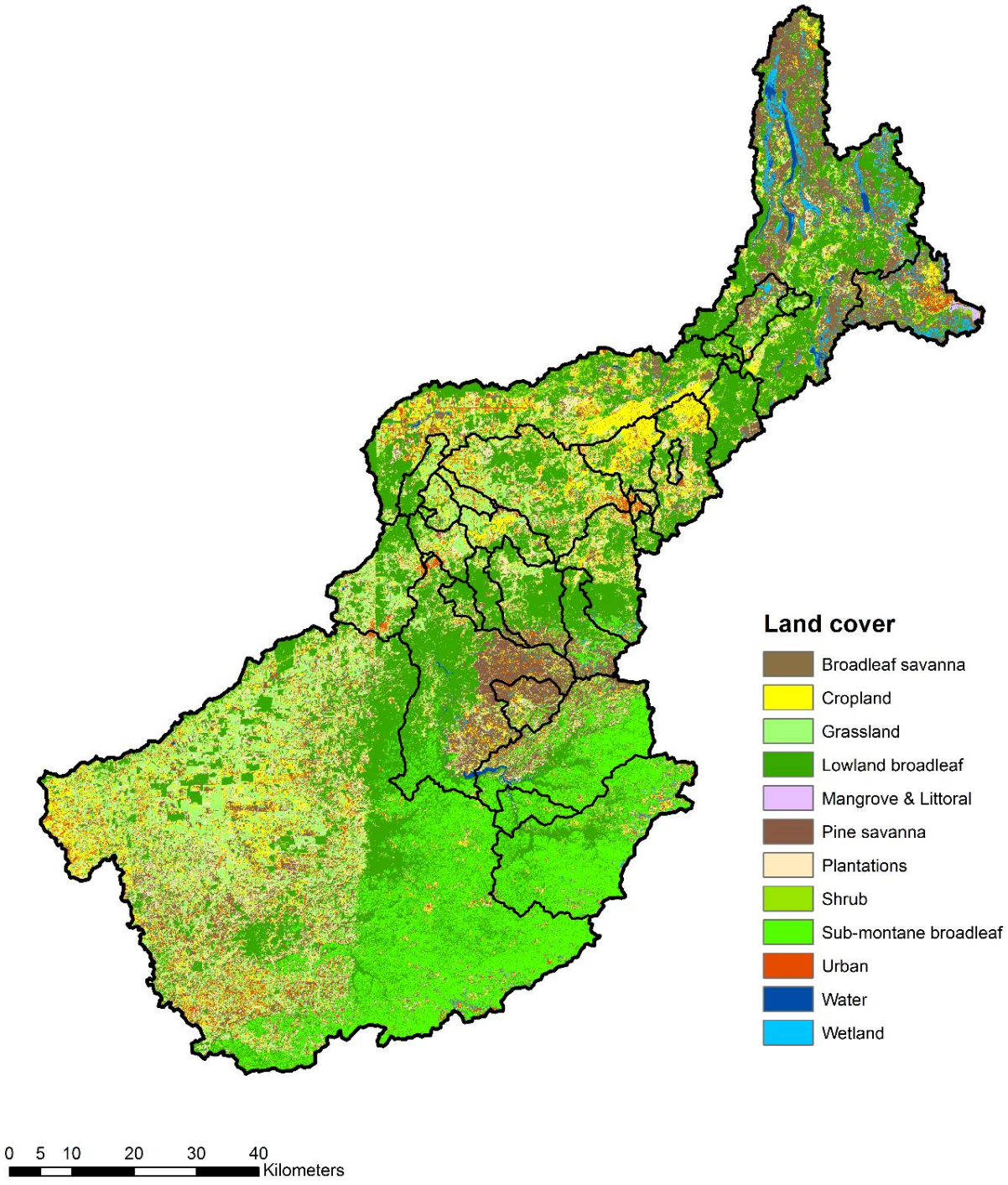

Figure 2-4. Land cover map for the Belize River watershed, with sub-catchments delineated.

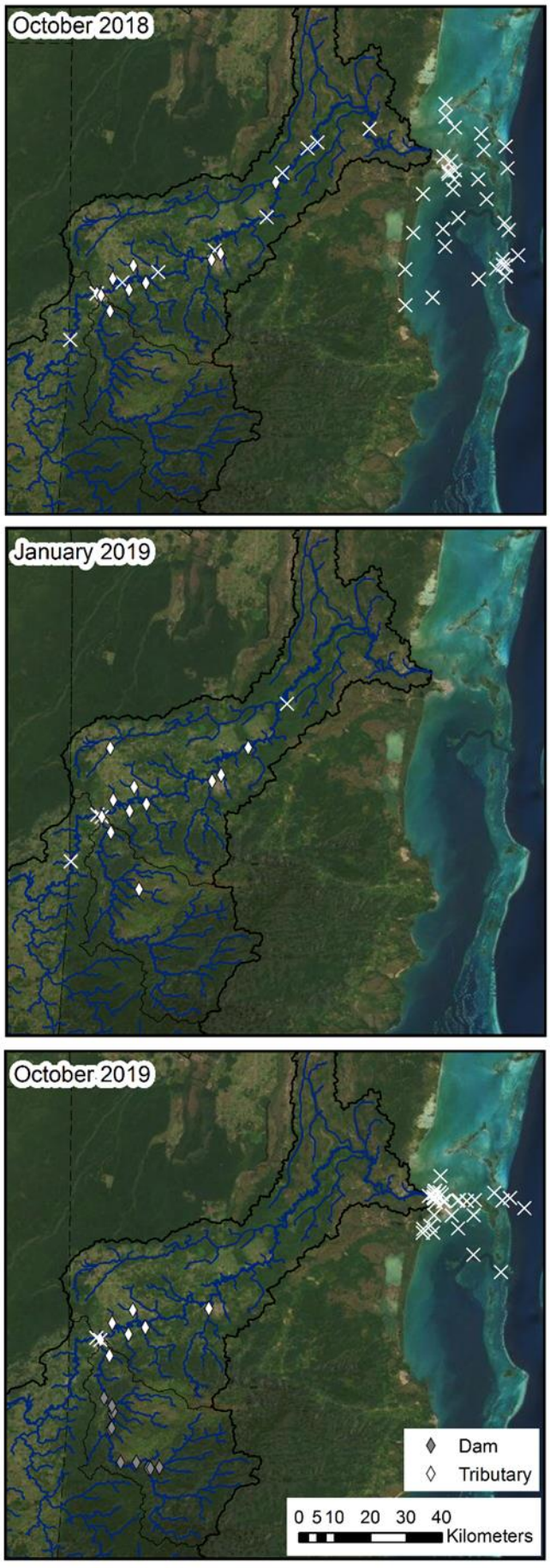

Figure 2-5. Map of the Belize River Watershed showing sampling points associated with each sampling trip: November 2018 (top), January 2019 (middle), and October 2019 (bottom). Main river and coastal samples are shown as crosses, with tributaries shown as white diamonds and dams shown as grey diamonds. Background map source: Source: Esri, DigitalGlobe, GeoEye, Earthstar Geographics, CNES/Airbus DS, USDA, USGS, AeroGRID, IGN, and the GIS User Community

Samples for determination of DOC concentration were filtered (0.45 µm Fischer® cellulose acetate) into Nalgene® HDPE bottles and stored cool and dark until their return to the laboratory. Freshwater DOC samples were then stored at 4°C. Saline DOC samples were frozen prior to analysis in 2018 and chilled in 2019. A comparison of absorbance spectra (Section 2.5.4) produced by samples subject to each treatment indicated no statistically significant differences (ANOVA; p value > 0.05) and so the DOC data are considered comparable. Samples for optical measurement were filtered (0.45 µm Fischer® cellulose acetate) into Wheaton® amber borosilicate glass vials bottles and stored cool and dark until their return to the laboratory, then at 4°C in the dark. All sample bottles were acid washed (24hrs in 10 % v/v Hydrochloric Acid) and Milli-Q® rinsed prior to use, and were triple rinsed with sample filtrate before use. Cellulose acetate filters were flushed with 100ml sample water prior to use.

2.5.4 Laboratory analysis

All laboratory analyses were conducted in the UK. DOC was determined by Pt-catalysed combustion against glycine and potassium hydrogen phthalate standards and pure water blanks using a TOC-VCPN analyser (Shimazdu, Japan). Standards and blanks were run every 10 samples. Reproducibility of standards was within 2 % in the range 0 – 50 ppm. Absorbance spectra (200-800 nm) were determined at 1nm intervals using a Cary 60 UV-Vis dual beam spectrophotometer (Agilent, USA) against ultrapure water (Milli-Q®). Absorbance at 254nm (a254) is presented as a measure of cDOM. Fluorescence was measured using a Cary Eclipse scanning fluorescence spectrophotometer (Agilent, USA), corrected for instrument specific biases following manufacturer protocols, for excitation (Ex) wavelengths of 255 – 400 nm (5nm intervals) and emission (Em) wavelengths of 280 – 500 nm (2nm intervals). Ex and Em slit widths of 5nm were employed, with a PMT voltage of 725 v and scan rate of 9600 nm/minute. Blanks were obtained using both ultrapure water in analytical cuvettes, and a sealed pure water standard (Starna® USA), and comparison of these were not statistically different. No samples were sufficiently optically dense to require dilution to enable robust inner-filter corrections (Kothawala et al., 2013).

2.5.5 PARAFAC modelling

Excitation-Emission Matrices produced via fluorescence spectrophotometry were modelled via parallel factor (PARAFAC) analysis, which is a tool commonly used to decompose the cDOM pool according to its fluorescent properties (Stedmon et al., 2003a). Fluorescence data were modelled by in R using the StaRdom package (version 1.1.14, Pucher et al., 2019; R Core Team, 2019). Non-negativity constraints were applied to normalized data, following standard pre-processing protocols

for which blanks specific to each analytical run were used for correction and normalization of Raman peaks (Murphy et al., 2010). Excitation wavelengths < 255 nm were discarded due to increased noise at those wavelengths. Identification of PARAFAC components was undertaken using the OpenFluor database of published fluorescence spectra (www.openfluor.org; accessed 06/07/2020), using a 95% similarity criterion (Murphy et al., 2014). Sample fluorescence was calculated as the sum of peak fluorescence values (F_{max}) associated with each PARAFAC component.

2.5.6 Theoretical mixing lines

Theoretical conservative mixing lines for component fluorescence and DOC were plotted according to a standard two-endmember mixing model (Equation 2-1) where F_{SW} is the theoretical fraction saline water in the sample, X_{SW} is the endmember concentration for saline water, F_{FW} is the theoretical fraction fresh water in the sample, and X_{FW} is the endmember concentration for fresh water. Conservative mixing indicates that any reduction in fluorescence or concentration within the coastal zone is the result of dilution (i.e. no net addition or removal of fluorescent DOM or bulk DOC). Divergence from the associated theoretical mixing line therefore indicates net addition (data points above the line) or removal (data points below the line) in transit. Endmember salinities were 0 and 36.1 ppt in 2018, and 3.3 and 37.8 ppt in 2019, with the model extrapolated from 0 – 38 ppt as required.

$$Modelled\ Value = (F_{FW}\ x\ X_{FW}) + (F_{SW}\ x\ X_{SW}) \qquad \boldsymbol{Eqn.2-1}$$

2.5.7 Hydrodynamic model

A coastal hydrodynamic model of 1/60° horizontal resolution was used to investigate the potential for the Belize River plume to influence the local region of the BBRRS, using salinity as a tracer (Figure 2-6). For this we used the NEMO (Nucleus of a European Model for the Ocean; https://www.nemo-ocean.eu/), largely following the shelf-sea configuration setup for high resolution operational forecasting in the NW European continental shelf (Graham et al., 2018; Guihou et al., 2018). NEMO integrates the three dimensional equations of motion on a regular horizontal grid (here approximately 1.0km). The domain spans the length of the eastern coast of the Yucatan peninsula (Figure 2-6). There are 31 terrain following coordinates in the vertical, giving the same number of levels at each horizontal cell, except where the coordinate surfaces are too steep, in which case levels 'beach' into the seabed using the envelope bathymetry approach, which alleviates the need for bathymetry smooth while still constraining the horizontal pressure gradient error. NEMO solves for 3D currents, temperature, salinity and turbulent properties with a 60s time step (internal mode).

Output is saved daily for 3D variables and hourly for surface and depth mean currents, and sea surface elevation. The model uses a pre-release version of NEMO V4, following setup approach used in the NEMO Regional Caribbean Model (https://zenodo.org/record/3228088#.YB0VcXmnxhE).

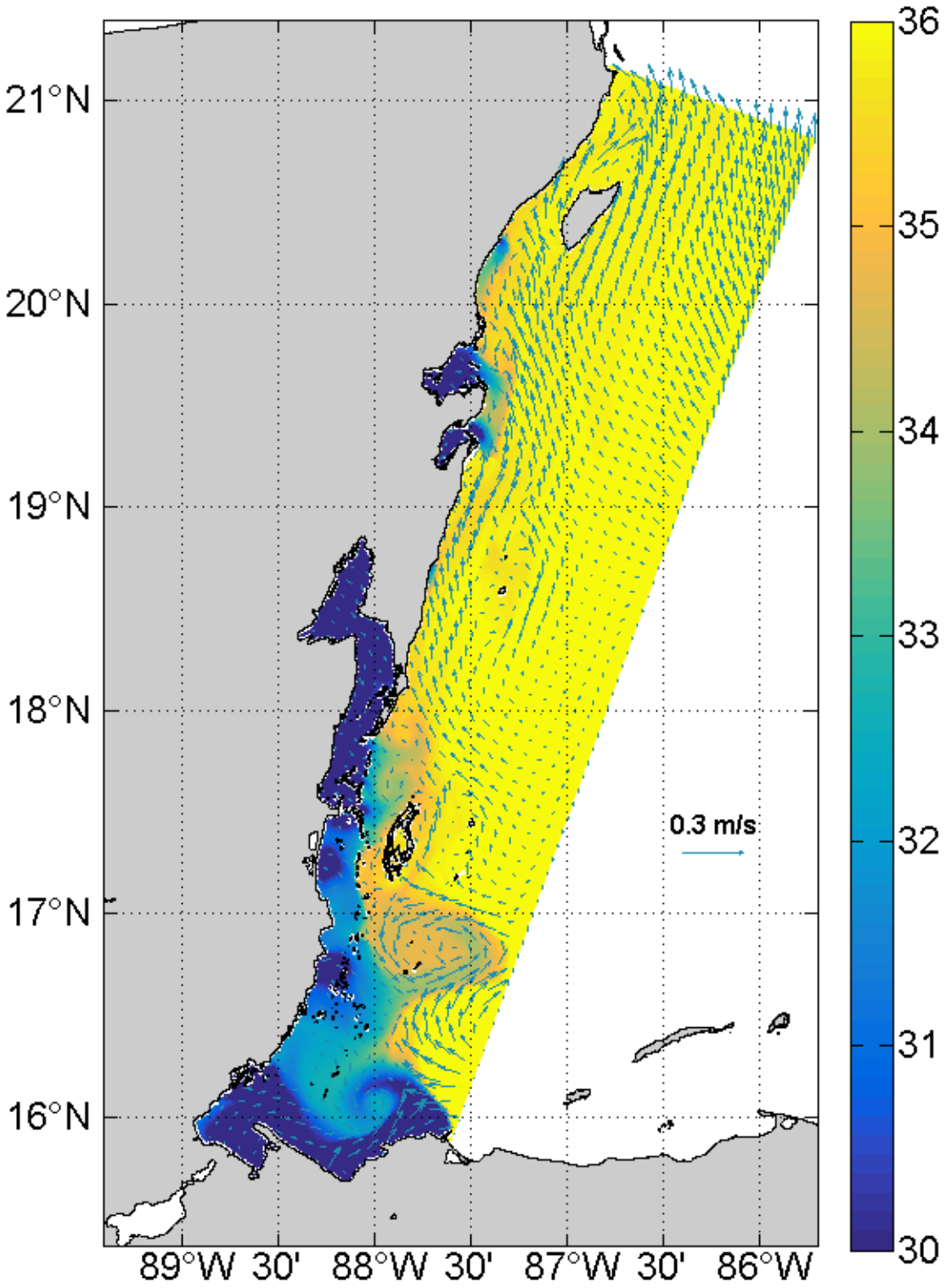

Figure 2-6. Hydrodynamic model domain and example current and salinity fields (1st October, 2015). Current vectors every 8th grid cell are shown.

The model was run for a 21-year period (1995 – 2015) and forced by atmospheric fields from the ERA5 reanalysis (European Centre for Medium-Range Weather Forecasts, 2019), hydrography, residual currents, and elevation from a 1/12° (~9km) global NEMO model, and tides from FES2014 (Lyard et al., 2020). River freshwater inflows from the four major rivers in the region (Hondo, Belize, Motaqua, and Ulua) were taken from GlobalNEWS2 (Mayorga et al., 2010), and modulated by the mean annual flow cycle from the Belize River 'DoublerunQ' flow gauge (data provided by Department of Natural Resources, Belize).

The Belize Barrier Reef was mapped into georeferenced coral reef polygons obtained from the Global Distribution of Coral Reefs dataset (UNEP-WCMC, 2018). Salinity thresholds were selected based on a combination of previous studies (Purdy et al., 1975; Sweetman et al., 2019), field data, and local knowledge of minimum salinity conditions overlying nearshore (~20 ppt) and offshore (~ 30 ppt) corals. The number of days when salinity went below these thresholds was counted for each reef polygon, and these data were converted to monthly averages across the 21-year model run.

2.5.8 Statistics

All statistics were done in R (R Core Team, 2019a) and all analyses used an alpha of 0.05. Assumptions of normality and heteroscedacity were met. Analysis of Variance (ANOVA) was used to identify differences between sampling trips and environments. No significant difference ($p > 0.05$) was observed between sampling year within the tributaries, and so those data were grouped for analysis. Cooks distance was used where appropriate to identify and examine outliers. Relationships between land-use, DOC, and component fluorescence intensities within the tributaries were investigated using stepwise multiple linear regression analysis, with the final model selected by Akaike information criterion (AIC). Collinearity between land-use classes was examined using Variance Inflation Factors (VIF; 'car' package, Fox and Weisberg, 2011) and explanatory variables were removed from models in decreasing order of VIF score until all scores were < 5. This resulted in the removal of broadleaf forest (collinear with grassland ($R^2 = 0.67$), cropland ($R^2 = 0.66$), urban ($R^2 = 0.54$), and plantation ($R^2 = 0.18$)), broadleaf savanna (collinear with wetland ($R^2 = 0.68$), pine savanna ($R^2 = 0.36$) and grassland ($R^2 = 0.14$)), and shrub (collinear with plantation ($R^2 = 0.61$), cropland ($R^2 = 0.18$), and pine savanna ($R^2 = 0.13$)). The relationship between land-use and the composition of the fluorescent DOM pool was then investigated using redundancy analysis (RDA; 'vegan' package, Oksanen et al., 2019), in which the best fit was backwards selected using F statistics.

2.6 Results

2.6.1 DOC vs. cDOM

We observed a significant positive relationship between DOC and absorbance (R^2 = 0.52; p = < 2.2 x 10^{-16}), but the strength of this relationship varied depending on location. It was stronger in the tributaries (R^2 = 0.75; p = 1.89 x 10^{-9}) and coastal zone (R^2 = 0.52; p = < 2.2 x 10^{-16}) and weaker in the main river (R^2 = 0.15; p = 0.07) and dam complex (R^2 = -0.47; p = 0.87). This is indicative of a variable decoupling between DOC and cDOM. The system contains a substantial and variable portion of non-colored, non-absorbing DOM. However, we observed a strong positive correlation between a254 and sample fluorescence (R^2 = 0.89; p = < 2.2 x 10^{-16}), indicating that the cDOM pool is highly fluorescent (Figure 2-7). We therefore present DOC data as an indicator of total DOM concentration and characterize the cDOM pool according to its fluorescent characteristics.

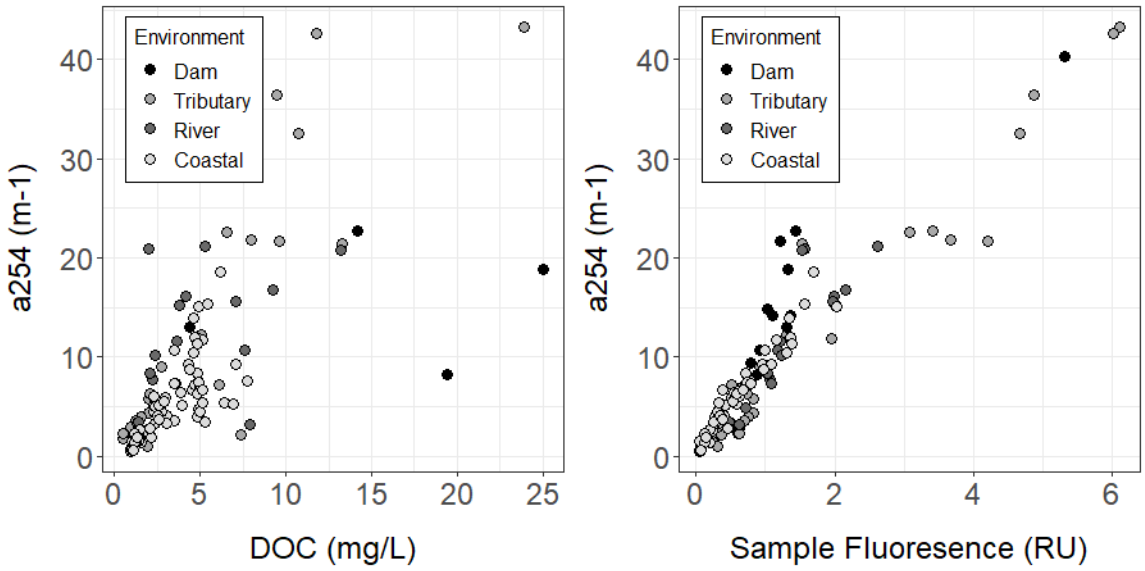

Figure 2-7 Plots of (left) DOC vs a_{254} showing a variable decoupling between the two measurements, and (right) sample fluorescence vs a_{254}.

2.6.2 PARAFAC results

A total of 207 excitation emission matrices were included in the analysis, resulting in a five-component model which explained 98.2 % of sample fluorescence, and which was split-half validated for randomized divisions of the dataset (Tucker's Congruence Coefficients > 0.91 for Ex loadings and > 0.96 for Em loadings). Loadings and contour plots are given in Figure 2-8 and Figure 2-9, respectively.

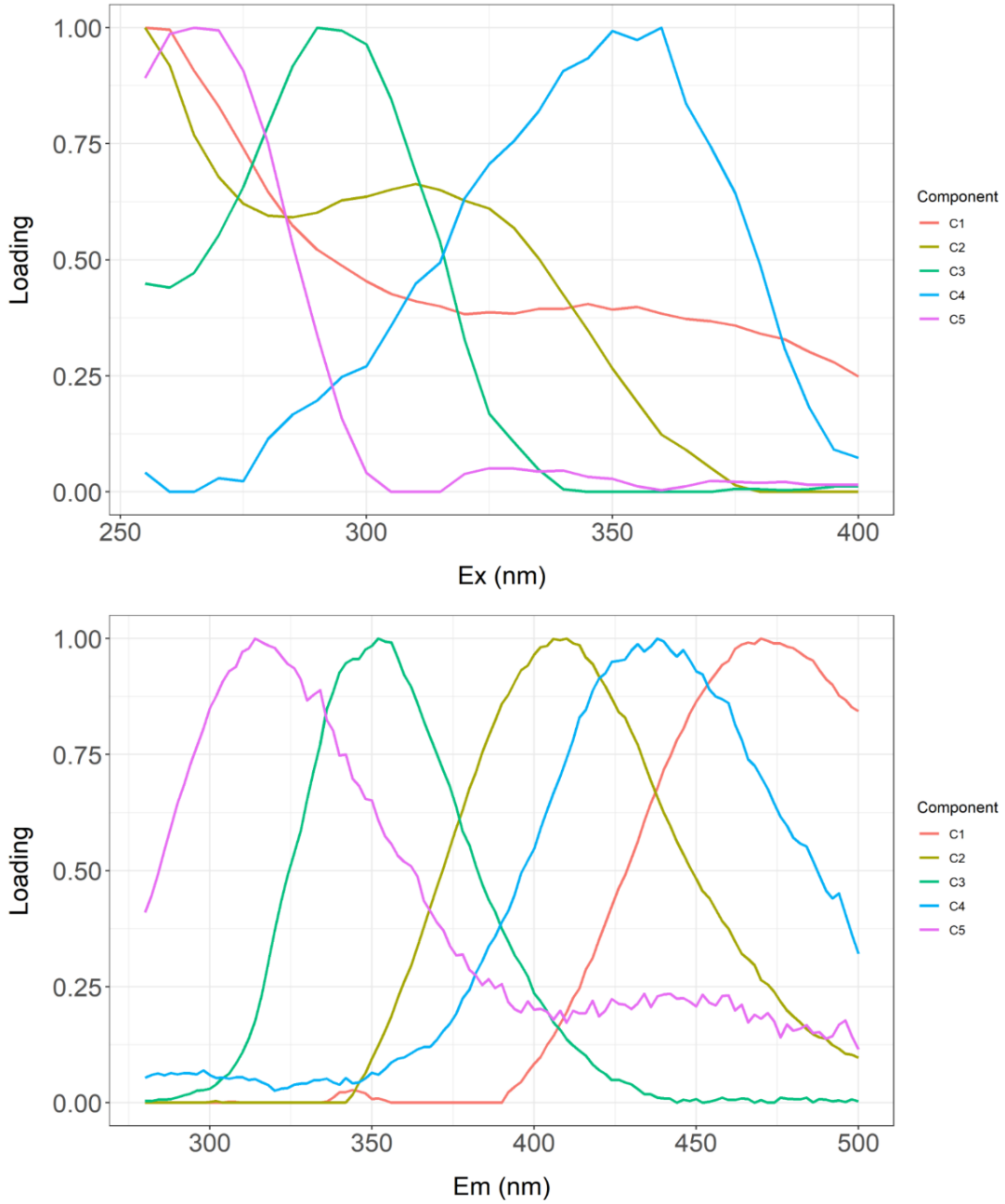

Figure 2-8. PARAFAC loadings plots for C1 – C5, showing (top) excitation wavelengths and (bottom) emission wavelengths.

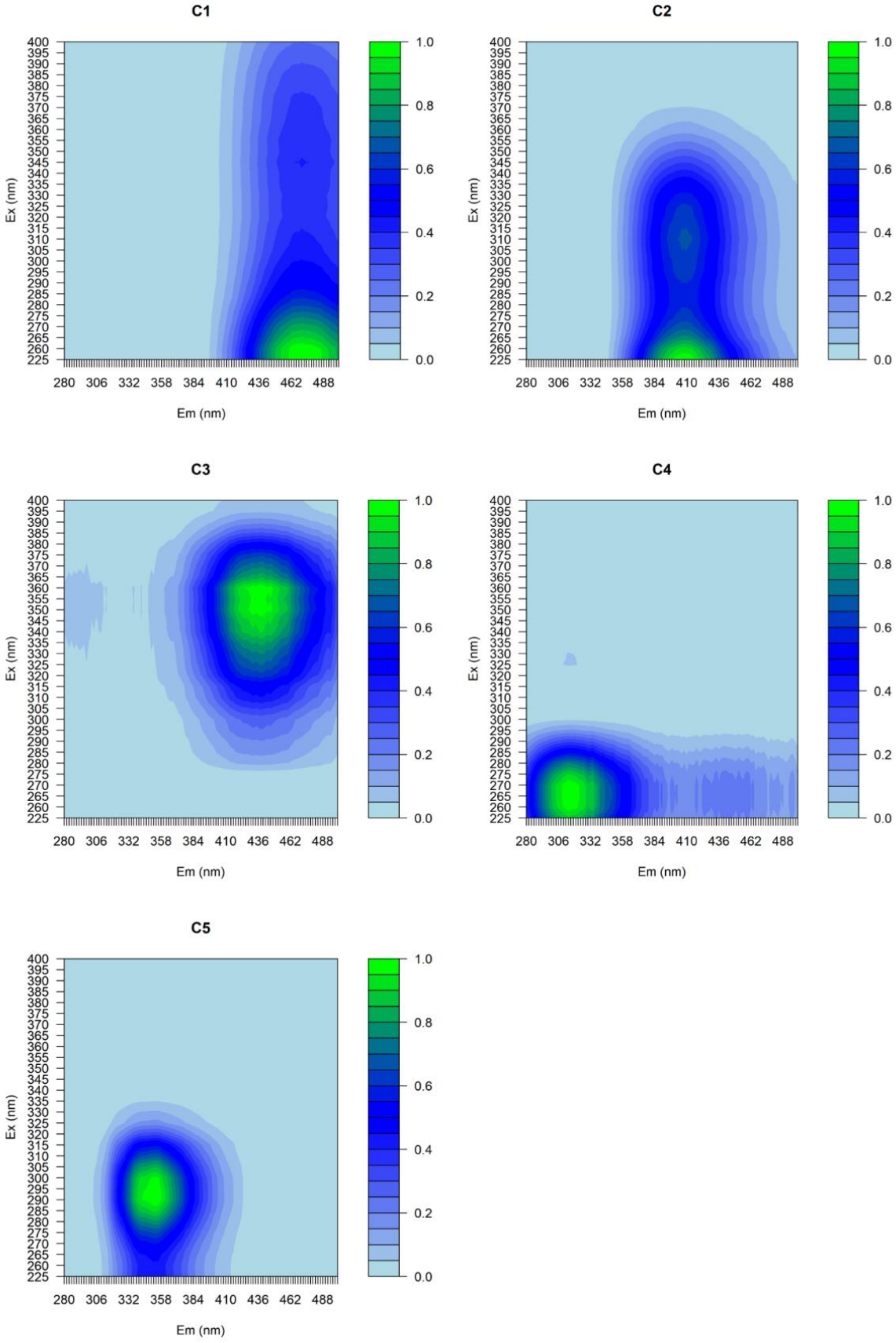

Figure 2-9. PARAFAC contour plots for Components C1 - C5.

The five components identified, henceforth termed C1 – C5, were characterized as terrestrial humic-like (C1 – C3) and protein-like (C4 and C5) through comparison with Coble Peaks (Coble, 1996) and two studies in which all components were also found: a large (~ 1,500 data point) model of fluorescence in municipal water schemes (Murphy et al., 2011), and a study of the Congo River network (Lambert et al., 2016) (Table 2-3). This characterization was further verified using the OpenFluor database (Murphy et al., 2014). The identified humic-like components (C1 – C3) have different sources and characteristics. C1 was characterized as highly aromatic material of terrigenous origin (likely SOM), C3 as lightly aromatic material of microbial origin, and C2 lightly aromatic material that may be linked to nutrient pollution and/or wastewater (Table 2-3). Previous work indicates that C1 may be susceptible to photodegradation, whilst C3 may be a product of photodegradation (Lambert et al., 2016). The protein-like components (C4 and C5) were both characterized as highly labile material of autochthonous origin, with C4 being tyrosine-like and C5 being tryptophan-like.

Table 2-3. Characterization of fluorophores C1 – C5 according to excitation and emissions maxima, Coble Peaks (Coble, 1996), a large PARAFAC model (Murphy et al., 2011), and a study of DOM composition in a tropical river network (Congo; Lambert et al., 2016) which gained supplemental insight using molecular techniques. That insight is given in italics.

	Ex max (nm)	Em max (nm)	Coble Peaks	Murphy et al. (2011)	Lambert et al. (2016)
C1	<255 (355)	470	C Humic-like (350, 420-480)	G1 – Terrestrial humic-like fluorescence	C1 – Terrestrial humic-like. *High aromaticity, high molecular weight (MW) , photo sensitive*
C2	<255 (310)	410	M Marine humic-like (312, 380-420)	G2 – Microbial humic-like fluorescence	C2 – Microbial humic-like. *Aliphatic, low MW*
C3	360	438	C Humic-like (350, 420-480)	G3 – Wastewater / nutrient enriched tracer	C5 – Humic-like *Low aromaticity, low MW. photoproduct*
C4	265	314	B Tyrosine-like (275, 310)	G7 – Tyrosine-like	C6 - Protein-like *Aliphatic, low MW, autochthonous, biolabile*
C5	290	352	T Tryptophan-like (275, 340)	G6 – Tryptophan-like	

2.6.3 DOM composition in the Mopan and Macal Rivers

The Mopan and Macal Rivers both have their headwaters in the Chiquibul Nature Reserve. The remote nature of the reserve made sampling difficult, and we could not gather sufficient samples within it to allow us to test the significance of our result. Given the lack of available data for the region, we present the data we could obtain as indicative only.

In 2018, two headwater samples were taken immediately before and after the confluence of a first and second order stream which feeds the Macal. Sample fluorescence was higher after the confluence (5.31 RU) than it was before it (1.16 RU), but the composition of the fluorescence pool was broadly similar across both samples (mean = 41% C1, 31% C2, 19% C3, 5% C4, and 3% C5). Water originating in the Chiquibul reserve is transported to the Belize River via either the Macal and the dam complex, or the Mopan and Guatemala. Fluorescence in the Macal had dropped to 0.8 RU after transit through the dam complex, whilst fluorescence in the Mopan had dropped to 1.1 RU after transit as it re-entered Belize at the Guatemalan border). Despite this similarity in post-transit fluorescence values, the composition of the fluorescence pools had clearly diverged in transit. In the Macal, we observed a net decrease in the contribution of highly aromatic fluorescence (C1 = -6%) and a net increase in the contribution of protein-like fluorescence (C4 = +3%; C5 = + 4%). In the Mopan, we observed a net decrease in the contribution of microbial humic-like fluorescence (C3 = -10%) and a net increase in the % contribution of both highly aromatic (C1 = + 3%) and lightly aromatic (C2 = + 7%) terrigenous material. In short, cDOM in the Macal became more autochthonous in nature after transit through the dams, and cDOM in the Mopan became more allochthonous in nature after transit through Guatemala's Western Uplands.

2.6.4 The influence of land use on DOM composition

Multiple regression analysis identified significant relationships between land use and both cDOM fluorescence and DOC concentration within the tributaries (Table 2-4). Agricultural land (cropland and grassland) was the primary explanator of both fluorescence and DOC concentration. Cropland was the major explanator of humic-like (C1- C3) fluorescence (69, 68, and 65 % variance explained, respectively). Grassland was the primary explanator of protein-like (C4 and C5) fluorescence and DOC concentration (64, 56, and 51 % variance explained, respectively). Urban land was correlated with protein-like (C4 and C5) fluorescence (5 % and 7 % variance explained, respectively). The extent of inland water upstream of the sampling point explained a consistent portion of humic-like (C1 – C3) and C5 protein-like fluorescence (3 – 5 % variance explained) but was not significant for C4 protein-like fluorescence or DOC concentration.

Table 2-4. Multiple linear regression models for predicting DOM fluorescence intensity and DOC concentration as a function of % land-use. Coefficient standard errors and % variance explained are given in parentheses. For each parameter, the primary land use explanator is highlighted in bold.

	R^2	Intercept	Grassland	Cropland	Water	Urban
C1	0.79	-0.54 (0.15)	0.02 (0.01, 6.58)	**0.13 (0.02, 69.24)**	1.08 (0.03, 5.13)	-
C2	0.83	-0.43 (0.12)	0.02 (0.01, 11.81)	**0.09 (0.02, 68.35)**	0.89 (0.30, 5.04)	-
C3	0.73	-0.11 (0.05)	0.01 (0.00, 7.58)	**0.03 (0.01, 65.22)**	0.22 (0.11, 3.46)	
C4	0.67	0.03 (0.01)	**0.001 (0.001, 64.00)**	-	-	0.004 (0.002, 5.10)
C5	0.68	-0.03 (0.03)	**0.01 (0.001, 55.56)**	-	0.20 (0.11, 4.26)	0.02 (0.01, 6.94)
DOC	0.56	-1.03 (1.59)	**0.16 (0.06, 51.24)**	0.46 (0.22, 6.22)	-	-

Redundancy analysis identified broadly similar relationships to multiple linear regression modelling (Figure 2-7). Grassland (F statistic = 35.11 on 1 and 26 degrees of freedom (DF)), cropland (F = 8.78 on 1 and 25 DF) and inland water (F = 3.39 on 1 and 24 DF) all significantly increased the amount of variance explained for cDOM fluorescence and DOC concentration ($p < 0.05$ in all cases). RDA 1 explained 70 % of total variance in DOC and DOM fluorescence and ordinated the data points along a land use gradient whereby samples from sites with > 50 % broadleaf forest cover has positive loadings and samples with < 40 % broadleaf forest cover had negative loadings. RDA 2 explained a further 3% of variance.

Sites draining land with < 40 % broadleaf forest cover (henceforth termed 'agri-urban dominated') had significantly higher sample fluorescence intensities and DOC concentrations than sites draining > 40% broadleaf forest (henceforth termed 'broadleaf dominated') ($p > 0.002$). Agri-urban dominated sites contained significantly higher proportions of humic-like C1 ($p = 0.03$) and C2 ($p = 0.04$) fluorescence, whilst broadleaf dominated sites contained a significantly higher proportion of protein-like C4 fluorescence ($p = 0.02$). No significant difference was observed for the proportions of

humic-like C3 (p = 0.17) and protein-like C5 (p = 0.95) found in these samples. Mean sample fluorescence was 3.86 ± 1.83 RU for agri-urban dominated sites, and 0.80 ± 0.72 RU for broadleaf dominated sites, with associated mean DOC concentrations of 10.1 ± 5.6 mg L^{-1} 3.2 ± 4.1 mg L^{-1}, respectively. Fluorescence contributions were 42 ± 4 % C1, 36 ± 4 % C2, 11 ± 2 % C3, 3 ± 1 % C4, and 7 ± 5 % C5 for agri-urban, and 38 ± 5 % C1, 33 ± 4 % C2, 12 ± 2 % C3, 10 ± 8 % C4, and 7 ± 3 % C5 for broadleaf dominated sites.

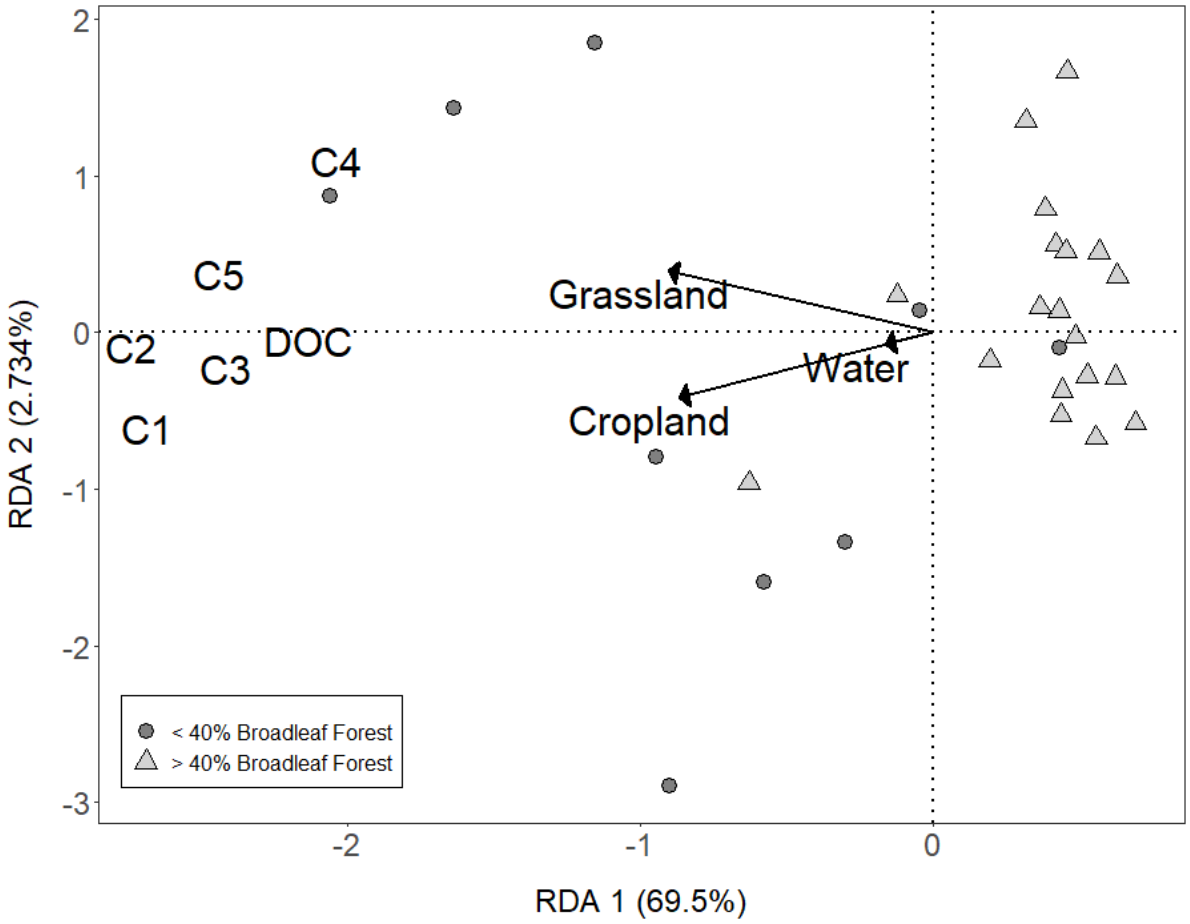

Figure 2-10. Redundancy analysis plot showing the relationships between land-use, DOC, and cDOM fluorescence. Data points represent individual samples, and are categorized according to % broadleaf forest. Land-use classes as plotted as arrow vectors, and DOC concentration and cDOM fluorescence are shown as text labels

2.6.5 Behaviour of cDOM and DOC in downstream receiving waters

In 2018, we found a net increase in DOM fluorescence and DOC concentration between the start of the Belize River (at the confluence of the Mopan and Macal Rivers) and the limit of freshwater extent during the 2018 Belize River transect (Figure 2-11). This was duplicated during our 2019 coastal sampling trip (Figure 2-11). Humic-like DOM components (C1 – C3) increased with increasing

distance from the confluence in a linear fashion within the main river stem (R^2 = 0.89, 0.88, and 0.86) and appeared to decline as a linear function of salinity (i.e. behaved conservatively) within the coastal zone (Figure 2-11). There is some evidence of the addition of humic-like fluorescence in the mid-salinity range which we attribute to the mixing of waterbodies (carried south from the outflow from the Rio Hondo, for example) as opposed to in-situ addition.

C4 protein-like DOM fluorescence exhibited a non-linear increase in the main river stem, and behaved non-conservatively within the coastal zone, with evidence of net addition at higher salinities. DOC concentrations behaved similarly to C4. C5 fluorescence exhibited a linear increase with distance downstream, albeit to a lesser degree than C1 – C3 (R^2 = 0.55). During 2018, C5 behaved non-conservatively in the coastal zone with evidence of addition at high salinities during the 2018 sampling. In 2019 C5 appeared to behave somewhat conservatively, and was present at much lower intensity than 2018.

2.6.6 Does DOM from the Belize River Watershed reach the Belize Barrier Reef?

The conservative behaviour of humic-like (C1 – C3) DOM allowed the associated fluorescence values to be statistically modelled across the full salinity range (0 – 38 ppt) using theoretical mixing lines (section 2.6). We found no significant difference between modelled fluorescence intensities across years ($p < 0.04$), and so the modelled values were averaged to provide an estimate of DOM fluorescence at any given salinity point.

Modelled salinity over the outer reefs adjacent to the river outflow had a mean value of 34.07 ± 1.16 (SD) ppt (range = 30.60 – 35.33), with a mean yearly minimum value of 29.1 ± 0.51 ppt (range = 28.2 ppt - 29.9 ppt). Salinities overlying this portion of the reef dropped below 30 ppt for an average of 10 ± 11 days yr^{-1} (Table 2-6; Figure 2-12), during which time estimate fluorescence intensities in overlying waters were more than double those predicted under 'normal' (34 ppt) conditions (C1 = 121 %; C2 = 111 %; C3 = 108 %).

Near-shore coral formations in close proximity to the Belize River outflow were subject to low-salinity (< 30 ppt) conditions throughout most of the year (356 ± 12 days yr-1), and mean salinity was 24.33 ± 3.08 ppt (range = 18.57 – 31.01). Salinity dropped below 20 ppt for 113 ± 24 days yr^{-1} Table 2-7), during which time estimated fluorescence intensities in overlying waters were around 30 % higher than those predicted at 'normal' (24 ppt) conditions (C1 = 30 %; C2 = 29 %; C3 = 20 %), and around 130% higher than those predicted at 30 ppt (C1 = 136 %; C2 = 132 %; C3 = 130 %).

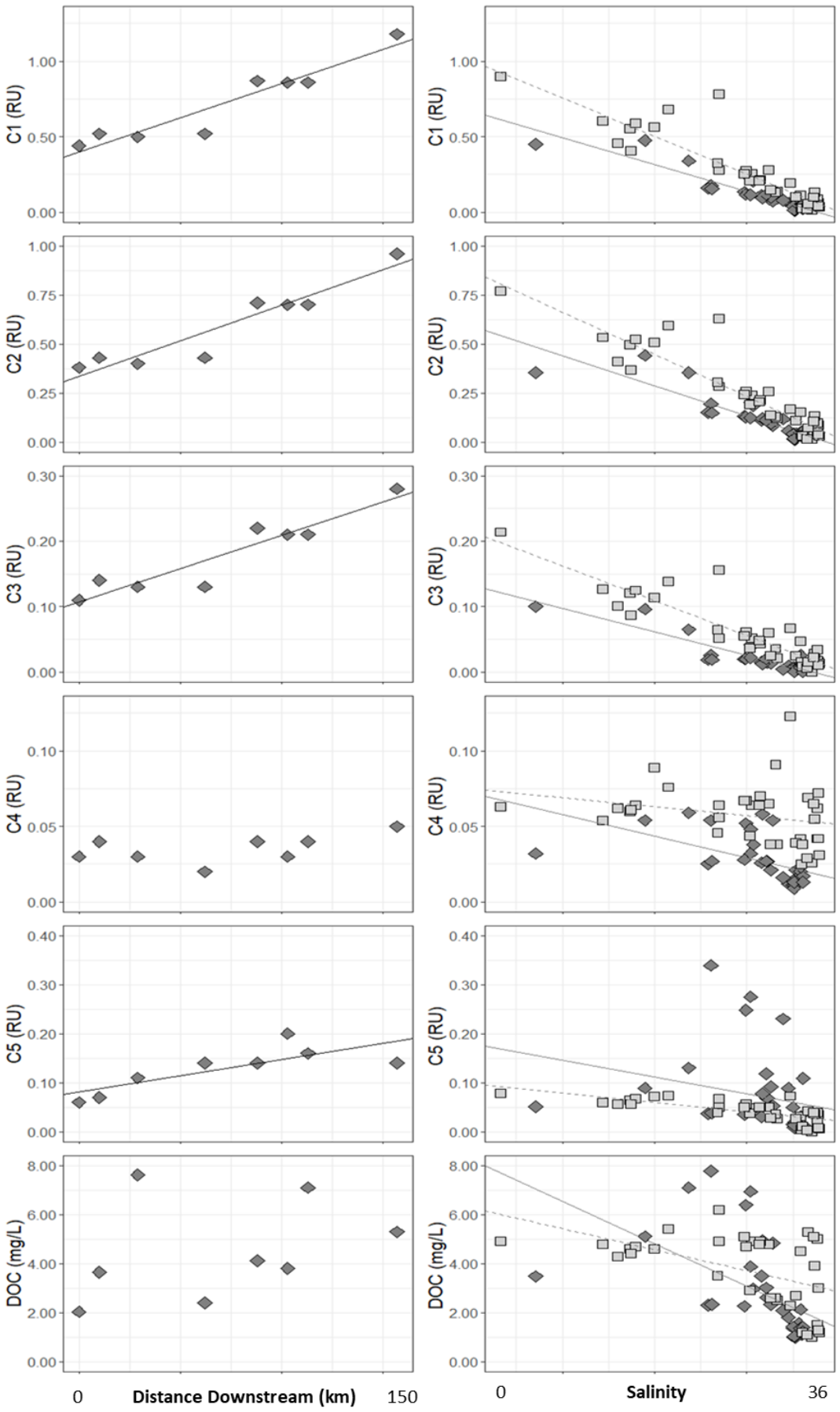
C1 (RU)
C2 (RU)
C3 (RU)
C4 (RU)
C5 (RU)
DOC (mg/L)
0
Distance Downstream (km)
150
0
Salinity
36

Figure 2-11 (previous page). Relationships between cDOM fluorescence and DOC concentration as a function of (left) distance downstream from the start of the Belize River, with solid line black line indicating significant linear relationships ($p < 0.05$) and (right) salinity within the adjacent coastal environment, with theoretical mixing lines indicated by solid (2018) and dashed (2019) dark grey lines. Data from 2018 are shown as dark grey diamonds. Data from 2019 are shown as light grey squares.

Table 2-5. Modelled fluorescence for DOM components and DOC at 20, 24, 30, and 34 ppt in November 2018 and October 2019. Values were obtained via theoretical mixing lines. Conservative components (C1 – C3) are discussed in the text. Conservative fits for other (non-conservative) components (C4, C5, and DOC) are provided for interest only.

Salinity (ppt)	Year	C1 (RU)	C2 (RU)	C3 (RU)	C4 (RU)	C5 (RU)	DOC (mg L^{-1})
20	2018	0.545	0.451	0.131	*0.030*	*0.070*	*3.13*
	2019	0.421	0.361	0.103	*0.045*	*0.039*	*2.85*
	Mean	**0.483**	**0.406**	**0.117**	***0.038***	***0.055***	***2.99***
24	2018	0.418	0.348	0.100	*0.027*	*0.056*	*2.70*
	2019	0.325	0.279	0.080	*0.042*	*0.031*	*2.44*
	Mean	**0.371**	**0.314**	**0.090**	***0.034***	***0.044***	***2.57***
30	2018	0.227	0.194	0.055	*0.022*	*0.035*	*2.06*
	2019	0.181	0.157	0.047	*0.036*	*0.019*	*1.83*
	Mean	**0.204**	**0.175**	**0.051**	***0.029***	***0.027***	***1.94***
34	2018	0.100	0.091	0.024	*0.019*	*0.021*	*1.63*
	2019	0.085	0.075	0.025	*0.033*	*0.011*	*1.42*
	Mean	**0.093**	**0.083**	**0.024**	***0.026***	***0.016***	***1.52***

Table 2-6. Number of days per month in which salinity dropped below 30 ppt in cells which overly the outer BBRS. Data are presented from January 1995 to December 2015.

	Jan	Feb	Mar	Apr	May	Jun	Jul	Aug	Sep	Oct	Nov	Dec
1995	0	0	0	0	0	0	0	0	1	1	0	0
1996	0	0	0	0	0	0	0	0	0	0	10	4
1997	0	0	0	0	0	0	0	0	3	1	2	1
1998	0	0	0	0	0	0	0	0	0	2	14	4
1999	0	0	0	0	0	0	0	0	7	0	0	0
2000	0	0	0	0	0	0	0	0	0	0	1	0
2001	0	0	0	0	0	0	0	0	0	1	6	0
2002	0	0	0	0	0	0	0	0	0	0	1	0
2003	0	0	0	0	0	0	0	0	0	2	1	0
2004	0	0	0	0	0	0	0	0	0	2	0	0
2005	0	0	0	0	0	0	0	0	0	3	0	0
2006	0	0	0	0	0	0	0	0	2	0	3	0
2007	0	0	0	0	0	0	0	0	0	2	0	0
2008	0	0	0	0	0	0	0	0	0	6	2	0
2009	0	0	0	0	0	0	0	0	0	0	7	0
2010	0	0	0	0	0	0	0	0	6	4	0	0
2011	0	0	0	0	0	0	0	0	5	26	4	8
2012	0	0	0	0	0	0	0	0	0	5	0	0
2013	0	0	0	0	0	0	0	0	3	2	28	7
2014	0	0	0	0	0	0	0	1	1	5	8	2
2015	0	0	0	0	0	0	0	0	3	6	1	0

Table 2-7. Number of days per month in which salinity dropped below 20 ppt in cells which overly the inshore corals adjacent to the Belize River outflow. Data is presented from January 1995 to December 2015.

	Jan	Feb	Mar	Apr	May	Jun	Jul	Aug	Sep	Oct	Nov	Dec
1995	0	0	0	0	0	0	0	0	11	24	30	6
1996	0	0	0	0	0	0	0	3	16	34	28	11
1997	0	0	0	0	0	0	5	28	20	33	30	9
1998	0	0	0	0	0	0	1	8	15	37	30	11
1999	0	0	0	0	0	0	1	4	20	32	30	12
2000	0	0	0	0	0	0	0	7	14	29	30	6
2001	0	0	0	0	0	0	3	9	28	32	23	23
2002	0	0	0	0	0	0	4	11	21	34	27	9
2003	0	0	0	0	0	0	2	1	18	41	28	0
2004	0	0	0	0	0	0	0	1	25	35	29	14
2005	0	0	0	0	0	0	0	0	16	29	22	14
2006	0	0	0	0	0	0	2	7	21	35	30	20
2007	1	0	0	0	0	0	3	23	36	33	30	12
2008	0	0	0	0	0	0	10	17	23	38	28	15
2009	2	0	0	0	0	0	3	22	30	42	38	20
2010	0	0	0	0	0	0	3	24	27	31	32	28
2011	6	0	0	0	0	0	7	20	30	44	37	25
2012	0	0	0	0	0	0	10	14	29	33	35	19
2013	0	0	0	0	0	0	5	11	29	38	28	23
2014	0	0	0	0	0	0	18	11	24	39	30	15
2015	6	0	0	0	0	0	9	16	28	35	38	30

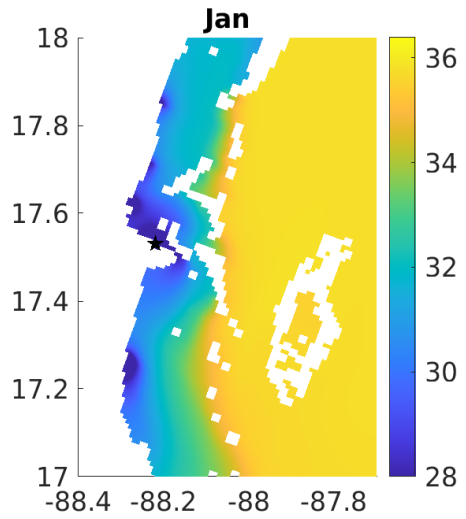
Jan
18
17.8
17.6
17.4
17.2
17
-88.4
-88.2
-88
-87.8
36
34
32
30
28

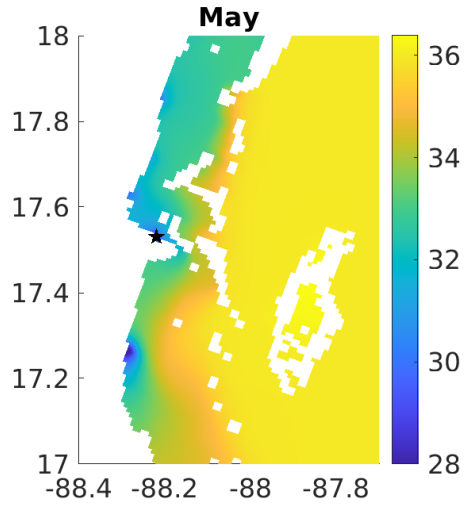
May
18
17.8
17.6
17.4
17.2
17
-88.4
-88.2
-88
-87.8
36
34
32
30
28

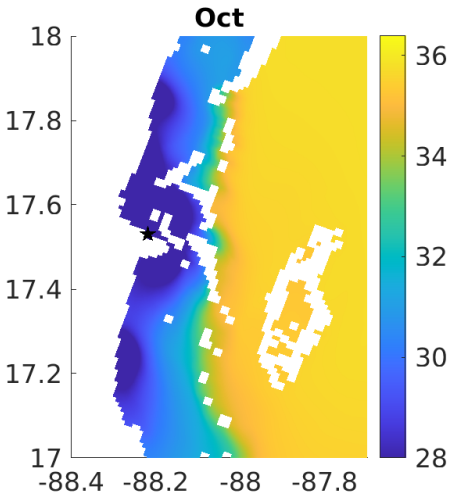
Oct
18
17.8
17.6
17.4
17.2
17
-88.4
-88.2
-88
-87.8
36
34
32
30
28

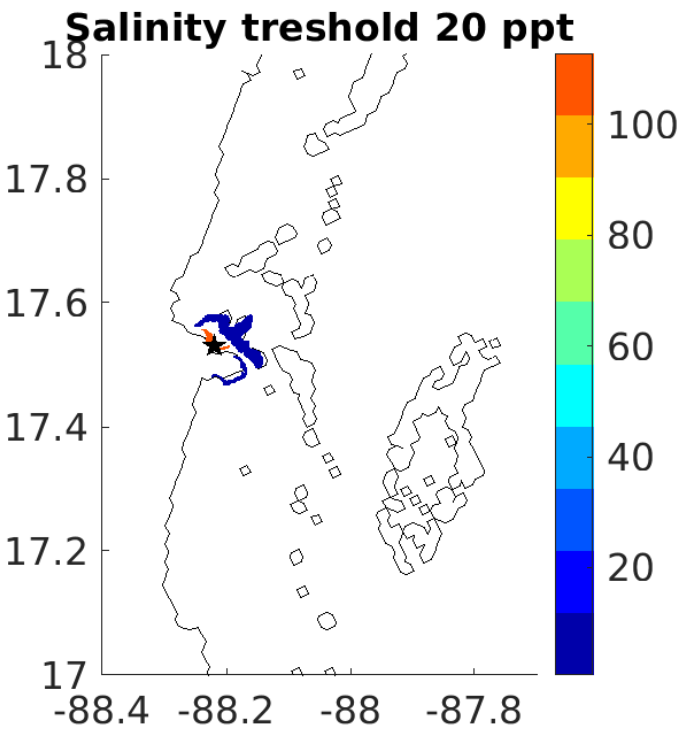
Salinity treshold 20 ppt
18
17.8
17.6
17.4
17.2
17
-88.4
-88.2
-88
-87.8
100
80
60
40
20

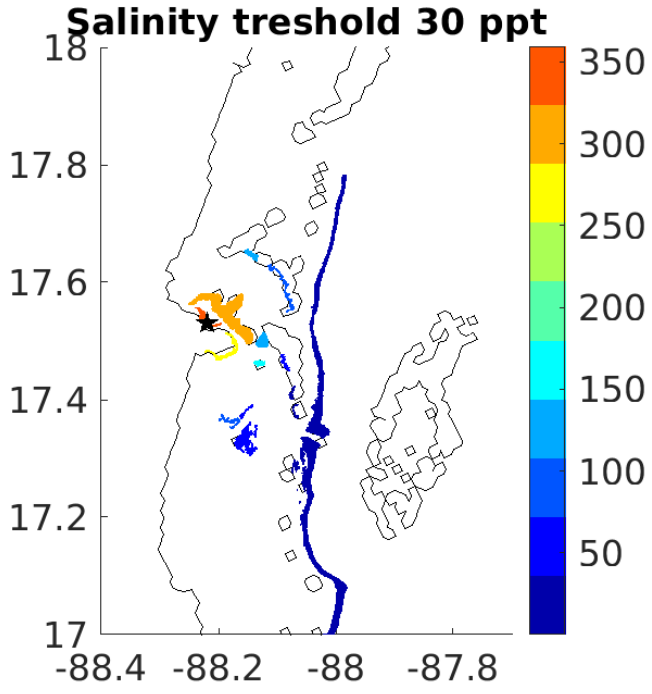
Salinity treshold 30 ppt
18
17.8
17.6
17.4
17.2
17
-88.4
-88.2
-88
-87.8
350
300
250
200
150
100
50

Figure 2-12 (previous page). Outputs from hydrodynamic modelling (1996 – 2015). Left panel (top to bottom) shows average monthly salinity distribution for January (end of wet season), May (peak dry season), and October (peak wet season). Right panel shows average number of days per year at which the defined salinity thresholds were breached in water overlying coral structures. The Belize River outflow is marked as a black star. Axis show latitude and longitude.

2.7 Discussion

2.7.1 The effect of land-use on the DOM pool

Within the tributaries, we observed a strong positive relationship between agri-urban land and DOM fluorescence. The relationship between DOM fluorescence and cDOM concentration has been well established (Stedmon et al., 2003a). An historic regional trend from broadleaf forest to agri-urban has also been established for Belize (Cherrington et al., 2010; Voight et al., 2019), and is predicted to continue (Cherrington et al., 2014). Our findings therefore suggest that conversion of land from forested to agri-urban has, and will continue to, drive an increase in the amount of cDOM entering the Belize River aquatic continuum.

Humic-like, SOM-derived material (C1) was the primary DOM type found within the tributaries. The export of SOM following deforestation has been shown to peak immediately following land use modification as the historic SOM stock is remobilized, and this peak export period lasts for between 5 to 50 years (West et al., 2004 and references therein). Beyond that period, SOM export will continue at a reduced rate owing to ongoing perturbation relating to crop production and, to a lesser extent, grazing (Fujisaki et al., 2017; West et al., 2004). Much of the agricultural land in Belize is < 50 years old and thus within the time window of SOM depletion. These cleared and cultivated lands are likely exporting SOM laid down by the preceding forest at elevated rates relative to farms which have been established for longer, and the associated SOM export can be expected to decline with time. It is possible that SOM exported from deforested tropical landscapes may be less aromatic and more biolabile than SOM exported from the preceding forest (Drake et al., 2019). On average, agri-urban dominated sites contained a higher proportion of highly aromatic C1 and lightly aromatic C2 fluorescence than was observed in broadleaf dominated sites. C1 is a typical humic-like recalcitrant SOM signal, whilst C2 is associated with less humic SOM (Table 2-4) and may be a signal of this biolabile pool.

This is further supported by our observation that transit through Guatemala resulted in a 10% increase in the contribution of humic-like (C1 and C2) DOM. We could not access the Guatemalan

portion of the Mopan, but the increase observed at the border relative to the headwaters may have resulted from the heavily deforested and highly agricultural landscape through which the Mopan flows (visible in Figure 2-1). In the ~ 32 km between the Belize-Guatemala border and the confluence of the Belize River, sample fluorescence in the Mopan increased from 1.1 RU to 1.6 RU, but the composition of the fluorescence pool shifted away from C1 and C2 type DOM and towards microbially derived (C3) and protein-like (C4 and C5) type DOM. This suggests that the Belizean portion of the Mopan is either more productive than the Guatemalan portion, and/or that the Belizean portion receives less C1 and C2 type SOM from the surrounding landscape than the Guatemalan portion. We cannot say whether this shift occurs at the border, or whether it begins further upstream.

The dominant grassland use was as animal pasture. Over-grazing of pasture by cattle and other livestock may be partially responsible for enhanced SOM export (Dlamini et al., 2016). Protein-like fluorescence typically increases with increasing anthropogenic DOM inputs from household (i.e. sewage) and farm wastes (Baker et al., 2004). Protein-like fluorescence was significantly elevated in agri-urban tributaries and anecdotal evidence suggests that animal agriculture (i.e. cattle and chicken rearing) in Belize does result in the dumping of animal waste, including bones and blood, into the river system (Pers. obs. and Carrias et al., 2018). The observed co-occurrence of elevated protein-like fluorescence with grassland may therefore be related, at least in part, to the discharge of agricultural waste associated with livestock farming. This link between protein-like fluorescence and farm wastes, including silage liquor and animal slurry, has been made elsewhere (Baker et al., 2004), but with much higher ratios of protein-like : fulvic/humic-like fluorescence (0.5 – 20) than we observed in this study (mean = 0.22 ± 0.24; range = 0.02 – 1.02).

It is also of note that a high proportion of the population live in non-urban areas. Due to the resolution of our land cover mapping, stand-alone rural dwellings with a footprint less than 10 m^2 were not captured. These dwellings are especially prevalent on the edge of grassland where farmers reside near to their grazing stock. Whilst Belize's largest population centres benefit from sanitation facilities, these non-urban dwellings typically dispose of waste directly into the river or connecting streams. Therefore, a portion of protein-like DOM fluorescence originating from grassland may relate to rural household waste, and it may have been possible to explain a greater proportion of the variance in these components if we had been able to better resolve all of the urban settlement within our study area. Other population and/or household metrics might prove useful in this regard in future work.

The dam complex was not ascribed as a distinct land use class, but is nevertheless the result of

human activity. Dams increase residence time in the Macal, increasing the opportunity for removal via photodegradation, biodegradation, and flocculation (Evans et al., 2017; Queimaliños et al., 2019; Worrall et al., 2018). We observed a net reduction in sample fluorescence which could indicate either a reduction in the concentration of fluorescent DOM or a shift from highly fluorescent humic-like DOM towards less fluorescent protein-like DOM, for example. Whilst sample fluorescence decreased, indicating DOM removal within the dams, it is of note that the relative proportion of protein-like (C4 and C5) DOM fluorescence increased. This suggests the preferential removal of humic-like material, presumably through photodegradation and/or flocculation, coupled with enhanced microbial activity. This same removal of humic-like DOM does not appear consistent with patterns observed in the main river stem and coastal zone, but residence times in the Belize River are in the order of days whilst the dams have residence times in the order of months (Karper and Boles, 2004). Another factor may be the presence of riparian forest along the Belize River which shades much of the waterbody, whereas the scale of the dams leaves most of the water surface unshielded from incident light.

The relatively consistent positive relationship observed between inland water bodies and DOM fluorescence (between 3 and 5 % of variance explained for C1 – C3 and C5 fluorescence) arises due to the fact that a higher density of streams, rivers, drainage ditches, and other channels increases land-water connectivity and may therefore facilitate land-water DOM transfer. The conspicuous absence of a relationship between protein-like C4 fluorescence and inland water suggests it may predominantly originate from point sources (e.g. agri-urban waste) rather than in-situ production. However, given the presence of C4 in the relatively pristine Chiquibul reserve and in broadleaf dominated sites as well as agri-urban ones, it is more likely that C4 DOM is the product of low-level in-situ production which is added to and/or encouraged by point source inputs of highly bio-labile DOM.

2.7.2 Downstream transport of DOM

We observed a net decrease in DOM fluorescence and DOC concentration between land and sea which is consistent with globally observed patterns (Massicotte et al., 2017). However, a range of smaller, ecosystem-scale variations were also apparent. The Belize River is flanked by riparian forest, beyond which lies some of the most agriculturally suitable land in Belize (King et al., 1993). As a result, riparian land use along its length is extremely stable (Figure 2-3) and can be excluded as a source of variation in the composition of the main river DOM pool. C1 – C3 DOM increased linearly within the Belize River (Figure 2-11), which indicates that (1) these DOM forms are being added or produced faster than they are being removed; and / or (2) their rates of addition, production and

removal do not vary with distance. This is consistent with a terrigenous humic-like characterization (Table 2-4), whereby relatively recalcitrant DOM is being added from the surrounding environment. One protein-like component (C4) accumulated non-linearly, indicating that rates of addition, production, and removal are unbalanced. This is consistent with a highly labile DOM type which originates from distinct point sources and/or the production of which varies in response to external factors. This behaviour was mirrored in the coastal environment (Figure 2-11), where humic-like components behaved conservatively with salinity whilst C4 protein-like fluorescence behaved non-conservatively, with evidence of significant addition at high salinity. C5 behaviour was more mixed: it exhibited a weak linear relationship with distance downstream (R^2 = 0.53) and which appeared to behave conservatively during the 2019 coastal sampling period. This likely indicates subdued in-situ production rates relative to 2018, rather than the transport of conservative material from the terrigenous environment.

Our study therefore suggests that (1) land-use change increased the amount of humic-like and protein-like cDOM in receiving waterbodies; (2) humic-like cDOM increased in the river during transit from upland to lowland; and (3) humic-like cDOM behaved conservatively within the coastal zone. Thus, we have demonstrated a link between land-use change and the downstream DOM pool, specifically with regards to agri-urban land and the export of humic-like (C1 – C3) material.

2.7.3 Does land-use change influence the Belize Barrier Reef?

Frequent and/or chronic exposure to low-salinity, high DOM waters can negatively impact coral species, with effects including extended photosynthetic recovery periods, reduced growth, and increased mortality (Lirman and Manzello, 2009). Our modelling results indicate a substantial (up to 130 %) increase in humic-like DOM during periods of Belize River – Belize Barrier Reef connectivity. The number of days per year at which the offshore reef was subject to these conditions was low (10 ± 11 days yr^{-1}). This suggests that any deleterious effect of DOM exposure would manifest as a short-term stress response in near-surface corals which dissipated quickly upon return to normal conditions (Aronson et al., 2000). The nearshore corals which experience these < 30 ppt conditions for the majority of the year (356 ± 12 days yr^{-1}) are almost certainly adapted to this, but were exposed to their lower salinity limit (< 20 ppt) more frequently (113 ± 24 days yr^{-1}). Whilst the increase in DOM was lower in relative terms (30 % increase between 24 and 20 ppt at the nearshore corals relative to 120 % increase between 34 and 30 ppt at the outer reef), the length of exposure was much greater. Thus, it is these nearshore corals which we suggest might most be at risk due to increasing DOM as a result of land-use change. Previous, coarser scale modelling work of the Belizean coastal zone supports our findings, reporting that buoyant terrigenous matter was highest

(> 3 g m^{-3}) over the same nearshore reefs, and that it peaked during periods of high river discharge and under specific current conditions (Burke and Sugg, 2006).

The relationship between land use and protein-like DOM in the coastal zone is less straight forward due to in-situ production and removal for which we do not have a baseline. Table 2-5 shows fluorescence values for these parameters (and for DOC) under conservative conditions, but we observed significant addition of C4 and C5 in the coastal environment (Figure 2-11). Whilst it is clear that riverine inputs of protein-like DOM and DOC are higher than those observed in more saline waters, we cannot determine the extent to which material of terrigenous origin persists relative to fresh production.

Almost all future climate scenarios for the region result in a significant reduction in precipitation within the watershed, but projected land-use change is predicted to result in increased export of SOM into nearby waterbodies, the combination of which will likely result in increased sediment and SOM export from the catchment (Cherrington et al., 2014). At the same time, the number of heavy rainfall events and storms is predicted to increase in coming years (Parry et al., 2008). Combined, this could (a) enhance the export of terrigenous DOM into the Belize River watershed, and (b) increase the number of days within a year when the river plume interacts with the barrier reef. Thus, interactions between the terrestrial and marine environments is likely to increase with time, and further study is required to understand the consequences of this.

2.7.4 Limitations and future study

We infer from these results that DOM quantity and character vary along a dominant axis of variation, namely land-use, but land-use in the study catchment at least partially tracks intrinsic site properties such as geology, elevation, and soil type. In the absence of historic baseline data, a future temporal study might allow us to better quantify the degree to which some (if any) the observed variation could pre-date land-use change. In this regard, the data produced by this study might provide a suitable baseline, particularly for the less modified, broadleaf dominated sub-catchments.

Seasonality plays an important role in land-ocean DOM transport. In-stream concentrations are typically maximal at the onset of runoff, continuously decreasing after the initial flush (Xenopoulos et al., 2017), and residence time can be considered the dominant control on the fate and reactivity of DOM along a river network, owing to changes in in-stream processing time (Catalán et al., 2016). Our sampling was timed to coincide with wet and dry seasons, yet unpredictable weather resulted in broad scale similarities in terms of flow, and missed maximal runoff. In the dry season, DOM concentration has been shown to decrease in forested streams, but to increase in highly modified

sub-catchments (Liu et al., 2019), and other work in a tropical river catchment suggests a strong wet/dry season influence on DOM composition (Hong et al., 2012; Spencer et al., 2010). The lack of sampling during peak wet season may therefore have biased our findings towards agri-urban environments, and full flood sampling is required to elucidate this. Additionally, our hydrodynamic model used mean annual discharge data, with the observed interannual variability in the freshwater plume being mostly driven by variability in ocean currents and surface winds. Future work should aim to include interannual variability in river discharge, which could be achieved through on-going efforts to collect the in-situ hydrology data required to strengthen discharge estimates for the study catchment, or by including some more general forcing, for example precipitation averaged over the river catchment taken from an atmospheric model like the ERA5 reanalysis (European Centre for Medium-Range Weather Forecasts, 2019). Nonetheless, the range of modelled salinity conditions produced by the model are representative of typical conditions over the 21-year model run, and plume penetration is greatest during peak river-discharge months (October and November). Thus, under future climate scenarios, an increase in river-discharge can be expected to increase connectivity between the Belize River watershed and the adjacent portion of the reef. This is particularly relevant during peak river discharge months, where connectivity was estimated to reach > 40 days yr^{-1} under certain hydrodynamic regimes.

An interesting note is that we did not find good agreement between DOC and sample fluorescence. This indicates that the DOM pool contained a significant non-colored fraction which was not characterized via PARAFAC analysis. Such material is typically thought to be highly labile autochthonous and/or anthropogenic material which undergoes rapid remineralization (Pereira et al., 2014a). Thus, its omission from our study is unlikely to have influenced our overall finding: that recalcitrant humic-like material reaches the coastal environment. However, future studies may wish to employ different techniques such as high-resolution mass spectroscopy to characterize this non-colored fraction.

Finally, we note that cellulose acetate filters can leach DOC, cDOM, and fDOM. We pre-flushed our filters with 100 ml sample water in the field to negate this effect (Karanfil et al., 2003; Khan and Subramania-Pillai, 2007) and used the same batch of filters throughout our sampling campaigns, but did not collect filter blanks and therefore cannot therefore exclude the possibility of filter-based sample contamination. Nevertheless, the clear changes in DOC, and fluorescence that we observed in space and time indicate that any such effects, if apparent, were minor.

2.8 Summary and conclusions

In this study, we used PARAFAC analysis to investigate how the composition of the aquatic DOM pool varied across a land use gradient in a sub-tropical watershed. Agri-urban land use was negatively correlated with broadleaf forest, a result consistent with the documented regional land-use change trajectory from broadleaf forest to agri-urban land use. Five cDOM components were identified: three humic-like components (C1 – C3) and two protein-like components (C4 and C5).

We hypothesized that sub-catchments draining agri-urban land would contain more cDOM than sub-catchments draining forested land. Agri-urban land use was positively associated with all five cDOM components and measured DOC concentration. Agri-urban samples contained a higher proportion of aromatic, highly colored cDOM than broadleaf forest samples did. It is possible that this finding is an intrinsic outcome of changes in soil type and vegetation from upland to lowland, however we speculate that it could also be a transient pattern resulting from the relative infancy of Belize's agricultural land and the ongoing loss of SOM laid down by the preceding broadleaf forest. We also hypothesized that humic-like DOM would be transported downstream and into the coastal environment, whilst protein-like DOM would be rapidly remineralized. Our findings supported this hypothesis, with humic-like (C1 – C3) fluorescence exhibiting significant positive relationships with distance downstream and conservative mixing behaviour within the coastal zone whilst protein-like (C4 and C5) fluorescence exhibited no relationship with distance downstream and non-conservative mixing behaviour in the coastal zone.

Given the conservative nature of C1 – C3 DOM, it is likely that this terrigenous material is carried along the main river and into the coastal zone. Our final hypothesis was that humic-like DOM persists within the Belize River plume to reach the adjacent barrier reef, where it may have a deleterious effect. Hydrodynamic modelling of the Belize coastal zone over a period of 21 years found the Belize River plume interacted with the offshore reef infrequently and for short periods of time, and with the nearshore reef more frequently, and for longer periods of time. We suggest that any deleterious effect on the offshore corals is likely to be short-lived and minimal, but that nearshore corals are likely to be influenced more strongly. Interaction between the Belize River plume, the Belize Barrier Reef, and the coastal environment more widely may increase under future climate and land-use scenarios, and whilst it is possible that cDOM at the levels identified here may have little effect on the coastal environment, potential impacts (e.g. darkening) require careful study. This is particularly true in the context of compound stressors, particularly freshening, acidification, warming, and pollution from various compounds which may be bound to and carried

with terrigenous DOM. For example, dissolved mercury and pesticides associated with agricultural and urban land use have previously been reported overlying Belizean coral reefs (Alegria, 2009).

In summary, we find a strong link between land-use change and cDOM composition and quantity in receiving waters of the Belize River watershed, including those overlying the economically and environmentally important Belize Barrier Reef. The potential for human activities on land to negatively impact the coastal environment is not unique to Belize, and so our findings are relevant more broadly, particularly for coastal developing nations where agri-mediated deforestation is ongoing and reliance on the marine economy is high.

2.9 Acknowledgements

This work was supported by the UK government through the Commonwealth Marine Economies Programme, which aims to enable safe and sustainable marine economies across the Commonwealth Small Island Developing States. SLF and DMP received additional support from the NERC-funded SPITFIRE Doctoral Training Programme (grant number NE/L002531/1 and NE/N012070/1 respectively). DJM, CDE and RS were supported by the NERC Land Ocean Carbon Transfer programme (LOCATE; grant number NE/N018087/1). CE was supported by Natural Environmental Research Council (NERC) 'Omics' Independent Research Fellowship NE/M018806/1. The authors would like to acknowledge colleagues at the Coastal Zone Management Authority and Institute (CZMAI) and the University of Belize (UB) for access to laboratory facilities and logistical support during fieldwork. Additional fieldwork support was provided by the Belize Energy Company Ltd. (BECOL) and Friends of Conservation (FCD) Belize, for which we are most grateful. The authors wish to thank our reviewers, whose time and comments greatly improved the quality of this manuscript.

The authors declare no conflicts of interest. All data used in this study are freely available online. DOI: 10/f75z (All 2018); 10/f754 (Freshwater 2019); 10/f75t (Coastal 2019).

2.10 Author contributions

Conceptualization: RS, CDE and CE; Data curation: SLF; Formal analysis: SLF, CDGB, CGMA, JTH, and AP; Funding acquisition: CE and RS; Investigation: SLF. CDGB, AC, AF, GA, HB, SEC, MGD, BKH, DMP, and SR; Methodology: SLF and CDGB; Project Administration: SLF; Resources: AC, AY, DJL, and CE; Software: CGMA and AF; Supervision: DJM, RS, and CDE; Validation: SLF and CDGB; Visualization: SLF, AF, and CGMA; Writing – original draft: SLF; Writing – review & editing: All authors.

Chapter 3 Evidence of biologically stable 'invisible' dissolved organic carbon in a subtropical watershed

This project was conceived by S. Felgate and C. Barry. S. Felgate led logistics, data analysis, and manuscript preparation. Monthly data collection was undertaken by students at the University of Belize, under supervision of S. Felgate, C. Barry, and A. Carrias. Full detail of author contributions are provided at the end of the chapter.

Stacey L. Felgate[1,2*], Abel Carrias[3], Joaquin Urbina[3], Esther A. Hernandez[3], Josué Aké[3], Jair Valladarez[3], Chris D. G. Barry[4], B. B. Cael[2], Chris D. Evans[4,5], Claire Evans[2], Alice Fitch[4], Edward Mawji[2], Christopher R. Pearce[2], Richard Sanders[2,6], and Daniel J. Mayor[2].

[1]Ocean and Earth Sciences, University of Southampton, Southampton, SO14 SZH, UK
[2]Ocean Biogeosciences, National Oceanography Centre, Southampton, SO14 SZH, UK
[3]Faculty of Science and Technology, University of Belize, Belmopan, Belize
[4]UK Centre for Ecology and Hydrology, Bangor, LL57, 2UW, UK
[5]Swedish University of Agricultural Sciences, 756 61 Uppsala, Sweden
[6]Norwegian Research Centre, NO-5007 Bergen, Norway

This chapter has been prepared for submission to Geophysical Research Letters. Supplimentary material has been incorporated into the main text.

3.1 Key Points

- Biodegradation within a sub-tropical river catchment removed 14 ± 10 % of dissolved organic carbon (DOC) within five days.
- This was fuelled by colored DOC which accounted for 48 ± 29 % of the DOC pool and was highest in agricultural settings.
- The remaining 52 ± 29 % DOC was optically invisible, ubiquitous, and appeared biologically stable.

3.2 Abstract

Tropical rivers transport globally significant quantities of dissolved organic carbon (DOC) from land to ocean, but our understanding of the fate of this material remains limited. A substantial fraction of riverine DOC may be comprised of non-chromophoric and optically 'invisible' (iDOC) which is hypothesized to be bioavailable, but this has not been directly investigated. We found that 14 ± 10 % of a sub-tropical DOC pool was biodegraded within 5 days. iDOC constituted 52 ± 29 % of the DOC pool but appeared biologically stable during 5-day oxygen-consumption experiments whilst chromophoric or 'colored' DOC (cDOC) fuelled biodegradation. Agricultural sub-catchments appeared to increase cDOC, bioavailable DOC, and biodegradation rates, implying that land-use directly impacts the production and fate of DOC. The high concentrations and apparent stability of iDOC observed in this study suggest a significant gap in our understanding of riverine DOC fluxes and processes within the carbon cycle.

3.3 Plain language summary

Tropical rivers transport a large amount of land-derived organic carbon downstream, but we know relatively little about what happens to this material in transit. It tends to be highly colored, so much so that colour can often be used to estimate concentration, but some systems also contain considerable amounts of non-coloured organic carbon which cannot be estimated in this way. The chemical properties which cause colour tend to make carbon less available for biological degradation, whereas the chemical properties which cause an absence of colour tend to make carbon more available. We found that around half of the dissolved organic carbon in a sub-tropical river was non-colored, but found no evidence that it was more accessible. Indeed, biological degradation increased as the colored fraction increased, suggesting that it was colored organic carbon that fuelled biodegradation. Understanding what caused this result will help us better understand land-ocean carbon processing, which is an important part of the global carbon cycle.

3.4 Introduction

The lateral transport of terrigenous carbon (C) through inland waters is a significant biogeochemical term with widespread implications for ecosystem function, water quality, and C cycling (Drake et al., 2018; Regnier et al., 2013; Stanley et al., 2012). A substantial fraction of this flux occurs as dissolved organic carbon (DOC), a complex composite of molecules comprising a wide continuum of molecular weight, size, and structural and elemental composition (Hope et al., 1994). These properties

influence DOC reactivity, which in turn influences bio- and photo-degradation rates with implications for aquatic C cycling, riverine oxygen levels, land-ocean C export, and carbon dioxide (CO_2) emissions (Anderson et al., 2019; Catalán et al., 2016; Kellerman et al., 2015; Shen and Benner, 2020).

DOC composition and its reactivity are largely determined by source: terrigenous DOC exported to inland waters via surface and sub-surface flows and point source inputs tends to be predominantly comprised of higher molecular weight, higher aromaticity compounds which are less susceptible to biodegradation than the lighter, less aromatic compounds which typically comprise DOC produced in-situ (Köhler et al., 2002; Sharpless et al., 2014; Stubbins et al., 2010). This difference in bioavailability means that DOC produced in-situ is often the dominant driver of heterotrophic production in freshwaters, despite terrigenous DOC being a more plentiful substrate (Hotchkiss and Hall, 2015; Thorp and Delong, 2002). However, this picture is complicated by the fact that the composition and bioavailability of terrigenous DOC is strongly linked to catchment land use (Hagen et al., 2010; Webster et al., 2008; Wilson and Xenopoulos, 2009) which is rapidly changing. In turn, this has implications for the metabolic state of, and CO_2 emissions from, aquatic ecosystems (e.g. Lapierre et al., 2013).

The higher molecular weight, more aromatic compounds which predominantly compose terrigenous DOC absorb ultra-violet and visible (UV-Vis) light are typically referred to as chromophoric or 'colored'. In freshwaters where terrigenous DOC dominates, DOC concentrations tend to be strongly correlated with absorbance (e.g. Brezonik et al., 2015; Carter et al., 2012; Massicotte et al., 2017) and absorbance-based descriptors of intrinsic molecular characteristics, e.g. weight and aromaticity, are well-established (Chin et al., 1994; Helms et al., 2008; Weishaar et al., 2003a), and can be used to predict DOC concentrations (Carter et al., 2012; Tipping et al., 2009). However, the strength of coupling between DOC and absorbance varies in time and space, and the extent to which DOC concentrations can be accurately predicted from absorbance spectra declines as the fraction of the DOC pool comprised of low- or non-absorbing, optically 'invisible' DOC (iDOC) increases (Adams et al., 2018; Brezonik et al., 2015; Griffin et al., 2018), e.g. along the land-ocean aquatic continuum (Massicotte et al., 2017).

Substantial amounts of iDOC have been observed within eutrophic lakes, linked to algal production (Adams et al., 2018). However, appreciable concentrations of iDOC have also been linked to terrigenous sources. For example, iDOC derived from soil runoff and leaf litter has been shown to seasonally account for 4 – 89 % of the DOC in a tropical headwater stream (Pereira et al., 2014a). This terrigenous iDOC was characterized via size exclusion chromatography (SEC) as being comprised of low molecular weight, aliphatic molecules including amino acids and mono- and polysaccharides,

similar to the molecules which typically constitute algal DOC (Mühlenbruch et al., 2018). These low molecular weight, aliphatic molecules exhibit varying bioavailabilities, all of which tend to be greater than that of the terrigenous aromatics which dominate cDOM (e.g. Mühlenbruch et al., 2018 and references therin).

We hypothesize that iDOC is more bioavailable than cDOC, and examine this within a sub-tropical river catchment in which we have previously documented large and variable decoupling between absorbance and DOC concentrations (Felgate et al., 2021b). We quantify cDOC and iDOC using an absorbance-based DOC prediction model (Carter et al., 2012; Tipping et al., 2009) and measured DOC concentrations (Pereira et al., 2014a). The bioavailabilities of these fractions, determined by measuring oxygen-consumption in 5-day dark incubations, are then related to land-use activities in the surrounding eight sub-catchments with varying degrees of agricultural influence

3.5 Methods

3.5.1 Sample collection

The Belize River Watershed (Figure 3-1) is a highly forested sub-tropical river catchment which is experiencing rapid deforestation and agricultural expansion (Cherrington et al., 2014, 2010). Detailed descriptions of catchment physiogeography, soils, geology, and hydrological characteristics are provided elsewhere (Baillie et al., 1993; Esselman and Boles, 2001; Hartshorn et al., 1984; Heyman and Kjerfve, 1999; King et al., 1993).

Eight sub-catchments with varying land cover (Figure 3-1; Table 3-1) were sampled within the mid-catchment. Sites 1 (the Mopan River) and 2 (the Macal River) drain the upper catchment and combine to form the Belize River, which was sampled downstream at Site 7. All other sites drain tributaries with low (< 25 %; Site 3 and Site 4), medium (32%; Site 8) and high (> 60 %; Site 5 and Site 6) mixed agricultural and urban (agri-urban) influence. Samples were collected on May 28th, June 27th, August 6th, September 25th, and October 21st, 2019. These dates fell within the wet season which typically spans May – November, but monthly precipitation values during this period were considerably lower than the long-term mean (1980 – 2010; Figure 3-2).

Samples were collected from ~ 10 cm below the river surface using a plastic bucket. Water temperature, specific conductance, and dissolved oxygen (DO) were measured using an YSI ProDSS hand-held Multimeter (Yellow Springs Instrument Co., USA). Water was syringe filtered (0.45 µm Fischer® cellulose acetate) immediately upon collection into 60 mL Nalgene® HDPE bottles for

determination of DOC concentration and 30 mL Wheaton® amber borosilicate glass vials for measurement of absorbance. In addition a 1000 mL LDPE plastic bottle was filled with unfiltered water for determination of biodegradation rates. Samples were stored cool and dark until their return to the laboratory, which was within 6 hours of collection, then refrigerated at 4 °C.

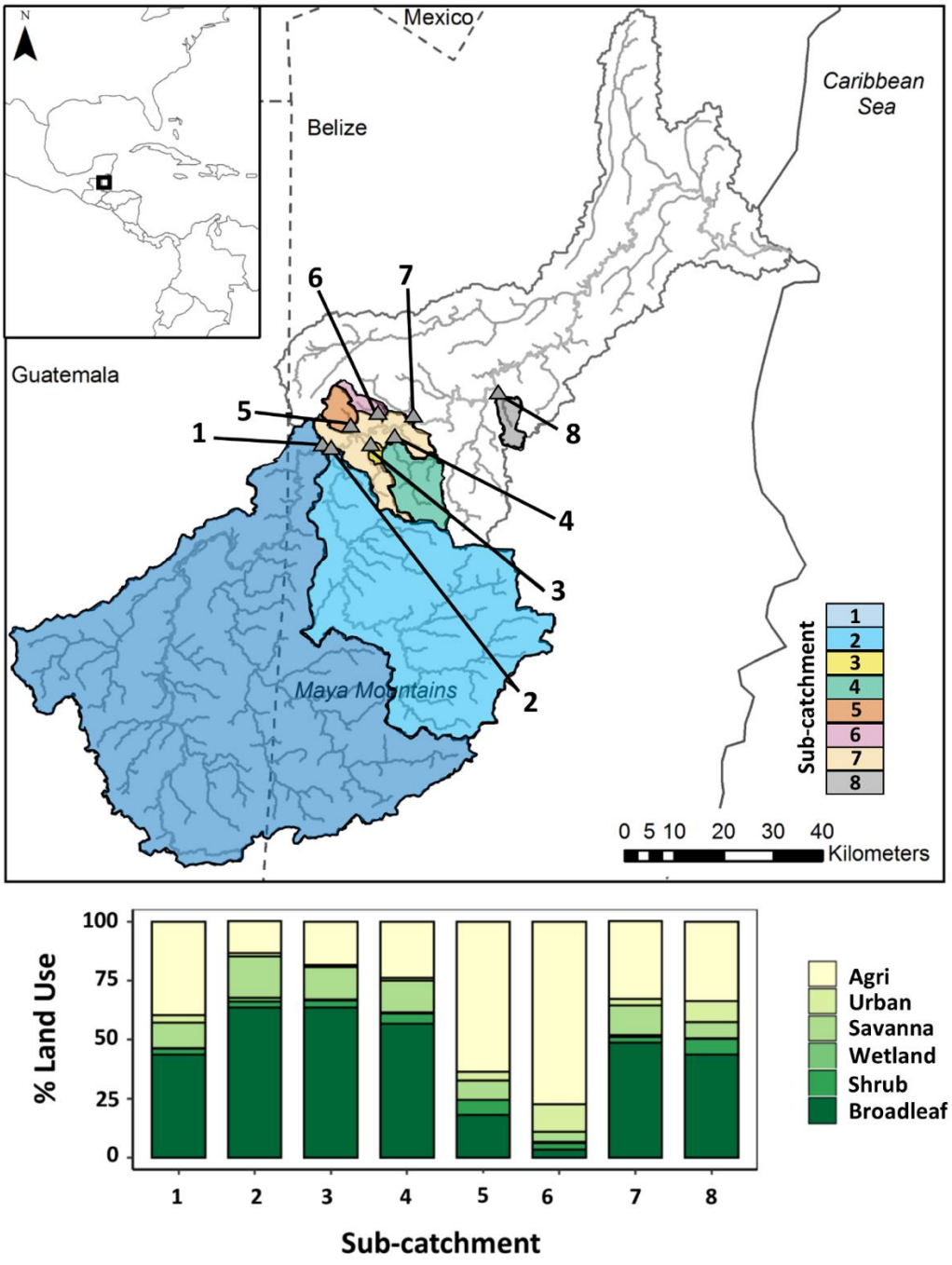

Figure 3-1. Map of the Belize River Watershed, with sampling locations (labelled) and sub-catchment boundaries (colorized) shown. Site 7 is on the main river and so its drainage area includes all upstream sub-catchments (1 - 6). Land use data obtained from Felgate et al. (2021).

Table 3-1 Locations and land use as a % value for each sampling site. Land use data taken from Felgate et al. (2021). Sites 1 and 2 drain the Mopan (3,690 km^2) and the Macal (1,466 km^2) sub-catchments which together represent the upper catchment and account for ~ 60% of the BRW by area. 'Site average (all)' = sites 1 - 8. 'Catchment Average' = BRW. Site 7 is located on the main river stem, and therefore drains land which includes sub-catchments 1 – 6. 'Site average (exc. 7)' = excluding site 7, to account for this.

Site	Lat	Long	Broadleaf	Agriculture	Urban	Savannah	Wetland and Inland Water	Shrub
1	17.17762	-89.08067	44	40	3	11	0	3
2	17.17743	-89.08000	64	13	2	18	2	3
3	17.18816	-88.99877	64	18	1	14	0	3
4	17.20173	-88.95625	57	24	1	13	1	4
5	17.21417	-88.03833	18	64	4	8	0	6
6	17.2261	-88.97483	3	77	12	5	0	3
7	17.23028	-88.92506	49	33	3	13	1	3
8	17.2774	-88.76781	44	34	9	7	0	7
Site Average (all)			43	38	4	11	1	4
Site Average (exc. 7)			42	39	4	11	1	4
Catchment Average			45	31	3	14	3	4

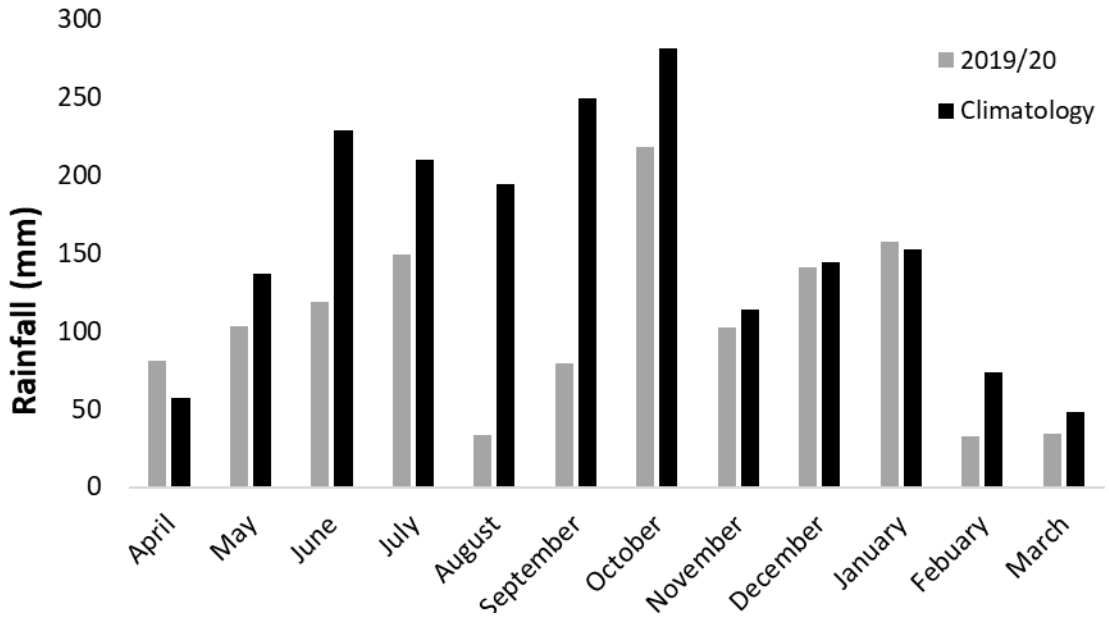

Figure 3-2. Monthly precipitation totals during the study period (2019/20) and long term mean monthly precipitation (Climatology: 1980 – 2010) taken for Belmopan (near Site 8; Figure 3-1). Data was provided by the Belize Department of Hydrology.

3.5.2 Laboratory analysis

DOC concentrations were determined as Non-Purgeable Organic Carbon (NPOC) by Pt-catalysed combustion against glycine and potassium hydrogen phthalate standards, using a TOC-VCPN analyser (Shimadzu, Japan). Samples were acidified to < pH 2 by adding hydrochloric acid at a rate of ~ 0.1 % sample volume, and sparged with high purity (> 0.99 %) oxygen prior to combustion. This method is not sensitive to dissolved inorganic carbon (DIC) concentrations (Findlay et al., 2010), and so was chosen to ensure that ambient DIC did not influence our results. Reproducibility of standards was within 2 % in the range 0 – 50 ppm. Absorbance spectra (200-800 nm) were determined at 1 nm intervals using a DR6000 spectrophotometer (Hach, Germany; May, June, and August, University of Belize) and a Cary 60 UV-Vis dual beam spectrophotometer (Agilent, USA; September and October, National Oceanography Centre, Southampton) using 1 cm path length quartz cuvettes against pure water blanks. In both cases sample reproducibility over the range 240 – 700 nm was within 0.2 %. Absorbance at 254 nm (a_{254}) is presented as a singular measure of absorbance, and DOC specific absorbance at 254 nm ($SUVA_{254}$) is presented as a metric of aromaticity (Weishaar et al., 2003a).

3.5.3 Estimating cDOC and iDOC

Concentrations of cDOC were calculated using the 'two wavelength' approach and associated extinction coefficients at 270 nm and 350 nm detailed by Carter et al. (2012) (Equation 3-1):

$$DOC = cDOC_a + cDOC_b + iDOC \qquad \boldsymbol{Eqn. 3-1}$$

This approach partitions cDOC into highly aromatic, strongly absorbing fraction, ($cDOC_a$) and a lightly aromatic, weakly absorbing fraction ($cDOC_b$), the latter being associated with more bioavailable substrates (Carter et al., 2012; Tipping et al., 2009), and adds a fixed intercept term (+ 0.8 mg L^{-1} in Carter et al., 2012) to account for a small iDOC concentration which is assumed to be constant. We omitted this fixed term, and instead estimated iDOC as the difference between total laboratory-determined DOC concentration and calculated cDOC concentration, using the method established by Pereira et al. (2014) (Equation 3-2):

$$iDOC = DOC - (cDOC_a + cDOC_b) \qquad \boldsymbol{Eqn. 3-2}$$

Full details of the cDOC model are given in Carter et al. (2012) but are summarized here, where a_λ is the absorbance of the sample at wavelength λ and $E_{AB,\lambda}$ is the cDOC extinction coefficient. If cDOC is composed of two fractions (f_A and f_B), each fraction will have its own extinction coefficient at any given wavelength λ ($E_{A,\lambda}$ and $E_{B,\lambda}$) (Equation 3-3):

$$cDOC = \frac{a_\lambda}{E_{AB,\lambda}} = \frac{a_\lambda}{(f_A * E_{A,\lambda}) + (f_B * E_{B,\lambda})} = \frac{a_\lambda}{(f_A * E_{A,\lambda}) + (1 - f_A)E_{B,\lambda}} \qquad \textbf{Eqn. 3 - 3}$$

$E_{AB,\lambda}$ can be written at two wavelengths to derive a ratio R which is equivalent to the ratio of measured absorbances at those wavelengths (Equation 3-4):

$$R = \frac{E_{AB,\lambda 1}}{E_{AB,\lambda 2}} = \frac{(f_A * E_{A,\lambda 1}) + (f_B * E_{B,\lambda 1})}{(f_A * E_{A,\lambda 2}) + (f_B * E_{B,\lambda 2})} = \frac{a_{\lambda 1}}{a_{\lambda 2}} \qquad \textbf{Eqn. 3 - 4}$$

Thus, if the extinction coefficients and associated absorbance are known at two wavelengths, f_A and f_B (as 1 - f_A) can be derived (Equation 3-5):

$$f_A = \frac{E_{B,\lambda 2} - (R * E_{B,\lambda 2})}{R * (E_{A,\lambda 2} - E_{B,\lambda 2}) + (E_{B,\lambda 2} - E_{A,\lambda 1})} \qquad \textbf{Eqn. 3 - 5}$$

These values can then be substituted back into Equation 3-3 to calculate cDOC, which is then multiplied by f_A and f_B to derive $cDOC_a$ and $cDOC_b$, respectively.

3.5.4 Biodegradation assays

Sample bottles were placed in a dark room until they had equilibrated to ambient temperature. This typically took ~ 2 hours, which allowed the majority of any suspended material to settle out. Unfiltered sample water from each site was then transferred into three 22 mL Supelco® gas-tight borosilicate glass vials, taking care not to re-suspend any particulates, and sealed without headspace. Each vial was pre-fitted with a SP-PSt3 oxygen planar sensor spot (Presens, Germany) which permits non-invasive oxygen determinations with a detection limit of 15 µg L^{-1} and a reported accuracy > 0.5 %. Vials were incubated at simulated *in-situ* temperature conditions (temp range = 21.1 – 29.3 °C) using an insulated cool box filled with water to ~ 30 cm depth and maintained at ambient temperature. Dissolved oxygen concentration (DO) was measured using a Fibox 4 oxygen optode (Presens, Germany) calibrated each month (0 and 100 % saturation). Initial measurements were taken two hours after the start of the incubation, and at 9 am, 1 pm, and 5 pm for two consecutive days. A final measurement was recorded at 9 am on day 5. Exact time points varied according to start time, and are given in Table 3-2 alongside details of incubation temperatures, which ranged from 21.2 °C to 27.9 °C.

3.5.5 Modelling biodegradation rates

The removal of DO was modelled according to first-order exponential decay (Equation 6) where

DO(t) is the oxygen removed at time *t*, $DO_{initial}$ is the total oxygen available, and *k* is the rate constant.

$$DO(t) = DO_{initial} * e^{-kt} \qquad \textbf{Eqn. 3-6}$$

The removal of DO is assumed to be caused by biodegradation alone as incubations were conducted in the dark. We converted DO to DOC assuming a pragmatic respiratory quotient of 1 (Guillemette and del Giorgio, 2011; Hunt et al., 2012), and calculated bioavailable DOC (BDOC) which we defined operationally as DOC consumed within five days. This duration was selected to encompass the maximum estimated mean water transit time for the watershed (Figure 3-3), and is also the incubation period frequently used to determine Biological Oxygen Demand (BOD), an ongoing and globally used metric of water quality (Mallin et al., 2006). DOC that was not consumed within five days was considered refractory (RDOC) over time scales relevant to the study catchment. We also calculated linear biodegradation rates (ΔDOC / Δt) to allow direct comparison with other studies which report in this way.

3.5.6 Statistics

Statistical analyses were undertaken using R software (R Core Team, 2019a). Decay models were fitted according to a non-linear least squares approach using the package 'lme4' (Bates et al., 2015). Linear regression (ANOVA) was used to examine the relationship between DOC concentration, absorbance, and cDOC concentration. For all other relationships, Spearman's Rank Correlation (r_s) was used to assess correlation between parameters, and Kruskal-Wallis tests were used to identify statistically significant variations by site and month. In all cases, $\alpha = 0.05$. Values in the text are reported as mean ± SD, unless otherwise stated.

3.6 Results and Discussion

Measured DOC concentrations ranged from 0.78 – 19.77 mg L^{-1} (6.61 ± 4.90 mg L^{-1}) and were positively correlated with absorbance (a_{254}) ($R^2 = 0.63$; $p = 3.50 \times 10^{-9}$; Figure 3-4a). This relationship held at other wavelengths, including those used in the 'two-wavelength' model (270 and 350 nm), and varied according to site (Figure 3-4a). Calculated cDOC concentrations ranged from 0.30 – 10.85 mg L^{-1} (mean = 2.88 ± 2.75 mg L^{-1}) and were, on average, 3.86 ± 4.15 mg L^{-1} lower than measured DOC (Figure 3-4b). This difference between DOC and cDOC represented an iDOC fraction equivalent to 51 ± 29 % of the DOC pool (range = 0 – 97 %).

Mean k was 0.15 ± 0.30 day^{-1}. DOC decay appeared linear in all but five instances in agricultural settings (Figure 3-4c; Sites 5 and 6). Linear decay rates (mean = 0.14 ± 0.12 mg L^{-1} day^{-1}) were

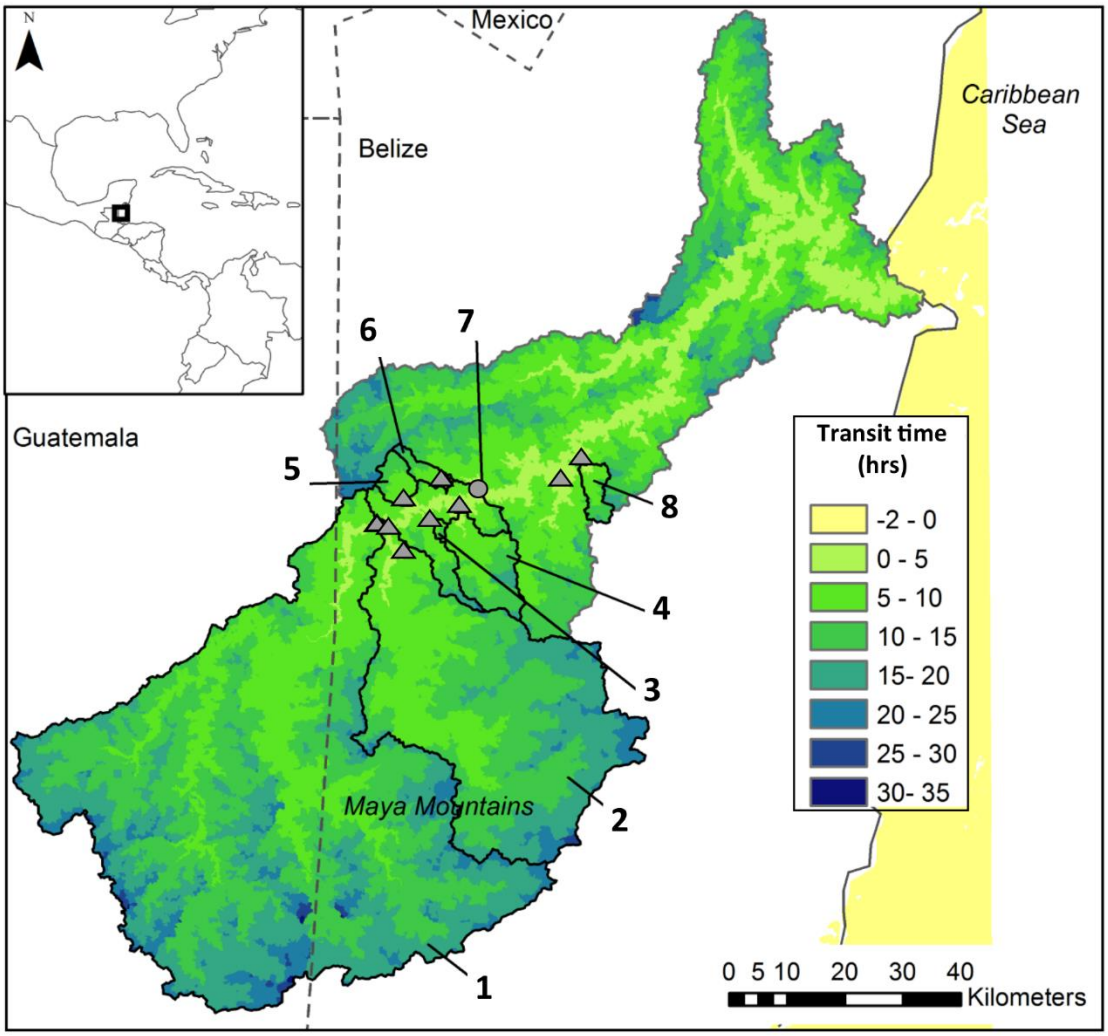

Figure 3-3. Map of the Belize River Watershed showing estimated transit time, which was derived as the number of hours taken for water to exit the river system from point of entry to the coast. Data are presented as estimated values under natural conditions (i.e. excluding effects of dams and other water course modifications). Transit times were calculated from spatial datasets of flow length (generated in ArcGIS) and velocity (calculated using Manning's equation), and are likely to be underestimates.

comparable with reports from the Tana River in Kenya (0.13 ± 0.10 mg L^{-1} day^{-1}; Geeraert et al., 2016) where sampling included agri-urban land, but were approximately twice as high as reports from near-natural sites within the Amazon Basin (Amon and Benner, 1996; Ward et al., 2013; both 0.06 mg L^{-1} day^{-1}). In this study, agricultural sub-catchments (Sites 5 and 6) exhibited higher k values than elsewhere in the catchment (Figure 3-4d). Excluding these settings reduced mean k by ~ 75 %, to 0.04 ± 0.03 day^{-1} and reduced linear degradation rates by ~ 50 % to 0.09 ± 0.04 mg L^{-1} day^{-1}. This supports previous work showing that agricultural land use can increase the susceptibility of riverine DOC to microbial degradation (Williams et al., 2010; Wilson and Xenopoulos, 2009).

Table 3-2. Measurement time (local), time since start of assay (days), and incubation temperature (°C) associated with biodegradation assays.

Time Point	May			June			August			September			October		
	Time	Days	Temp	Time	Days	Temp	Time	Days	Temp	Time	Days	Temp	Time	Days	Temp
0	13:30	0.00	22.4	06:42	0.00	25.8	18:28	0.00	26.5	20:12	0.00	23.0	09:14	0.00	21.1
1	16:06	0.11	23.3	16:26	0.40	25.1	08:02	0.57	26.3	08:24	0.51	24.3	17:17	0.34	24.2
2	18:02	0.19	24.7	08:30	1.08	25.9	11:18	0.7	26.8	16:34	0.85	27.2	08:20	0.96	24.3
3	08:47	0.80	26.1	17:04	1.43	25.8	15:58	0.9	26.1	08:21	1.51	26.8	17:44	1.35	24.6
4	12:04	0.94	27.9	06:31	1.99	26.3	08:38	1.59	27.0	15:42	1.81	27.6	08:00	1.95	23.2
5	17:44	1.18	27.1	08:27	4.08	25.2	11:13	1.70	26.5	09:00	2.53	26.9	08:50	3.98	25.4
6	08:37	1.80	25.1				15:49	1.89	29.3	09:23	4.55	22.4			
7	12:19	1.95	26.0				08:18	2.58	28.6						
8	16:33	2.13	26.3				08:33	4.59	29.3						
9	08:36	2.80	26.4												
10	08:56	5.81	27.9												

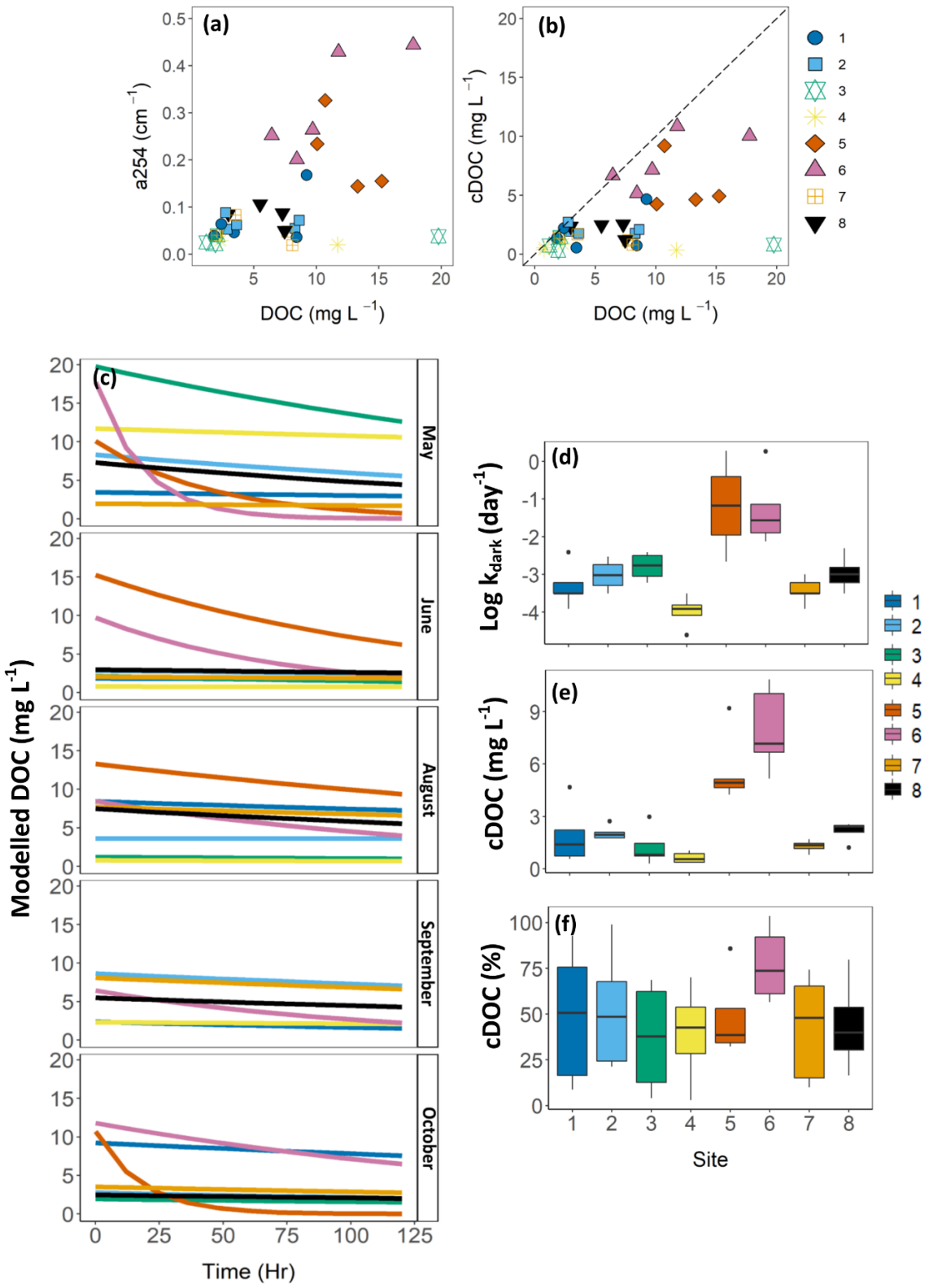

Figure 3-4. Plot of (a) DOC concentration vs. absorbance at 254 nm (a254) and (b) DOC concentration vs. cDOC concentration by site, where filled points denote significant relationships and the dotted line represents a 1:1 relationship where all DOC is colored and deviation from that

line indicates an iDOC contribution; (c) exponential decay curves for DOC, based on oxygen consumption data, grouped by month and colour coded by site; and (d – f) box plots of k, cDOC concentration, and cDOC contribution averaged by site. k is presented on a natural log scale to show small-scale variations. Note that DOC decay in (c) appears linear in most cases. Where explicit exponential decay was observed, this occurred at sites 5 and 6.

Agricultural sub-catchments also exhibited the highest cDOC concentrations (Figure 3-4e and f), in agreement with earlier work showing a strong relationship between agricultural land use and riverine colored dissolved organic matter (cDOM) concentrations in the study catchment (Felgate et al., 2021b) and elsewhere (e.g. Lambert et al., 2015; Stanley et al., 2012). The cDOC pool was split 33 ± 20 % $cDOC_a$ and 67 ± 20 % $cDOC_b$, accounting for 14 ± 8 % and 35 ± 24 % of the DOC pool, respectively.

Given the expected negative relationship between absorbance and bioavailability, we anticipated rapid remineralization of the low ($cDOC_b$) and non-absorbing (iDOC) fractions, which together accounted for 86 ± 26 % of the initial DOC pool. However, only 14 ± 10 % of total DOC was removed during our 5-day incubations (BDOC; range = 1 – 43 %). This suggests that a substantial fraction of low ($cDOC_b$) and/or non-absorbing (iDOC) material was not biologically remineralized during transit through the river network.

We did not find any correlation between iDOC and either BDOC or k (Figure 3-5). Instead, iDOC was strongly correlated with RDOC (r_s= 0.81) whilst cDOC was strongly correlated with both BDOC and k (both r_s = 0.71). We therefore suggest that the Belize River Watershed contains a significant pool of iDOC (51 ± 29 % DOC) which does not undergo substantial biological remineralization in transit, and that a small cDOC fraction (≤ BDOC = 14 ± 10 % DOC) fuels biodegradation rates. This is in agreement with isotopic evidence from the Amazon Basin where biodegradation rates are driven by a rapidly cycled, typically small, fraction of the terrigenous DOC pool (Mayorga et al., 2005), is supported by studies which demonstrate preferential utilization of cDOC over iDOC (e.g. Clark and Mannino, 2021).

RDOC was more strongly correlated with $cDOC_a$ than $cDOC_b$ (r_s = 0.60 vs. 0.41), in agreement with the theoretical characterization of $cDOC_a$ as being more aromatic (Carter et al., 2012). In direct opposition to this and against a priori expectations, $SUVA_{254}$ was more strongly correlated with $cDOC_b$ than with $cDOC_a$. However, when derived per unit cDOC ($cSUVA_{254}$) instead of per unit DOC, this finding was reversed: $cSUVA_{254}$ was positively correlated with the most aromatic fraction ($cDOC_a$; rs = 0.42) and not with the least aromatic material ($cDOC_b$), illustrating the potential for

iDOC concentrations to confound absorbance-based proxies.

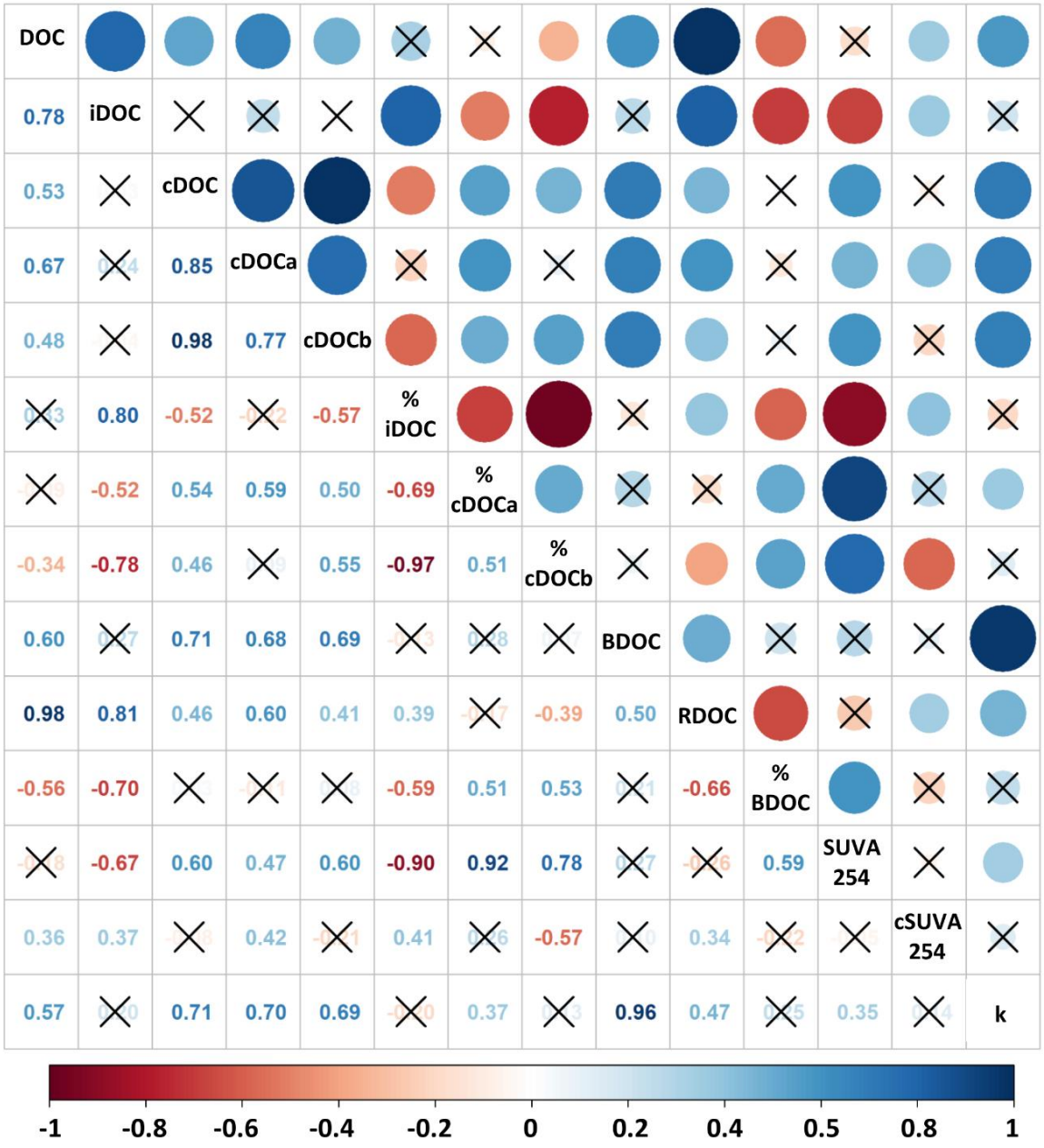

Figure 3-5. Correlogram illustrating Spearman's Rank correlations between all DOC and biodegradation related parameters, where rs > 1 indicates a positive correlation and rs < 1 indicates a negative correlation. Circle size increases with degree of correlation. Colour scale indicates direction and strength of correlation. Non-significant relationships ($\alpha > 0.05$) are marked with a cross.

Despite this evidence that $cDOC_b$ was less aromatic than $cDOC_a$, we found no evidence that it was more bioavailable: both fractions were similarly correlated with k and BDOC (r_s = 0.68 - 0.71) which suggests a potentially similar degree of utilization. Previous work has shown that lignin and other

terrestrially derived, typically $cDOC_a$-type macromolecules, may account for ~ 50 % of bulk respiration in tropical river settings (Ward et al., 2013), and so this is not an unrealistic suggestion. Incorporating time-point sampling into future incubation studies would elucidate this further.

3.7 Conclusions and implications

This study indicates that a small cDOC fraction (≤ BDOC = 14 ± 10 % DOC) fuels riverine biodegradation within the Belize River Watershed, contrary to our hypothesis that iDOC, which comprised 51 ± 29 % of the DOC pool, would be the most bioavailable fraction. This agrees with recent work indicating that a tropical microbiome may be capable of altering a wide range of DOC compositions, including highly aromatic cDOC, on daily time scales, and in the presence of a substantial iDOC pool (Spray et al., 2021).

Further study is required to understand the provenance and behaviour of iDOC. As with the wider DOC pool, freshwater iDOC is likely to originate from multiple sources and to be subject to both protective and destructive processes, all of which likely vary in space and time. The fate of iDOC is therefore uncertain, and will largely depend upon the mechanism(s) underpinning its stability. For example, abiotically stabilized iDOC, e.g. via mineral preservation (Blattmann et al., 2019) is likely to persist within the coastal ocean, whereas iDOC which is inaccessible for biotic reasons, e.g. if the local microbiome preferentially utilize cDOC, might be remineralized upon reaching a more genetically diverse downstream microbiome, similar to how 'semi-labile' surface ocean DOC is stable in the surface layer only to undergo rapid remineralization at depth (Hansell and Carlson, 1998; Sunagawa et al., 2015). The latter might contribute to coastal CO_2 outgassing, and could go some way to explaining why the amount of DOC entering the ocean far exceeds its annual turnover within the ocean interior (Bianchi, 2011; Hedges et al., 1997).

A better understanding of the fate of iDOC in tropical and sub-tropical river systems will improve our ability to quantify global land-ocean carbon export and may help reduce uncertainties in CO_2 emission estimates for these globally important regions. However, identification of iDOC in temperate systems (e.g. Adams et al., 2018; Tzortziou et al., 2015) suggests that significant iDOC contributions exist beyond the tropics, and so it is also important to determine the geographic prevalence of iDOC in order to ensure our use of absorbance based DOC prediction and characterization tools is appropriate.

3.8 Acknowledgements

SLF was supported by the NERC-funded SPITFIRE Doctoral Training Programme (grant number NE/L002531/1). DJM, BBC, and RS, and CDGB and CDE were supported by the NERC (Natural Environment Research Council, UK) Land Ocean Carbon Transfer programme (LOCATE; grant numbers NE/N018087/1 & NE/C05686, respectively). CE was supported by the NERC 'Omics' Independent Research Fellowship (grant number NE/M018806/1). This work received additional support from the UK government through the Commonwealth Marine Economies Programme, which aims to enable safe and sustainable marine economies across the Commonwealth Small Island Developing States, and from the Belize Electrical Company Ltd. (BECOL). The authors acknowledge colleagues from the Belize Department of the Environment for their assistance with logistics, and students at the University of Belize, in particular Ian Oliva, Carissa Sabido, Kelvin Requena, and Melissa Berjes, who assisted with fieldwork and whose enthusiasm and persistence made this study possible. The authors also acknowledge colleagues from the Belize Department of Hydrology for providing the data behind Figure 3-2 and David Cooper (UK CEH) for his contribution to Figure 3-3.

The authors declare no conflict of interest. All data used in this study will be made freely available prior to publication.

3.9 Author contributions

Conceptualisation: SLF; Data curation: SLF and EAH; Formal analysis: SF and EAH; Funding acquisition: RS, CE, and AC; Investigation: SLF, CDGB, and EAH; Methodology: SLF; Project administration: SLF and AC; Resources: AC, JU, JA, JV, and EM; Validation: SLF and CDGB; Visualisation: SLF and AF. Writing – original draft: SLF; Writing – review and editing: All authors.

Chapter 4 A simple, quantitative method to partition dissolved organic carbon fractions using absorbance and fluorescence measurements

This chapter was conceptualised by S. Felgate and C. Barry. S. Felgate conducted the data analysis and wrote the manuscript. Full details of author contributions are provided at the end of the chapter.

Stacey L. Felgate[1,2], Christopher D. G. Barry[3], Chris D. Evans[3], and Daniel J. Mayor[2].

[1]Ocean and Earth Sciences, University of Southampton, Southampton, UK.
[2]Ocean Biogeosciences, National Oceanography Centre, Southampton, UK.
[3]UK Centre for Ecology and Hydrology, Bangor, UK.

This chapter has been prepared for submission to Limnology and Oceanography: Methods.

Key words: Dissolved organic matter; Dissolved organic carbon; PARAFAC; Absorbance; Fluorescence

4.1 Abstract

Dissolved organic carbon (DOC) makes up ~ 50 % of the aquatic dissolved organic matter (DOM) pool. It is a significant term in the global carbon (C) cycle, and a major determinant of surface water chemistry and biology. It is of paramount importance that we understand not only the concentration and fluxes of aquatic DOC, but also its composition. Spectral techniques, including Excitation Emission Matrix - Parallel Factor Analysis (EEM-PARAFAC) are commonly used to infer DOM character, with these inferences extended to the associated DOC pool. However, variability in DOM stoichiometry means that compositional shifts in the DOM pool may not be reflected in the DOC pool with any degree of predictability, and an inability to account for the non-coloured or 'invisible' fraction (iDOC) limits our ability to interpret PARAFAC in low-color systems. Here we present a method to quantitatively partition the DOC pool into coloured and invisible fractions, the former being further partitioned according to humic-like and protein-like characteristics. We apply this method to a sub-tropical land-ocean gradient (Belize, Central America) where the contribution of non-coloured DOM is thought to be significant and variable. Our findings provide quantative values for the various DOC fractions, and suggest that PARAFAC-derived fluorescence intensity is a poor predictor for the relative contribution of fluorophore-associated DOC. We believe this method is a

small but important step forward for aquatic biogeochemistry which opens up exciting new avenues of enquiry with regards the aquatic C cycle.

4.2 Introduction

Dissolved organic matter (DOM) is a complex mixture of thousands if not millions of compounds (Wagner et al., 2020). It is typically composed of ~ 50 % humic-fulvic substances, 30 % hydrophilic acids, and 20 % low molecular weight compounds such as carbohydrates and amino acids (Aitkenhead-Peterson et al., 2003). An estimated 20 – 70 % of DOM pool is chromophoric or 'coloured'(cDOM), and the remainder is non-coloured or 'invisible' (iDOM) (Laane and Koole, 1982).

Investigations of DOM character have increasingly focused on cDOM, using absorbance and fluorescence spectroscopy to classify it according to broad chemical and structural characteristics (i.e. humic-like vs protein-like). Excitation Emission Matrix – Parallel Factor Analysis (EEM-PARAFAC) is a powerful tool for characterizing and quantifying changes in cDOM fluorescence, enabling the tracing of different fractions in the natural environments. However, different fluorescence intensities associated with different compounds mean that PARAFAC cannot be used to quantify the compounds themselves without first identifying them. Thus, in natural systems PARAFAC identifies broad component classes rather than specific and known compounds, and is therefore a qualitative rather than quantitative tool. Using PARAFAC modelling, fluorescence intensity can be derived for each component, but the fact that one component has a higher fluorescence intensity than another does not mean that it has a higher concentration, only a higher fluorescence. Data must therefore be interpreted with care. Fluorescence is not only dependent on concentrations, but on molar absorptivity and quantum efficiency, which is unknown. However, relative changes and ratios between component fluorescence can be used to illustrate the qualitative differences between samples, and if certain PARAFAC components can be identified as specific chemical analytes, absolute calibration can be performed (Stedmon et al., 2003b)

Dissolved organic carbon (DOC) makes up approximately 50% of the aquatic DOM pool, but that value is highly variable (e.g. 67 % (Bolan et al., 2011); 44 % (Moody and Worrall, 2017)). It is a major term in the global carbon (C) cycle, and so its quantification is commonplace and its fluxes oft-studied. DOC is also a major source of reduced C to aquatic ecosystems and thus an important determinant in controlling surface water chemistry and biology. It is therefore important to better understand the composition of the DOC pool, and how that composition shifts in response to various drivers, is desirable. To this end, DOC is often examined in conjunction with EEM-PARAFAC outputs to infer some degree of characterization. However, variability of DOM stoichiometry, and in the

contribution of coloured vs. non-coloured material, means that compositional shifts in the cDOM pool may not be reflected in the DOC pool, and vice versa, at least with any degree of predictability.

A first step towards improving the relatability of cDOM and DOC might be to adequately account for (and remove) the non-coloured DOC fraction (iDOC), thus comparing like with like (cDOM with cDOC). Developed by Tipping et al. (Tipping et al., 2009) and refined by Carter et al. (Carter et al., 2012), the 2-wavelength method to predict [DOC] from DOM absorbance has been well established in the literature. This model is highly successful (R^2 = 0.98) in natural waters with a high degree of coloration, but underpredicts in eutrophic or anthropogenically modified environments which commonly have high iDOC contributions. Whilst attempts to account for iDOC have been made, (Carter et al. add a uniform 0.8 mg L^{-1}) they cannot account for the high degree of variability observed in some systems (e.g. Pereira et al., 2014). Whilst this could be viewed as a failure to predict [DOC], we suggest the model be used in such systems as a predictor of [cDOC] only, and that where [DOC] is known, [iDOC] can be calculated as the residual.

Here we present a method which not only accounts for the iDOC pool, but which combines the 2-wavelength method with EEM-PARAFAC analysis to quantitatively partition the cDOC pool according to its broad chemical composition and character (i.e. invisible vs coloured, humic vs protein). Thus, we provide a technique to quantify iDOC, cDOC, humic-like DOC, and protein-like DOC, with scope to further decompose humic-like and protein-like components in line with the number of components produced via EEM-PARAFAC.

A recent study of land cover controls on the composition and fate of DOM along a sub-tropical land-ocean aquatic continuum (LOAC) used EEM-PARAFAC modelling to identify five DOM components representative of three humic-like, and two protein-like DOM types (Chapter 2). No relationship was found between [DOC] and DOM fluorescence, and whilst shifts in the relative contribution of humic-like and protein-like DOM were observed, these were not quantified. The authors remarked on their inability to quantify iDOM, and on the need to develop new ways of quantifying compositional shifts in the aquatic DOM and DOC pool. This is a problem implicit to all such studies, and one to which there has been no better solution. Here we reanalyse the data from Chapter 2, using [DOC], absorbance, and fluorescence to assign a quantitative value to the DOC associated with each of the DOM components identified.

4.3 Methods

4.3.1 Study site and sampling

DOC, absorbance, and fluorescence data were obtained from across a land-ocean gradient in the Belize River Watershed (BRW), Belize, Central America. Sampling occurred between October 2018 and October 2019 during three discrete sampling trips. DOC quantification , spectral analysis, and EEM-PARAFAC modelling were conducted according to standard methods (Badr et al., 2003; Stedmon et al., 2007). Full details are available in Chapter 2.

4.3.2 Using absorbance to quantify cDOC

UV optical absorbance of DOM can be explained by a 2 end-member model, and these end-members can be used to accurately estimate DOC concentrations in natural systems (Carter et al., 2012; Tipping et al., 2009). DOC is composed of an invisible and a coloured fraction, the latter of which can be derived according to Equation 4-1:

$$DOC = iDOC + cDOC_A + cDOC_B = iDOC + \frac{A_\lambda}{E_{AB,\lambda}} \qquad \boldsymbol{Eqn.4-1}$$

where A and B represent the 2 endmembers, A_λ is the absorbance at wavelength λ (nm), and $E_{AB,\lambda}$ is the extinction coefficient (absorbance cm^{-1} DOC_{AB}^{-1}) of the cDOM fraction. This extinction coefficient can be calculated according to Equation 4-2:

$$E_{AB,\lambda} = f_A E_{A,\lambda} + f_B E_{B,\lambda} = f_A E_{A,\lambda} + (1 - f_A)E_{B,\lambda} \qquad \boldsymbol{Eqn.4-2}$$

where f_A and f_B are the fractions of components A and B that comprise the light absorbing DOM (here $f_A + f_B = 1$), and $E_{A,\lambda}$ and $E_{B,\lambda}$ are the extinction coefficients at wavelength λ. Equation 2 can be written for two different wavelengths, λ1 and λ2, and then the ratio R defined in Equation 4-3:

$$R = \frac{E_{AB,\lambda1}}{E_{AB,\lambda2}} = \frac{f_A E_{A,\lambda1} + (1 - f_A)E_{B,\lambda1}}{f_A E_{A,\lambda2} + (1 - f_A)E_{B,\lambda2}} = \frac{A_{\lambda1}}{A_{\lambda2}} \qquad \boldsymbol{Eqn.4-3}$$

The value of R can thus be obtained from Equation 4-4 as the measured absorbance at the two wavelengths. Its combination with the extinction coefficients of components A and B yields:

$$f_A = \frac{E_{B,\lambda1} - R E_{B,\lambda2}}{R\left(E_{A,\lambda2} - E_{B,\lambda2}\right) + \left(E_{B,\lambda1} - E_{A,\lambda1}\right)} \qquad \boldsymbol{Eqn.4-4}$$

Therefore, if the values of $E_{A,\lambda1}$, $E_{B,\lambda1}$, $E_{A,\lambda2}$ and $E_{B,\lambda1}$ are known, f_A can be calculated, and then substituted back into Equation 4-2 to obtain E_{AB} at either of the two wavelengths. E_{AB} can in turn be substituted back into Equation 4-1 to obtain cDOC. DOC prediction using this method relies upon the addition of a standard iDOC term (in Carter et al. this term is 0.8 mg L^{-1}), however in systems where DOC is already known, and where confidence in cDOC prediction is high, iDOC can be calculated as the residual of DOC and cDOC.

We selected λ_{270} and λ_{350}, based on good unbiased estimations of DOC in natural, highly coloured systems (R^2 = 0.98) in Carter et al. (2012). The associated extinction coefficients are defined by as follows: $E_{A,270}$ = 77.1 L g^{-1} cm^{-1}; $E_{A,350}$ = 69.3 L g^{-1} cm^{-1}; : $E_{B,270}$ = 21.31 L g^{-1} cm^{-1}; : $E_{B,350}$ = 15.4 L g^{-1} cm^{-1}.

4.3.3 Using EEM-PARAFAC modelling to partition cDOC

PARAFAC modelling decomposes sample fluorescence into a number of distinct fluorophores, thus the total fluorescence of these components (sumFL) represents the total fluorescence of the DOM pool. As per Felgate et al. (2021), EEM-PARAFAC modelling identified five DOM components, henceforth termed C1 – C5. Excitation and emission (ex/em) maxima were as follows (secondary maxima in parentheses): C1 = <255 (355) / 470nm; C2 = <255 (310) / 410nm; C3 = 265 / 314nm; C4 = 290 / 352nm; C5 = 360 / 438nm. These components were characterised as terrestrial humic-like (C1, C2, and C5) and protein-like (C3 and C4) using the OpenFluor database (Murphy et al., 2014).

A strong linear relationship was observed between cDOC and sumFL, which allows for the calculation of DOC concentrations associated with each fluorescence component using the relevant coefficient. These can be solved for using a multiple linear regression model (Equation 4-5):

$$cDOC \sim (a\ xC1_{FL}) + (b\ x\ C2_{FL}) + (c\ x\ C3_{FL}) + (d\ x\ C4_{FL}) + (e\ x\ C5_{FL}) + 0 \qquad \boldsymbol{Eqn.4-5}$$

where $C1_{FL}$ is the peak fluorescence intensity of C1, and so on. However, an assumption of linear regression modelling is independence. A strong linearity was observed between the humic-like components in this instance (C1 ~ C2, R^2 = 0.98; C1 ~ C5, R^2 = 0.82; C2 ~ C5, R^2 = 0.75; Figure 4-1), and so these components were grouped together and termed 'humic' moving forward (Equation 4-6):

$$cDOC \sim (a\ xHumic_{FL}) + (b\ x\ C3_{FL}) + (c\ x\ C4_{FL}) + 0 \qquad \boldsymbol{Eqn.4-6}$$

This produced coefficients (a = 1.60; b = 0.44; c = 2.11; R^2 = 0.95, RSE = 0.58 on 162 DF) which allowed the calculation of component-specific cDOC concentrations (Equations 4-7 to 4-9):

$$Predicted\ Humic\ cDOC = (a\ x\ cDOC) \qquad \boldsymbol{Eqn.4-7}$$

$$Predicted\ C3\ cDOC = (b\ x\ cDOC) \qquad \boldsymbol{Eqn.4-8}$$

$$Predicted\ C4\ cDOC = (c\ x\ cDOC) \qquad \boldsymbol{Eqn.4-9}$$

These predicted cDOC concentrations were corrected as a proportion of the cDOC pool to account for variation imposed by the model fit (Equation 4-10), i.e. if predicted humic cDOC represented

30 % of the sum of the predicted cDOC components produced by this model, the corrected humic cDOC concentration would be cDOC x 0.3:

$$Humic\ cDOC = cDOC\ x\ \frac{Predicted\ Humic\ cDOC}{Total\ Predicted\ cDOC} \qquad \textbf{Eqn. 4 - 10}$$

These cDOC concentrations were then converted to a percentage of the DOC pool to allow a proportional, quantitative interrogation of the dataset in relation to the qualitative findings of Felgate et al. (2021).

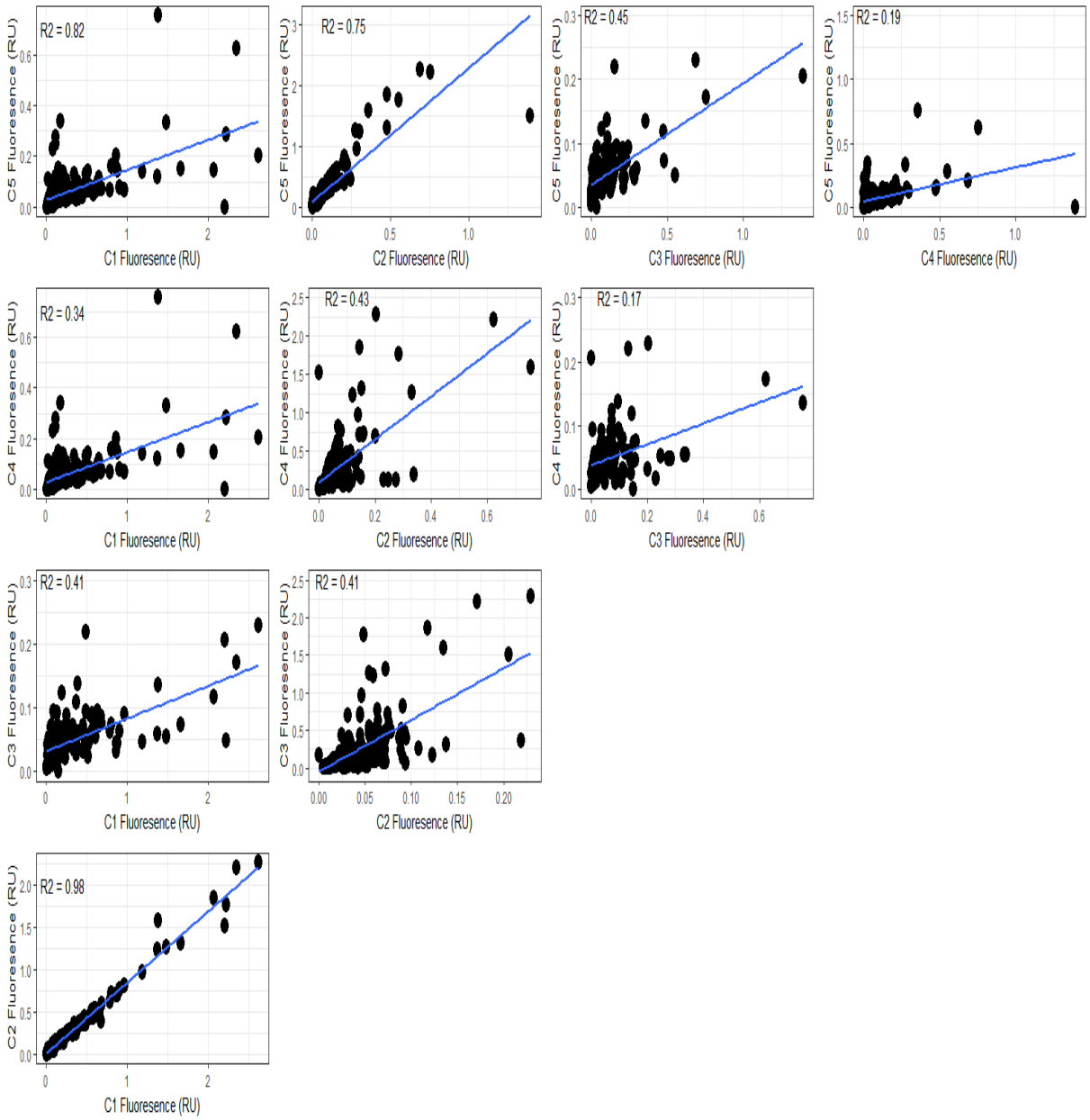

Figure 4-1. Correlation plot showing component fluorescence intensities for C1-C5. C1, C2, and C5 exhibit strong correlations with each other (R^2 = 0.75 – 0.98), whilst all other relationships are weak (R^2 > 0.45).

4.4 Assessment

4.4.1 Appropriateness of using absorbance to quantify cDOC

Whilst a strong relationship between [DOC] and cDOM has been established globally, particularly for rivers (Carter et al., 2012; Jeong et al., 2012; Weishaar et al., 2003), tropical and sub-tropical examples are less common (Spencer et al., 2010; Yamashita et al., 2010). Still fewer studies have tested this relationship in the wider tropical and sub-tropical aquatic continuum, and where such studies do exist, they are from highly-coloured systems such as wetlands (Yamashita et al., 2010), peatlands (Cook et al., 2017), and blackwater streams (Waterloo et al., 2006). To our knowledge, only (Pereira et al., 2014) have applied the 2-wavelength method in a low-colour tropical setting, and they found a high degree of variability in terms of its effectiveness, attributing this to seasonal shifts in the contribution of iDOM which could not be accounted for. In a similar vein, was it our purpose to use the 2 wavelength model to predict DOC, we would have considered it an inappropriate tool. As shown in Figure 4-2, DOC exhibited only weak correlations with a_{270} (R^2 = 0.53) and a_{350}, (R^2 = 0.50), and the model consistently under-predicted by ~ 50 % (mean under prediction = 0.48 % (SE = 0.02); mean residual = 1.98 mg L^{-1} (SE = 0.23)).

Our use of the 2-wavelength model to instead predict [cDOC] and [iDOC] represents a paradigmatic departure from previous utilizations, whereby the apparent failure of the model to predict [DOC] is in fact confirmation of a significant and variable iDOC pool. Thus, while the 2-wavelength method may not be suitable as a bulk [DOC] prediction tool in low-colour systems such as ours, we believe it can be repurposed to provide a powerful ability to separate coloured and non-coloured DOC fractions where [DOC] measurements are available. Given the fact that DOC is a standard parameter across the majority of PARAFAC studies, this makes the method presented here a small and eminently feasible additional step with the potential to yield new insight into the composition and variability of the aquatic DOC pool.

4.4.1 Appropriateness of our DOC partitioning model

The model proposed relies upon a simple assumption, which is that absorbance and fluorescence both account for the total cDOM pool. By extension, the 2-wavelength method is assumed to account for the cDOC pool in its entirety, and PARAFAC modelling is assumed to produce components which represent the cDOM pool in its entirety. In this study, a strong positive relationship was observed between cDOC and sumFL (R^2 = 0.94; Figure 4-2), which supports this (i.e.

the 2-wavelength and PARAFAC models are strongly correlated, and therefore the fractions of the DOC/DOM pool described are the same, or at least so different that it becomes significant).

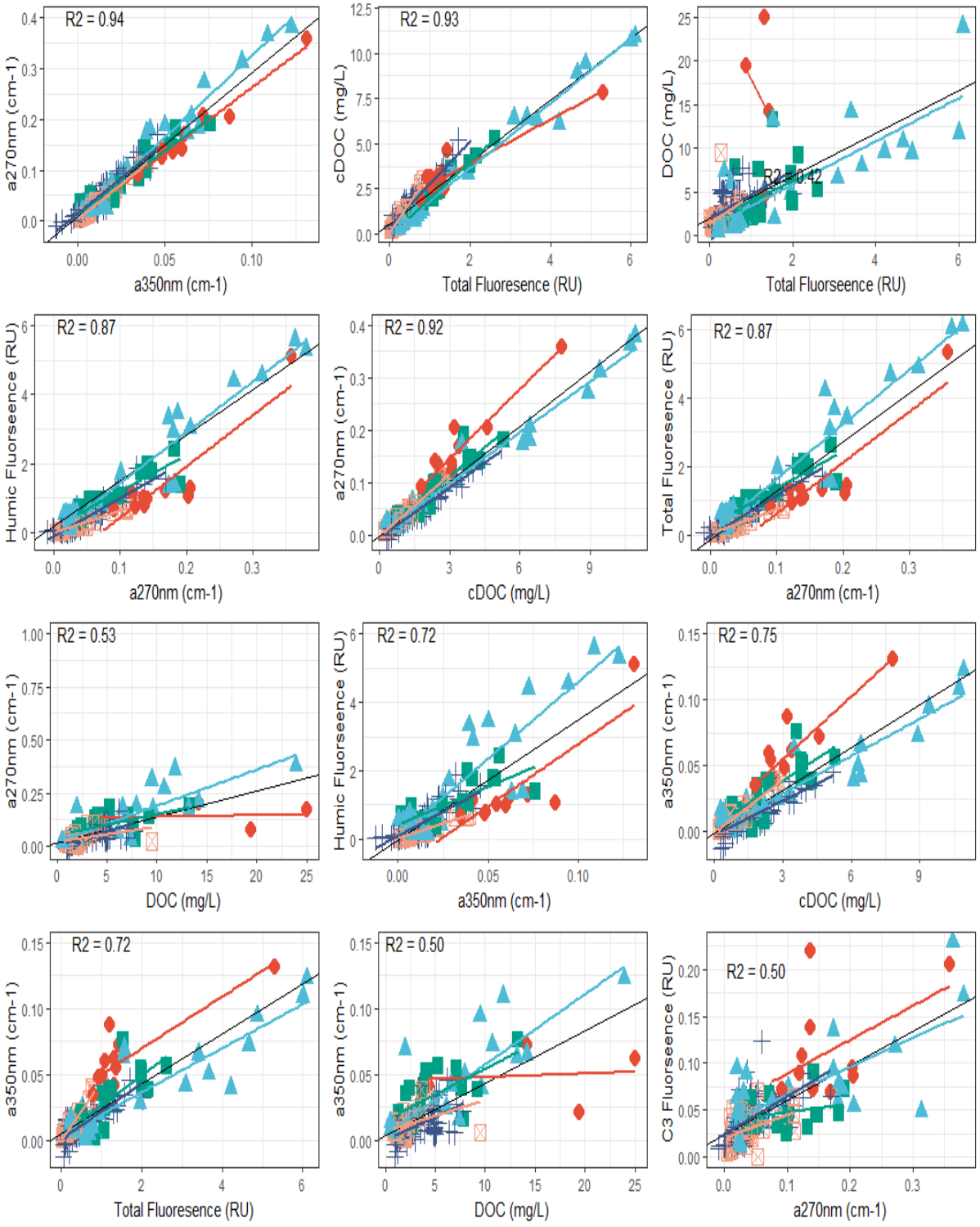

Figure 4-2. Correlations between key parameters. Key denotes sample source: red diamonds = dam; blue triangles = tributary; green squares = river; navy pluses = coastal; peach empty squares = atoll.

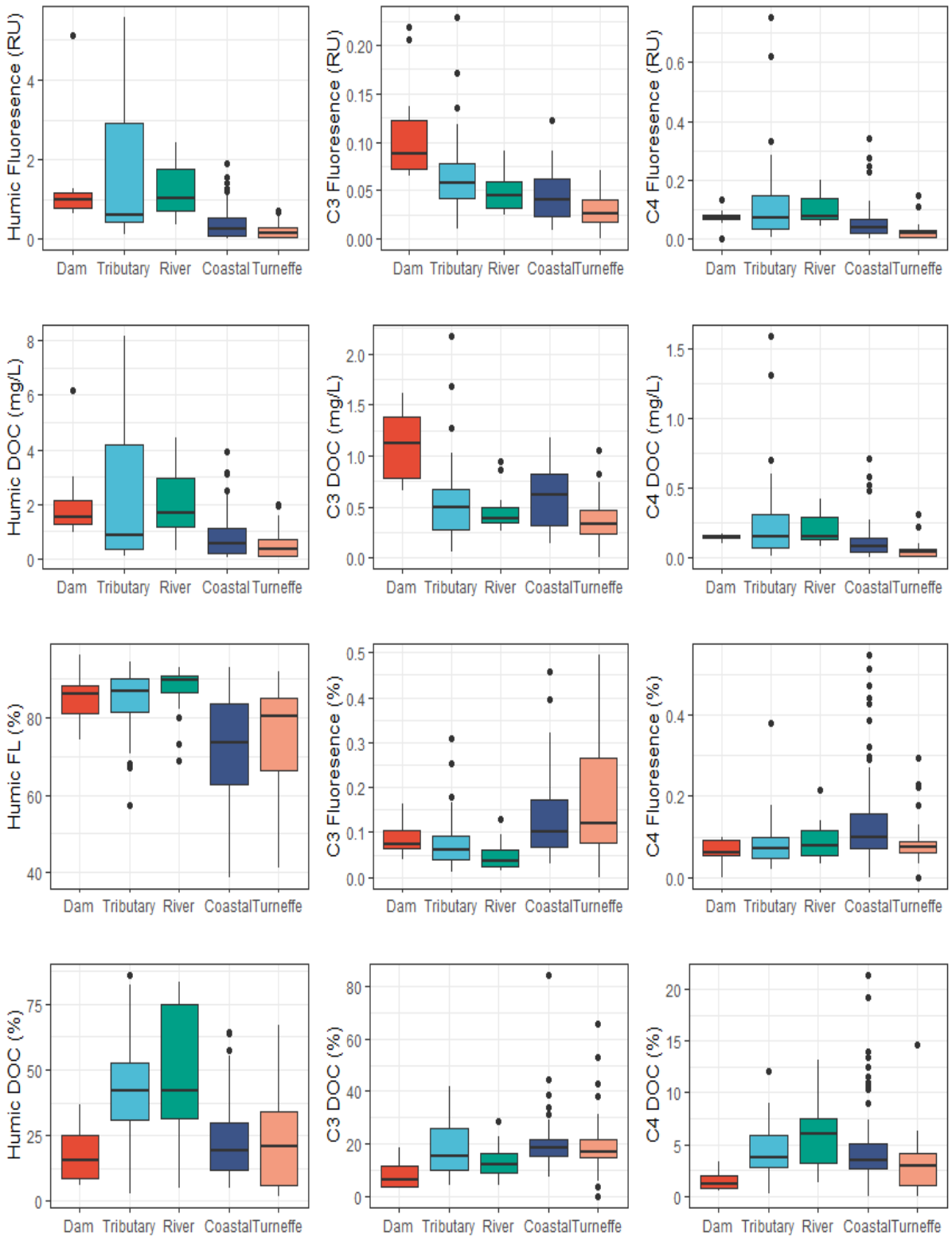

Figure 4-3. Fluorescence and fluorophore-associated DOC along a land-ocean continuum in Belize, Central America, given as absolute and percentage values.

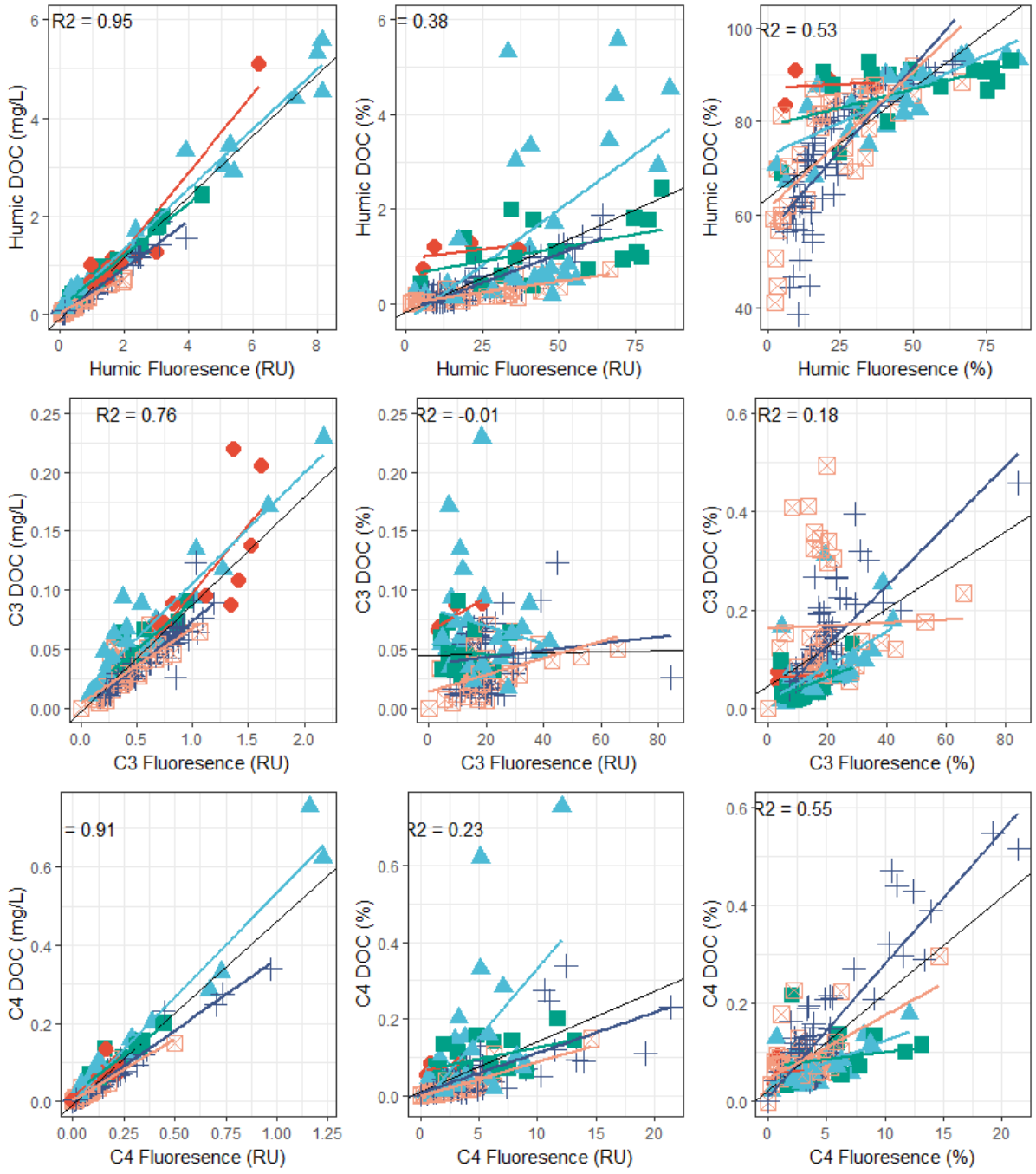

Figure 4-4. Relationships between fluorescence and fluorophore-associated DOC, given as absolute and percentage values. Key as per Figure 4-2.

4.1 Discussion

4.1.1 A low-resource tool compared to other existing options

Whilst 1000s of studies have investigated the composition of the DOM pool and extended this to DOC, fewer studies have investigated the composition of the aquatic DOC pool directly (e.g. not

relative to DOM; Hedges et al., 1994; Heikkinen, 1994; Sachse et al., 2005, 2001; Wu et al., 1997). These studies classify DOC according to a recalcitrant or labile categorization model, separating recalcitrant compounds (e.g. humics and fulvics) from more labile compounds (e.g. carbohydrates, peptides, and amino acids). For example, Sachse et al. (2005) used automated size exclusion chromatography to fractionate DOC according to different groups, and to quantify those fractions. Other studies have used ultra-high resolution mass spectrometry to characterise the aquatic DOC pool according to its chemical composition (e.g. Kim et al., 2006). Whilst such non-optical techniques have the advantage of being able to treat coloured and non-coloured fractions as one pool, each has their own weaknesses, the discussion of which is beyond the scope of this paper. What is clear is that they each require specific analytical techniques which go beyond the scope of most contemporary investigations of the aquatic DOM pool, and thus their application requires significant additional resource. The method we present utilizes data already commonly collected in such studies, and therefore has the potential to add similar value at no additional financial cost and requires only a modest additional step during data analysis.

We note that this method does not account for variable fluorescence efficiencies. Humic-like compound classes have broadly similar efficiencies and thus, this method is likely to work well where humics dominate, but may work less well in the presence of a larger proportion of protein-like material .Further validation is required to test this and further refine the model.

4.1.2 New insights

For those using optical techniques to study the aquatic DOM pool, DOC has represented a ‘black box’ whereby absolute concentrations masked internal compositional dynamics and fluctuations which could not be identified. The method presented in this paper provides a simple additional step to traditional absorbance and fluorescence analysis which moves us from qualitative to quantitative understanding, at least in so far as the DOC pool is concerned. We therefore consider this to be a small but important step forward for aquatic biogeochemistry which opens up new possibilities and exciting research questions.

In particular, by applying this method across a land-ocean continuum, we have demonstrated its suitability across a wide range of environments: fresh, brackish, and saline waters; headwaters, dams, tributaries, rivers, the coastal zone, and a mangrove atoll. A major gap in the global C cycle lies in our understanding of what controls the export of DOC from land to sea. The wide range of environments involved in the production, transfer, and processing of terrigenous DOC across the LOAC results in a high degree of variation with regards cDOM composition, but little is known about

changes in the relative contribution of DOC components. This method therefore represents a new opportunity to investigate how e.g. land use change, nutrient pollution, point-source pollution, or extreme weather events alter the internal dynamics which underpin bulk DOC measurements without the caveats of an undetermined iDOC contribution and/or qualitative rather than quantative findings.

4.2 Conclusion

DOC makes up ~50% of the aquatic dissolved organic matter (DOM) pool. It is a significant term in the global carbon (C) cycle, and a major determinant of surface water chemistry and biology. It is of paramount importance that we understand not only the concentration and fluxes of aquatic DOC, but also its composition. Spectral techniques, including Excitation Emission Matrix - Parallel Factor Analysis (EEM-PARAFAC) are commonly used to infer DOM character, with these inferences transferred to the associated DOC pool. However, variability in DOM stoichiometry means that compositional shifts in the DOM pool may not be reflected in the DOC pool with any degree of predictability, and an inability to account for the non-coloured fraction limits our ability to interpret PARAFAC in low-color systems. Here we present a method to quantitatively partition the DOC pool into coloured and invisible fractions, the former being further split into humic-like and protein-like fractions. We apply this method to sub-tropical land-ocean gradient where the contribution of non-coloured DOM is thought to be significant and variable. Our findings provide quantative values for the various DOC pools, and suggest that PARAFAC-derived fluorescence intensity is a poor predictor for the relative contribution of fluorophore-associated [DOC] across a sub-tropical land-ocean gradient. Such shifts have the potential to provide new insight to biogeochemical investigations of aquatic DOM/DOC.

4.3 Acknowledgements and data

This work was supported by the NERC Land Ocean Carbon Transfer programme (LOCATE; grant number NE/N018087/1). SF received additional funding from the NERC-funded SPITFIRE Doctoral Training Programme (grant number NE/L002531/1). The authors declare no conflicts of interest. The data used in this study is freely available from the following DOI: 10/f75z (All 2018); 10/f754 (Freshwater 2019); 10/f75t (Coastal 2019). Data from Turneffe Atoll will be made available prior to publication.

4.4 Author contributions

SF and CB conceptualized the method. SF conducted formal data analysis, visualisation, and wrote the original manuscript draft. All authors contributed to reviewing and editing of the manuscript

Chapter 5 The prevalence of 'invisible' dissolved organic carbon in freshwaters

S. Felgate conceptualised this study with input from D. Mayor and C. Evans, and led data analysis and manuscript preparation. M. Peacock assisted with collation of a global data set. Full details of author contributions are provided at the end of this chapter.

Stacey L. Felgate[1,2], Daniel J. Mayor[2], Jennifer Williamson[3], B. B. Cael[2], Michael Peacock[4], Daniel J. Lapworth[5], Suman Acharya[6], Roxane Anderson[7], Rupak Aryal[8], Christopher D. G. Barry[3], Joshua Dean[9,10], Martyn Futter[4], M. Gloria Pereira[11], Jasmin Godbold[1], Al Grinham[12], Alicia Holland[6], Alex Hunt[11], Elizabeth Jakobsson[13], Paddy Keenan[11], Vasilis Kitidis[14], Dolly Kothawala[13], Thibault Lambert[15,16], Ruth Matthews[18], Filip Moldan[19], Don Monteith[3], Alan Radbourne[3], Andy P. Rees[14], Richard Sanders[2,20], Ewen Silvester[6], Bryan Spears[21], John Stephens[14], Barry Thornton[22], and Chris D. Evans[3].

[1]Ocean and Earth Sciences, University of Southampton, Southampton, UK.
[2]Ocean Biogeosciences, National Oceanography Centre, Southampton, UK.
[3]UK Centre for Ecology and Hydrology, Bangor, UK.
[4]Swedish University of Agricultural Sciences, Uppsala, Sweden
[5]British Geological Survey, Wallingford, UK
[6]Department of Ecology, Environment, and Evolution, La Trobe University, Wodonga, Australia
[7]Environmental Research Institute, University of the Highlands and Islands, Thurso, UK
[8]School of Civil and Environmental Engineering, University of Technology, Sydney, Australia
[9]Department of Earth Sciences, Vrije Universiteit Amsterdam, Netherlands
[10]School of Environmental Sciences, University of Liverpool, Liverpool, UK
[11]UK Centre for Ecology and Hydrology, Lancaster, UK
[12]School of Civil Engineering, University of Queensland, Australia
[13]Uppsala University, Uppsala, Sweden
[14]Plymouth Marine Laboratory, Plymouth, UK
[15]Chemical Oceanography Unit, University of Liege, Belgium
[16]Institute of Earth Surface Dynamics, University of Lausanne, Lausanne, Switzerland
[17]Nanyang Technical University, Singapore
[18]School of Environmental Sciences, University of East Anglia, Norwich, UK
[19]IVL Swedish Environmental Institute, Gothenburg, Sweden
[20]Norwegian Research Centre, Bergen, Norway
[21]UK Centre for Ecology and Hydrology, Edinburgh, UK
[22]James Hutton Institute, Aberdeen, UK

This chapter has been prepared for submission to Nature Geoscience. Methods text and supplimentary information are included at the end of the Chapter.

5.1 Abstract

Freshwater dissolved organic carbon (DOC) fluxes are a significant and changing component of the global carbon cycle. These fluxes are widely considered to be dominated by chromophoric or 'coloured' material (cDOC), and DOC is often characterised and quantified using optical tools which specifically target this fraction. However, multiple studies now point towards a sizeable non-coloured or optically 'invisible' DOC (iDOC) pool, which is not captured by such characterisations. Few studies have directly investigated iDOC, such that the magnitude of iDOC fluxes as well as their source, composition, behaviour, and geographic variation all remain poorly understood. Here we combine detailed catchment and national-scale river data to show that iDOC accounts for over 20 % of annual riverine DOC export (0.23 Tg C yr^{-1}) in Great Britain, with spatial variation in catchment-scale mean annual export positively associated with forest cover and dairy cattle density. Using > 2,900 samples from the range of climatic settings found across five continents we find a similar result: iDOC accounts for 26 % (range = 0 – 97 %) of measured DOC fluxes. Our results indicate that iDOC is more prevalent in systems with a high degree of anthropogenic influence and/or a high residence time. We conclude that iDOC is a globally significant pathway for carbon transport, the broad-scale importance of which has yet to be studied in detail. This has implications for our understanding of aquatic biogeochemistry, and for the use of optical parameters to quantify and characterise DOC.

5.2 Introduction

Dissolved organic matter (DOM) is a complex mixture of thousands if not millions of compounds, the reactivity of which is determined by a combination of intrinsic (e.g. chemical) and extrinsic (e.g. environmental) variables (Hansen et al., 2016; Nebbioso and Piccolo, 2013; Raymond and Spencer, 2015; Wagner et al., 2020). The concentration and composition of DOM has widespread ecological and biogeochemical implications for water quality, and carbon cycling in aquatic systems (Nebbioso and Piccolo, 2013). It is therefore critical that we have the means and understanding with which to adequately quantify and characterise it.

Concentrations of DOM are generally expressed in terms of their carbon content, as dissolved organic carbon (DOC). Studies have repeatedly demonstrated a strong relationship between DOC and chromophoric or 'coloured' DOM (cDOM), including a study of 34 North American sites spanning cold-temperate, temperate, and sub-tropical climates (R^2 = 0.93; Brezonik et al., 2015), and a global study incorporating > 12,000 paired measurements taken across a range of environmental settings

(R^2 = 0.92; Massicotte et al., 2017). This relationship underpins efforts to model DOC concentrations from cDOM absorbance spectra. The frequently adopted 'two-wavelength model'(Carter et al., 2012) found good agreement between DOC and cDOM absorbance across ~1700 samples from a range of freshwater environments (R^2 = 0.98; Carter et al., 2012). These findings have been replicated many times across a range of diverse environments including headwater streams (Peacock et al., 2014), peatlands (Cook et al., 2017), lakes (Griffin et al., 2018), and rivers (Spencer et al., 2012). However, the relationship between DOC and cDOM is not universally robust and most studies report a sub-set of samples for which it does not hold (Adams et al., 2018; Brezonik et al., 2015; Griffin et al., 2018; Spencer et al., 2012). This decoupling of DOC and cDOM absorbance is commonly attributed to the presence of a non-coloured or 'invisible' DOC fraction (iDOC), and is particularly prevalent in systems subject to high degrees of anthropogenic influence (Massicotte et al., 2017; Spencer et al., 2012) or with long residence times (Adams et al., 2018). The frequency with which this decoupling is reported suggests that it is pervasive. However, very few studies have explicitly investigated iDOC, adapting the aforementioned 'two-wavelength' model to quantify it in a tropical headwater stream (Pereira et al., 2014), a series of eutrophic lakes (Adams et al., 2018), and a sub-tropical river catchment (Chapter 3). In each case, iDOC has accounted for a significant yet variable fraction of the DOC pool. However, these studies present a number of apparent contradictions, characterizing iDOC as both algogenic (Adams et al., 2018) and terrigenous (Pereira et al., 2014), and comprising low-molecular weight moieties thought to be bioavailable (Pereira et al., 2014) yet behaving as though biologically stable (Chapter 3). Major uncertainties exist in our understanding of the prevalence of iDOC and its role in aquatic carbon cycling around the world.

Here we estimate freshwater iDOC contributions at catchment, land-mass, and global scales. We used paired DOC and absorbance data to determine the prevalence of iDOC at catchment, land-mass, and global scales. The underlying data were derived from (a) year-round monitoring of two GB river catchments with contrasting land-use; (b) year-round monitoring of the Great British (GB) land-mass; and (c) a collated dataset of > 2,900 time-point samples covering a range of aquatic, climatic, and geographic settings from across five continents (see Section 5.5).

5.3 Results and Discussion

5.3.1 Catchment scale

We analysed monthly DOC and absorbance samples from May 2019 to February 2020 at 23 sites across two GB river catchments with contrasting land cover: the Conwy (North Wales), a near-

natural catchment dominated by peatland and rough grazing, and the Tamar (South England), a highly modified catchment dominated by intensive grazing. Full site descriptions are given in Supplementary Information (Text S1) alongside detailed land cover mapping (Figures S1 – S4).

DOC concentrations in the Conwy (6.8 ± 5.0 mg L^{-1}; mean ± SD) were within the expected range (e.g. 3.0 – 7.9 mg L^{-1}; Mattsson et al., 2009). DOC and cDOC exhibited a strong positive correlation (Figure 5-1; R^2 = 0.98, p = < 0.001) in agreement with the established relationship for this catchment (Austnes et al., 2010) and for natural temperate systems more broadly (Carter et al., 2012; Massicotte et al., 2017; Spencer et al., 2012). Mean iDOC accounted for just 3 ± 15 % of the Conwy DOC pool, but was consistently > 20 % DOC in the most modified sub-catchments (Figure 5-2).

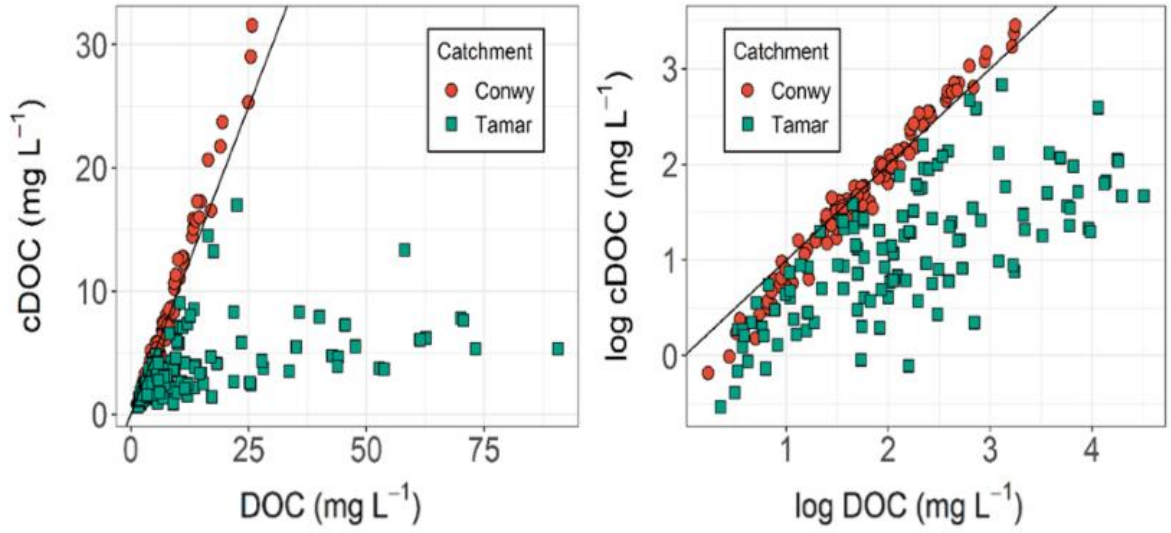

Figure 5-1. : Plots of DOC vs. cDOC as absolute and natural log values in the Conwy (red circles) and Tamar (green squares). Black line indicates 1:1 relationship where cDOC = 100% DOC.

DOC concentrations in the Tamar (15.2 ± 18.1 mg L^{-1}) were higher than expected based on previous work in the catchment (e.g. 2.3 – 5.3 mg L^{-1}; Miller, 1999 and 5.4 – 6.1 mg L^{-1}; Lloyd et al., 2019). We were unable to identify any sample processing or analytical issues to suggest that our DOC data were incorrect: samples from the Tamar and Conwy were collected, handled, and analysed following standard protocols and using centralised facilities such that any systematic issue would be present across both catchments (see Section 5.5), and we could find no evidence of a catchment-specific issue in the Tamar (Text S2; Figures S5 – S6). The correlation between DOC and cDOC was strongest in near-natural, moorland-dominated sub-catchments (R^2 = 0.73; p = < 0.001), but weak at catchment scale (R^2 = 0.21, p = < 0.001) which reflected a mean iDOC contribution of 57 ± 25 % DOC. Mean iDOC concentrations for each sub-catchment exhibited a strong and linear increase with dairy

cattle density (R^2 = 0.82; p = 0.002) and were also positively correlated with average flow (R^2 = 0.39; p = 0.002; Table S2 and Figure S7). Dairy farming produces large volumes of liquefied manure in the

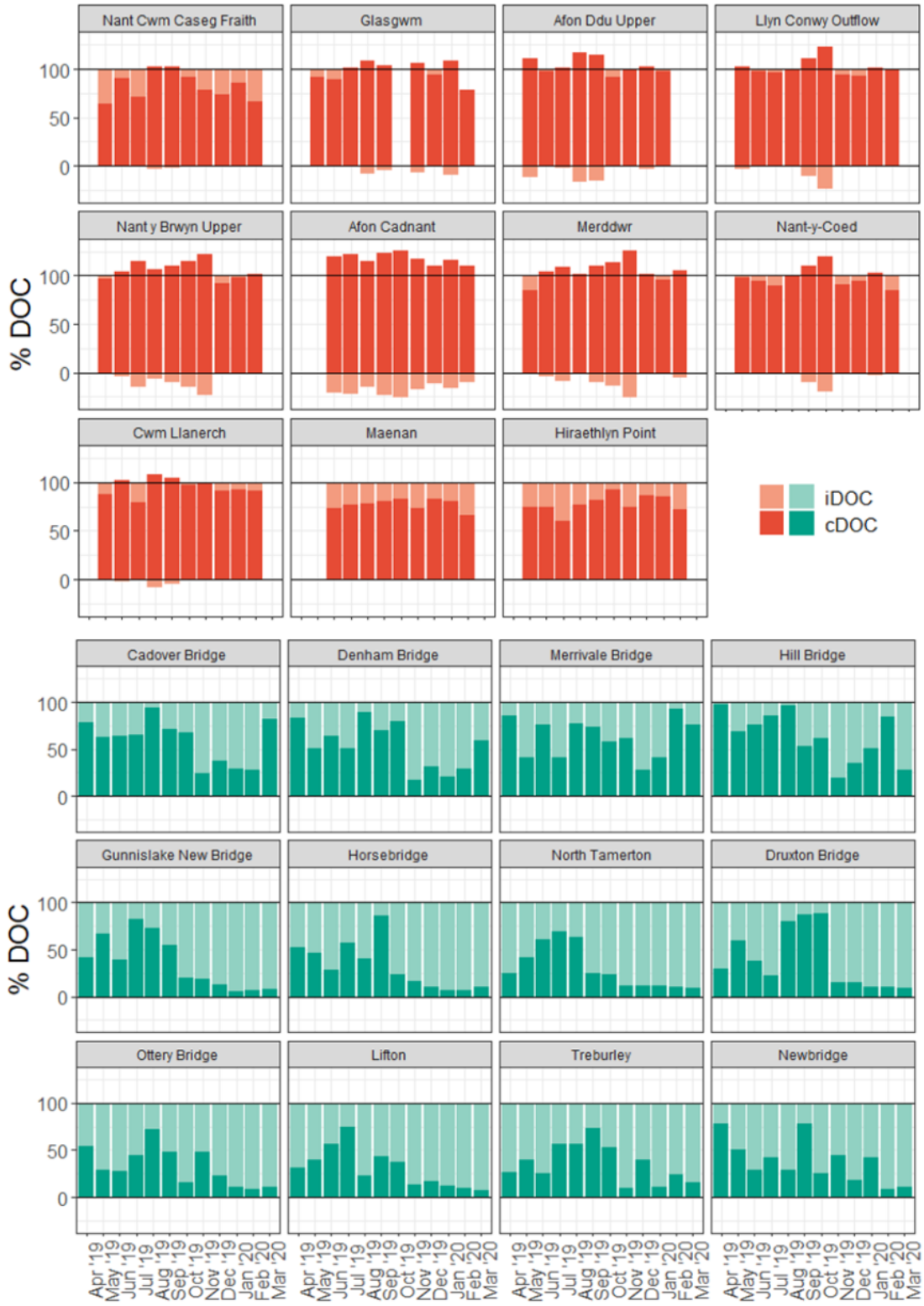

Figure 5-2. DOC composition in the Conwy and Tamar, plotted by site and month. Black lines indicate 0 and 100%. Instances where cDOC > 100% and iDOC < 0% are model artefacts, likely due

to elevated absorbance values. In such cases, the DOC pool can be considered 100% cDOC. The associated DOC concentration values are presented in Supplementary Information (Figure S9; Table S4).

form of slurry, which is stored in tanks and applied to the land as fertilizer. If poorly timed relative to rainfall, this application can result in large quantities of DOM being washed into waterways (e.g. Ramos et al., 2006). Dairy manure contains a high % of molecules associated with iDOC including mono- and polysaccharides (Jarde et al., 2007). Thus, iDOC runoff from slurry is a plausible explanation for these results.

5.3.2 GB landmass-scale

Monthly DOC concentrations were measured in rivers covering 38% of the land-mass of Great Britain (GB) by catchment area between January and December 2017, producing an estimated GB-scale annual flux to estuaries of 1.15 Tg DOC yr^{-1} (Williamson et al., 2021). Here we combine these data with absorbance scans to partition that flux into cDOC and iDOC fractions, using multiple linear regression modelling to scale export fluxes at 1 km^2 resolution (Text S3; Tables S5 – S10; Figures S10 – S13). Spatial variation in DOC export was best explained by % forest, % peat soils, and % acid grass (Equation 5-1; $R^2 = 0.91$; $p = < 2.2 \times 10^{-16}$). These land cover types are associated with organic-rich, wet environments which typically export highly coloured material (Xenopoulos et al., 2021). Unsurprisingly, these same catchment characteristics also explained a high degree of variability in cDOC export (Equation 5-2; $R^2 = 0.92$; $p = < 2.2 \times 10^{-16}$), whereas iDOC export was best explained by % forest and mean dairy cattle density (Equation 5-3; $R^2 = 0.73$; $p = 1.45 \times 10^{-10}$). This result is consistent with the understanding that forests release iDOC via leaf inputs, and suggests that dairy farms are an important additional source of iDOC at a national scale.

$$Areal\ DOC\ flux = (0.19 * \%\ Forest) + (0.10 * \%\ Peat\ Soils) + (0.07 * \%\ Acid\ Grass) \quad \boldsymbol{Eqn.\ 5-1}$$

$$Areal\ cDOC\ flux = (0.15 * \%\ Forest) + (0.01 * \%\ Peat\ Soils) + (0.05 * \%\ Acid\ Grass) \quad \boldsymbol{Eqn.\ 5-2}$$

$$iDOC\ flux = (0.05 * \%\ Forest) + (0.032 * Mean\ Dairy\ Cattle\ \ Density) \quad \boldsymbol{Eqn.\ 5-3}$$

Using these models to predict per-area yields at GB scale gave a total DOC export flux of 1.15 Tg yr^{-1} with an uncertainty range of 0.96 – 1.33 Tg yr^{-1}. This flux was split 79 % cDOC (mean = 0.91 Tg yr^{-1}; range = 0.77 – 1.06 Tg yr^{-1}) and 21 % iDOC (mean = 0.23 Tg yr^{-1}; range = 0.19 – 0.27 Tg yr^{-1}).

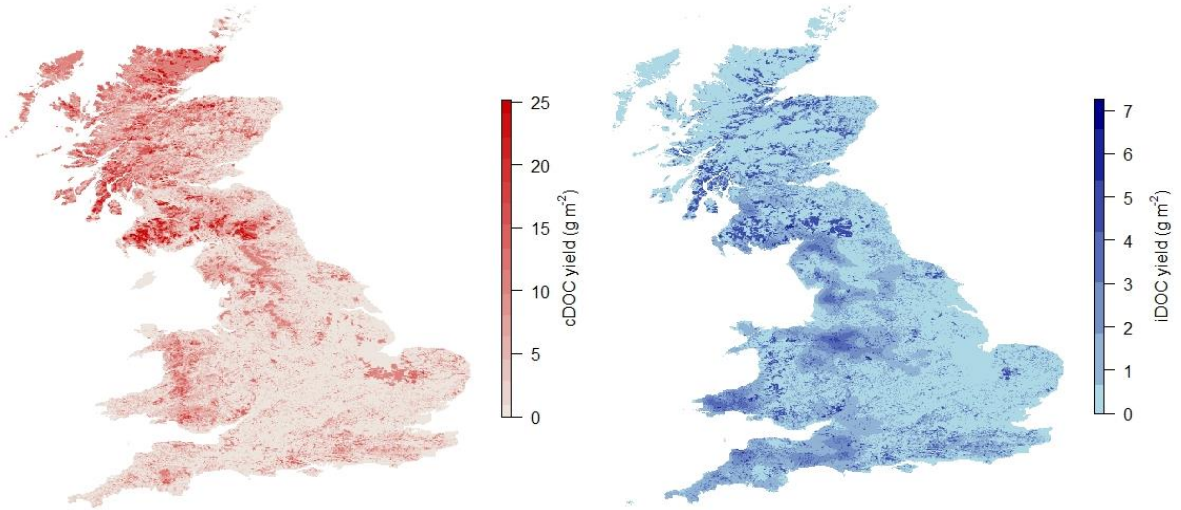

Figure 5-3. Modelled annual yields for cDOC and iDOC (g m^{-1} yr^{-1}) at 1km grid scale across GB. Note that this extrapolation effectively predicts observed fluxes at the sampling points closest to the tidal limit and thus cannot strictly be considered a map of the cDOC / iDOC produced by each grid cell.

5.3.3 Global scale

Finally, we collated a dataset of paired DOC and absorbance samples (n = 2911) from a range of published (13 studies, n = 1603) and unpublished (17 studies, n = 1208) datasets spanning a wide range of climatic and geographic settings (Table S11 and Spreadsheet S1). Whilst iDOC was not present in every sample, it was present in every data set (Table S11). The mean iDOC contribution across all samples was 26 ± 25 % DOC (Figure 5-4). The application of reasonable uncertainties (up to 20 % DOC; Table S12) did not significantly alter our findings.

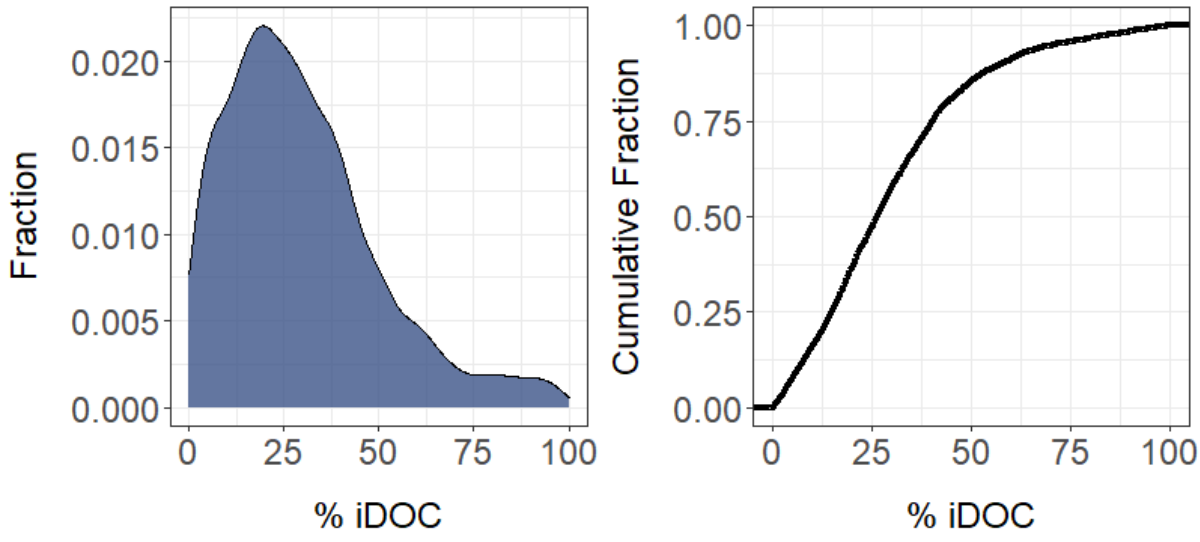

Figure 5-4. Distribution plot for % iDOC in a collated dataset of freshwater samples (n = 2911).

The lowest iDOC contributions were observed in near-natural, organic-rich systems, such as the relatively pristine Flow Country peatlands in northern Scotland (iDOC = 7 ± 8 %) and some Swedish rivers and lakes (iDOC = 9 ± 11 %). However, sites from the Uppland region of Sweden had larger iDOC contributions (iDOC = 16 ± 35 %). The highest iDOC contributions were observed in more modified settings. For example rivers in Belize (iDOC = 37 ± 37 %) and Brazil (iDOC = 40 ± 13 %), both of which are subject to ongoing deforestation and agricultural expansion (e.g. Chapter 2). However, substantial iDOC concentrations were also observed in systems which are not subject to high levels of anthropogenic influence, however, such as Greenland (iDOC = 56 ± 17 %), Siberia (iDOC = 23 ± 22 %), and remote ponds sampled on West Falkland (iDOC = 75 ± 12 %) where a more natural source seems likely. At the same time, some rivers subject to relatively high levels of catchment modification contained very low levels of iDOC (e.g. Malaysian Borneo; iDOC 12 ± 14 %). It is likely that the mode of modification (e.g. conversion of forested land to livestock and crop agriculture in Belize vs. palm plantation in Malaysia) is highly influential. We therefore conclude that iDOC is a pervasive and highly variable component of the global DOC pool which is most prevalent in waterbodies subject to substantial anthropogenic perturbation, but which can also be found in less modified settings.

5.4 Implications

Our study demonstrates that iDOC constitutes a significant, and sometimes dominant, fraction of the terrigenous DOC pools across a broad range of water body types and environments, from the Arctic to the tropics. The presence of iDOC has been recognised previously, but its prevalence and extent was unknown. Our analysis suggests that it may comprises around 25 % of the total DOC pool on average, and that it is highest in anthropogenically modified catchments. Estimates of DOC concentrations based on optical properties will therefore under-estimate DOC concentrations by a similar amount, and may lead to inaccurate conclusions regarding the composition and function of aquatic DOC, as well as errors in calculations of land-ocean carbon fluxes. Optically-based approaches to monitor aquatic DOC concentrations via both satellites and in situ platforms will require careful calibration and understanding of iDOC variability before the resulting data can be robustly interpreted and understood. Failing to do so may exclude a sizeable fraction of DOC that is most susceptible to anthropogenic perturbation. Greater understanding of the source, composition, and reactivity of iDOC is required in order to better characterise its role in aquatic systems, including its contribution to CO_2 degassing and land-ocean carbon transport, and thus its role in the global carbon cycle.

5.5 Methods

Catchment scale sample collection occurred on a monthly basis between May 2019 and February 2020 in the Conwy and Tamar catchments. GB scale sample collection occurred on a monthly basis between January and December 2017. In both cases, sampling trips were planned to coincide across catchments where ever possible, and in all cases were conducted within 1 week of each other. Water samples were syringe filtered (Fisher® 0.45µm cellulose acetate) into a 60ml HDPE Nalgene® bottle for DOC analysis and a 30ml amber glass Whatman® bottle fitted with a PTFE cap for spectral analysis. Sample bottles were pre-washed (10% HCl for 24hrs) and rinsed with Milli-Q® water, and triple rinsed with sample filtrate in the field. Samples were kept cool and dark in transit, and then stored at 4°C until they could be analysed. DOC concentrations were quantified using the NPOC (Non-Purgeable Organic Carbon) method on a Shimadzu TOC-L analyser (Shimadzu, Japan). Prior to analysis, filtered samples were acidified to pH 2 using 1M HCl, then purged with zero grade air for 6 minutes to remove any inorganic carbon. DOC (as NPOC) was measured using infrared absorbance as CO_2 following combustion at 720°C over a Pt-catalyst. Two calibration ranges were used (0 – 10 mg L^{-1} and 10 – 50 mg L^{-1}) depending on the concentration of the samples, and samples which fell out with this calibration range were re-run post dilution. Limits of detection for DOC were 0.6 mg L^{-1}. Certified reference materials (WR1, 2, and 3) were run every 30 samples or less at concentrations of 5, 10, and 40 mg L^{-1}. Instrument precision was checked on ~ 5 % of samples with an expected precision of within 10%. Absorbance scans were conducted on a Cary 60 UV-Vis spectrophotometer (Agilent, USA) using a 1cm quartz cuvette and scanning at 1nm intervals between 200 and 800nm. Scans were corrected for instrument drift by subtracting the mean value between 600 and 700nm. UV optical absorbance of cDOM can be explained by a two end-member model, and these end-members can be used to accurately estimate DOC concentration (Carter et al., 2012; Tipping et al., 2009). This method relies upon the addition of a fixed residual iDOC term (0.8 mg L^{-1} in Carter et al. 2012). Where DOC is already known, iDOC can be derived as the residual of DOC and cDOC (Pereira et al., 2014b). We applied this method using 270 nm and 350 nm as end-members, based on good unbiased estimations made in natural, highly coloured systems (R^2 = 0.98; Carter et al., 2012).

For collated data where absorbance was not available at one or both of the specified wavelengths (270 and 350 nm) these were derived via modelling of the complete spectra, and the error associated with this process derived via comparison with data derived from complete spectra using the same method. For hyperspectral measurements with data present at < 270 nm, > 350 nm, and between 271 and 349 nm, absorption at the desired wavelengths was estimated using a cubic spline interpolation (median error = 0.1 %). For hyperspectral measurements with no data < 270 nm,

absorbance at 350 nm was estimated as above if not measured, and absorption at 270 nm was estimated by fitting an exponential decay function to the absorption spectra which we then evaluated at 270 nm (median error = 1%). For multispectral measurements where measurements were not made at 270 and 350 nm, absorption was estimated by fitting the same exponential decay function to the absorption spectra, including a zero absorption point at 700 nm (median error = 8 % at 270 nm and 6 % at 350 nm). Interpolations and fits were performed in Matlab R2019a. Code will be made freely available on Zenodo for publication.

5.6 Acknowledgements

SLF was supported by the NERC-funded SPITFIRE Doctoral Training Programme (grant number NE/L002531/1). This study was supported by the NERC (Natural Environment Research Council, UK) Land Ocean Carbon Transfer programme (LOCATE) as follows: DJM, BBC, DJL, and RS (grant number NE/C05686/1), CDE, JW, CDGB, MJP, AR, PK, DM, and BS (grant number NE/C05686/1) and APR, VK, and JS (grant number NE/ NE/N018087/1).

The authors declare no conflict of interest. Land-mass scale data (GB dataset) are available from Environmental Information Data Centre (EIDC) here: (https://doi.org/10.5285/08223cdd-5e01-43ad-840d-15ff81e58acf). Catchment scale (Tamar and Conwy) will be archived with the EIDC and made freely available prior to publication. Unpublished global-scale data will be provided as a supplementary spreadsheet on publication.

5.7 Author contributions

DJM, CDE, RS, BS, APR, VK, and DJL obtained funding and conceptualised the LOCATE sampling strategy. SLF and CDE conceptualised this study. SLF wrote the original manuscript draft, in consultation with CDE, MP, DJM, CDGB, and DJL. SLF conducted data analysis and modelling in collaboration with JW (GB-scale) and BBC (global-scale). DM provided additional data investigation and validation. MGP, AH, and PK conducted laboratory analyses. DJM, CDE, JG, and BT provided supervision. JS and AR led field work in the Tamar and Conwy catchments, respectively. Unpublished data were provided by SLF, MP, SA, RAn, RAr, JD, MF, AG, AH, EJ, DK, TL, RM, FM, and ES.

5.8 Supplementary Information

Text S1. Site descriptions (Tamar and Conwy)

The River Conwy (North Wales) has a catchment area of 580 km^2, a maximum altitude of 1064 m above sea level (ASL), an annual average rainfall (AAR) of 2042 mm (1961 – 1990), and a base flow index (BFI) of 0.28 (NRFA Station 66011). Catchment population is skewed towards the lower reaches. The Conwy finds its source in an extensive are of blanket bog (the Migneint), and drains north into the Irish Sea through a mixed landscape characterised by acid grassland (36%), intensive grassland (30%), forest (18%), and blanket bog (12%). Catchment geology is characterised by Cambrian igneous and sedimentary rock to the west, and Silurian mud stones to the east.

The River Tamar (South East England) is approximately 270 km south of the River Conwy. It has a catchment area of 916 km^2, a maximum altitude of 586 m ASL, an AAR of 1216 mm (1961 – 1990), and a BFI of 0.46 (NRFA station 47001)(Rawlins et al., 2003). The Tamar finds its source in Wooley Moor and drains south into the Plymouth Sound, through a landscape dominated by intensive grassland (63%) and some arable land (14%), with some forest (10%), and acid grassland (7%). Catchment geology is predominantly Carboniferous sandstones and fine-grained sedimentary sequences. The catchment is bracketed by Dartmoor to the east (> 500m elevation) and Bodmin moor to the west (> 300m elevation), both characterised by granite outcrops interspersed with Lower Carboniferous and Devonian slates. In the middle of the catchment, quaternary deposits of alluvial sediments run along the larger rivers. Soils are predominantly brown earths (podzols and cambic stognogley soils), with ironpan stagnopodzols to the west and alluvial grey soils to the south.

Table S1. Habitat groupings used for analysis of land cover on DOM and DOC composition, and associated % land cover for the Tamar and Conwy catchments. Land cover data were derived from the 2015 CEH Land Cover Map (LCM 2015) whereby satellite imagery is used to categorise land cover according to 21 broad habitat types (Rowland et al., 2017). These types were grouped into larger, more internationally meaningful groupings for analysis in order to reduce the number of potential explanatory variables relative to study sites, as per Williamson et al. (2021).

Grouped Habitat	LCM 2015 Broad Habitat Types	Conwy (%)	Tamar (%)
Acid Grassland	Acid Grassland; Heather Grassland	36	7
Arable	Arable and Horticulture	0	14
Broadleaf	Broadleaf Woodland	7	7
Conifer	Conifer Woodland	11	3
Intensive Grassland	Improved Grassland; Neutral Grassland; Calcareous Grassland	30	63
Urban	Urban; Suburban	2	2
Water	Freshwater	1	0
Wetland and Moor	Bog; Fen, Marsh and Swamp; Heather	12	2
Other	Inland Rock; Littoral Rock; Saltmarsh; Supralittoral Sediment; Supralittoral Rock; Saltwater; Littoral Sediment	1	0

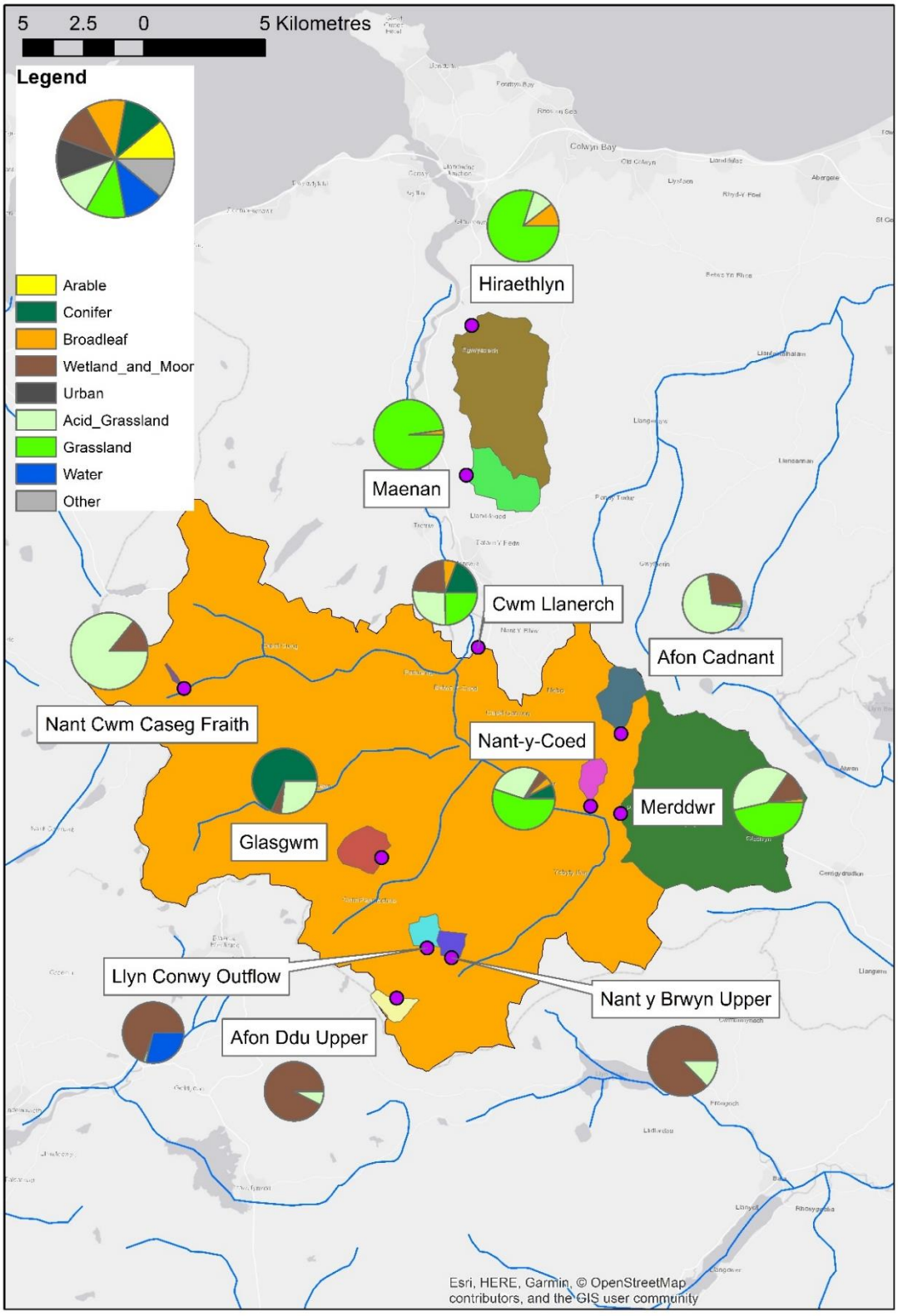

Figure S1. Map of the Conwy catchment, showing sub-catchment boundaries. Land cover is summarised as pie charts.

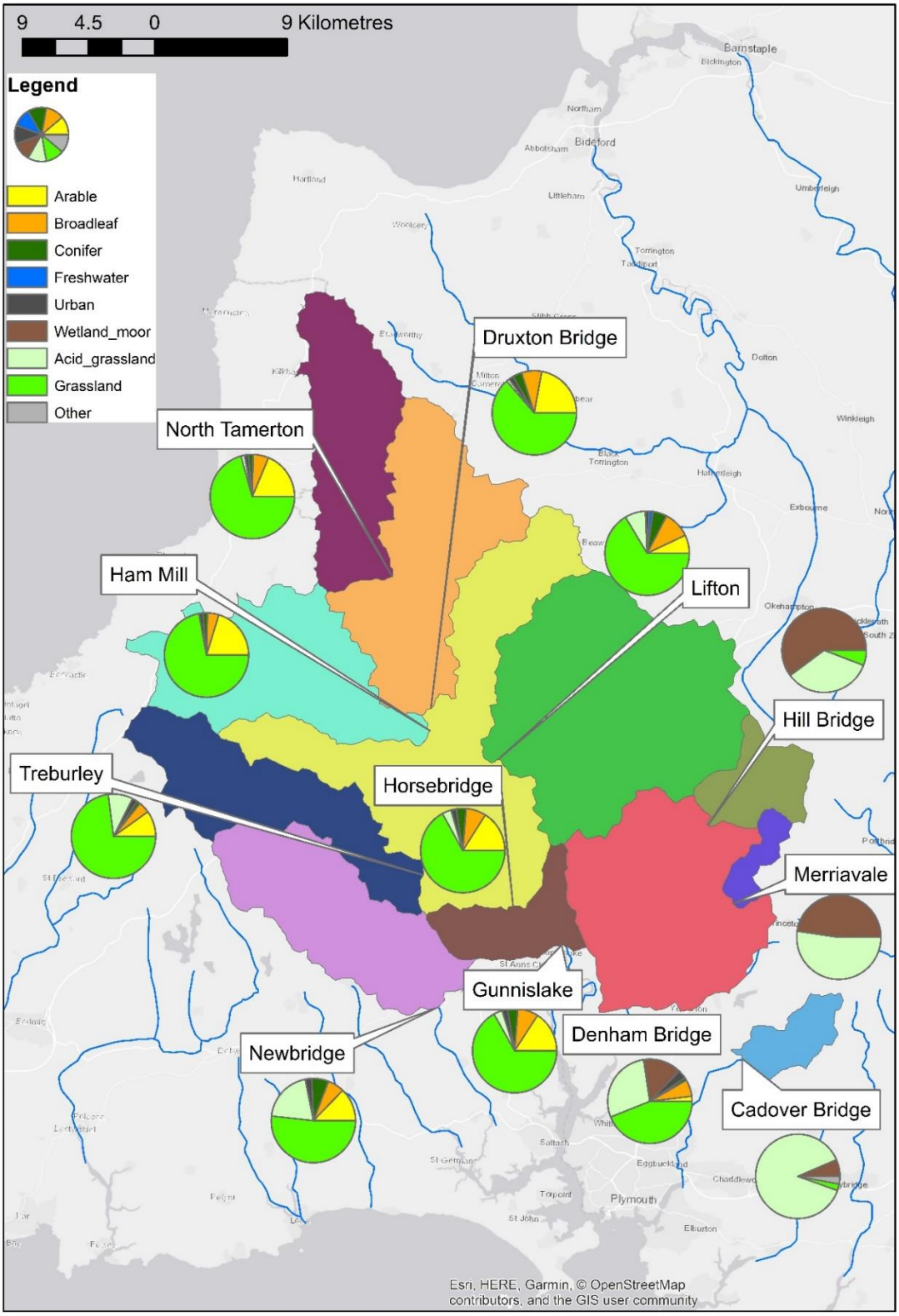

Figure S2. Map of the Tamar catchment, showing sub-catchment boundaries. Land cover is summarised as pie charts.

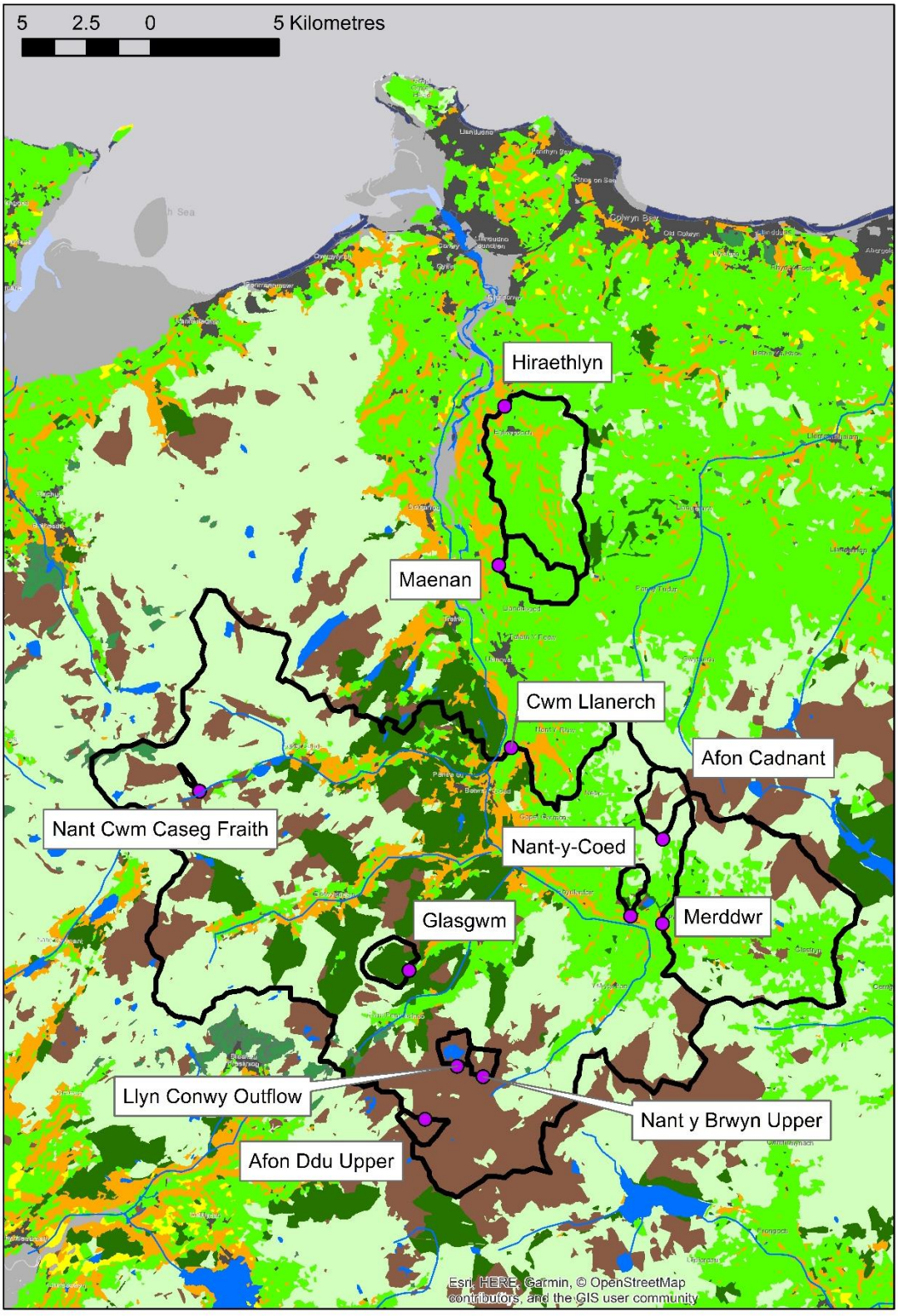

Figure S3. Land cover map for the Conwy catchment, with sub-catchment boundaries highlighted.

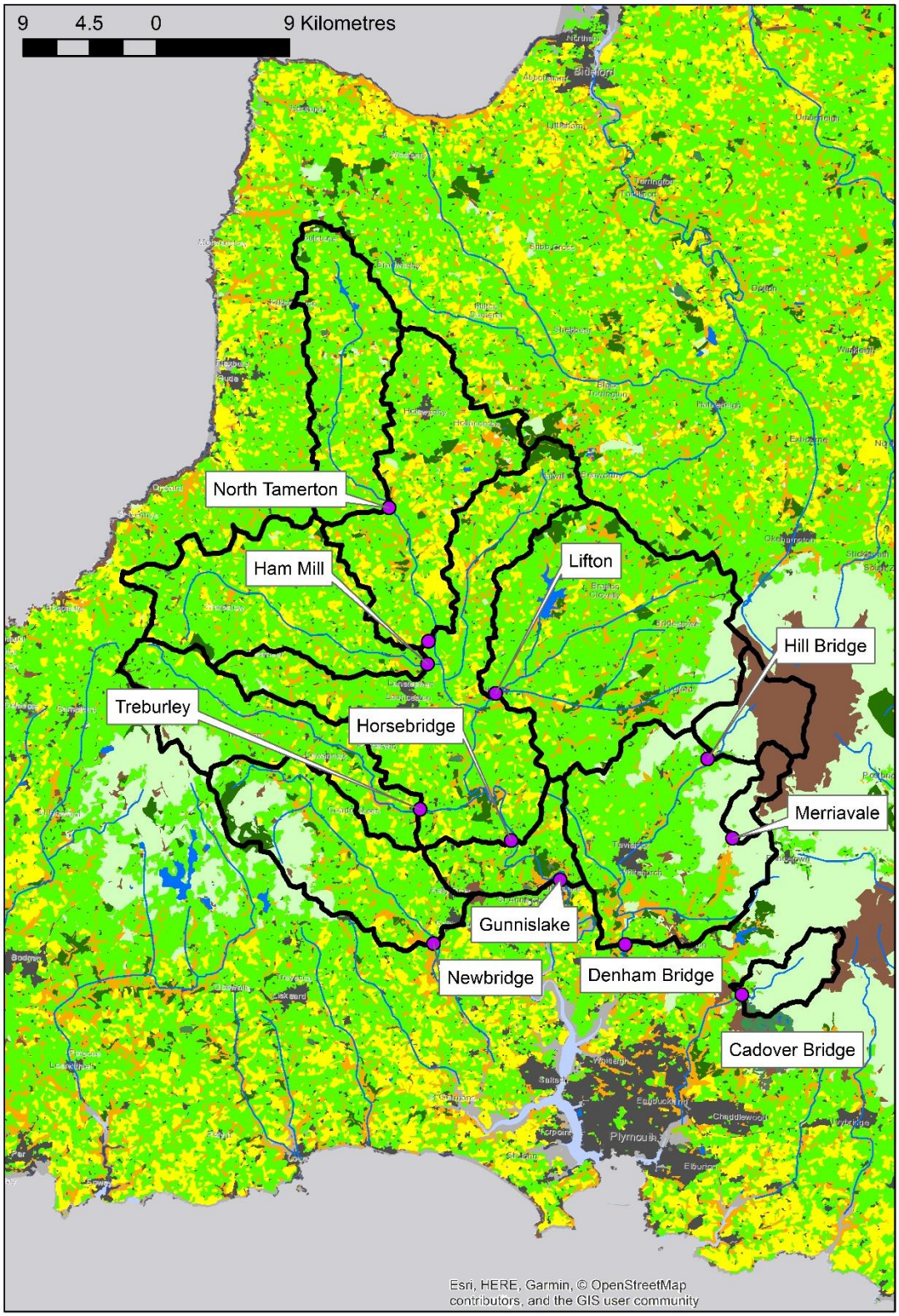

Figure S4. Land cover map for the Tamar catchment, with sub-catchment boundaries highlighted.

Text S2. Are our DOC data robust?

The determination of DOC via the Non-Purgeable Organic Carbon (NPOC) method is known to produce a linear overestimation of DOC concentrations in instances of incomplete purging of dissolved inorganic carbon (DIC) (Findlay et al., 2010). Were this the case, we would expect to find a relationship between DOC and carbonate cycle. We found no evidence of a relationship between DOC and pH (Figure S5). DIC was not measured as part of this study, but using the method outlined by Findlay et al. (2010), we calculated that it would take > 130 mg L^{-1} un-purged DIC to produce a DOC overestimation equivalent to mean iDOC in the Tamar (11.15 mg L^{-1}), and > 1000 mg L^{-1} in order to produce iDOC at the top of our range (85.28 mg L^{-1}). DIC values in the Tamar are typically < 10 mg L^{-1} (Jarvie et al., 2017). DIC was measured in the Tamar estuary during the sampling period (July 2019 sampling run), and concentrations ranged from 15.19 – 25.45 mg L^{-1} (Figure S6). Thus, despite being marginally higher than usual, DIC cannot account for the presence of a DOC residual term (i.e. iDOC).

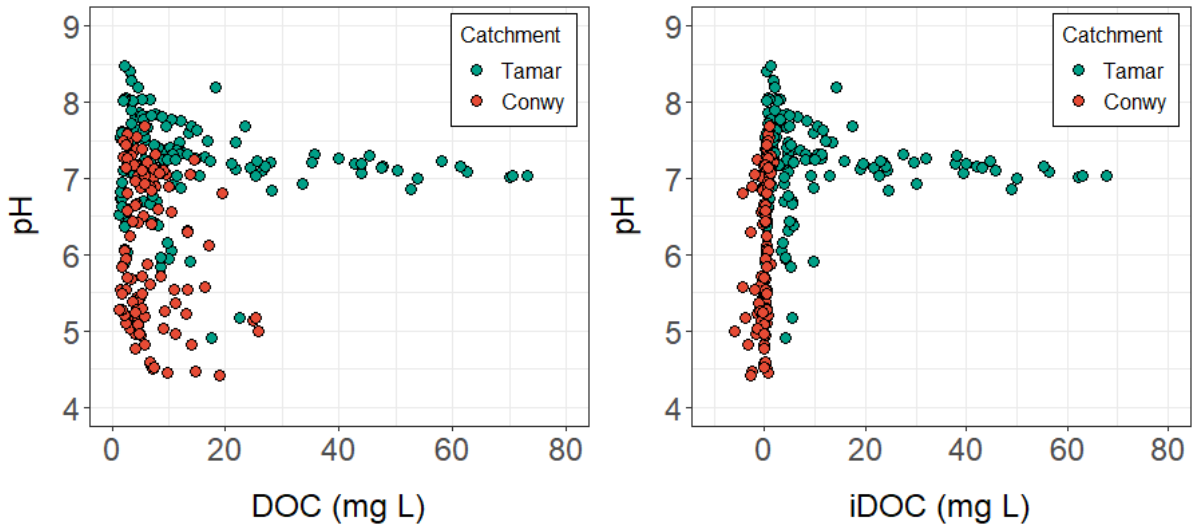

Figure S5. Plot of (left) DOC vs. pH and (right) iDOC vs. pH in the Tamar and Conwy catchments. If DOC (and thus iDOC) was being overestimated due to high DIC concentrations, we would expect to see a relationship with pH. Whilst samples with a pH of around 7 did contain higher DOC and iDOC concentrations, we did not observe a relationship between these parameters more broadly.

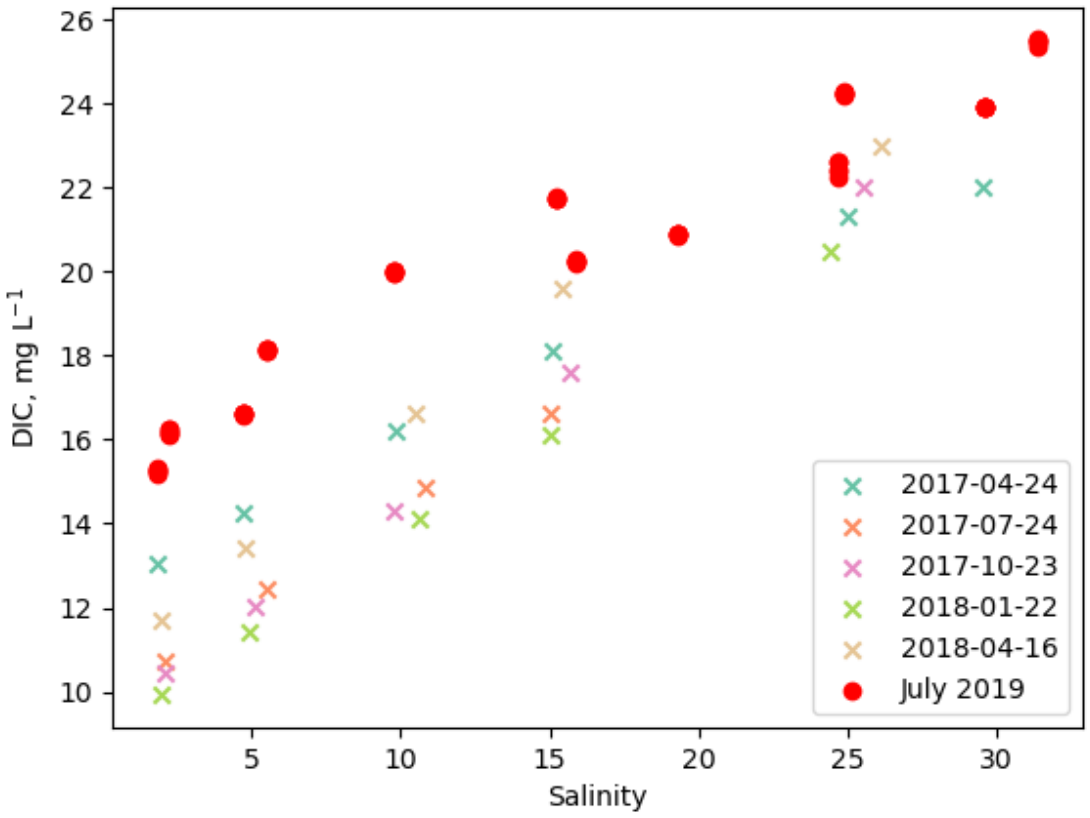

Figure S6. Plot of DIC (mg L^{-1}) vs. salinity (ppt) in the Tamar estuary during July 2019, and on several occasions previously. Whilst DIC during the sampling period (July 2019) was higher than it had been during earlier trips, the increase was in the order of a few mg L^{-1} and nowhere near high enough to produce the kind of NPOC over-estimation required to explain our findings. DIC samples were collected in quintuplicate at each sampling location, and stored in the dark in 250ml borosilicate bottles which were gas-sealed with grease stoppers and fixed with 50 µl saturated mercuric chloride solution. Samples were analysed using the Versatile Instrument for the Determination of Total inorganic carbon and titration Alkalinity (VINDTA 3C, Marinada, Germany), which measures DIC by coulometric titration (CM5011 C02 coulometer, UIC, Inc, USA). The VINDTA 3C measures a known volume of sample and acidifies that subsample with 10 % phosphoric acid (H_3PO_4) to convert all DIC into CO2, which is carried to the coulometer cell by a nitrogen gas. The measurements were calibrated using Certified Reference Materials (CRMs) from A. Dickson (Scripps Institution of Oceanography, US; Dickson et al., 2003). DIC concentrations were calculated using the coulometric titration data, in addition to temperature and salinity data collected using a handheld Hach™ Multimeter which were used to calculate density using Calkulate (Version 2.2.0; Humphreys and Matthews, 2021). The 1σ precision uncertainty for the DIC measurements was 0.05 mg L^{-1}, calculated using the CRM measurements and the quintuplicate sample measurements.

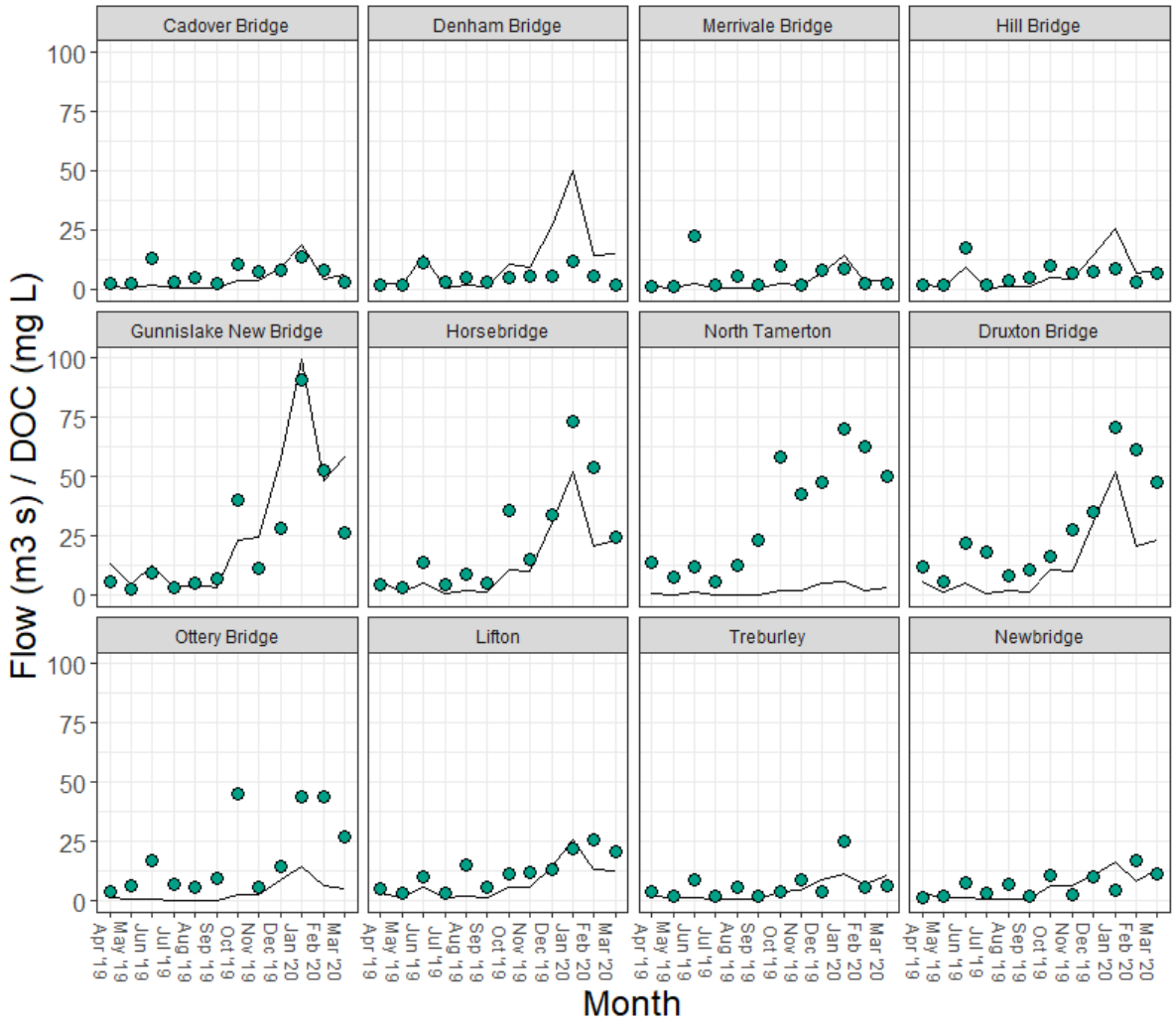

Figure S7. DOC and daily averaged flow data (m^3 s^{-1}) taken from the nearest National River Flow Archive (NRFA) gauging station to each sampling station. Flow data were downloaded from the NRFA and Environment Agency websites (https://nrfa.ceh.ac.uk/data and https://environment.data.gov.uk/hydrology, both accessed 20/01/2020). Sampling locations were often several 100m from the gauging station, meaning that the NRFA data are indicative of conditions at the sampling station, but are not directly related. Nonetheless, they show that high DOC concentrations were often accompanied by high flow conditions. Flow data were not available for the sub-catchments within the Conwy.

Table S2. Linear fit for DOC vs Flow, given by site in the Tamar. Main river sites with highest iDOC values are highlighted in red.

Site	R^2
Cadover Bridge	0.33
Denham Bridge	0.56
Merrivale Bridge	0.06
Hill Bridge	0.21
Gunnislake New Bridge	0.79
Horsebridge	0.80
North Tamerton	0.64
Druxton Bridge	0.78
Ottery Bridge	0.40
Lifton	0.60
Treburley	0.37
Newbridge	0.19

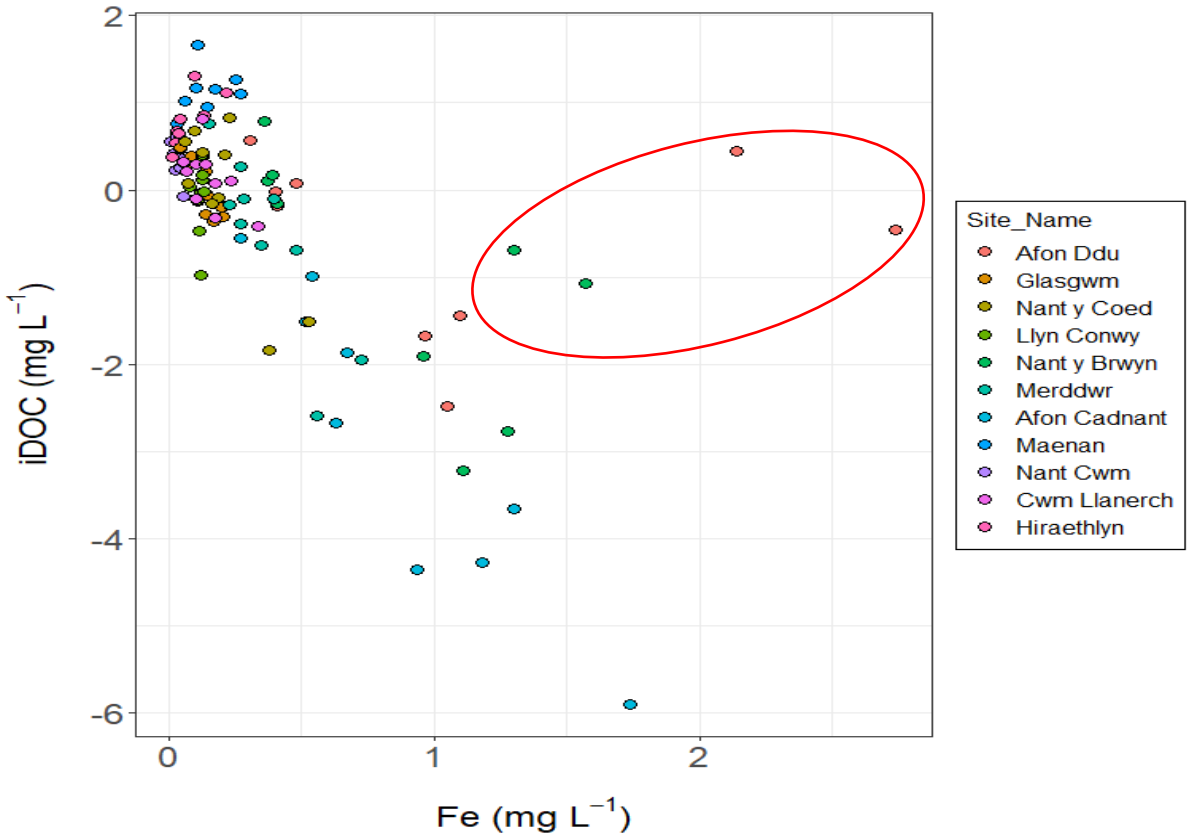

Figure S8. Plot of dissolved iron (Fe) vs. iDOC in the Conwy catchment. Some metals are known to absorb strongly at wavelengths commonly used for investigation of the DOM pool (including those used in this study). For example, Fe is known to increasing absorbance at a rate of ~ 0.01 cm^{-1} for every 1 mg L^{-1} Fe present (Lambert et al., 2015; Weishaar et al., 2003). Negative iDOC concentrations modelled for the Conwy catchment may have resulted from elevated absorbance values, and so we investigated the relationship between iDOC and Fe and found a significant negative correlation (R^2 = 0.39; p = < 0.01). Four points were identified as outliers (circled), originating from two sites (Afon Ddu and Nany y Brwyn) in July and August. Removing these points increased the R^2 to 0.77 (p < 0.01). Fe is used here to demonstrate the potential for a strongly absorbing metal to influence our prediction of iDOC. It is likely that metals in solution have a cumulative effect on absorbance values and thus, on estimated cDOC concentrations, particularly in peated catchments like the Conwy with an already highly coloured DOM pool and typically high metal concentrations.

Table S3. % Peat Cover vs % cDOC (sites ordered by catchment and by % peat). We observed a strong relationship between % peat cover and % cDOC in the Tamar catchment (R^2 = 0.84; p = 1.60 x 10^{-5}), and % cDOC was highest in sub-catchments draining the peat-dominated Dartmoor: Hill Bridge, Merrivale Bridge, Cadover Bridge, and Denham Bridge. In the Conwy, the relationship between % peat and % cDOC was weak (R^2 = 0.16; p = 0.16), despite the highest % cDOC values occurring at sites draining the peat-dominated Migneint: Afon Ddu Upper, Nant y Brwyn, and Llyn Conwy. This fit was improved (R^2 = 0.64; p = 0.01) by removing three sites with high cDOC concentrations and low % peat cover: Afon Cadnant, Merddwr, and Glasgwm. Local knowledge suggests this is an artefact of organic-rich sediments not classified as peat during mapping.

Site	% Peat Cover	% cDOC
Afon Ddu Upper	97	104
Nant y Brwyn Upper	84	106
Llyn Conwy Outflow	70	102
Nant y Coed	25	99
Cwm Llanerch	21	96
Afon Cadnant	*15*	*118*
Nant Cwm Caseg Fraith	12	83
Merddwr	*4*	*105*
Glasgwm	*4*	*97*
Hiraethlyn Point	0	78
Maenan	*0*	*66*
Hill Bridge	73	63
Merrivale Bridge	52	63
Cadover Bridge	47	59
Denham Bridge	18	54
Treburley	4	36
Newbridge	*4*	*38*
Lifton	*3*	*30*
Horsebridge	*1*	*32*
Gunnislake New Bridge	*1*	*36*
Ottery Bridge	*1*	*33*
Druxton Bridge	*0*	*39*
North Tamerton	0	30

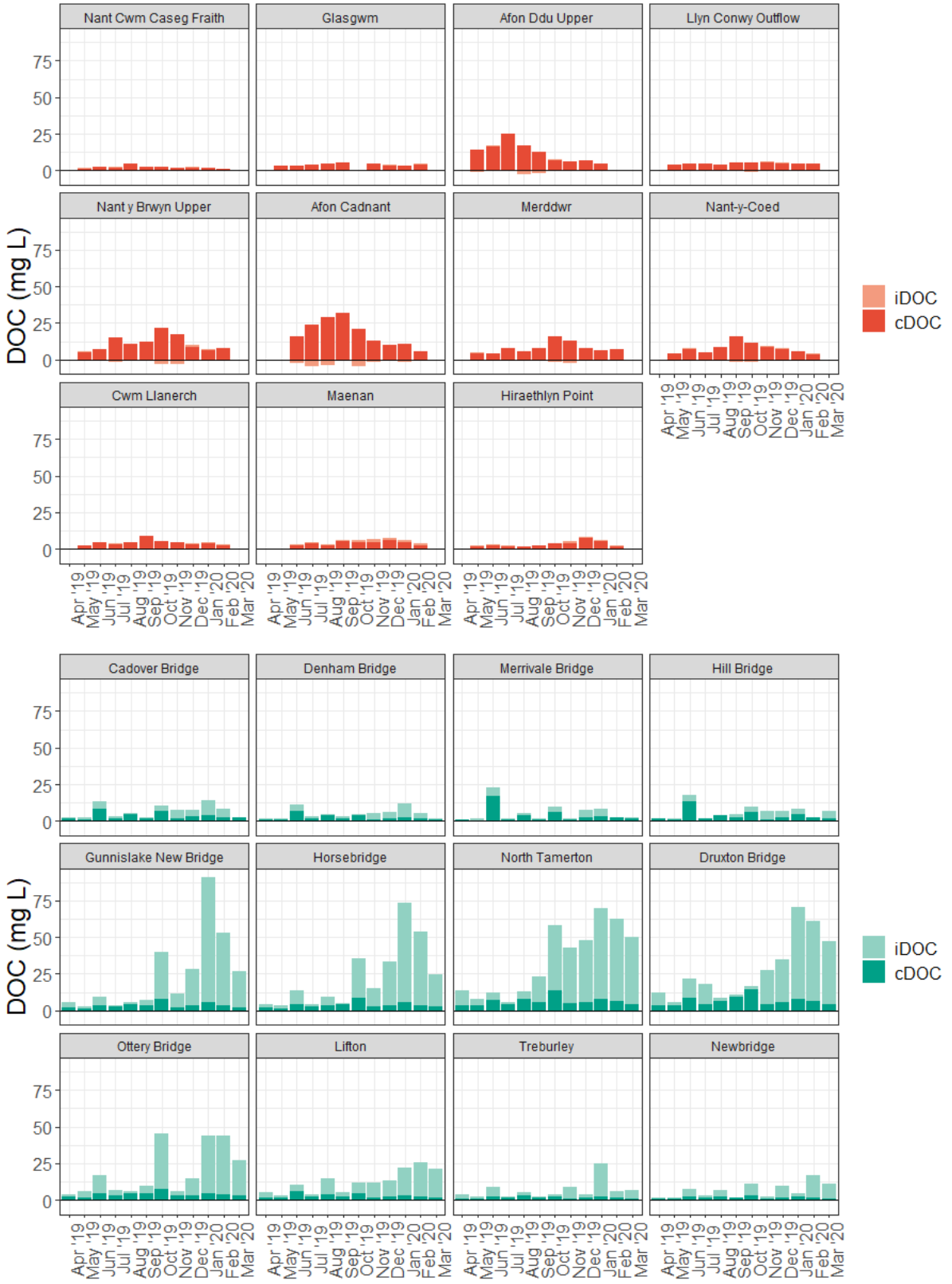

Figure S9. Raw DOC concentrations in the Conwy (top) and Tamar (bottom) catchments, plotted by site and month. Instances where cDOC > 100% and iDOC < 0% are model artefacts, likely due to elevated absorbance values. In such cases, the DOC pool can be considered 100% cDOC.

Table S4. Mean values for DOC concentrations and % composition in the Conwy and Tamar catchments (mean ± SE, range), given by site and catchment.

Site	DOC	cDOC		iDOC	
	mg L^{-1}	mg L^{-1}	%	mg L^{-1}	%
Nant Cwm Caseg Fraith	2.31 ± 0.31 (1.26 – 4.84)	2.00 ± 0.38 (0.84 – 4.97)	83 ± 4 (64 – 103)	0.31 ± 0.08 (-0.13 – 0.64)	17 ± 4 (-3 – 36)
Glasgwm	3.59 ± 0.26 (2.26 – 4.91)	3.54 ± 0.37 (1.77 – 5.10)	97 ± 3 (78 – 109)	0.05 ± 0.10 (-0.37 – 0.49)	3 ± 3 (-9 – 22)
Afon Ddu Upper	11.15 ± 2.03 (3.89 – 24.90)	12.23 ± 2.31 (4.34 – 25.35)	104 ± 3 (92 – 117)	-0.57 ± 0.35 (-2.48 – 0.57)	-4 ± 3 (-17 – 8)
Llyn Conwy	4.68 ± 0.18 (4.01 – 5.83)	4.73 ± 0.14 (4.04 – 5.46)	102 ± 3 (92 – 123)	-0.05 ± 0.13 (-0.98 – 0.40)	-2 ± 3 (-23 – 8)
Nant y Brwyn	10.41 ± 1.32 (5.32 – 19.00)	11.30 ± 1.69 (5.14 – 21.77)	106 ± 3 (92 – 123)	-0.90 ± 0.42 (-3.21 – 0.79)	-6 ± 3 (-23 – 8)
Afon Cadnant	14.96 ± 2.43 (5.30 – 25.70)	17.83 ± 2.98 (5.86 – 31.60)	118 ± 2 (110 – 126)	-2.86 ± 0.60 (-5.90 – -0.56)	-18 ± 2 (-26 – -10)
Merddwr	7.44 ± 0.86 (4.37 – 13.80)	8.00 ± 1.13 (4.19 – 15.74)	105 ± 3 (85 – 126)	-0.56 ± 0.32 (-2.59 – 0.77)	-5 ± 3 (-26 – 15)
Nant-y-Coed	7.66 ± 0.97 (4.33 – 14.50)	7.72 ± 1.17 (3.79 – 16)	99 ± 3 (85 – 119)	-0.06 ± 0.29 (-1.84 – 0.82)	1 ± 3 (-19 – 15)
Cwm Llanerch	4.39 ± 0.49 (2.59 – 8.10)	4.26 ± 0.57 (2.26 – 8.52)	96 ± 3 (80 – 108)	0.13 ± 0.11 (-0.42 – 0.82)	4 ± 3 (-8 – 20)
Maenan	4.96 ± 0.56 (2.69 – 7.35)	3.87 ± 0.44 (2.10 – 6.09)	77 ± 1 (66 – 84)	1.07 ± 0.10 (0.59 – 1.66)	23 ± 2 (16 – 34)
Hiraethlyn Point	3.64 ± 0.67 (1.66 – 8.29)	2.93 ± 0.61 (1.20 – 7.17)	78 ± 3 (60 – 93)	0.71 ± 0.10 (0.28 – 1.31)	22 ± 3 (7 – 40)
Conwy Av.	6.80 ± 0.48 (1.26 – 25.70)	6.53 ± 0.56 (0.60 – 31.60)	97 ± 1 (60 – 126)	-0.24 ± 0.12 (-5.90 – 1.66)	3 ± 1 (-26 – 40)
Cadover Bridge	6.59 ± 1.23 (2.15 – 13.80)	3.42 ± 0.67 (1.35 – 8.53)	59 ± 7 (25 – 94)	3.17 ± 0.87 (0.33 – 9.77)	41 ± 7 (6 – 75)
Denham Bridge	5.02 ± 0.99 (1.62 – 12.10)	2.38 ± 0.52 (0.85 – 7.05)	54 ± 7 (17 – 89)	2.64 ± 0.78 (0.28 – 9.63)	46 ± 7 (11 – 83)
Merrivale Bridge	5.56 ± 1.79 (1.31 – 22.50)	3.44 ± 1.31 (0.58 – 17.01)	63 ± 6 (28 – 93)	2.12 ± 0.65 (0.16 - 5.57)	27 ± 6 (7 – 72)
Hill Bridge	6.10 ± 1.31 (1.49 – 17.50)	3.53 ± 0.97 (1.24 – 13.24)	63 ± 8 (20 – 98)	2.57 ± 0.62 (0.03 – 5.45)	37 ± 8 (2 – 80)
Gunnislake New Bridge	23.48 ± 7.69 (2.42 – 90.60)	3.57 ± 0.50 (1.62 – 7.93)	36 ± 8 (6 – 83)	19.91 ± 7.42 (0.54 – 85.28)	64 ± 8 (17 – 94)
Horsebridge	22.92 ± 6.45 (3.35 – 73.10)	3.65 ± 0.52 (1.57 – 8.33)	32 ± 7 (7 – 86)	19.27 ± 6.20 (0.66 – 67.79)	68 ± 7 (14 – 93)
North Tamerton	33.88 ± 6.83 (5.79 – 70.00)	6.17 ± 0.81 (3.16 – 13.37)	30 ± 7 (9 – 70)	37.71 ± 6.53 (1.75 – 62.21)	70 ± 7 (30 – 91)
Druxton Bridge	27.90 ± 6.02 (5.37 – 70.60)	6.44 ± 0.91 (3.18 – 14.51)	39 ± 9 (9 – 88)	21.45 ± 6.30 (1.35 – 62.93)	61 ± 9 (12 – 91)
Ottery Bridge	19.16 ± 4.77 (4.00 – 45.40)	3.79 ± 0.42 (1.78 – 7.27)	33 ± 6 (9 – 72)	15.37 ± 4.51 (1.62 – 39.89)	67 ± 6 (28 – 91)
Lifton	12.32 ± 2.15 (3.30 – 25.50)	2.63 ± 0.37 (1.31 – 5.79)	30 ± 6 (7 – 75)	9.69 ± 2.17 (0.84 – 23.09	70 ± 6 (25 – 93)
Treburley	6.51 ±1.84 (1.93 – 25.20)	1.59 ± 0.21 (0.88 – 3.07)	36 ± 6 (10 – 74)	4.93 ± 1.75 (0.51 – 22.62)	64 ± 6 (26 – 90)
Newbridge	6.54 ± 1.42 (1.46 – 17.20)	1.58 ± 0.15 (0.94 – 2.64)	38 ± 7 (8 – 79)	4.96 ± 1.37 (0.32 – 15.79)	62 ± 7 (21 – 92)
Tamar Av.	14.66 ± 1.46 (1.31 – 90.60)	3.52 ± 0.23 (0.58 – 17.01)	43 ± 2 (6 – 98)	11.15 ± 1.37 (0.03 – 85.28)	57 ± 2 (2 – 94)

Text S3: Modelling the annual GB riverine iDOC flux

Williamson et al. (2021) derived an annual GB-scale riverine export flux of DOC using monthly resolution data from forty rivers draining 26 % of the GB land mass. We used the same data set to apportion this flux into cDOC and iDOC fractions, following the method set out in that paper. Using the full data set of Williamson et al., (2021), mean annual flow weighted DOC concentrations (FW DOC) were estimated at 7.8 $\pm$ 3.0 mg L^{-1} (range = 1.9 - 13.2 mg C L^{-1}) and the mean DOC export per unit area (DOC yield) was estimated at 5.98 + 4.40 g C m^{-2} yr^{-1} (range = 0.31 – 20.23 g C m^{-2} yr^{-1}). Using our slightly reduced data set, we estimated these values at 7.8 $\pm$ 3.2 mg L^{-1} (range = 1.9 - 13.2 mg C L^{-1}) and 5.87 + 4.47 g C m^{-2} yr^{-1} (range = 0.28 – 23.29 g C m^{-2} yr^{-1}), respectively.

We used step-wise linear regression modelling to investigate the relationship between FW DOC and DOC yield and a range of land-use and geoclimatic variables known to exert influence over DOC fluxes. Catchment characteristics considered were peat soil area (km^2), % peat soil, base flow index (BFI), annual average rainfall (SAAR), mean altitude, and % carbonate rock. Land-use classes were grouped as per Table S1. Models were run in R software (R Core Team, 2019) and best-fit models were selected by Akaike Information Criterion (AIC) (Equations 5-4 and 5-5). Model outputs are given in Tables S5 and S6. The relationships identified were the same as in Williamson et al. (2021), except the inclusion of BFI in Model 2, and explained 74 % and 78 % of variation in FW DOC and DOC yield, respectively. These relationships were applied at 1 km^2 grid resolution to produce a GB-scale flux estimate of 1.01 Tg C yr^{-1}. Williamson et al.'s estimate was 1.15 Tg C yr^{-1}.

$$FW\ DOC \sim \%\ Peat + BFI + SAAR + \%\ Forest + \ MeanAlt + \ \%\ Grassland \qquad \boldsymbol{Eqn.5-4}$$

$$DOC\ yield \sim \%\ Peat \ + \ \%\ Forest + \ BFI \ + \ SAAR \qquad \boldsymbol{Eqn.5-5}$$

Table S5. Model output associated with Equation 5-4.

R^2 = 0.74; p = 1.31 x 10^{-7}	Estimate	Std. Error	t value	p value	Significance
Intercept	10.74	2.56	4.20	2.20 x 10^{-4}	***
% Peat	0.09	0.02	4.79	4.20 x 10^{-5}	***
BFI	-8.86	2.76	-3.21	3.15 x 10^{-3}	**
SAAR	-0.004	0.001	-4.55	8.40 x 10^{-4}	***
% Forest	0.05	0.03	1.58	0.12	
Mean Altitude	0.01	0.004	2.22	0.03	*
% Grassland	0.05	0.02	2.01	0.05	.

Table S6. Model output associated with Equation 5-5.

R^2 = 0.78; p = 4.31 x 10^{-10}	Estimate	Std. Error	t value	p value	Significance
Intercept	2.45	2.63	0.93	0.36	
% Peat	0.08	0.02	4.24	1.75 x 10^{-3}	***
% Forest	0.22	0.04	4.94	2.36 x 10^{-5}	***
BFI	-7.54	3.53	-2.14	0.04	*
SAAR	0.01	0.001	2.12	0.04	*

The same method was applied to derive a GB-scale cDOC flux, producing a mean FW cDOC estimate of 6.26 ± 2.99 mg L-1 (range = 1.27 – 13.46 mg L^{-1}) and a mean cDOC yield estimate of 4.78 ± 4.07 g C m^{-2} yr^{-1} (range = 0.21 – 19.86 g C m^{-2} yr^{-1}). Best-fit models explained 80 % and 84 % of variation in FW cDOC and cDOC yield (Equations 5-6 and 5-7), with model outputs given in Tables S7 and S8.

$$FW\ cDOC \sim\ \%\ Peat + BFI + SAAR\ + \%\ MeanAlt + \%\ Forest \qquad \boldsymbol{Eqn.\ 5-6}$$

$$cDOC\ yield \sim Peat + \%\ Forest + BFI + SAAR \qquad \boldsymbol{Eqn.\ 5-7}$$

Table S7. Model output associated with Equation 5-6.

R^2 = 0.80; p = 5.83 x 10^{-10}	Estimate	Std. Error	t value	p value	Significance
Intercept	10.30	1.63	6.32	4.92 x 10^{-7}	***
% Peat	0.08	0.01	6.68	1.79 x 10^{-7}	***
BFI	-8.00	2.16	-3.71	8.11 x 10^{-3}	***
SAAR	-0.003	0.0007	-4.82	3.56 x 10^{-5}	***
Mean Altitude	0.01	0.003	2.29	0.03	*
% Forest	0.05	0.03	1.74	0.09	.

Table S8. Model output associated with Equation 5-7.

R^2 = 0.84; p = 4.15 x 10^{-12}	Estimate	Std. Error	t value	p value	Significance
(Intercept)	1.29	1.96	0.66	0.52	
Peat	0.09	0.01	6.07	8.84 x 10^{-7}	***
Forest	0.19	0.03	5.76	2.18 x 10^{-6}	***
BFI	-5.35	2.62	-2.04	0.05	*
SAAR	0.002	0.0007	2.02	0.05	.

FW iDOC was estimated at 1.55 ± 0.89 mg L-1 (range = 0.34 – 5.08 mg L-1) and iDOC yield was estimated at 1.08 ± 0.97 g C m^{-2} yr^{-1} (range = 0.07 – 3.72 g C m^{-2} yr^{-1}). The relationship between iDOC and regression variables was decidedly weaker than for cDOC, explaining just 17% of variation in FW iDOC and 30% of variation in iDOC yield (Equations 5-8 and 5-9), and model outputs are given in Tables S9 and S10.

$$FW\ iDOC \sim \%\ Grassland \qquad \boldsymbol{Eqn\ 5-8}$$

$$iDOC\ yield \sim \%\ Forest + SAAR \qquad \boldsymbol{Eqn\ 5-9}$$

Table S9. Model output associated with Equation 5-8.

R^2 = 0.17; p = 6.27 x 10^{-3}	**Estimate**	**Std. Error**	**t value**	**p value**	**Significance**
Intercept	0.94	0.25	3.78	5.92 x 10^{-1}	***
% Grassland	0.02	0.01	2.91	6.27 x 10^{-3}	**

Table S10. Model output associated with Equation 5-9.

R^2 = 0.30; p = 2.74 x 10^{-3}	**Estimate**	**Std. Error**	**t value**	**p value**	**Significance**
Intercept	1.29	1.96	0.66	5.15 x 10^{-1}	
% Forest	0.04	0.01	6.07	8.84 x 10^{-7}	***
SAAR	0.002	0.001	2.02	5.17 x 10^{-2}	.

To derive GB-scale export fluxes for cDOC and iDOC, we first derived cDOC export at 1 km^2 resolution then derived iDOC by subtraction (DOC – cDOC). This produced final estimates of 0.77 Tg cDOC yr^{-1} cDOC and 0.24 Tg iDOC yr^{-1}, equivalent to 77 % and 23 % of the total DOC export flux, respectively. Minimum and maximum estimates of these flux estimates were calculated according to the uncertainty of the linear regression approach.

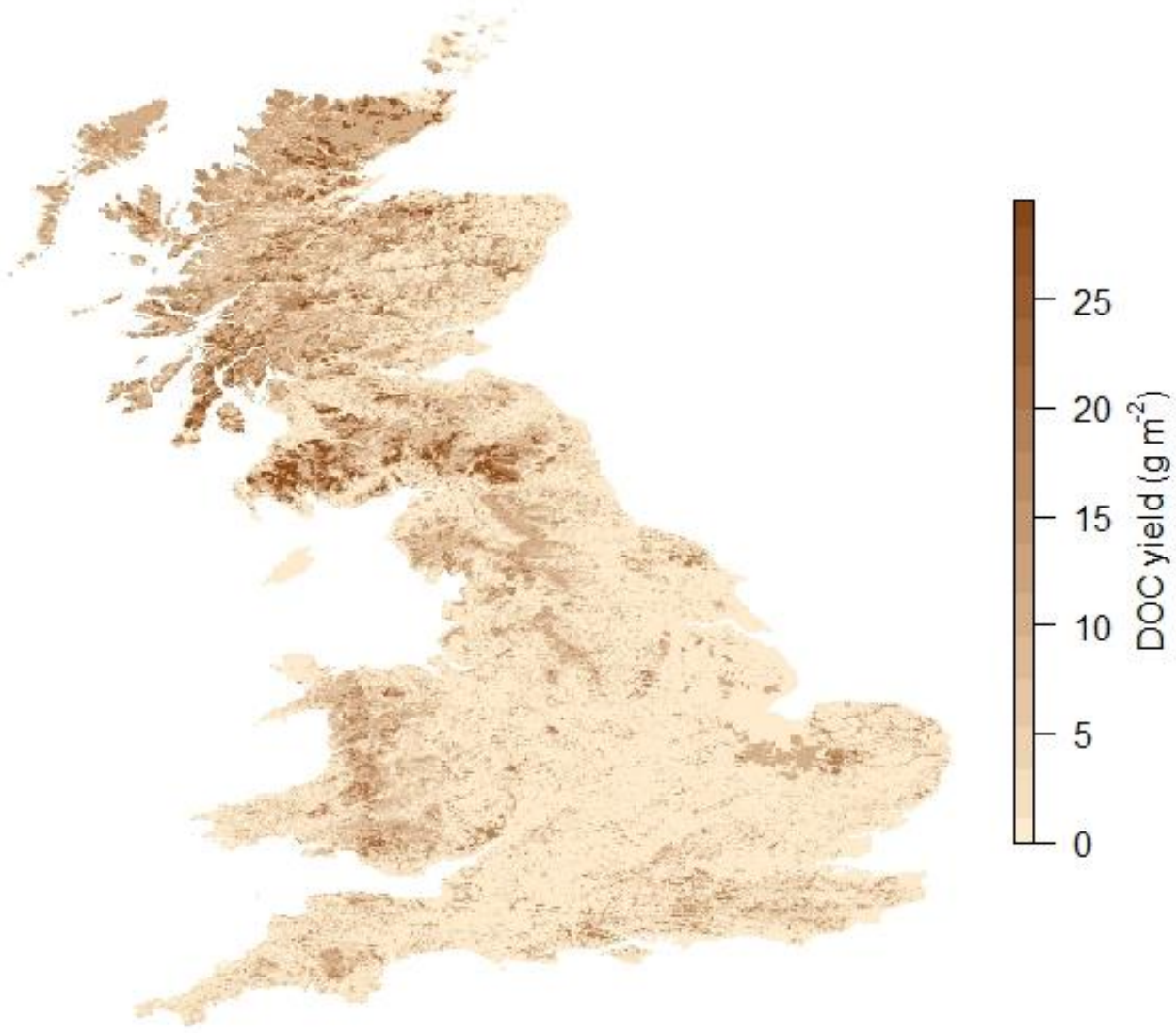

Figure S11. Map of Great Britain showing estimated DOC yields, modelled at 1 km^2 resolution.

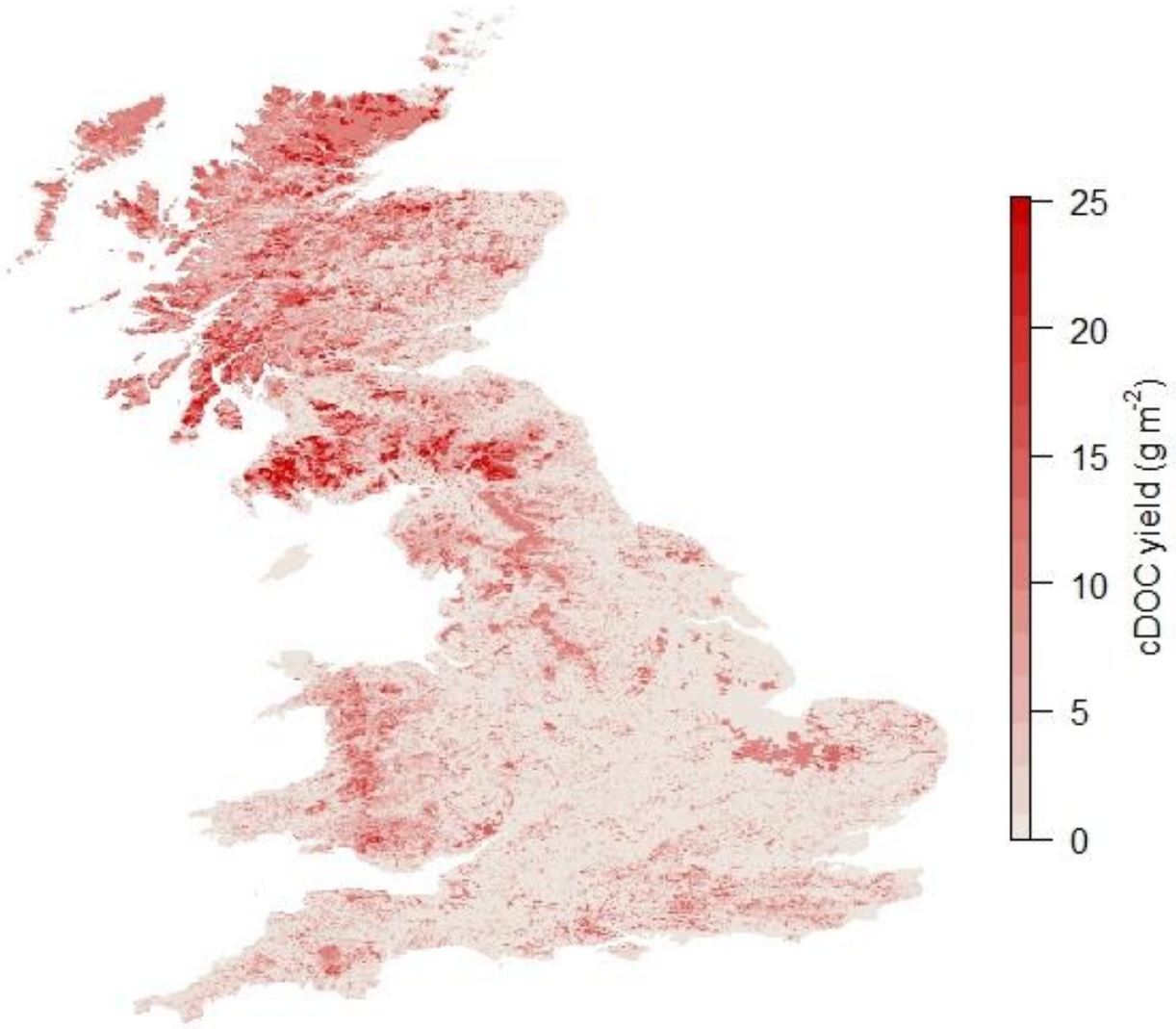

Figure S12. Map of Great Britain showing estimated cDOC yields, modelled at 1 km^2 resolution.

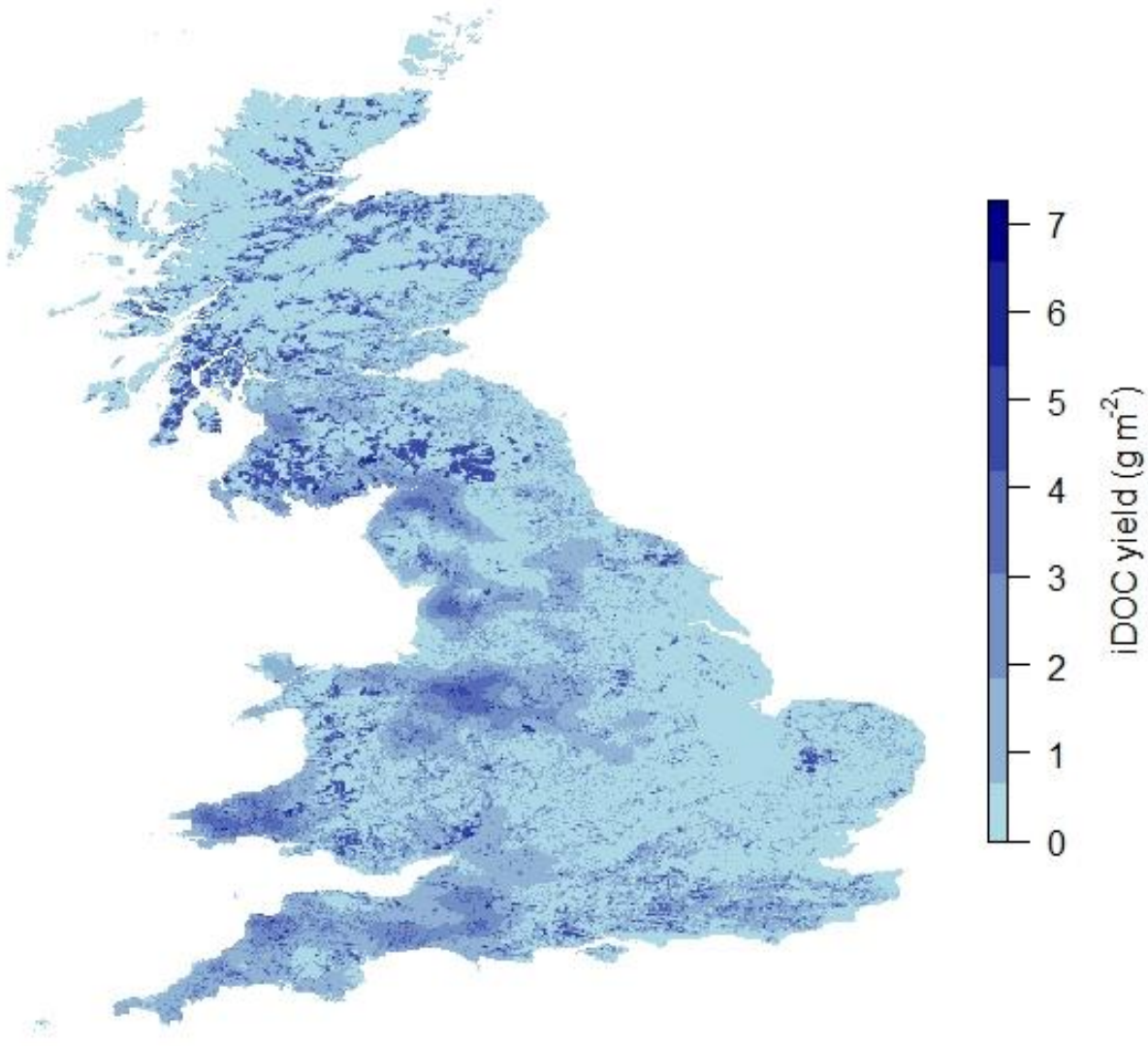

Figure S13. Map of Great Britain showing estimated iDOC yields modelled at 1 km^2 resolution.

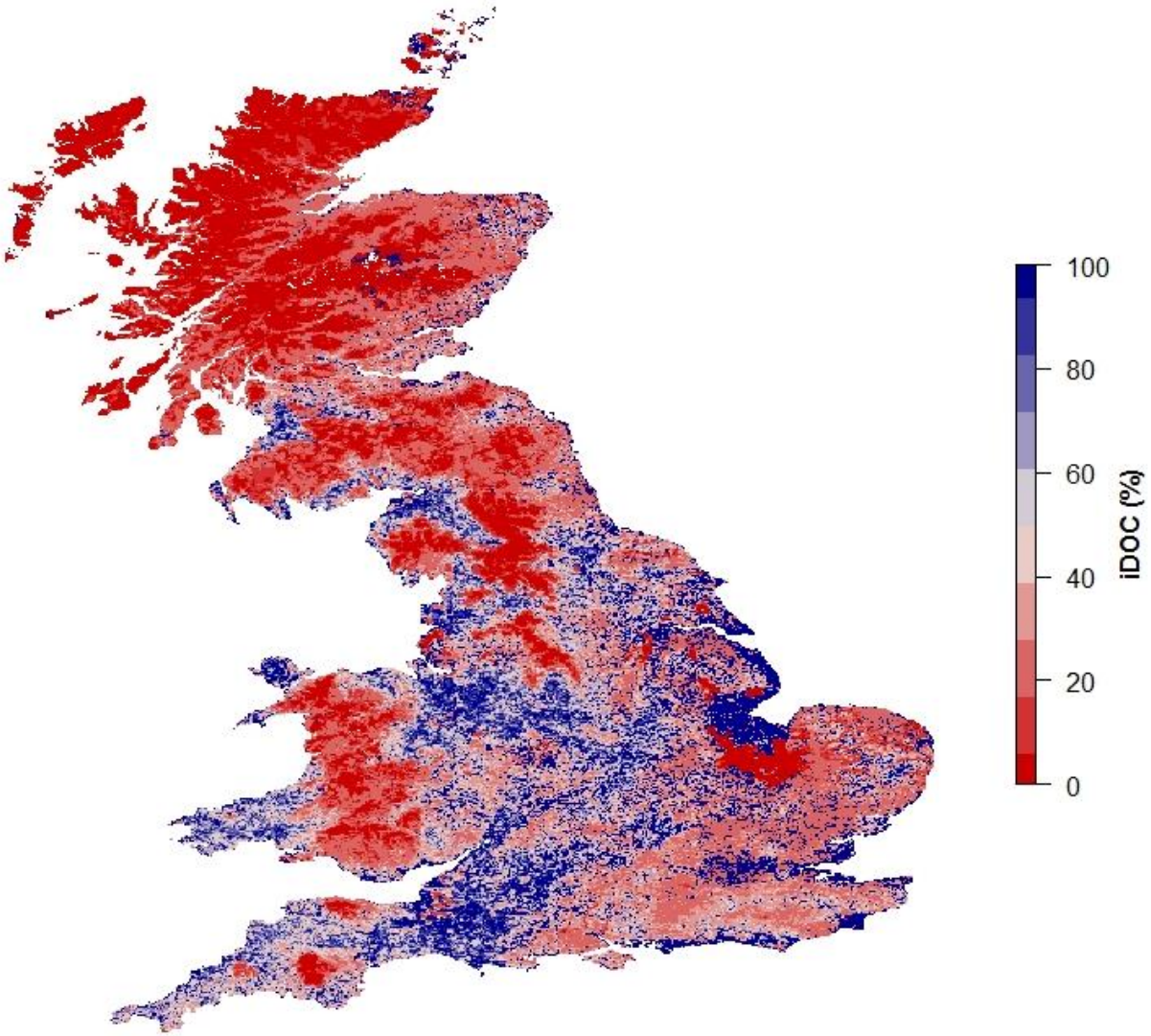

Figure S14. Map of Great Britain showing estimated % iDOC yields modelled at 1 km^2 resolution.

Table S10. Summary of collated dataset, showing source (ref), status (published vs. unpublished), continent, environment, number of data points (n), and iDOC as a concentration and a % value (mean ± standard deviation).

Ref	Status	Continent	Environment	n	iDOC (mg L^{-1})	iDOC (%)
Agro	Pub	Arctic	River	246	2.09 ± 1.53	29 ± 14
Asmala	Pub	Europe	River	22	-0.67 ± 2.02	-5 ± 12
Chen	Pub	N. America	River	5	0.89 ± 0.28	24 ± 10
Belize	Pub	S. America	River	48	2.14 ± 3.14	34 ± 37
Belize	Pub	S. America	Reservoir	3	15.81 ± 6.05	79 ± 12
Greenland	Pub	Arctic	Lake	38	21.99 ± 22.40	56 ± 17
Heinz	Pub	Europe	River	139	0.75 ± 1.12	17 ± 19
Horsens	Pub	Europe	River	272	0.91 ± 1.04	17 ± 14
Horsens	Pub	Europe	Lake	58	0.89 ± 0.95	13 ± 12
Lambert	Pub	Africa	River	569	2.56 ± 2.59	41 ± 20
LTER	Pub	N. America	Lake	102	2.17 ± 1.85	21 ± 16
Massiciotte	Pub	N. America	River	59	0.84 ± 0.65	26 ± 17
Patrick	Pub	Asia	River	42	2.05 ± 6.68	12 ± 14
Shen	Pub	N. America	Groundwater	28	0.97 ± 1.22	57 ± 10
Xi	Pub	Asia	River	7	2.54 ± 1.49	48 ± 10
Zhang	Pub	Asia	Lake	16	12.61 ± 3.37	96 ± 0.28
Basal	Unpub	Oceania	River	18	0.25 ± 0.57	15 ± 28
Beaulieu	Unpub	Europe	River	12	1.48 ± 3.01	12 ± 19
Brazil	Unpub	S. America	River	9	2.56 ± 0.91	40 ± 15
Brazil	Unpub	S. America	Lake	6	3.14 ± 1.03	42 ± 12
Conwy	Unpub	Europe	River	107	-0.23 ± 1.27	3 ± 15
Daemons	Unpub	Europe	River	23	0.53 ± 0.40	6 ± 5
Daemons	Unpub	Europe	Stream	51	0.56 ± 0.77	6 ± 8
Daemons	Unpub	Europe	Lake	17	1.18 ± 0.50	22 ± 13
Derwent	Unpub	Oceania	River	318	1.40 ± 1.27	24 ± 18
Falklands	Unpub	S. America	Ponds	5	25.55 ± 11.47	75 ± 12
Gardsjon	Unpub	Europe	Stream	16	0.81 ± 1.06	5 ± 6
Gardsjon	Unpub	Europe	Lake	27	1.14 ± 0.86	25 ±20
Grinham	Unpub	Oceania	Reservoir	15	5.66 ± 0.46	48 ± 2
Halladale	Unpub	Europe	River	130	0.97 ± 1.48	7 ± 8

Kitex	Unpub	Europe	River	18	4.17 ± 10.30	8 ± 44
Malaren	Unpub	Europe	Lake	44	1.73 ± 1.08	17 ± 8
Siberia	Unpub	Asia	River	9	2.46 ± 1.09	23 ± 7
Siberia	Unpub	Asia	Lake	28	3.29 ± 1.68	34 ± 8
Siberia	Unpub	Asia	Pond	25	3.34 ± 6.34	9 ± 28
Spur	Unpub	Oceania	Stream	63	-0.32 ± 0.30	-9 ± 10
Tamar	Unpub	Europe	River	144	11.15 ± 16.38	57 ± 26
Uppland	Unpub	Europe	Stream	20	1.54 ± 2.76	0 ± 43
Uppland	Unpub	Europe	Ditch	19	-0.28 ± 8.36	-3 ± 58
Uppland	Unpub	Europe	Pond	19	3.97 ± 3.02	27 ± 19

Table S11. The use of data from multiple studies, instruments, and time periods makes measurement uncertainty attribution problematic, but we nonetheless give broad estimates here. Measurement uncertainty for DOC is typically in the order of 2 – 5%(Peacock et al., 2015a) and, in the case of the Tamar and Conwy, was specified at < 10 %. Intrinsic (instrument based) uncertainties associated with absorbance measurements are typically only a few tenths of a percent, whilst extrinsic (sample based) uncertainties are in the order of 1 – 3 %(Skoog et al., 2007; Sooväli et al., 2006). Model uncertainty associated with derived absorbance spectra were < 1% for hyperspectral data and 6 – 8 % for multispectral data. Thus, the combined uncertainties associated with the global model range from ~ 3 – 20 %. To understand how these uncertainties might influence our results, we undertook sensitivity testing which involved applying a range of uncertainty limits to estimated iDOC concentrations. A range of uncertainties (0 – 20% of DOC) were applied whereby only iDOC concentrations > the given uncertainty were considered significant. The inclusion of uncertainties reduced mean iDOC contributions in the order of a few %, but did not substantially alter our findings, i.e. iDOC represents a significant fraction of the aquatic DOC pool irrespective of which uncertainty level is applied.

% Uncertainty	% iDOC (mean ± SD)
0	27 ± 22
5	27 ± 22
10	26 ± 22
15	25 ± 24
20	23 ± 24

Chapter 6 Non-conservative behaviour of estuarine dissolved organic carbon is driven by optically 'invisible' material.

S. Felgate conceptualised and led this manuscript, including data analysis and manuscript preparation. Full details of author contributions are provided at the end of this chapter.

Stacey L. Felgate[1,2], Chris D. Evans[3], and Daniel J. Mayor[2]

[1]Ocean and Earth Sciences, University of Southampton, Southampton, SO14 3ZH, UK.
[2]Ocean Biogeosciences, National Oceanography Centre, Southampton, SO14 3ZH, UK.
[3]UK Centre for Ecology and Hydrology, Bangor, LL57 2UW, UK.

This chapter has been formatted for submission to Limnology and Oceanography Letters. Supplimentary material has been incorporated into the main text.

Key Words: Dissolved organic carbon; Dissolved organic matter; Estuaries; Non-conseravtive; iDOM

6.1 Abstract

The flux of terrigenous dissolved organic carbon (DOC) through estuaries is an important component of the global carbon cycle which is subject to change and poorly understood. Here we use an absorbance-based DOC prediction model to partition this flux into its coloured (cDOC) and non-coloured or 'invisible' (iDOC) fractions in 12 British estuaries, sampled at quarterly resolution between April 2017 and April 2018. We show that these fractions exhibit contrasting behaviours, and that their contributions ultimately control bulk DOC behaviour. We show that riverine cDOC inputs behaved conservatively irrespective of initial concentrations, whilst riverine iDOC inputs behaved non-conservatively. Within-estuary point-source iDOC inputs were considerable and highly influential, irrespective of catchment land-use, whilst point-source cDOC inputs were minimal and exerted less influence. We conclude that non-conservative estuarine DOC transport can almost entirely be explained by shifts in iDOC concentrations, and suggest consideration of the non-coloured fraction might yield an increased understanding of estuarine DOC transport.

6.2 Introduction

Each year ~ 5.1 Pg of terrigenous carbon (C) enters the land-ocean aquatic continuum (LOAC), the network of aquatic systems (streams, wetlands, lakes, reservoirs, rivers and estuaries) linking soil water to the open ocean (Bouwman et al., 2013; Drake et al., 2018). This is equivalent to ~ 50 % of terrestrial net ecosystem production (Drake et al., 2018), making the terrigenous export flux an important component of the global carbon cycle. Around 25 % of the land to water carbon flux occurs in the form of dissolved organic carbon (DOC; Cole et al., 2007). Carbon is the largest elemental component of most dissolved organic matter (DOM), so DOC typically contributes about 50 % of DOM by molecular weight (Moody and Worrall, 2017).

The quantity and composition of terrigenous DOM entering the LOAC is determined by a combination of catchment characteristics (e.g. soil type and land cover; hydrology; geology; morphology; climate) and human activities (e.g. land use change; wastewater discharge; water extraction; pollution) (Felgate et al., 2021b; Williams et al., 2016; Williamson et al., 2021a; Xenopoulos et al., 2021). Within the LOAC it mixes with the autochthonous DOM (i.e. DOM produced through autotrophic processes within aquatic systems, e.g. by algae) and their combined C content is subject to three potential fates: remineralisation (via photo- and/or biodegradation), which may lead to outgassing to the atmosphere as carbon dioxide (CO_2); aggregation and flocculation, which may lead to burial within sediments; and export to the ocean for additional processing and/or storage (Cole et al., 2007). The extent to which different removal, transformation, and production processes influence DOM concentration and composition is determined by a combination of intrinsic (e.g. molecular structure and stoichiometry) and extrinsic (e.g. water chemistry, climate, light attenuation, temperature) factors (Kothawala et al., 2020). The balance of DOM input, removal, and production along the LOAC plays an important role in determining its contribution to greenhouse gas (GHG) emissions as well as the quantity and composition of DOC entering marine ecosystems. The terrigenous C flux is believed to have increased by ~ 1 Pg C yr^{-1} since the start of the industrial revolution, mostly as OC resulting from human activities (e.g. enhanced export of soil OC and increased wastewater inputs; Regnier et al., 2013), meanwhile oceanic DOC export has been relatively constant (Drake et al., 2018), implying that rates of C processing, outgassing and/or burial within the LOAC have increased.

Terrigenous DOM is predominantly chromophoric or 'coloured' (cDOM), and so cDOM is commonly used as a tracer for terrigenous material in marine waters. The majority of cDOM is thought to be fluorescent (fDOM; Coble, 2007; Laane and Koole, 1982), such that fDOM properties are often used to characterize cDOM. Compounds associated with terrigenous inputs tend to fluoresce more

strongly than those associated with anthropogenic inputs (e.g. wastewater) and *in situ* microbial processes (Stedmon and Bro, 2008). Non-chromophoric or optically 'invisible' DOM (iDOM) typically accounts for ~ 25 % of freshwater DOM (Chapter 5) but can represent a substantially larger fraction (Adams et al., 2018; Pereira et al., 2014, Chapter 3 and Chapter 5) and is more prevalent in highly productive and/or modified catchments (e.g. Massicotte et al., 2017; Spencer et al., 2012). Specifically, iDOC has been associated with remobilized surface soils (Pereira et al., 2014), algal production in eutrophic lakes (Adams et al., 2018), and inputs of dairy cattle waste (Chapter 5). The production of cDOM in the ocean is sufficiently low that its presence in seawater can be used as a tracer for terrigenous material (Painter et al., 2018).

Estuaries represent the boundary between fresh and marine waters and present the last barrier between terrigenous DOM and the ocean. Different estuarine morphologies and settings give rise to a multitude of different behaviours (Abril et al., 2002). Where processes of removal, transformation, and addition are minimal or balanced, DOC transport is controlled by dilution and therefore decreases linearly with increasing salinity (conservative mixing). Where these processes are not balanced, DOC changes non-linearly with increasing salinity, indicating non-conservative mixing. A sharp increase or decrease in DOC concentration at low salinities (< 5 ppt) is frequently reported (Abril et al., 2002; Li et al., 2019; Spencer et al., 2007) and is often attributed to environmental shifts associated with the mixing of waterbodies, including salinity-mediated cell plasmolysis (Morris et al., 1978) and geochemical changes (i.e. flocculation, resuspension, and desorption; Sholkovitz, 1976; Uher et al., 2001). Above 5 ppt, sharp shifts in DOC concentration can result from inflowing tributaries, current-driven sediment resuspension and dissolution, and point source anthropogenic inputs of DOC from e.g. wastewater treatment plants or agriculture (Imai et al., 2002), the latter of which is often accompanied by nutrients which can also stimulate *in situ* DOC production (Schlesinger and Melack, 1981) and consumption (Li et al., 2019). Non-linear DOC increases associated with additional inputs (tributaries and point sources) are not in themselves indicative of non-conservative behavior and must therefore be interpreted with caution. Linear increases in DOC concentration have also been observed, and are associated with high levels of baseline *in situ* production and/or steady inputs from the surrounding catchment via e.g. runoff (Lee et al., 2020). It has been suggested that DOC removal within estuaries is regulated by the DOC concentration of the initial riverine input (DOC_{in}), with higher DOC_{in} leading to greater removal (Spencer et al., 2007), but variations in the composition of this input also play a role (Asmala et al., 2016). Recent work found that British estuaries draining near-natural catchments tended to transport DOC conservatively, whilst estuaries draining more modified catchments tended to transport DOC non-conservatively (García-Martín et al., 2021). This behaviour was mainly attributed to shifts in the composition of the

fDOM fraction, but there was evidence of a substantial non-fluorescent (and therefore, mostly non-chromophoric) DOM fraction in estuaries that drained highly modified (e.g. arable and urban) land.

The molecular structure of DOM contributes to its bio-lability (Catalán et al., 2016; Kothawala et al., 2014; Mosher et al., 2015). iDOM lacks the double and triple bonds and aromatic structures that give cDOM its absorptive properties, and this structural simplicity may make it more susceptible to biological remineralisation. Thus, the relative abundances of cDOM and iDOM may control bulk DOC behaviour. Here we use an absorbance-based DOC prediction model (Pereira et al., 2014a) to quantify cDOC and iDOC in 12 British estuaries, sampled at quarterly resolution between April 2017 and April 2018. We explore the influence of cDOC and iDOC on estuarine DOC transport, and hypothesize that DOC transport is conservative where cDOC is dominant, and non-conservative where iDOC is dominant.

6.3 Methods

Full methodological details of sample collection, storage, and analysis are provided in (García-Martín et al., 2021) and are only summarized here. DOC, absorbance, and fluorescence samples were collected during quarterly visits (April, July and October 2017 and January and April 2018) to 12 estuaries which were selected as representative of the broad range of catchment types and land-use patterns found across GB (Figure 6-1). This produced a total of 60 salinity transects (12 sites x 5 visits), each with a salinity range of ~ 0 – 25 ppt (mean salinity range = 0.31 ± 0.49 ppt – 24.03 ± 3.29 ppt). DOC was quantified as non-purgeable organic carbon (NPOC) using a Shimadzu TOC-L analyser. Samples were run in triplicate against laboratory standards. Absorbance was measured using a Cary 60 UV-vis spectrophotometer set to scan between 200 and 800 nm at 1nm intervals. Samples were run against pure water (MilliQ) blanks in a quartz cuvette. Terrigenous samples are typically measured using a 1 cm pathlength cuvette, whilst marine samples tend towards a 5 cm pathlength cuvette. All samples in this study were measured using a 1 cm pathlength, which was deemed sufficient because (a) none of the samples were fully marine and (b) sufficiently strong and consistent absorbance signals were obtained across all samples.

The DOC pool was partitioned into cDOC and iDOC fractions using the absorbance-based method outlined in Pereira et al. (2014) using absorbance at 270 nm and 350 nm. The influence cDOC and iDOC fractions on DOC concentration was assessed via non-linear correlation ($\alpha = 0.05$), using the '*nclor*' package (v2.1; Ranjan and Nahari, 2020) in R (v4.1.1; R Core Team, 2019). Plotted concentration data were normalized to concentrations at zero salinity in order to more clearly show their behaviour relative to one another. Theoretical dilution lines were derived by modelling a linear

relationship between the lowest and highest salinity value for each individual transect. Estuarine behaviour was considered conservative where measured and modelled data exhibited linear correlation with an $R^2 > 0.80$. This cut-off is an operational one, allowing estuaries to be classified according to behaviour.

Previous studies investigating the transport of DOC through estuaries have intentionally avoided point-source inputs or removed data points which appear influenced by them (e.g. Spencer et al., 2007), thus any concentration increase in those studies could be attributed to internal processing rather than external inputs. In the present study this was not possible due to the nature of the estuaries sampled and the temporary nature of some point sources: sharp concentration increases rarely occurred every month (See Section 6.4 and Figure 6-2). Removal of data points associated with point-source increases was considered, but this obscured the DOC ~ iDOC relationship, and often resulted in too few data points per estuary with which to assess mixing behaviour

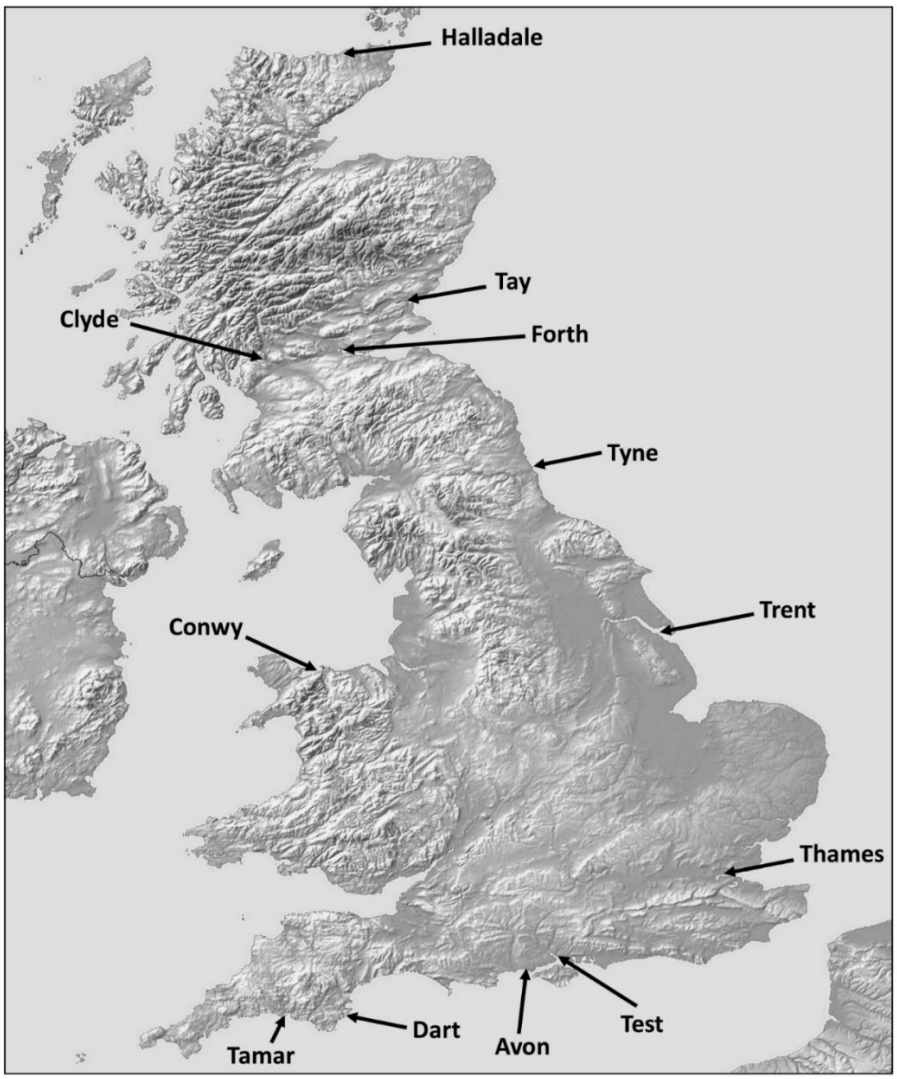

.

Figure 6-1. Map of Great Britain showing the location of each of the 12 study estuaries. Base map obtained from https://maps-uk.com.

6.4 Results and discussion

Estuarine DOC concentrations ranged from 0.91 to 34.40 mg L^{-1}, and were typically more strongly coloured and ~ 2 times higher at the freshwater end of the estuary (DOC_{in} = 6.74 ± 4.04 mg L^{-1}; 75 ± 22 %) relative to the saltwater end (DOC_{out} = 3.76 ± 3.12 mg L^{-1}; 57 ± 18 % cDOC). DOC exhibited a mix of behaviours during transport (conservative dilution (*n = 20*); non-conservative dilution (*n = 36*); increasing (*n = 5*). DOC_{in} was positively correlated with DOC_{out} (R^2 = 0.28, p = < 2.2 x 10^{-16}) and net DOC removal (ΔDOC; R^2 = 0.40, p = < 2.2 x 10^{-16}), but these correlations were weak. Thus, these results indicate that the concentration of the bulk riverine DOC input exerts only limited influence over its fate within the estuary (i.e. DOC_{in} is not a major driver of DOC_{out} or ΔDOC).

Estuarine cDOC concentrations ranged from 0.79 to 18.22 mg L^{-1} and exhibited net declines across all transects (n = 60) which were mostly conservative (*n = 51*). The correlation between the riverine cDOC input ($cDOC_{in}$) and the estuarine cDOC output ($cDOC_{out}$ R^2 = 0.68, p = < 2.2 x 10^{-16}) was much stronger than that observed for bulk DOC, as was the correlation between $cDOC_{in}$ and net cDOC removal (ΔcDOC; R^2 = 0.88, p = < 2.2 x 10^{-16}). These correlations and the mostly conservative nature of cDOC transport suggest that $cDOC_{in}$ exerts a substantial influence over $cDOC_{out}$ and ΔcDOC. However, the influence of cDOC on the behaviour and fate of bulk DOC was minimal, with $cDOC_{in}$ only weakly correlated with DOC_{out} (R^2 = 0.18, < 2.2 x 10^{-16}) and ΔDOC (R^2 = 0.24, p = < 2.2 x 10^{-16}).

Exceptions to this occurred where DOC transport was conservative (*n = 20*). $cDOC_{in}$ was strongly correlated to both DOC_{out} (R^2 = 0.78, p = < 2.2 x 10^{-16}) and ΔDOC (R^2 = 0.76, p = < 2.2 x 10^{-16}) in these transects, which received the largest, most highly coloured riverine inputs (DOC_{in} = 7.72 ± 4.05 mg L^{-1}; 85 ± 22 % cDOC). These conservative transects also exhibited strong within-estuary relationships between DOC and cDOC (R^2 = 0.93 – 1.00, p = < 2.2 x 10^{-16}) (Table 6-1), and riverine iDOC inputs were considerably lower in conservative ($iDOC_{in}$ = 1.10 ± 1.77 mg L^{-1}) relative to non-conservative ($iDOC_{in}$ = 2.09 ± 2.49 mg L^{-1}) and/or increasing ($iDOC_{in}$ = 1.68 ± 2.84 mg L^{-1}) transects, with minimal mid-estuary addition and/or removal (Figure 6-2). Thus, conservative DOC transport occurred when the initial riverine input was strongly coloured and within-estuary additions of iDOC were low. This is not to say that iDOC was not produced within or added to these estuaries, but that this was balanced by removal.

In the minority of transects where cDOC behaved non-conservatively (*n* = *9*), this was because of sharp cDOC increases within the estuary (Avon and Dart in April and July ’17), indicative of point-source inputs and/or rapid internal production or resuspension across the salinity gradient, or because initial deviations from conservative mixing occurred at low salinity (< 4 ppt), whether as an increase (Tamar in October ’17; Test in January and April ’18) or as a decrease (Dart and Tamar in January ’18). However, cDOC was not the most influential fraction in these instances.

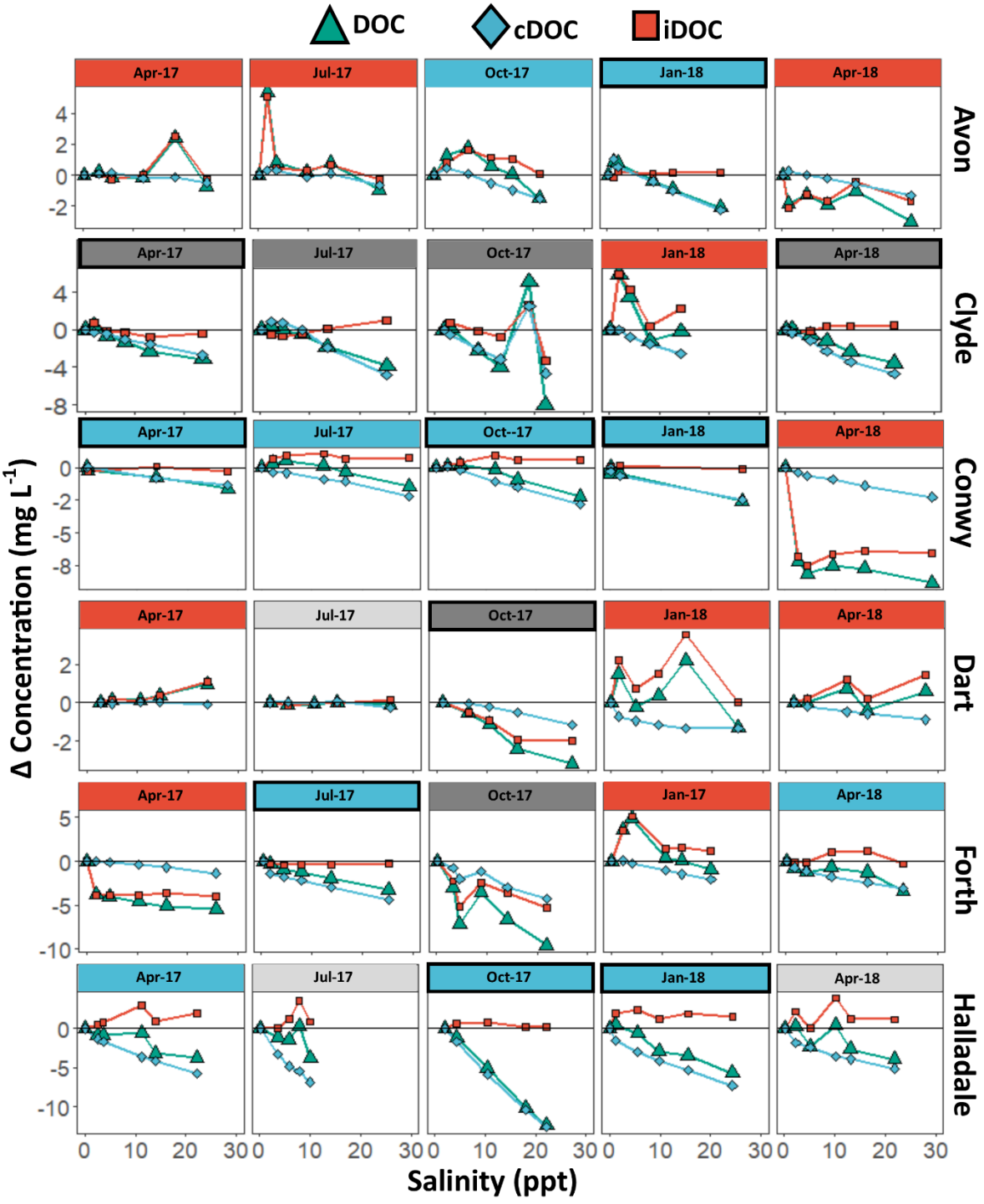

Figure 6-2. Relative changes in DOC concentrations across the salinity gradients within the studied

estuaries on each sampling occasion. DOC data are normalized to concentrations at zero salinity (solid black line) to facilitate visualization. Top bars are color coded according to significant non-linear correlations: (iDOC = red; cDOC = blue; both = dark grey; none = light grey). Black outline top bar indicates conservative DOC mixing.

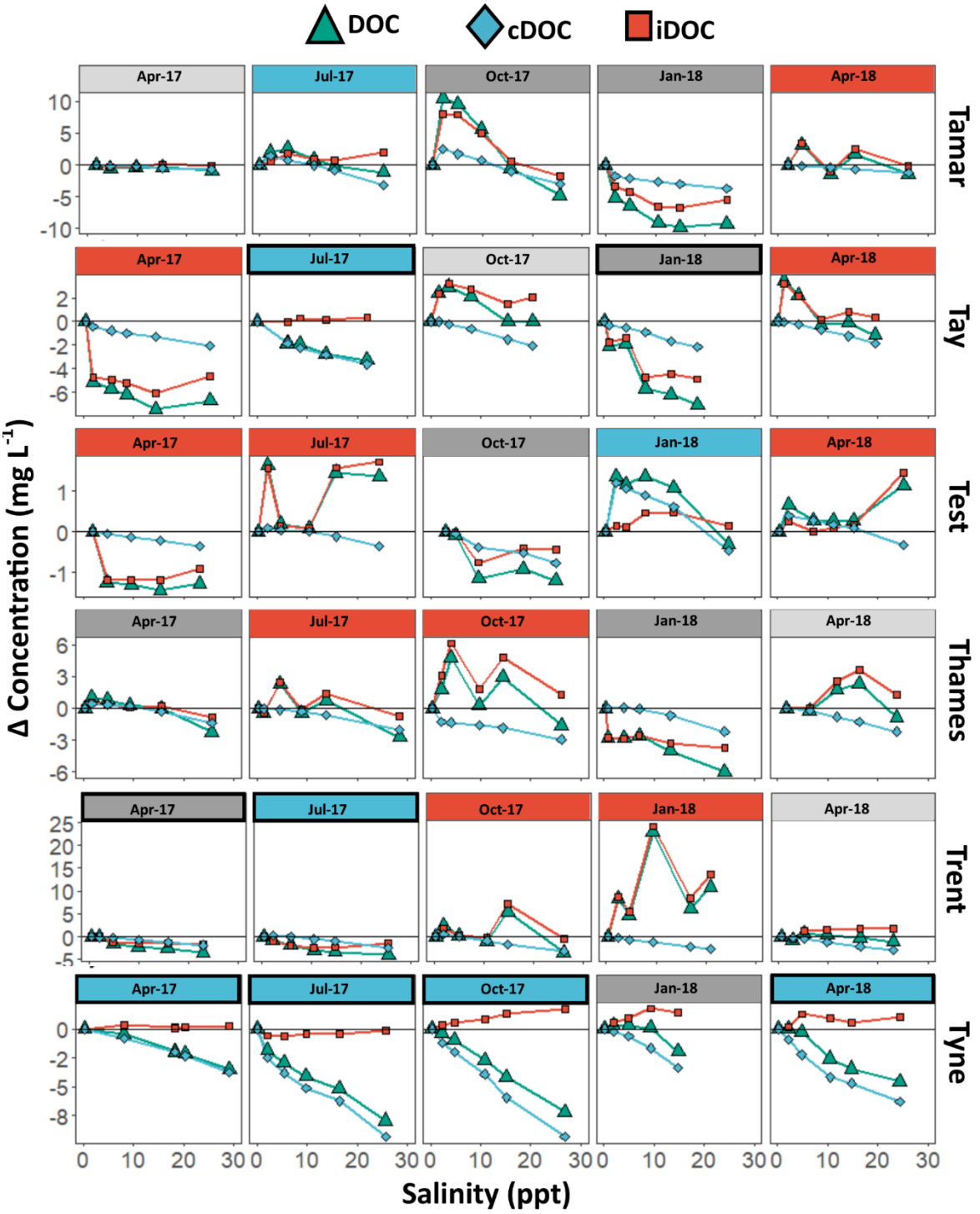

Figure 6-2 (Continued). Relative changes in DOC concentrations across the salinity gradients within the studied estuaries on each sampling occasion. DOC data are normalized to concentrations at

zero salinity (solid black line) to facilitate visualization. Top bars are color coded according to significant non-linear correlations: (iDOC = red; cDOC = blue; both = dark grey; none = light grey). Black outline top bar indicates conservative DOC mixing.

Table 6-1. Non-linear correlations between DOC and cDOC and iDOC. The strongest significant correlation is marked in bold in each instance. Non-significant relationships are shown as n.s. (α = 0.05).

Estuary	Fraction	Apr-17	Jul-17	Oct-17	Jan-18	Apr-18
Avon	cDOC	*n.s.*	*n.s.*	**0.85**	**0.99**	*n.s.*
	iDOC	**0.98**	**0.99**	*n.s.*	*n.s.*	**0.83**
Clyde	cDOC	**0.96**	**0.99**	**0.99**	*n.s.*	**0.99**
	iDOC	0.81	-0.92	0.98	**0.94**	-0.83
Conwy	cDOC	**0.96**	**0.88**	**0.96**	**0.99**	*n.s.*
	iDOC	*n.s.*	*n.s.*	*n.s.*	*n.s.*	**0.98**
Dart	cDOC	*n.s.*	*n.s.*	0.94	*n.s.*	*n.s.*
	iDOC	**1.00**	*n.s.*	**0.98**	**0.93**	**0.88**
Forth	cDOC	*n.s.*	**0.97**	0.95	*n.s.*	**0.85**
	iDOC	**0.95**	*n.s.*	**0.97**	**0.93**	*n.s.*
Halladale	cDOC	**0.86**	*n.s.*	**1.00**	**0.95**	*n.s.*
	iDOC	*n.s.*	*n.s.*	*n.s.*	*n.s.*	*n.s.*
Tamar	cDOC	*n.s.*	**0.88**	0.96	0.96	*n.s.*
	iDOC	*n.s.*	*n.s.*	**0.99**	**0.99**	**0.97**
Tay	cDOC	*n.s.*	**0.99**	*n.s.*	0.93	*n.s.*
	iDOC	**0.98**	*n.s.*	*n.s.*	**0.99**	**0.95**
Test	cDOC	*n.s.*	*n.s.*	**0.92**	**0.97**	*n.s.*
	iDOC	**0.98**	**0.99**	0.91	*n.s.*	**0.92**
Thames	cDOC	**0.99**	*n.s.*	*n.s.*	0.82	*n.s.*
	iDOC	0.97	**0.9**	**0.91**	**0.93**	*n.s.*
Trent	cDOC	0.93	**0.83**	*n.s.*	*n.s.*	*n.s.*
	iDOC	**0.95**	*n.s.*	**0.90**	**0.99**	*n.s.*
Tyne	cDOC	**0.99**	**1.00**	**1.00**	**0.88**	**0.96**
	iDOC	*n.s.*	*n.s.*	*n.s.*	*-0.97.*	*n.s.*

Where DOC behaved non-conservatively (*n = 35*) or increased (*n* = 5), within-estuary DOC concentrations were correlated with iDOC (*n* = 27/40; R^2 = 0.83 – 0.99) almost twice as often as with cDOC (*n* = 14/40; R^2 = 0.82 – 0.99), and cDOC was the singular significant correlation on just seven occasions. Furthermore, iDOC appeared locally influential on several occasions where the overall correlation with DOC was not statistically significant (i.e. a sharp increase in iDOC coincided with a sharp increase in DOC, but the two were not correlated overall). This can be seen in the Halladale estuary, where repeated mid-estuary spikes occur at approximately the same salinity (and geographical location) on multiple occasions (see Figure 6-2). These measurements were taken over

a macroalgal mat which may be the source of this iDOC input. We are unaware of any studies quantifying macroalgal iDOC, but they are known to exude compounds associated with it (e.g. saccharides and aliphatic acids). Mid-estuary spikes which appear in more urban estuaries (e.g. Thames, Trent) may instead be associated with point source wastewater outputs. The increase in iDOC observed in the Tamar in October '17 may relate to agricultural inputs, as per Chapter 5. which found evidence of substantial iDOC inputs in the lower Tamar associated with both dairy farming and runoff.

Thus, non-conservative mixing appears to be to be driven by iDOC than by cDOC. This finding is particularly important in the context of studies which have previously used optical characteristics to quantify and/or characterize estuarine DOC and/or DOM. These studies typically assume that cDOM ultimately controls the behavior and fate of the riverine DOC input within estuaries, however our results indicate that the iDOC may be considerably more influential. This should be considered as part of efforts to use *in-situ* sensors and/or remote sensing of cDOM as a proxy for terrigenous DOC. The present study finds that iDOC accounted for 25 ± 22 % DOC_{in} on average, in agreement with previous work showing that iDOC accounted for ~ 22 % of the British riverine DOC flux (Chapter 5). Thus, the riverine flux can contain a substantial fraction iDOC which originated in freshwaters, enters estuaries, and cannot be accounted for using optical methods in isolation. In comparison, iDOC accounted for 43 ± 18 % DOC_{out} on average, which suggests net-production and/or addition of iDOC within the 12 study estuaries. ΔcDOC and ΔiDOC exhibited ranges of -12.62 to -0.13 mg L^{-1} and -6.57 to 13.67 mg L^{-1}, respectively, which demonstrates how much more variable iDOC behaviour is relative to cDOC, which universally showed a net decrease.

In the small number of conservative transects where both cDOC and iDOC concentrations were significantly correlated with DOC (*n = 7*), the correlation between iDOC and its theoretical mixing line was relatively high (R^2 = 0.71 ± 0.19, p = < 2.2 x 10^{-16}). Whilst this was not high enough to meet the operational cut-off for conservative transport (R^2 = 0.80, p = < 2.2 x 10^{-16}; see Section 6.3), this is suggestive of minimal addition and/or removal of iDOC. The fact that the riverine input of iDOC behaves near-conservatively in the absence of external inputs suggests that it is less labile than iDOC received via point-source inputs, which was rapidly removed in most cases. In these instances, any *in situ* production of iDOC would have to be tightly cycled such that it exhibited minimal net change. Future work should look to provenance iDOC such that any source-driven spectrum of labilities can be assessed. Molecular characterization of iDOM is also required to unpick the relative importance of DOM pool composition vs. environmental conditions which may favour the remineralisation of specific moieties. The latter has been observed in the open ocean where semi-labile DOM can

persist for weeks at the surface despite being structurally simple, only to be rapidly degraded at depth (Hansell and Carlson, 1998lo; Sunagawa et al., 2015), and may explain why iDOC appears to gradually accumulate in some transects (e.g. the Tyne). The iDOC which is accumulating may represent a less labile iDOC fraction which is produced during the remineralisation of more labile material. Thus, our results may well have missed the turnover of a rapidly cycled and hyper labile iDOC pool produced *in situ*. Quantifying the contribution of each fraction to estuarine outgassing is an important next step in understanding the true contribution of iDOC (and hence DOC as a whole) to the estuarine carbon cycle.

6.5 Conclusion

This study shows that the loss of riverine DOC across estuarine salinity gradients is not always simply related to the concentrations imported by the rivers; its fate frequently depends upon the abundances and individual behaviours of cDOC and iDOC. The refractory nature of most cDOC results in its conservative transport across estuaries, and exported concentrations of this fraction are therefore highly correlated with concentrations entering the estuary from freshwaters. Therefore, when the DOC pool is predominantly comprised of cDOC, and where no obvious inputs occur at intermediate salinities, bulk DOC behaves conservatively. By contrast, where within-estuary addition, removal, and production processes are substantial, iDOC is highly influential. Whilst shifts in cDOC can contribute to non-conservative DOC transport, variations in iDOC concentration were the most common driver. These results point towards iDOC being considerably more influential than cDOC in terms of estuarine DOC dynamics, and are particularly relevant to conversations about the appropriateness of using cDOM to quantify and characterize estuarine DOC dynamics.

6.6 Acknowledgements

SLF was supported by the NERC-funded SPITFIRE Doctoral Training Programme (grant number NE/L002531/1). DJM and CDE were supported by the NERC (Natural Environment Research Council, UK) Land Ocean Carbon Transfer programme (LOCATE; grant numbers NE/N018087/1 & NE/C05686/1, respectively).

The authors declare no conflict of interest. The data used in this study are available on request from the British Oceanographic Data Centre (BODC) under Accession Number SOC210158.

6.7 Author contributions

SLF conceptualised the study, conducted formal analysis, and wrote the original manuscript draft. All authors contributed to the review and editing process.

Chapter 7 Discussion

7.1 Restatement of aims and objectives

The overarching objective of this thesis was to improve our understanding of the land-ocean DOC flux. Specifically, this thesis aimed to investigate:

1. The effect of land use on the quantity and composition of terrigenous DOC export (Chapter 2 and 4);

2. The behaviour, source, and prevalence of iDOC in multiple settings and at multiple scales (catchment; land-mass; global) (Chapters 3, 5, and 6); and

3. The importance of including iDOC quantification in absorbance-based investigations of DOC (Chapters 5 and 6).

7.2 Thesis Summary

The transport of terrigenous DOM and DOC from land to sea is a significant and changing component of the global carbon cycle. This thesis used optical tools (absorbance and fluorescence spectrophotometry) to investigate its composition and fate across a range of aquatic settings.

The common thread running through this thesis is that human activities on land are influencing aquatic and coastal ecosystems. Chapter 1 sets the scene for this, detailing the scale of the land-ocean C flux and the various anthropogenic pressures which act upon it. Chapter 1 also addresses the uncertainties associated with current estimates of the terrigenous C flux, and finds that our existing estimates may be biased in favour of large, highly coloured river systems.

Chapter 2 shows that deforestation and agricultural expansion in the Belize River Watershed has increased terrigenous DOM export, with implications for the health of coastal ecosystems including the world's second largest coral reef system. However, this study focusses explicitly on cDOM, and reports a decoupling between cDOM and DOC. The scale of this decoupling is not unprecedented, but it is unusual as far as the literature goes. Chapter 3 investigates this, quantifying iDOC as ~ 50 % of the DOC pool. To my knowledge, this is only the third study to have explicitly quantified the iDOC fraction. One of the major uncertainties around iDOC is how it behaves in aquatic systems, and so

Chapter 3 investigates this using dark biodegradation assays to show that iDOC in the Belize River Watershed may be more refractory than the cDOC pool. Chapter 4 remains within the Belize River Watershed and presents a new method to provide quantitative estimates of DOC associated with fluorescence-derived PARAFAC components. PARAFAC has previously been limited to qualitative characterisation of the DOC pool in environmental samples.

Chapter 5 quantifies freshwater iDOC at GB-scale, where it accounted for 21 % of the annual DOC flux. This was reflected more broadly in a compiled data set of ~ 3,000 samples from a range of geo-climatic settings where it represented ~ 20 % of the DOC pool. Thus, iDOC is a globally significant C fraction, the broad scale importance of which has been overlooked. Chapter 6 moves into GB estuaries where iDOC appears to drive estuarine DOC behaviour. Previous studies have generally focussed on using cDOC and/or catchment characteristics to explain DOC transport through estuaries, but this study suggests that neither are particularly influential. Instead, in-estuary iDOC inputs appear to be the dominant control.

7.3 Implications

7.3.1 Implications for sensor-based estimates of DOC concentration

To improve our understanding of the land-ocean DOC and DOM flux, we require much more data than is presently available. Sensor-based measurements offer a way to do this at much higher resolution than would be possible through sample collection, with *in situ* sensors offering high temporal resolution across a limited number of locations and satellite remote sensing offering high spatial resolution at up to global scale, with the option to look back in time using archived images. It has been the recommendation of multiple agencies and reports that sensor-based estimates of DOC and DOM fluxes be used inorder to reach the scale required for useful regional and global understanding of this important pathway, including the National Environmental Research Council (NERC)'s 'Constructing a Digital Environment' strategic priorities fund (www.digitalenvironment.org) and the Integrated Carbon Observatory System (ICOS) (Felgate et al., 2021a). However, in light of the findings of this thesis, such estimates seem likely to significantly underpredict DOC fluxes across a wide range of systems where iDOC is a significant fraction. This must be given careful consideration, as without adequate calibrations and/or caveating of sensor-based estimates, a substantial fraction of the global DOC pool may be missed.

7.3.2 Implications for optical characterisations

Optical proxies for the molecular characteristics of DOM and DOC are commonly used and compared across systems and studies. Given the highly variable contribution of iDOC identified in this thesis, such comparisons have the potential to be misleading.

This can be demonstrated using catchment-scale data from the Conwy and Tamar catchments. PARAFAC analysis revealed that fDOM in these catchments exhibited broadly similar fluorescence component compositions (Figure 7-1), and a general interpretation of these results would suggest broadly similar molecular composition and thus, broadly similar reactivities assuming all other factors are equal. We also see that the composition of the fDOM pool is relatively consistent across time and space within each sub-catchment, with occasional spikes in more microbially mediated material (C4 and C5) which do not appear to be the main driver of increased total fluorescence (sumFL), which is an indicator of how much of material is present (Figure 7-3). Without knowledge of the scale and variability of the iDOM fraction, these data suggest DOM pools which are relatively stable in terms of their composition, and which are dominated by humic-like (C1 and C2) material which is typically refractory.

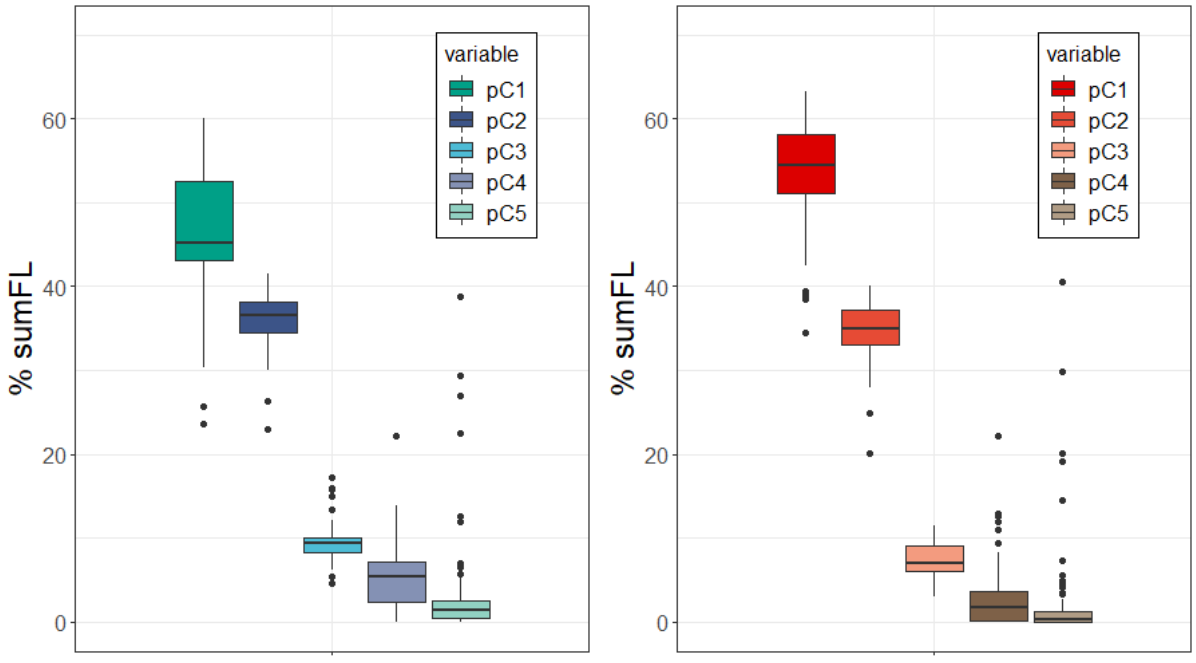

Figure 7-1. Mean fDOM composition in the Tamar (left) and Conwy (right) catchments (10 monthly measurements across 11 sites per catchment) presented as a box plot. pC1 – pC5 are the proportion of C1 – C5 PARAFAC components.

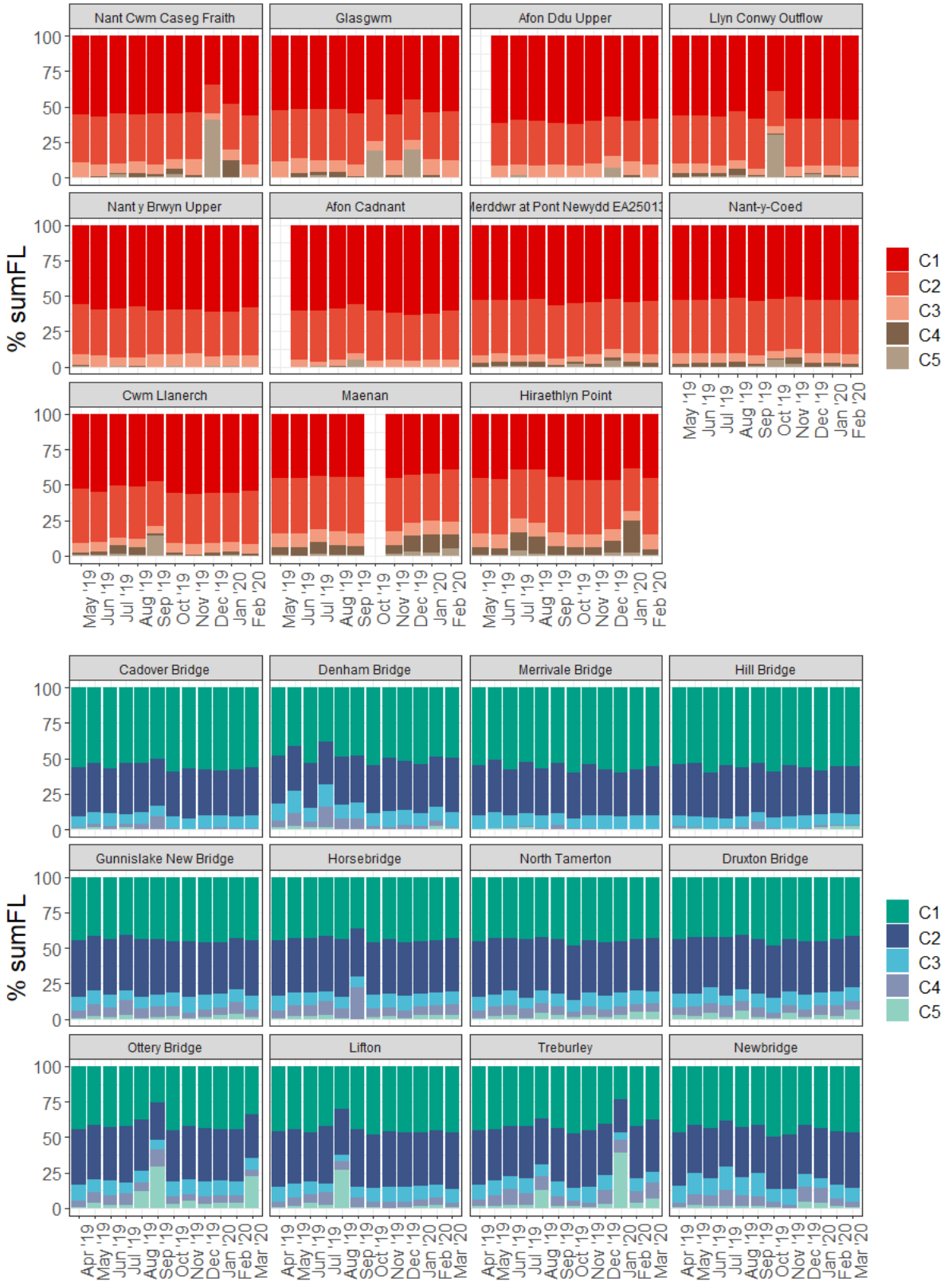

Figure 7-2. Monthly composition of the fluorescence DOM pool in the Conwy (top) and Tamar (bottom), plotted as a % of sumFL and given by site and month. Note that no data were collected in April 2019 and March 2020 for the Conwy.

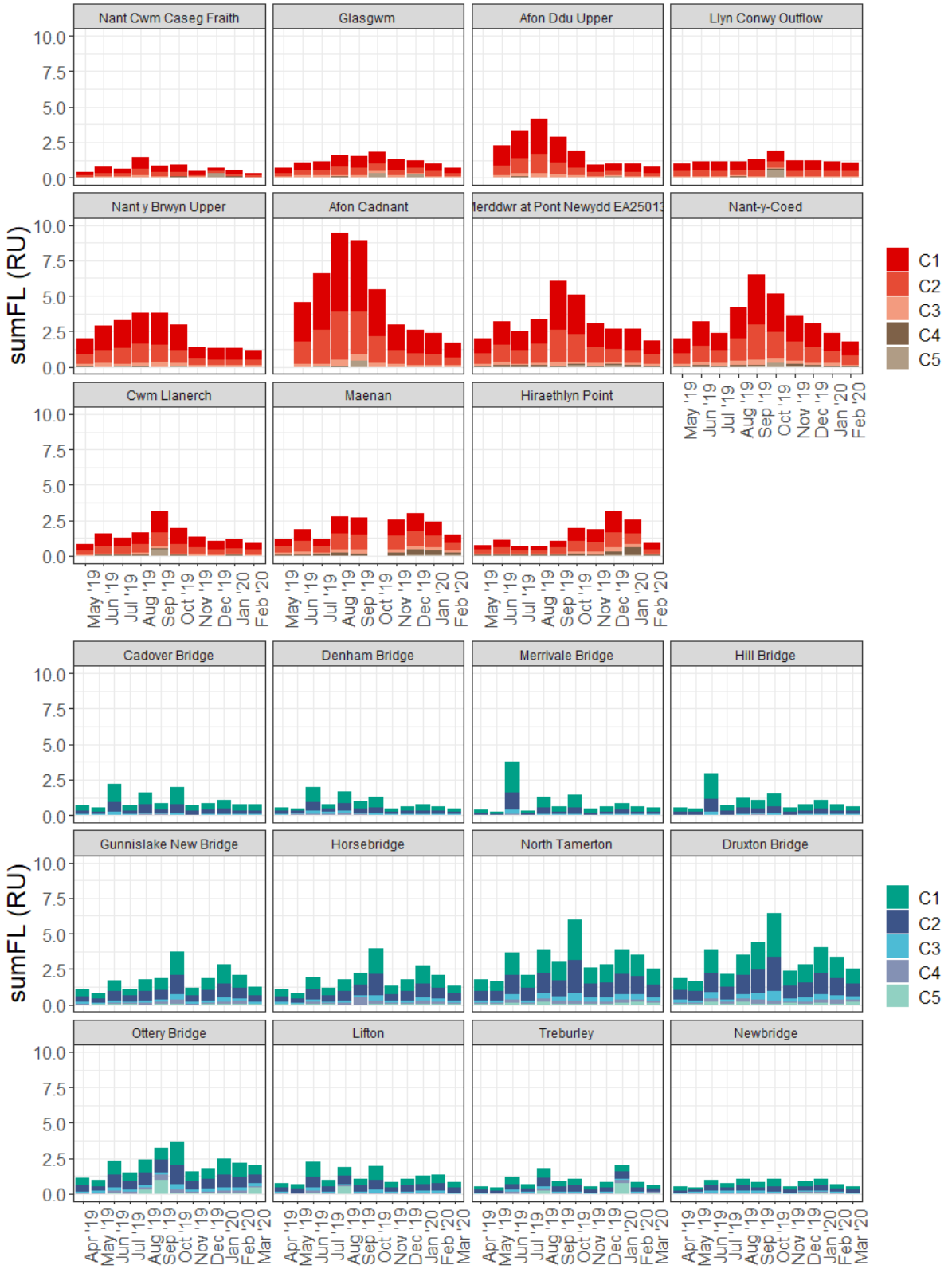

Figure 7-3. Monthly fluorescence intensity in the Conwy (top) and Tamar (bottom), plotted by site and month. Note that no data were collected in April 2019 and March 2020 for the Conwy.

However, cDOM accounts for ~ 100 % of the Conwy DOC pool, and only ~ 50 % of the Tamar DOC pool. If iDOM is more labile than humic-like cDOM, the associated DOC pools are likely to exhibit very different reactivities. Without quantifying cDOC and iDOC, there is no way to know how much of the DOC pool is accounted for using PARAFAC analysis, and this may therefore bias our interpretation.

Similar caution should be applied for absorbance-based proxies, such as DOC specific UV absorbance at 254nm ($SUVA_{254}$) which is commonly used to approximate aromaticity, and is derived according to Equation 7-1:

$$SUVA_{254} = \frac{a254\ (m^{-1})}{DOC\ (mg\ L^{-1})} \qquad \boldsymbol{Eqn.7-1}$$

Because of its structure, iDOC can be considered to have zero aromaticity, and so $SUVA_{254}$ can be seen as a measure of aromaticity in the cDOC fraction and in the DOC fraction as a whole. Take two theoretical samples, A and B, both of which have the same DOC concentration and the same absorbance at 254nm. A standard interpretation of $SUVA_{254}$ would be to infer a similar degree of aromaticity. This approach works when the DOC pool as a whole is being compared, but where inferences are being made about cDOC, the iDOC contribution has the potential to confound this interpretation. If, for example, sample A contains 100 % cDOC and sample B contains 50 % cDOC, sample B would have to contain a cDOC fraction which was twice as aromatic as the cDOC which comprises sample A. Thus, the DOC in each sample is likely to be functionally different in terms of its bio- and photo-lability, and to have come from different sources and/or experienced different degrees of bio- and photo-processing. It may therefore be more appropriate to calculate $SUVA_{254}$ for the coloured fraction in isolation where cDOC is the target of the investigation ($cSUVA_{254}$).

7.3.3 Implications for ongoing monitoring activities

The highly variable nature of the relationship between DOC and iDOC means that absorbance-based monitoring of DOC fluxes may not be reliable in systems where iDOC represents a significant fraction of the DOC pool, and a lack of interest and/or the previous absence of a reliable method for quantifying iDOC means that we do not necessarily know which systems these are. It therefore seems sensible that the composition of the DOC pool should be ascertained before initiating absorbance-based monitoring activities, and that regular checks on the variability of that composition will be required to ensure ongoing appropriateness. However, it is possible that iDOC may also be problematic for some direct DOC quantification methods.

As part of the data validation process for Chapter 5, DOC data for the Tamar catchment were investigated relative to existing monitoring data obtained from the UK Environment Agency (EA). The EA undertake monthly monitoring of the Tamar River at Gunnislake New Bridge, and reported data were considerably lower than those measured by the LOCATE program (Figure 7-4):

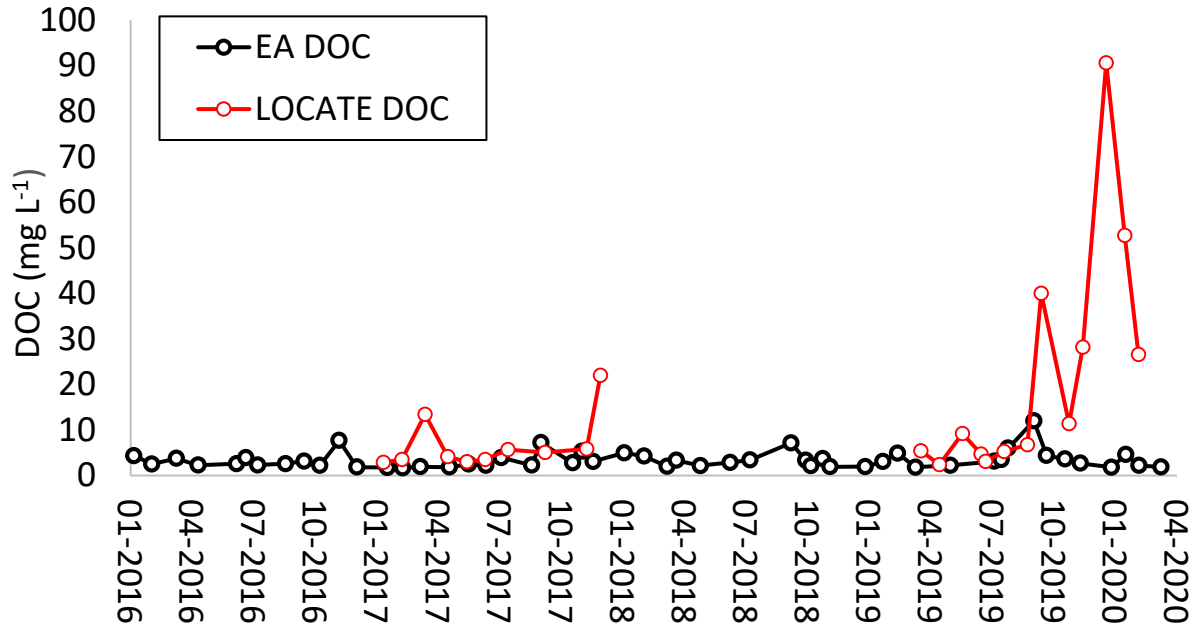

Figure 7-4. Plot showing EA DOC data (black line) at Gunnislake Bridge between January 2016 and April 2020, showing previous trend, and LOCATE DOC data (red line) during the WP1 (January – December 2017) and WP2 (April 2019 – March 2020) sampling periods.

Several potential methodological issues with the LOCATE data were considered, details of which are given in Chapter 5. In addition, a more than coincidental relationship was identified between measured DOC and suspended solids (SS) in the Tamar (Figure 7-2). Filtration of highly turbid samples can block filter capsules very quickly, increasing the likelihood of inappropriate pressure being applied. This could result in a break-down of colloidal and particulate C into DOC, artificially elevating measured DOC values. However, for this to produce iDOC as an artefact of filtering, the effect would need to be present in DOC and absent in absorbance samples or all the 'additional' DOC added via filtering would need to be non-coloured. Absorbance samples were collected in the same way as DOC samples, so the former seems unlikely. As a rough check on the latter, we estimated POC as 50 % of SS. To produce a 50 mg L^{-1} DOC, filtration would need to force 100 mg L^{-1} or 1/3 of the highest SS reported (300 mg L^{-1}) through the filter. Whilst this seems unlikely, it is technically possible. However, SS loads were often insufficient to account for estimated iDOC concentrations.

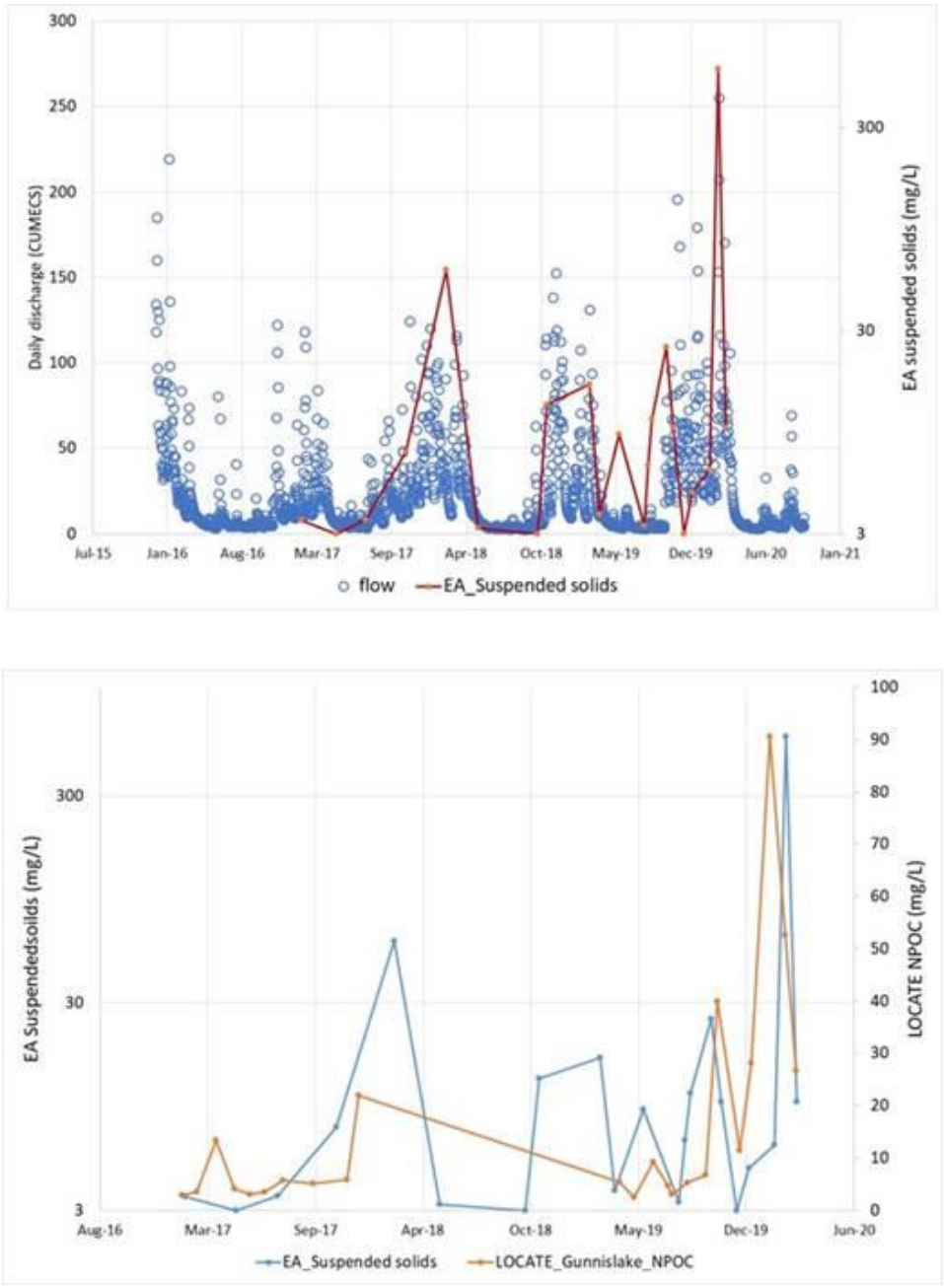

Figure 7-5. Relationship between (top) EA suspended solid data and daily discharge (m^3s^{-1}), and (bottom) shifts in EA suspended solids and LOCATE measured DOC data over time. EA data obtained from the EA Harmonised Monitoring System.

Taking October 2019 as an example, LOCATE DOC was 40 mg L^{-1} and the EA DOC was around 4 mg L^{-1}, with a SS load of 30 mg L^{-1}. Forcing all 30 mg L^{-1} SS through the filter, even if it was entirely composed of POC, would not explain the DOC value. Thus, SS concentrations are insufficient to generate the difference between LOCATE and EA DOC values. It is more likely that the apparent highly sensitive SS vs. discharge relationship (Figure 7-5) in the Tamar is an indicator of a state change in flow paths at times of prolonged heavy rainfall, which in addition to bringing more

particulates could also deliver more DOC from e.g. agricultural storm drains, manure from fields, slurry tanks, much of which is iDOC.

EA data are determined colorometrically via UV oxidation, which provides an indirect quantification of DOC based upon a secondary chemical reaction. Previous work has demonstrated the potential for similar methods to significantly underestimate DOC concentrations. A recent study identified this underestimation as the result of agglomeration and 'foaming' which specifically affects proteins and some humic substances (Yang et al., 2021). If this is the cause of the differences shown in Figure 7-4, it is likely that the EA monitoring data are under predicting DOC by ~ 50 % in the Tamar River, and that this is a wider-scale issue. EA data underpin historic DOC records held within the Harmonised Monitoring Scheme (HMS) database (available here) and several GB flux estimates (e.g. Worrall et al., 2020), highlighting the importance of selecting the correct DOC quantification method. In this context, the fact that our GB-scale DOC estimate (Williamson et al., 2021) was ~ 20 % higher than previous estimates made using EA data (e.g. Worrall et al., 2012) is unsurprising, given that ~ 20 % of our calculated flux was iDOC. A comparison exercise involving the EA laboratory, CEH Lancaster (where the LOCATE samples were run), and at least one independent laboratory would be a useful next step, and talks are ongoing to arrange this.

7.4 Limitations

7.4.1 Limitations of the catchment characteristics selected

Chapter 2 infers that DOM quantity and character vary along a dominant axis of variation in the Belize River Watershed, namely land-use, but land-use in that catchment at least partially tracks intrinsic site properties such as geology, elevation, and soil type. This tracking of land use with other catchment characteristics is also true elsewhere. In Chapter 5, for example, land use types most closely aligned with human activities (e.g. crop and livestock agriculture and urban settlement) tended to dominate at lower altitudes and more fertile soil types, whereas higher altitudes and less fertile soil types tend to be used for e.g. forestry and rough grazing. The type of modification also appears to play a role, an example of this being the difference in iDOC content in highly deforested regions of Belize and Malaysian Borneo (Chapter 5). Both systems have been subject to intensive land use realignment, but to different ends: in Belize, forested land has been replaced with intensive crop and livestock agriculture, whereas in Borneo, conversion is almost exclusively to make room for palm plantation. Whilst both regions have experienced high levels of anthropogenic modification, Belize has a much larger human presence and a much greater iDOC fraction. However, these systems also have very different soil types with Belize draining mostly carbonate and mineral soils and

Borneo draining organic-rich peat soils. Thus, the effect of land use modification is highly context dependent, and more work is required to understand exactly how different systems will respond to various combinations of catchment characteristics and human influence.

An additional limitation exists in the GB-scale modelling conducted in Chapter 5, which assumes that different DOC fractions respond similarly to e.g. flow and precipitation, whereas differences in flow paths and solubility might result in different responses from cDOC and iDOC, and indeed from different cDOC and iDOC fractions. Resolving such differences was out with the scope of this thesis, but further investigation would be valuable.

7.4.2 Limitations of the iDOC prediction model

The iDOC prediction model used throughout this thesis uses the extinction coefficients presented in Carter et al. (2012). Whilst these coefficients were derived for a reasonable number of samples (n = 1700) from multiple geographic settings, their use assumes that the characteristics of components A and B are universal. In reality, it is likely that these the absorbance characteristics of these components vary according to catchment and source characteristics, and bespoke derivations of their extinction coefficients may yield different results. Future work to assess the influence of universal vs. bespoke calibrations would be a useful contribution, however the broad classification of just two components means that any influence is likely to be small. The iDOC model also assumes that DOC can be adequately represented by three components (cDOCa, cDOCb, and iDOC), but this distinction is an arbitrary one. Adams et al. (2018) identified an additional component (cDOCc) associated with low-colour algal material which I considered including, but this carried a risk of overfitting the model in systems where this component was not significant. Again, more specific calibrations of each sample set might allow additional components to be added and improve the accuracy of the model.

7.4.3 Limitations of the biodegradation method

A methodological limitation of the biodegradation method presented in Chapter 3 was a lack of adequate temperature control. Incubating at ambient temperatures produces two temperature effects. The first is a measurement effect whereby O_2 concentrations vary according to water temperature and pressure, and this is easily corrected for by recording these parameters with each O_2 measurement. The second is a functional effect whereby microbial biodegradation rates vary with temperature. It is possible to attempt a correction for this (i.e. Q_{10}) if an adequate temperature record can be obtained and, indeed, if the correct Q_{10} value is known, but the sensors deployed to

capture this were lost within hours of the first experiment, making this impossible. As a result, the complexity of the biodegradation model which could be fit to these data was limited to a basic exponential fit. More information could be obtained if these temperature issues could be removed, allowing the fit of a multiple pool and/or continuum model.

A possibility not considered in Chapter 3 is that a substantial fraction of iDOC which was captured in the DOC and absorbance samples which were filtered immediately, but was remineralized before the first O_2 measurement could be taken (1 - 5 hours post-collection). This would fit with the initial hypothesis that iDOC would be highly labile, and could result from iDOC having a non-pelagic source within the river (e.g. benthic production diffusing into the water column) which was not captured in surface water samples. If we assume that any O_2 lost between sampling and the initial bioassay measurement was the result of iDOC remineralisation, and that this remineralisation occurred at a ratio of 1 iDOC: 2 O_2 (i.e. DOC –> CO_2), the mean potential loss of iDOC in transit can be estimated at 2.43 ± 4.35 mg L^{-1}, relative to an initial iDOC pool of 4.02 ± 4.34 mg L^{-1}. The O_2 consumed in transit could have resulted in total iDOC removal at 8 sites (27 %), but at the remaining 22 sites (73 %) available iDOC exceeded O_2 consumption: on average, at least 67 ± 31 % of the initial iDOC would still have been present at the start of the bioassay (3.87 ± 4.23 mg L^{-1}). Thus, even if all the O_2 lost in transit resulted from the remineralisation of a highly labile iDOC fraction, a substantial iDOC fraction would have remained. It is unclear whether taking the possible removal of iDOC into account would fundamentally change the findings presented in Chapter 3, but if rapidly removed iDOC is a confounding factor in these data, it is likely to also have been a factor in any other studies which investigate DOC biodegradation kinetics using bioassay experiments which involve a delay between collection and incubation. The potential for this to be an issue could be further investigated by repeating the correlation analysis in Chapter 3 using iDOC values calculated to take into account O_2 loss (and assumed iDOC loss) during transit, and validated in the longer term by repeating the experiment with a revised methodology whereby samples were placed into vials and the bioassay initiated immediately. Additionally, collecting DOC and cDOM samples at the end of the assays would allow model fits to be truthed, and would further validate their findings.

7.5 Future research priorities

The primary recommendation of this thesis is that iDOM should be quantified as standard in future land-ocean DOC export studies, whether they operate within a single component or the entire continuum. DOC and absorbance measurements are often core to such studies, in which case all that is required is a simple calculation. Where absorbance is not also included, the analysis is inexpensive,

fast, and the samples can be stored and transported in the same was as DOC and so the additional resource is low. Beyond this, some specific research priorities have been identified.

7.5.1 The effect of increasing terrigenous cDOM concentrations on coral health

A major conclusion of Chapter 2 was that sub-catchments dominated by agricultural land use contained higher concentrations of terrigenous humic-like cDOM than sub-catchments dominated by pristine rainforest. This material accumulated with distance downstream and behaved conservatively in the adjacent coastal environment, were hydrodynamic modelling indicated that this material could be found in waters overlying the regions' environmentally and economically valuable coral reefs. Thus, an historic land-use trajectory away from forest and towards agriculture has likely increased the amount of cDOM reaching the reef. However, this inference was based on data collected over a short time scale (12 months) and under a very narrow set of hydrological conditions. Furthermore, it is unclear whether cDOM concentrations in overlying waters have any measurable effect on coral health. Both of these questions are critical from an ecosystem management perspective. A recently published method which uses luminescence as a proxy for terrigenous cDOM in a Malaysian coral system (Kaushal et al., 2021) might provide a useful way to validate the model and conclusions presented in Chapter 2 against historic data. To this end I have been awarded a Global Partnership Award from the University of Southampton to reconstruct historic terrigenous cDOM concentrations in Belizean corals (Appendix B). If this validation is successful, an important next step will be to investigate the effect of increasing water column cDOM concentrations on coral health. Laboratory mesocosm studies which would allow corals to be subjected to a range of past, present, and predicted cDOM concentrations under controlled conditions are likely to be the best way forward for this research, and would ideally be run as multi-factorial experiments which consider the effects of multiple stressors including temperature increase and ocean acidification.

7.5.2 Characterising iDOM

More fundamentally, there is a need to more adequately characterise iDOM in terms of its composition, source, and behaviour. Whilst iDOC appears to be most associated with anthropogenic land use and/or activities, we cannot assume that all iDOC is anthropogenic in nature – it is also found in more natural settings and evidence suggests it may have a substantial source in leaf litter and/or surface soil run-off. This thesis has taken a binary approach to iDOC and cDOC reactivity, which was a pragmatic approach in the face of limited evidence and the limitations of the available methodology. However, Chapter 3 suggests that iDOC in Belize may be less reactive than cDOC, and

Chapter 5 suggests variable reactivities according to source (i.e. *in situ* vs. point-source inputs). Acceptance of variable cDOM reactivities is long-standing, and it is likely that iDOC similarly exhibits a spectrum of labilities which must be understood in order to move this research forward. Combining stable isotope analysis with biodegradation assays might help elucidate the relationship between source and reactivity, and whilst field studies might most accurately reflect the complex microbial, biogeochemical, and environmental interactions found in nature, targeted laboratory based incubations of ^{13}C labelled iDOM compounds might be a more appropriate first line of enquiry. To better constrain iDOM composition, higher resolution techniques such as size exclusion chromatography and Fourier Transmission Infrared Mass Spectrometry (FT-IRMS) could be applied. Whilst each of these options carries its own limitations, a combination of optical, high resolution, and chemical analyses would likely yield new understanding.

7.6 Conclusions

This thesis has two central conclusions. The first is that human activities on land are having a meaningful influence over the composition of the aquatic DOC pool, in agreement with a large and growing body of literature. The second is that iDOC is a substantial and variable component of the aquatic DOC pool, about which a great deal of uncertainty exists. Better constraining and understanding iDOC composition, source, and reactivity is critical to our understanding of the land-ocean C flux and, more broadly, to our understanding of the global C cycle and how it is changing.

Appendix A DOM and DOC Preservation Methods

This appendix details considerations and decision making around the preservation of samples for measurement of DOC concentration and DOM absorbance.

A.1 Filtration

Filtration works by removing the biodegradation organisms before they can alter the sample. Prokaryotes are typically > 0.2 µm in diameter (Krieg, 2001), and so a 0.2 µm is standard in saline waters. However, 0.45 µm is typical in freshwaters where organic complexes in the 0.2 – 0.45 µm range are more common. The literature suggests that this difference in pore size does not have a significant effect on measured DOC concentrations (Zsolnay, 2003; Sanderman et al., 2008; Gandois et al., 2010; Denis et al., 2017), but some studies do contradict this. For example, Chow et al. (2005) reported a ~ 10 % reduction in DOC concentration using a 0.2 µm filter relative to a 0.45 µm filter. To ensure comparability of results when working across fresh and saline waters, a singular filter size should therefore be used. 0.45 µm was selected as most sampling was to occur in fresh waters.

Filters come in a range of materials, with glass fibre (GF) and cellulose acetate (CA) filters being the most common (Karanfil et al., 2002). GF filters pore sizes were considered unsuitable because they are only nominally sized, whereas CA filters come in an absolute sizing. Disposable filter capsules were selected to limit handling of the filter itself, which in turn reduced the risk of contamination.

Filters have the potential to alter the concentration and/or composition of the sample via leaching of DOM/DOC from and adsorption of DOM/DOC onto the filter disk. The extent and nature of these alterations varies according to filter material, pore size, brand, and even batch number. Pre-treatment of filters is recommended, and is usually done by flushing the filters with a fixed volume of organic-free water prior to use. Karanfil et al. (2003) recommended flushing CA filters with 150 ml, but the remote locations studied in this thesis meant that organic-free water was not always available. Fouling of the filter by particulates and/or colloidal matter is another issue associated with filtering, and 150 ml sample water was often sufficient to block the filter. As such, a pragmatic flushing protocol was adopted whereby 50 ml sample water was pushed through each CA filter prior to use. Comparison of filtered and unfiltered samples (Figure A-1) show that this protocol led to minimal contamination, and the fact that the results presented in this thesis are physically sensible and interpretable lends further confidence to this.

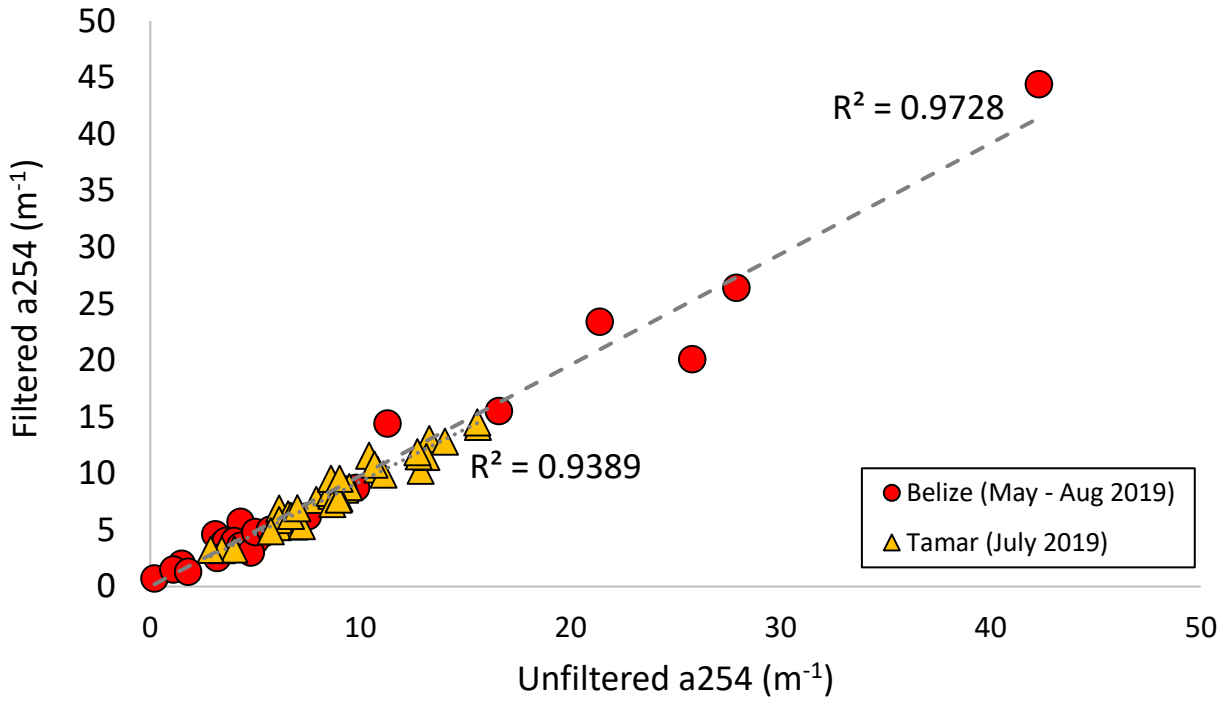

Figure A-1. Plot showing the effect of filtering freshwater absorbance samples in the Tamar catchment (yellow triangles) and the Belize River Watershed (red circles). Comparable data for DOC are not available.

A.2 Cold storage

Whilst filtration is designed to stop biodegradation, the 3D nature of prokaryotes makes it inevitable that some will pass through the filter. Biodegradation kinetics are temperature dependent, and so cold storage can be used to limit the activity of those remaining. Saline samples are typically frozen at – 20 °C, whereas freshwater samples tend to be stored chilled at < 4 °C. This methodological difference is largely because freshwaters contain a much higher concentration of humics and fulvics, both of which are known to react badly to freezing. This was confirmed by two comparison exercises, the first comprising 10 oceanic samples (> 25 psu) and 14 tributaries of varying land use from Belize, Central America and the second comprising 4 tributary, 3 lake, and 2 estuarine (< 5 psu) samples from Halladale, North Scotland. We did not detect any significant variation between chilled and frozen DOC concentrations in oceanic samples ($p < 0.01$), but found that cold storage method had a variable effect on DOC concentrations in freshwaters.

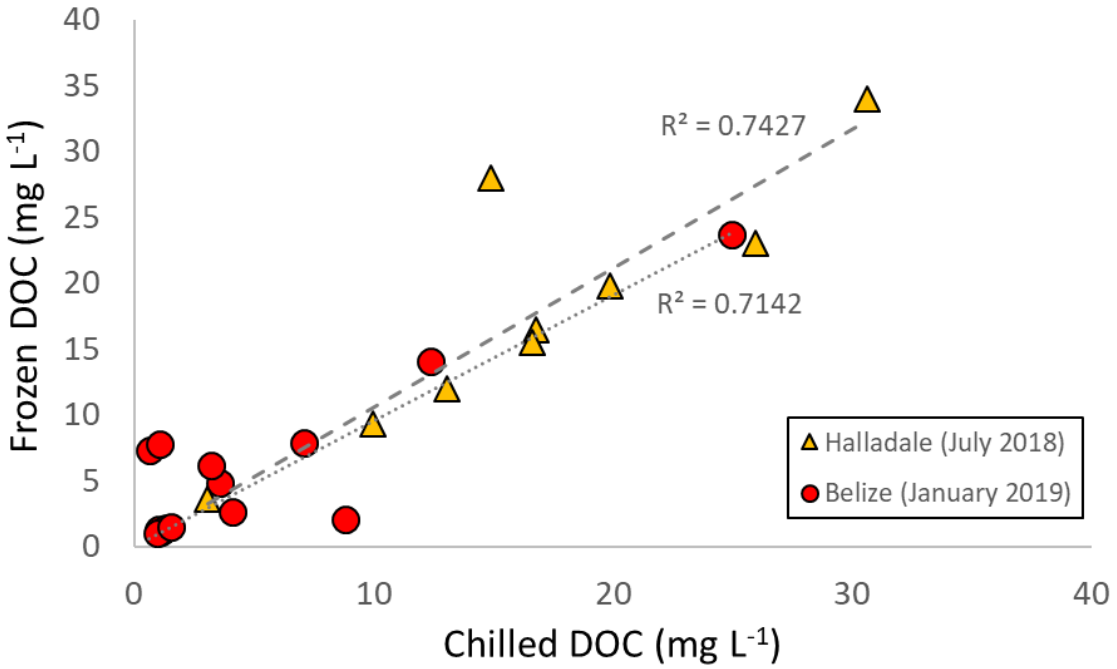

Figure A-2. Plot showing the effect of freezing freshwater samples in the Halladale catchment (yellow triangles) and the Belize River Watershed (red circles). In the Halladale, nine samples from a range of environments (lakes, rivers, estuary) and land use types (peat, forest, and mixed agriculture) were stored at 4°C for four weeks, measured via NPOC, frozen at -20°C, and then re-analysed. In the Belize River Watershed, fourteen river samples from a range of land-use types (pristine forest to intensive agriculture) were stored for four weeks in duplicate (one chilled and one frozen) then measured via NPOC. In the Halladale, freezing produced a mean Δ DOC of 1.35 ± 4.51 mg L^{-1} (mean ± SD) with a range of -13.00 to +2.95 mg L^{-1} whilst in Belize mean Δ DOC was 0.77 ± 3.33 mg L^{-1} with a range of -6.79 to + 6.73 mg L^{-1}.

A.3 Acidification

As a final preservation step, saline DOC samples are often acidified in the field. However, acidification of freshwater samples has been shown to result in DOC losses which increase with time (up to 11 % after 2 weeks storage; (Peacock et al., 2015). These losses occur as a result of hydrolysis, which means that the effect varies according to DOC composition and is therefore difficult to predict or standardise. A comparison exercise confirmed this (Figure A-3): across nine samples from the Belize River Watershed, acidification had a variable effect on measured DOC concentration. Interestingly, a254 exhibited a stronger relationship with DOC measured in acidified samples than in non-acidified samples, which suggests that acidification might preferentially remove (or alter) non-chromophoric DOC species (Figure A-4).

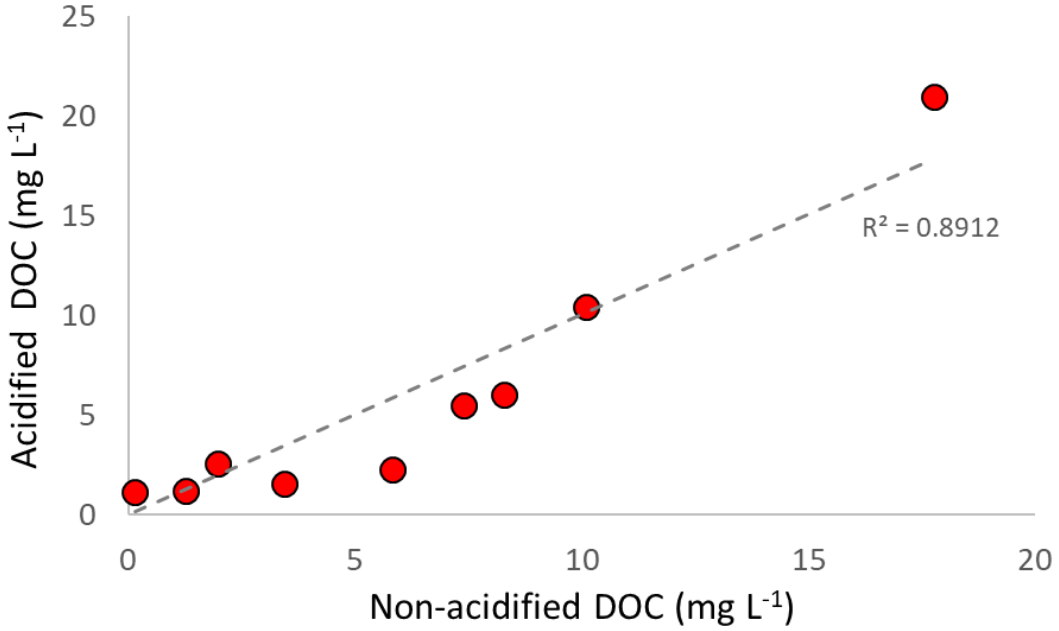

Figure A-3. Plot showing the effect of acidification on DOC concentrations measured in freshwater samples in the Belize River Watershed (May 2019), comprising samples from nine rivers with a range of land-use types (pristine forest to intensive agriculture). Samples were taken in duplicate, one of which was acidified. Both were stored chilled at 4 °C for four weeks before DOC was measured via NPOC. Acidification produced a Δ DOC of -0.01 ± 2.43 mg L^{-1} (mean ± SD) with a range of = -3.54 to 4.65 mg L^{-1}.

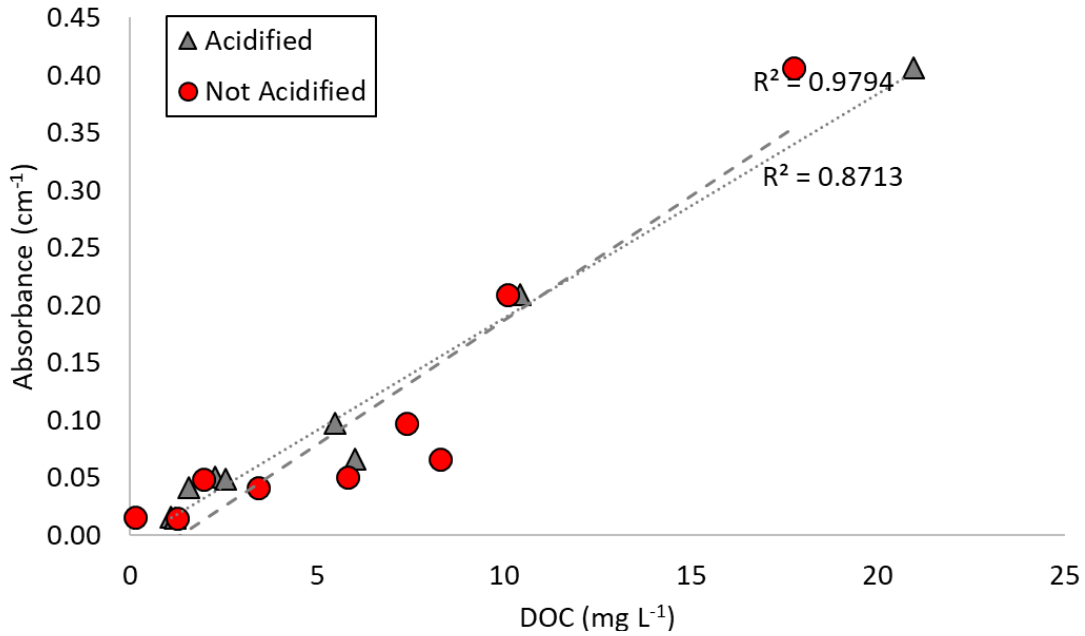

Figure A-4. DOC data from Chapter 2 plotted against absorbance at 254 nm measured on the chilled sample. The relationship between DOC and absorbance was weaker in non-acidified

samples (R^2 = 0.87) than it was in acidified samples (R^2 = 0.98), suggesting that acidification may preferentially remove and/or alter non-chromophoric material.

Appendix B Quantifying the effect of upstream deforestation on downstream ecosystems: using coral skeletal luminescence to reconstruct historic land-ocean carbon transport.

This project was successfully funded as part of the University of Southampton's Global Partnership Award 2022, and will allow follow-on activities to the study presented in Chapter 2.

Stacey L. Felgate *(University of Southampton) and* ***Patrick Martin*** *(Nanyang Technical University)*

B.1 Project Summary

This project will leverage freely available satelite data, a published water chemistry dataset, and newly obtained coral cores to reconstruct the transport or terrigenous dissolved organic matter (tDOM) from the Mesoamerican rainforest to the world's second largest barrier reef system (Belize, Central America). We will produce a temporal record which can be investigated relative to historic land-use change and climate records in order to better understand the relationship between upstream activities (including deforestation and agricultural expanison) and downstream tDOM export, increasing scientific capacity and knowledge in Belize, providing crucial information for local ecosystem managers, and enabling collaboration between UoS and NTU.

B.2 Project Description

Belize is home to substantial portions of the Mesoamerican rainforest and the Mesoamerican barrier reef system, two of the world's most important biodiversity hotspots. Doyle et al. (2021) found that Belize's forests and wetlands were being lost at 'alarming' rates, with 2014 - 2016 losses of 8% and 28%, respectively. In Felgate et al. (2021), we showed that this deforestation leads to increased transport of terrigenous dissolved organic matter (DOM) into nearby waterbodies, and a decrease in water clarity above the reef which has the potential to negatively influence coral growth and survival. However, no long-term records exist for the region, and so we cannot identify the historic relationships which might help us understand and predict future change. Kaushal et al. (2021) solved this lack of data issue in Malaysian corals using luminescence banding in coral skeleton cores, which

are caused by the incorporation of terrigenous humic acid-rich coloured DOM (cDOM, which is the light-absorbent fraction of DOM) within the coral skeletal structures. These bandings were used to reconstruct a 24-year time series which related coral luminescence intensity to rainfall-driven changes in surface water terrigenous cDOM concentrations. Because cDOM is an integral constituent of terrigenous DOM, this means that it is now possible to reconstruct past terrigenous DOM fluxes from coral core luminescence.

This project will leverage freely available satelite data, a published water chemistry dataset, and newly obtained coral cores to reconstruct the tDOM transport in Belize's largest watershed and adjacent coastal zone. In so doing, we will produce a temporal proxy record which can be investigated relative to historic land-use change and climate records. This will allow us derive a more quantitative understanding of how what happens in the upsteam catchment (e.g. deforestation and agricultural expanison) influences the quantity and fate of material transported downstream and into the coastal environment. This will provide ecosystem managers with the data and understanding they need to support informed decision making at local and national scales, and will be an important contribution to our scientific understanding of past, present, and future land-ocean interactions.

We will also increase scientific capacity within Belize, providing equipment and virtual training to local stakeholders and students who will then collect coral cores under supervison of SF, who will fly to Belize to oversee fieldwork. These cores will shipped to Singapore for analysis. Local students will be invited to take part in sample collection (UoB) and analysis (NTU), further supporting knowledge transfer. The data obtained will be written up for publication as a collaborative exercise, based around a small online writing workshop.

B.3 Previous Activities

SF has previously worked in Belize on numerous occasions and with the proposed stakeholders, including orchestrating field campaigns and obtaining marine research and export permits in collaboration with local governmental agencies and the FCDO / British High Commission. SF founded a mentorship programme involving several UK scientists who work with UoB faculty and undergraduate thesis students to deliver research projects of a similar scale to the one proposed here. PM has previously published using the proposed luminescence method. Parties have had previous discussions about conducting this work, should suitable funding become available.

B.4 Evidence of Quality and Interdisciplinarity

PM led the development of the proposed luminescence method, with access to the required specialist coral scanning equipment. This equipment is not available at UoS. SF led a recent study linking land use change to coastal cDOM concentrations overlying the coral reef in question. This study was the first of its kind to demonstrate a qualitative link between deforestation and increased terrigenous cDOM in the region, and utilised hydrodynamic modelling to pinpoint key areas of interest along the reef system where that material is thought to settle under varying hydrodynamic and oceanographic current regimes. By combining these expertise and knowledge sets, this project will advance the previous work and solidify the luminescence method within the literature. This project mainly has relevance to SDGs 14 (life below water) and 17 (partnerships), but will also help inform SDG 6 (clean water), 8 (economic growth), 12 (sustainable production), and 13 (climate action).

B.5 Evidence of Sustainability

This project will build capacity within Belize, providing training and equipment that will enable local stakeholders to play an active part in future research and collaborations around coral reef health and environmental trends. It will build a relationship between UoS and a number of Belizean partners, and strengthen the relationship between UoS and NTU. Specifically, it will foster a new collaboration between UoS and PM, an expert in coastal and shelf sea carbon cycling and land-ocean DOM fluxes. By feeding into the existing 3-year long UoB mentorship scheme for undergraduate thesis students, this project will contribute to the sustainability of the scheme, extending it by one additional semester and allowing time to apply for additional funds (for example, from the FCDO) to continue this scheme into the future. It is hoped that this study will act as a pilot ahead of a larger fellowship application which would further this collaboration, for example the NTU President's Fellowship (a 2 year independent research fellowship) looking at the link between land use change, climate change, and land-ocean carbon fluxes at global scale.

B.6 Impact and Benefits

Funding under this scheme will allow collection of samples and analysis of the resultant data. Costs associated with laboratory analysis will be covered by PM. Objectives: (1) train local stakeholders in the construction and deployment of coral coring equipment; (2) obtain coral cores from priority regions of the Belize Barrier Reef; (3) demonstrate the utility of the luminescence cDOM method under different environmental (a mineral soil catchment in Belize relative to a peatland catchment in Malaysia) and hydrological (exposed vs. sheltered reef) conditions; and (4) produce a peer-reviewed

manuscript detailing our findings. Participation in this research will increase access to bespoke core scanning equipment, increase the international profile of UoS by introducing a range of Belizian stakeholders, with the potential for future collaboration and partnerships, and increase the reach and influence of existing work by a UoS PhD student (Felgate et al. 2021). The proposed project includes a priority partner (NTU). All parties have an interest in a wide range of research across land and sea, making future faculty (and university wide) collaboration an attractive possibility. SF previously oversaw negotiation and delivery of two separate Memorandum of Understanding between NOC, UoB, and CZMAI which could reasonably be sought for UoS. The project is interdisciplinary, combining previous terrestrial/limnological and marine hydrodynamic research with oceanographic and palaeo techniques to synthesise land-ocean fluxes from source to sink in a new and innovative way.

Table B.1. Proposed timeline for project completion

Date (Months/weeks)	**Activity**
February / March 2022	Finalise field method (SF and PM), source required equipment (SF and UoB), and construct and test core drill (UoB and CZMAI).
March 2022	Permit application prepared and submitted to the Belize Fisheries Department. CITES Licence application submitted. Applications will be prepared by SF, with assistance from CZMAI.
April 2022	Virtual training workshop, covering coral growth, use of field kit, handling of samples, and a field briefing.
May 2022 (5 days)	Sample collection, led SF with assistance from CZMAI and UoB personnel.
May 2022	Shipping of samples from Belize to Singapore, organised by SF and CZMAI using a local customs agent.
June 2022 (1 week)	Preparation and analysis of cores (PM)
June 2022	Data analysis / Manuscript drafting (PM + SF)
July 2022	Writing workshop, sharing analysis and preliminary MS draft.

Table B.2. Proposed budget for project completion

Items		Totals
Compressed air	*Hire of extra SCUBA tanks to power drilling (5 – 10 tanks per core x 3 cores)*	**£** 500
Pneumatic core drills	*Compressed air drills (2 drills @ £200 each)*	**£** 400
Core bits	*Diamond core drill bits*	**£** 200
Other drill kit	*SCUBA tank fittings, gas hose, misc.*	**£** 400
Vessel costs	*60 units per day x 5 days @ $13 BZD per unit*	**£** 1,443
Staff costs	*Payment to CZMAI to cover staff costs during week (3 staff x 5 days @ $70 BZD per day)*	**£** 388.50
Dive gear	*Hire of SCUBA dive gear (2 sets x 5 days @ $70 BZD per day)*	**£** 260
Shipping	*Transport of samples from Belize to Singapore for analysis, including payment to local customs agent*	**£** 900
Contingency	*Contingency (10 %)*	**£** 449.15
	Subtotal for fieldwork costs	**£ 4940.65**
PCR Tests	*2 x PCR tests required for travel*	**£** 200
Travel	*Return bus from Southampton to LHR*	**£** 30
Flights	*Return flights from LHR to Belize City (via USA)*	**£** 620
Hotel (USA)	*Hotel in Texas during 17 hour layover (outbound)*	**£** 100
Hotel (Belize)	*Hotel in Belize City for 7 nights, including breakfasts and airport transfers @ £100 per night.*	**£** 700
Food	*Lunch and dinner for 8 days @ £30 per day*	**£** 240
Insurance	*Mandatory insurance in Belize*	**£** 10
	Subtotal for travel costs	**£ 1900**
	TOTAL COST	**£ 6840.65**

List of References

Abril, G., Borges, A.V., 2019. Ideas and perspectives: Carbon leaks from flooded land: Do we need to replumb the inland water active pipe? Biogeosciences. https://doi.org/10.5194/bg-16-769-2019

Abril, G., Bouillon, S., Darchambeau, F., Teodoru, C.R., Marwick, T.R., Tamooh, F., Ochieng Omengo, F., Geeraert, N., Deirmendjian, L., Polsenaere, P., Borges, A.V., 2015. Technical note: Large overestimation of pCO2 calculated from pH and alkalinity in acidic, organic-rich freshwaters. Biogeosciences. https://doi.org/10.5194/bg-12-67-2015

Abril, G., Nogueira, M., Etcheber, H., Cabeçadas, G., Lemaire, E., Brogueira, M.J., 2002. Behaviour of organic carbon in nine contrasting European estuaries. Estuar. Coast. Shelf Sci. https://doi.org/10.1006/ecss.2001.0844

Adams, J.L., Tipping, E., Feuchtmayr, H., Carter, H.T., Keenan, P., 2018. The contribution of algae to freshwater dissolved organic matter: implications for UV spectroscopic analysis. Inland Waters. https://doi.org/10.1080/20442041.2017.1415032

Aitkenhead, J.A., McDowell, W.H., 2000. Soil C:N ratio as a predictor of annual riverine DOC flux at local and global scales. Glob. Biogeochem. Cycles 14, 127–138. https://doi.org/10.1029/1999GB900083

Albu, A.C., Albu, L.L., 2020. The Impact of Climate Change on Income Inequality. Evidence from European Union Countries. Stud. Bus. Econ. 15. https://doi.org/10.2478/sbe-2020-0055

Alegria, V.E., 2009. Land-Based Sources of Pollutants to Coastal Waters of Southern Belize - Comparison of Predictive Model with Empirical Data.

Amon, R.M.W., Benner, R., 1996. Photochemical and microbial consumption of dissolved organic carbon and dissolved oxygen in the Amazon River system. Geochim. Cosmochim. Acta. https://doi.org/10.1016/0016-7037(96)00055-5

Anderson, T.R., Rowe, E.C., Polimene, L., Tipping, E., Evans, C.D., Barry, C.D.G., Hansell, D.A., Kaiser, K., Kitidis, V., Lapworth, D.J., Mayor, D.J., Monteith, D.T., Pickard, A.E., Sanders, R.J., Spears, B.M., Torres, R., Tye, A.M., Wade, A.J., Waska, H., 2019. Unified concepts for understanding and modelling turnover of dissolved organic matter from freshwaters to the ocean: the UniDOM model. Biogeochemistry 1, 1–19. https://doi.org/10.1007/s10533-019-00621-1

Arango, C.P., Beaulieu, J.J., Fritz, K.M., Hill, B.H., Elonen, C.M., Pennino, M.J., Mayer, P.M., Kaushal, S.S., Balz, A.D., 2017. Urban infrastructure influences dissolved organic matter quality and bacterial metabolism in an urban stream network. Freshw. Biol. 62, 1917–1928. https://doi.org/10.1111/fwb.13035

Aronson, R.B., Precht, W.F., Macintyre, I.G., Murdoch, T.J.T., 2000. Coral bleach-out in Belize. Nature. https://doi.org/10.1038/35011132

Asmala, E., Carstensen, J., Raike, A., 2019. Multiple anthropogenic drivers behind upward trends in organic carbon concentrations in boreal rivers. Environ. Res. Lett. https://doi.org/10.1088/1748-9326/ab4fa9

Asmala, E., Kaartokallio, H., Carstensen, J., Thomas, D.N., 2016. Variation in riverine inputs affect dissolved organic matter characteristics throughout the estuarine gradient. Front. Mar. Sci. https://doi.org/10.3389/fmars.2015.00125

Asmala, E., Stedmon, C.A., Thomas, D.N., 2012. Linking CDOM spectral absorption to dissolved organic carbon concentrations and loadings in boreal estuaries. Estuar. Coast. Shelf Sci. https://doi.org/10.1016/j.ecss.2012.06.015

Austnes, K., Evans, C.D., Eliot-Laize, C., Naden, P.S., Old, G.H., 2010. Effects of storm events on mobilisation and in-stream processing of dissolved organic matter (DOM) in a Welsh peatland catchment. Biogeochemistry. https://doi.org/10.1007/s10533-009-9399-4

Badr, E.S.A., Achterberg, E.P., Tappin, A.D., Hill, S.J., Braungardt, C.B., 2003. Determination of dissolved organic nitrogen in natural waters using high-temperature catalytic oxidation. TrAC - Trends Anal. Chem. https://doi.org/10.1016/S0165-9936(03)01202-0

Baillie, I.C., Wright, A.C.S., Holder, M.A., Fitzpatrick, E.A., 1993. Revised Classification of the Soils of Belize.

Baker, A., Ward, D., Lieten, S.H., Periera, R., Simpson, E.C., Slater, M., 2004. Measurement of protein-like fluorescence in river and waste water using a handheld spectrophotometer. Water Res. https://doi.org/10.1016/j.watres.2004.04.023

Banoub, M.W., 1973. Ultraviolet absorption as a measure of organic matter in natural waters in Bodensee. Achiv Hydrobiol. 159–165.

Barros, N., Cole, J.J., Tranvik, L.J., Prairie, Y.T., Bastviken, D., Huszar, V.L.M., Del Giorgio, P., Roland, F., 2011. Carbon emission from hydroelectric reservoirs linked to reservoir age and latitude. Nat. Geosci. https://doi.org/10.1038/ngeo1211

Bastviken, D., Tranvik, L.J., Downing, J.A., Crill, P.M., Enrich-Prast, A., 2011. Freshwater methane emissions offset the continental carbon sink. Science. https://doi.org/10.1126/science.1196808

Bates, D., Mächler, M., Bolker, B.M., Walker, S.C., 2015. Fitting linear mixed-effects models using lme4. J. Stat. Softw. https://doi.org/10.18637/jss.v067.i01

Bates, N.R., Astor, Y.M., Church, M.J., Currie, K., Dore, J.E., González-Dávila, M., Lorenzoni, L., Muller-Karger, F., Olafsson, J., Santana-Casiano, J.M., 2014. A time-series view of changing surface ocean chemistry due to ocean uptake of anthropogenic CO2 and ocean acidification. Oceanography. https://doi.org/10.5670/oceanog.2014.16

Bauer, J.E., Cai, W.-J., Raymond, P. a, Bianchi, T.S., Hopkinson, C.S., Regnier, P. a G., 2013. The changing carbon cycle of the coastal ocean. Nature 504, 61–70. https://doi.org/10.1038/nature12857

Berggren, M., Klaus, M., Panneer Selvam, B., Ström, L., Laudon, H., Jansson, M., Karlsson, J., 2017. Quality transformation of dissolved organic carbon during water transit through lakes: contrasting controls by photochemical and biological processes. Biogeosciences Discuss. 1–22. https://doi.org/10.5194/bg-2017-279

Bianchi, T.S., 2011. The role of terrestrially derived organic carbon in the coastal ocean: A changing paradigm and the priming effect. Proc. Natl. Acad. Sci. 108, 19473–19481. https://doi.org/10.1073/pnas.1017982108

Bianchi, T.S., Allison, M.A., 2009. Large-river delta-front estuaries as natural “recorders” of global environmental change. Proc. Natl. Acad. Sci. U. S. A. https://doi.org/10.1073/pnas.0812878106

Blanchet, M., Pringault, O., Panagiotopoulos, C., Lefèvre, D., Charrière, B., Ghiglione, J.F., Fernandez, C., Aparicio, F.L., Marrasé, C., Catala, P., Oriol, L., Caparros, J., Joux, F., 2017. When riverine dissolved organic matter (DOM) meets labile DOM in coastal waters: changes in bacterial community activity and composition. Aquat. Sci. 79, 27–43. https://doi.org/10.1007/s00027-016-0477-0

Blattmann, T.M., Liu, Z., Zhang, Y., Zhao, Y., Haghipour, N., Montluçon, D.B., Plötze, M., Eglinton, T.I., 2019. Mineralogical control on the fate of continentally derived organic matter in the ocean. Science. https://doi.org/10.1126/science.aax5345

Bolan, N.S., Adriano, D.C., Kunhikrishnan, A., James, T., McDowell, R., Senesi, N., 2011. Dissolved Organic Matter. Biogeochemistry, Dynamics, and Environmental Significance in Soils., Advances in Agronomy. https://doi.org/10.1016/B978-0-12-385531-2.00001-3

Borges, A.V., Abril, G., Darchambeau, F., Teodoru, C.R., Deborde, J., Vidal, L.O., Lambert, T., Bouillon, S., 2015. Divergent biophysical controls of aquatic CO2 and CH4 in the World's two largest rivers. Sci. Rep. https://doi.org/10.1038/srep15614

Bouwman, A.F., Bierkens, M.F.P., Griffioen, J., Hefting, M.M., Middelburg, J.J., Middelkoop, H., Slomp, C.P., 2013. Nutrient dynamics, transfer and retention along the aquatic continuum from land to ocean: Towards integration of ecological and biogeochemical models. Biogeosciences 10. https://doi.org/10.5194/bg-10-1-2013

Brezonik, P.L., Olmanson, L.G., Finlay, J.C., Bauer, M.E., 2015. Factors affecting the measurement of CDOM by remote sensing of optically complex inland waters. Remote Sens. Environ. 157, 199–215. https://doi.org/10.1016/j.rse.2014.04.033

Briones, M.J.I., Garnett, M.H., Ineson, P., 2010. Soil biology and warming play a key role in the release of "old C" from organic soils. Soil Biol. Biochem. 42, 960–967. https://doi.org/10.1016/j.soilbio.2010.02.013

Broecker, W.S., Takahashi, T., Simpson, H.J., Peng, T.-H., 1979. Fate of Fossil Fuel Carbon Dioxide and the Global Carbon Budget. Science 206, 409–418.

Brown, C.D., Turner, N., Hollis, J., Bellamy, P., Biggs, J., Williams, P., Arnold, D., Pepper, T., Maund, S., 2006. Morphological and physico-chemical properties of British aquatic habitats potentially exposed to pesticides. Agric. Ecosyst. Environ. https://doi.org/10.1016/j.agee.2005.10.015

Burdige, D.J., 2007. Preservation of organic matter in marine sediments: Controls, mechanisms, and an imbalance in sediment organic carbon budgets? Chem. Rev. 107, 467–485. https://doi.org/10.1021/cr050347q

Burke, L., Sugg, Z., 2006. Hydrologic Modelling of Watersheds Discharging Adjacent to the Mesoamerican Reef. World Resour. Inst.

Butler, J.R.A., Wong, G.Y., Metcalfe, D.J., Honzák, M., Pert, P.L., Rao, N., van Grieken, M.E., Lawson, T., Bruce, C., Kroon, F.J., Brodie, J.E., 2013. An analysis of trade-offs between multiple ecosystem services and stakeholders linked to land use and water quality management in the Great Barrier Reef, Australia. Agric. Ecosyst. Environ. https://doi.org/10.1016/j.agee.2011.08.017

Butman, D., Raymond, P.A., 2011. Significant efflux of carbon dioxide from streams and rivers in the United States. Nat. Geosci. https://doi.org/10.1038/ngeo1294

Butman, D.E., Wilson, H.F., Barnes, R.T., Xenopoulos, M.A., Raymond, P.A., 2015. Increased mobilization of aged carbon to rivers by human disturbance. Nat. Geosci. https://doi.org/10.1038/ngeo2322

Cai, W.-J., 2011. Estuarine and coastal ocean carbon paradox: CO2 sinks or sites of terrestrial carbon incineration? Annu. Rev. Mar. Sci. 3, 123–145. https://doi.org/10.1146/annurev-marine-120709-142723

Carr, N., Davis, C.E., Blackbird, S., Daniels, L.R., Preece, C., Woodward, M., Mahaffey, C., 2019. Seasonal and spatial variability in the optical characteristics of DOM in a temperate shelf sea. Prog. Oceanogr. https://doi.org/10.1016/j.pocean.2018.02.025

Carrias, A., Cano, A., Saqui, P., Ake, J., Boles, E., 2018. Management Plan for the Belize River Watershed , Belize.

Carstensen, J., Duarte, C.M., 2019. Drivers of pH Variability in Coastal Ecosystems. Environ. Sci. Technol. https://doi.org/10.1021/acs.est.8b03655

Carter, H.T., Tipping, E., Koprivnjak, J.F., Miller, M.P., Cookson, B., Hamilton-Taylor, J., 2012. Freshwater DOM quantity and quality from a two-component model of UV absorbance. Water Res. https://doi.org/10.1016/j.watres.2012.05.021

Catalán, N., Marcé, R., Kothawala, D.N., Tranvik, L.J., 2016. Organic carbon decomposition rates controlled by water retention time across inland waters. Nat. Geosci. https://doi.org/10.1038/ngeo2720

Cherrington, E.A., Ek, E., Cho, P., Howell, B.F., Hernandez, B.E., Anderson, E.R., Flores, A.I., Garcia, B.C., Sempris, E., Irwin, D.E., 2010. Forest Cover and Deforestation in Belize: 1980-2010 1980–2010.

Cherrington, E.A., Kay, E., Waight-Cho, I., 2014. Modelling the impacts of climate change and land use change on Belize's water resources: potential effects on erosion and runoff 1–32. https://doi.org/10.13140/RG.2.2.16952.75524

Chin, Y.P., Alken, G., O'Loughlin, E., 1994. Molecular Weight, Polydispersity, and Spectroscopic Properties of Aquatic Humic Substances. Environ. Sci. Technol. https://doi.org/10.1021/es00060a015

Clark, J.B., Mannino, A., 2021. Preferential loss of Yukon River delta colored dissolved organic matter under nutrient replete conditions. Limnol. Oceanogr. https://doi.org/10.1002/lno.11706

Clark, J.M., Lane, S.N., Chapman, P.J., Adamson, J.K., 2007. Export of dissolved organic carbon from an upland peatland during storm events: Implications for flux estimates. J. Hydrol. https://doi.org/10.1016/j.jhydrol.2007.09.030

Coble, P.G., 2007. Marine optical biogeochemistry: The chemistry of ocean color. Chem. Rev. 107. https://doi.org/10.1021/cr050350+

Coble, P.G., 1996. Characterization of marine and terrestrial DOM in seawater using excitation-emission matrix spectroscopy. Mar. Chem. 51, 325–346. https://doi.org/10.1016/0304-4203(95)00062-3

Cole, J.J., Caraco, N.F., Kling, G.W., Kratz, T.K., 1994. Carbon dioxide supersaturation in the surface waters of lakes. Science. https://doi.org/10.1126/science.265.5178.1568

Cole, J.J., Prairie, Y.T., Caraco, N.F., McDowell, W.H., Tranvik, L.J., Striegl, R.G., Duarte, C.M., Kortelainen, P., Downing, J.A., Middelburg, J.J., Melack, J., 2007. Plumbing the global carbon cycle: Integrating inland waters into the terrestrial carbon budget. Ecosystems 10, 171–184. https://doi.org/10.1007/s10021-006-9013-8

Collier, K.J., 1987. Spectrophotometric determination of dissolved organic carbon in some south island streams and rivers (note). N. Z. J. Mar. Freshw. Res. https://doi.org/10.1080/00288330.1987.9516230

Condron, L.M., Hopkins, D.W., Gregorich, E.G., Black, A., Wakelin, S.A., 2014. Long-term irrigation effects on soil organic matter under temperate grazed pasture. Eur. J. Soil Sci. 65, 741–750. https://doi.org/10.1111/ejss.12164

Cook, S., Peacock, M., Evans, C.D., Page, S.E., Whelan, M.J., Gauci, V., Kho, L.K., 2017. Quantifying tropical peatland dissolved organic carbon (DOC) using UV-visible spectroscopy. Water Res. https://doi.org/10.1016/j.watres.2017.02.059

Cory, R.M., Kling, G.W., 2018. Interactions between sunlight and microorganisms influence dissolved organic matter degradation along the aquatic continuum. Limnol. Oceanogr. Lett. 3, 102–116. https://doi.org/10.1002/lol2.10060

Cory, R.M., McNeill, K., Cotner, J.P., Amado, A., Purcell, J.M., Marshall, A.G., 2010a. Singlet Oxygen in the Coupled Photochemical and Biochemical Oxidation of Dissolved Organic Matter. Environ. Sci. Technol. 44, 3683–3689. https://doi.org/10.1021/es902989y

Cory, R.M., Miller, M.P., McKnight, D.M., Guerard, J.J., Miller, P.L., 2010b. Effect of instrument-specific response on the analysis of fulvic acid fluorescence spectra. Limnol. Oceanogr. Methods 8, 67–78. https://doi.org/10.4319/lom.2010.8.67

Dachs, J., Calleja, M.L., Duarte, C.M., del Vento, S., Turpin, B., Polidori, A., Herndl, G.J., Agustí, S., 2005. High atmosphere-ocean exchange of organic carbon in the NE subtropical Atlantic. Geophys. Res. Lett. 32. https://doi.org/10.1029/2005GL023799

Dagg, M., Sato, R., Liu, H., Bianchi, T.S., Green, R., Powell, R., 2008. Microbial food web contributions to bottom water hypoxia in the northern Gulf of Mexico. Cont. Shelf Res. 28, 1127–1137. https://doi.org/10.1016/j.csr.2008.02.013

Dai, M., Martin, J.M., Cauwet, G., 1995. The significant role of colloids in the transport and transformation of organic carbon and associated trace metals (Cd, Cu and Ni) in the Rhône delta (France). Mar. Chem. https://doi.org/10.1016/0304-4203(95)00051-R

Dai, M., Yin, Z., Meng, F., Liu, Q., Cai, W.J., 2012. Spatial distribution of riverine DOC inputs to the ocean: An updated global synthesis. Curr. Opin. Environ. Sustain. https://doi.org/10.1016/j.cosust.2012.03.003

de Carlos, A., Martínez-Carreño, N., Barros-García, D., Luis, J.R., García-Gil, S., 2017. Geochemical and microbial context of the gassy sediments in the Ría de Vigo (NW of Spain). Mar. Geol. https://doi.org/10.1016/j.margeo.2016.12.004

De Haan, H., 1977. Effect of benzoate on microbial decomposition of fulvic acids in Tjeukemeer (the Netherlands). Limnol. Oceanogr. 22, 38–44. https://doi.org/10.4319/lo.1977.22.1.0038

Deemer, B.R., Harrison, J.A., Li, S., Beaulieu, J.J., Delsontro, T., Barros, N., Bezerra-Neto, J.F., Powers, S.M., Dos Santos, M.A., Vonk, J.A., 2016. Greenhouse gas emissions from reservoir water surfaces: A new global synthesis. BioScience. https://doi.org/10.1093/biosci/biw117

Degens, E.T., Kempe, S., Richey, J.E., 1991. Biogeochemistry of major world rivers, SCOPE 42 - Biogeochemistry of Major World Rivers.

Deirmendjian, L., Loustau, D., Augusto, L., Lafont, S., Chipeaux, C., Poirier, D., Abril, G., 2018. Hydro-ecological controls on dissolved carbon dynamics in groundwater and export to streams in a temperate pine forest. Biogeosciences. https://doi.org/10.5194/bg-15-669-2018

DelSontro, T., del Giorgio, P.A., Prairie, Y.T., 2018. No Longer a Paradox: The Interaction Between Physical Transport and Biological Processes Explains the Spatial Distribution of Surface Water Methane Within and Across Lakes. Ecosystems. https://doi.org/10.1007/s10021-017-0205-1

Denfeld, B.A., Wallin, M.B., Sahlée, E., Sobek, S., Kokic, J., Chmiel, H.E., Weyhenmeyer, G.A., 2015. Temporal and spatial carbon dioxide concentration patterns in a small boreal lake in relation to ice-cover dynamics. Boreal Environ. Res.

Devlin, M., Schaffelke, B., 2012. Catchment-to-reef continuum: Case studies from the Great Barrier Reef. A special issue - Marine Pollution Bulletin 2012. Mar. Pollut. Bull. https://doi.org/10.1016/j.marpolbul.2012.04.013

Dhillon, G.S., Inamdar, S., 2014. Storm event patterns of particulate organic carbon (POC) for large storms and differences with dissolved organic carbon (DOC). Biogeochemistry. https://doi.org/10.1007/s10533-013-9905-6

Dhillon, G.S., Inamdar, S., 2013. Extreme storms and changes in particulate and dissolved organic carbon in runoff: Entering uncharted waters? Geophys. Res. Lett. https://doi.org/10.1002/grl.50306

Dickson, A.G., Afghan, J.D., Anderson, G.C., 2003. Reference materials for oceanic CO2 analysis: A method for the certification of total alkalinity. Mar. Chem. https://doi.org/10.1016/S0304-4203(02)00133-0

Dlamini, P., Chivenge, P., Chaplot, V., 2016. Overgrazing decreases soil organic carbon stocks the most under dry climates and low soil pH: A meta-analysis shows. Agric. Ecosyst. Environ. 221, 258–269. https://doi.org/10.1016/j.agee.2016.01.026

Dobbs, R.A., Wise, R.H., Dean, R.B., 1972. The use of ultraviolet absorbance for monitoring the total organic content of water and wastewater. Water Res. 1173–1180.

Doney, S.C., Fabry, V.J., Feely, R.A., Kleypas, J.A., 2009. Ocean Acidification: The Other CO 2 Problem. Annu. Rev. Mar. Sci. 1, 169–192. https://doi.org/10.1146/annurev.marine.010908.163834

Downing, B.D., Boss, E., Bergamaschi, B.A., Fleck, J.A., Lionberger, M.A., Ganju, N.K., Schoellhamer, D.H., Fujii, R., 2009. Quantifying fluxes and characterizing compositional changes of dissolved organic

matter in aquatic systems in situ using combined acoustic and optical measurements. Limnol. Oceanogr. Methods. https://doi.org/10.4319/lom.2009.7.119

Downing, J.A., 2010. Emerging global role of small lakes and ponds: Little things mean a lot. Limnetica.

Downing, J.A., Striegl, R.G., 2018. Size, age, renewal, and discharge of groundwater carbon. Inland Waters. https://doi.org/10.1080/20442041.2017.1412918

Drake, T.W., Raymond, P.A., Spencer, R.G.M., 2018. Terrestrial carbon inputs to inland waters: A current synthesis of estimates and uncertainty. Limnol. Oceanogr. Lett. 3, 132–142. https://doi.org/10.1002/lol2.10055

Drake, T.W., Van Oost, K., Barthel, M., Bauters, M., Hoyt, A.M., Podgorski, D.C., Six, J., Boeckx, P., Trumbore, S.E., Cizungu Ntaboba, L., Spencer, R.G.M., 2019. Mobilization of aged and biolabile soil carbon by tropical deforestation. Nat. Geosci. https://doi.org/10.1038/s41561-019-0384-9

Duarte, C.M., Middelburg, J.J., Caraco, N., 2005. Major role of marine vegetation on the oceanic carbon cycle. Biogeosciences 2, 1–8. https://doi.org/10.5194/bgd-1-659-2004

Duarte, C.M., Middelburg, J.J., Caraco, N., 2004. Major role of marine vegetation on the oceanic carbon cycle. Biogeosciences Discuss. 1, 659–679. https://doi.org/10.5194/bgd-1-659-2004

Duc, N.T., Crill, P., Bastviken, D., 2010. Implications of temperature and sediment characteristics on methane formation and oxidation in lake sediments. Biogeochemistry. https://doi.org/10.1007/s10533-010-9415-8

Dürr, H.H., Laruelle, G.G., van Kempen, C.M., Slomp, C.P., Meybeck, M., Middelkoop, H., 2011. Worldwide Typology of Nearshore Coastal Systems: Defining the Estuarine Filter of River Inputs to the Oceans. Estuaries Coasts 34, 441–458. https://doi.org/10.1007/s12237-011-9381-y

Esselman, R.E., Boles, E., 2001. Status and Future Needs of Limnological in Belize. Int. Assoc. Limnol.

European Centre for Medium-Range Weather Forecasts, 2019. ERA5. Reanalysis Datasets. https://doi.org/10.24381/cds.adbb2d47

Evans, Chris D., Futter, M.N., Moldan, F., Valinia, S., Frogbrook, Z., Kothawala, D.N., 2017. Variability in organic carbon reactivity across lake residence time and trophic gradients. Nat. Geosci. https://doi.org/10.1038/NGEO3051

Evans, C. D., Malcolm, I.A., Shilland, E.M., Rose, N.L., Turner, S.D., Crilly, A., Norris, D., Granath, G., Monteith, D.T., 2017. Sustained Biogeochemical Impacts of Wildfire in a Mountain Lake Catchment. Ecosystems. https://doi.org/10.1007/s10021-016-0064-1

Evans, C.D., Renou-Wilson, F., Strack, M., 2016. The role of waterborne carbon in the greenhouse gas balance of drained and re-wetted peatlands. Aquat. Sci. https://doi.org/10.1007/s00027-015-0447-y

Evans, R., 2007. The Impact of Groundwater Use on Australias Rivers Technical Report.

Felgate, S.L., Ala-Aho, P., Anderson, T.R., Bastviken, D., Burba, G., Evans, C.D., Giani, M., Gkritzalis, T., Hartman, S.E., Hargreaves, G., Hastie, A., Kitidis, V., Klemedtsson, L., Lapworth, D.J., Lauerwald, R., Lindroth, A., Lohila, A., Luchetta, A., Mammarella, I., Marttila, H., Peacock, M., Pickard, A., Rutgersson, A., Sanders, R., Stinchcombe, M., Vaha, A., Vesala, T., Wood, T., Wieslien, P., Mayor, D.J., 2021a. Requirements for the monitoring of land-ocean carbon fluxes at pan-European scale (D 1.4).

Felgate, S.L., Barry, C.D.G., Mayor, D.J., Sanders, R., Carrias, A., Young, A., Fitch, A., Mayorga-Adame, C.G., Andrews, G., Brittain, H., Cryer, S.E., Evans, C.D., Goddard-Dwyer, M., Holt, J., Hughes, B.K., Lapworth, D., Pinder, A., Price, D.M., Rosado, S., Evans, C., 2021b. Conversion of forest to agriculture increases colored dissolved organic matter in a sub-tropical catchment and adjacent coastal environment. J. Geophys. Res. Biogeosciences. https://doi.org/10.1029/2021jg006295

Fennel, K., Alin, S., Barbero, L., Evans, W., Bourgeois, T., Cooley, S., Dunne, J., Feely, R.A., Martin Hernandez-Ayon, J., Hu, X., Lohrenz, S., Muller-Karger, F., Najjar, R., Robbins, L., Shadwick, E., Siedlecki, S., Steiner, N., Sutton, A., Turk, D., Vlahos, P., Aleck Wang, Z., 2019. Carbon cycling in the North American coastal ocean: A synthesis. Biogeosciences. https://doi.org/10.5194/bg-16-1281-2019

Fernandes, J.A., Papathanasopoulou, E., Hattam, C., Queirós, A.M., Cheung, W.W.W.L., Yool, A., Artioli, Y., Pope, E.C., Flynn, K.J., Merino, G., Calosi, P., Beaumont, N., Austen, M.C., Widdicombe, S., Barange, M., 2017. Estimating the ecological, economic and social impacts of ocean acidification and warming on UK fisheries. Fish Fish. 18, 389–411. https://doi.org/10.1111/faf.12183

Fichot, C.G., Benner, R., 2014. The fate of terrigenous dissolved organic carbon in a river-influenced ocean margin. Glob. Biogeochem. Cycles. https://doi.org/10.1002/2013GB004670

Fichot, C.G., Benner, R., 2011. A novel method to estimate DOC concentrations from CDOM absorption coefficients in coastal waters. Geophys. Res. Lett. https://doi.org/10.1029/2010GL046152

Findlay, S., McDowell, W.H., Fischer, D., Pace, M.L., Caraco, N., Kaushal, S.S., Weathers, K.C., 2010. Total carbon analysis may overestimate organic carbon content of fresh waters in the presence of high dissolved inorganic carbon. Limnol. Oceanogr. Methods. https://doi.org/10.4319/lom.2010.8.196

Forsberg, C., 1967. Dissolved Organic Carbon in Some Lakes in Uppland, Sweden. Oikos. https://doi.org/10.2307/3565099

Fox, J., Weisberg, S., 2011. An {R} Companion to Applied Regression.

Frankignoulle, M., Abril, G., Borges, A., Bourge, I., Canon, C., Delille, B., Libert, E., Théate, J.M., 1998. Carbon dioxide emission from European estuaries. Science. https://doi.org/10.1126/science.282.5388.434

Friedlingstein, P., Jones, M.W., O'Sullivan, M., Andrew, R.M., Hauck, J., Peters, G.P., Peters, W., Pongratz, J., Sitch, S., Le Quéré, C., DBakker, O.C.E., Canadell1, J.G., Ciais1, P., Jackson, R.B., Anthoni1, P., Barbero, L., Bastos, A., Bastrikov, V., Becker, M., Bopp, L., Buitenhuis, E., Chandra, N., Chevallier, F., Chini, L.P., Currie, K.I., Feely, R.A., Gehlen, M., Gilfillan, D., Gkritzalis, T., Goll, D.S., Gruber, N., Gutekunst, S., Harris, I., Haverd, V., Houghton, R.A., Hurtt, G., Ilyina, T., Jain, A.K., Joetzjer, E., Kaplan, J.O., Kato, E., Goldewijk, K.K., Korsbakken, J.I., Landschützer, P., Lauvset, S.K., Lefèvre, N., Lenton, A., Lienert, S., Lombardozzi, D., Marland, G., McGuire, P.C., Melton, J.R., Metzl, N., Munro, D.R., Nabel, J.E.M.S., Nakaoka, S.I., Neill, C., Omar, A.M., Ono, T., Peregon, A., Pierrot, D., Poulter, B., Rehder, G., Resplandy, L., Robertson, E., Rödenbeck, C., Séférian, R., Schwinger, J., Smith, N., Tans, P.P., Tian, H., Tilbrook, B., Tubiello, F.N., Van Der Werf, G.R., Wiltshire, A.J., Zaehle, S., 2019. Global carbon budget 2019. Earth Syst. Sci. Data 11. https://doi.org/10.5194/essd-11-1783-2019

Friedlingstein, P., O'Sullivan, M., Jones, M.W., Andrew, R.M., Hauck, J., Olsen, A., Peters, G.P., Peters, W., Pongratz, J., Sitch, S., Le Quéré, C., Canadell, J.G., Ciais, P., Jackson, R.B., Alin, S., Aragão, L.E.O.C., Arneth, A., Arora, V., Bates, N.R., Becker, M., Benoit-Cattin, A., Bittig, H.C., Bopp, L., Bultan, S., Chandra, N., Chevallier, F., Chini, L.P., Evans, W., Florentie, L., Forster, P.M., Gasser, T., Gehlen, M., Gilfillan, D., Gkritzalis, T., Gregor, L., Gruber, N., Harris, I., Hartung, K., Haverd, V., Houghton, R.A., Ilyina, T., Jain, A.K., Joetzjer, E., Kadono, K., Kato, E., Kitidis, V., Korsbakken, J.I., Landschützer, P., Lefèvre, N., Lenton, A., Lienert, S., Liu, Z., Lombardozzi, D., Marland, G., Metzl, N., Munro, D.R., Nabel, J.E.M.S., Nakaoka, S.I., Niwa, Y., O'Brien, K., Ono, T., Palmer, P.I., Pierrot, D., Poulter, B., Resplandy, L., Robertson, E., Rödenbeck, C., Schwinger, J., Séférian, R., Skjelvan, I., Smith, A.J.P., Sutton, A.J., Tanhua, T., Tans, P.P., Tian, H., Tilbrook, B., Van Der Werf, G., Vuichard, N., Walker, A.P.,

Wanninkhof, R., Watson, A.J., Willis, D., Wiltshire, A.J., Yuan, W., Yue, X., Zaehle, S., 2020. Global Carbon Budget 2020. Earth Syst. Sci. Data 12. https://doi.org/10.5194/essd-12-3269-2020

Frouin, P., 2000. Effects of anthropogenic disturbances of tropical soft-bottom benthic communities. Mar. Ecol. Prog. Ser. 194, 39–53. https://doi.org/10.3354/meps194039

Fujisaki, K., Perrin, A.S., Garric, B., Balesdent, J., Brossard, M., 2017. Soil organic carbon changes after deforestation and agrosystem establishment in Amazonia: An assessment by diachronic approach. Agric. Ecosyst. Environ. 245, 63–73. https://doi.org/10.1016/j.agee.2017.05.011

Galloway, J.N., Townsend, A.R., Erisman, J.W., Bekunda, M., Cai, Z., Freney, J.R., Martinelli, L.A., Seitzinger, S.P., Sutton, M.A., 2008. Transformation of the nitrogen cycle: Recent trends, questions, and potential solutions. Science. https://doi.org/10.1126/science.1136674

García-Martín, E.E., Sanders, R., Evans, C.D., Kitidis, V., Lapworth, D.J., Rees, A.P., Spears, B.M., Tye, A., Williamson, J.L., Balfour, C., Best, M., Bowes, M., Breimann, S., Brown, I.J., Burden, A., Callaghan, N., Felgate, S.L., Fishwick, J., Fraser, M., Gibb, S.W., Gilbert, P.J., Godsell, N., Gomez-Castillo, A.P., Hargreaves, G., Jones, O., Kennedy, P., Lichtschlag, A., Martin, A., May, R., Mawji, E., Mounteney, I., Nightingale, P.D., Olszewska, J.P., Painter, S.C., Pearce, C.R., Pereira, M.G., Peel, K., Pickard, A., Stephens, J.A., Stinchcombe, M., Williams, P., Woodward, E.M.S., Yarrow, D., Mayor, D.J., 2021. Contrasting Estuarine Processing of Dissolved Organic Matter Derived From Natural and Human-Impacted Landscapes. Glob. Biogeochem. Cycles 35. https://doi.org/10.1029/2021gb007023

Geeraert, N., Omengo, F.O., Govers, G., Bouillon, S., 2016. Dissolved organic carbon lability and stable isotope shifts during microbial decomposition in a tropical river system. Biogeosciences. https://doi.org/10.5194/bg-13-517-2016

Gibbs, H.K., Ruesch, A.S., Achard, F., Clayton, M.K., Holmgren, P., Ramankutty, N., Foley, J.A., 2010. Tropical forests were the primary sources of new agricultural land in the 1980s and 1990s. Proc. Natl. Acad. Sci. U. S. A. 107, 16732–16737. https://doi.org/10.1073/pnas.0910275107

Gmach, M.R., Cherubin, M.R., Kaiser, K., Cerri, C.E.P., 2020. Processes that influence dissolved organic matter in the soil: A review. Sci. Agric. https://doi.org/10.1590/1678-992x-2018-0164

Goldstone, J.V., Pullin, M.J., Bertilsson, S., Voelker, B.M., 2002. Reactions of hydroxyl radical with humic substances: Bleaching, mineralization, and production of bioavailable carbon substrates. Environ. Sci. Technol. 36, 364–372. https://doi.org/10.1021/es0109646

Gooddy, D.C., Darling, W.G., 2005. The potential for methane emissions from groundwaters of the UK. Sci. Total Environ. https://doi.org/10.1016/j.scitotenv.2004.07.019

Gooddy, D.C., Darling, W.G., Abesser, C., Lapworth, D.J., 2006. Using chlorofluorocarbons (CFCs) and sulphur hexafluoride (SF6) to characterise groundwater movement and residence time in a lowland Chalk catchment. J. Hydrol. https://doi.org/10.1016/j.jhydrol.2006.04.011

Graeber, D., Goyenola, G., Meerhoff, M., Zwirnmann, E., Ovesen, N.B., Glendell, M., Gelbrecht, J., Teixeira De Mello, F., González-Bergonzoni, I., Jeppesen, E., Kronvang, B., 2015. Interacting effects of climate and agriculture on fluvial DOM in temperate and subtropical catchments. Hydrol. Earth Syst. Sci. 19, 2377–2394. https://doi.org/10.5194/hess-19-2377-2015

Graham, J.A., O'Dea, E., Holt, J., Polton, J., Hewitt, H.T., Furner, R., Guihou, K., Brereton, A., Arnold, A., Wakelin, S., Sanchez, J.M.C., Adame, C.G.M., 2018. AMM15: A new high-resolution NEMO configuration for operational simulation of the European north-west shelf. Geosci. Model Dev. https://doi.org/10.5194/gmd-11-681-2018

Grieve, I., 1986. Determination of dissolved organic matter in streamwater using visible spectrophotometry: A reply. Earth Surf. Process. Landf. https://doi.org/10.1002/esp.3290110412

Griffin, C.G., Finlay, J.C., Brezonik, P.L., Olmanson, L., Hozalski, R.M., 2018. Limitations on using CDOM as a proxy for DOC in temperate lakes. Water Res. https://doi.org/10.1016/j.watres.2018.08.007

Grinham, A., Albert, S., Deering, N., Dunbabin, M., Bastviken, D., Sherman, B., Lovelock, C.E., Evans, C.D., 2018. The importance of small artificial water bodies as sources of methane emissions in Queensland, Australia. Hydrol. Earth Syst. Sci. https://doi.org/10.5194/hess-22-5281-2018

Gröger, M., Maier-Reimer, E., Mikolajewicz, U., Moll, A., Sein, D., 2013. NW European shelf under climate warming: Implications for open ocean - Shelf exchange, primary production, and carbon absorption. Biogeosciences. https://doi.org/10.5194/bg-10-3767-2013

Gücker, B., Silva, R.C.S., Graeber, D., Monteiro, J.A.F., Boëchat, I.G., 2016. Urbanization and agriculture increase exports and differentially alter elemental stoichiometry of dissolved organic matter (DOM) from tropical catchments. Sci. Total Environ. https://doi.org/10.1016/j.scitotenv.2016.01.158

Guérin, F., Abril, G., Richard, S., Burban, B., Reynouard, C., Seyler, P., Delmas, R., 2006. Methane and carbon dioxide emissions from tropical reservoirs: Significance of downstream rivers. Geophys. Res. Lett. https://doi.org/10.1029/2006GL027929

Guihou, K., Polton, J., Harle, J., Wakelin, S., O'Dea, E., Holt, J., 2018. Kilometric Scale Modeling of the North West European Shelf Seas: Exploring the Spatial and Temporal Variability of Internal Tides. J. Geophys. Res. Oceans. https://doi.org/10.1002/2017JC012960

Guillemette, F., del Giorgio, P.A., 2011. Reconstructing the various facets of dissolved organic carbon bioavailability in freshwater ecosystems. Limnol. Oceanogr. https://doi.org/10.4319/lo.2011.56.2.0734

Hagen, E.M., McTammany, M.E., Webster, J.R., Benfield, E.F., 2010. Shifts in allochthonous input and autochthonous production in streams along an agricultural land-use gradient. Hydrobiologia. https://doi.org/10.1007/s10750-010-0404-7

Hall, D.C., Behl, R.J., 2006. Integrating economic analysis and the science of climate instability. Ecol. Econ. 57. https://doi.org/10.1016/j.ecolecon.2005.05.001

Hansell, D.A., Carlson, C.A., 1998. Net community production in dissolved organic carbon. Glob. Biogeochem. Cycles. https://doi.org/10.1029/98GB01928

Hansen, A.M., Kraus, T.E.C., Pellerin, B.A., Fleck, J.A., Downing, B.D., Bergamaschi, B.A., 2016. Optical properties of dissolved organic matter (DOM): Effects of biological and photolytic degradation. Limnol. Oceanogr. https://doi.org/10.1002/lno.10270

Hartshorn, G.S., Nicolait, L., Hartshorn, L., Bevier, G., Brigtman, R., Cal, J., Cawich, A., Davidson, W., Dubois, R., Dyer, C., Gibson, J., Hawley, W., Leonard, J., Nicolait, R., Weyer, D., White, H., Wright C., 1984. Belize country environmental profile: A field study. USAID Contract No. 505-0000-C-00-3001-00. San Jose.

Hastie, A., Lauerwald, R., Weyhenmeyer, G., Sobek, S., Verpoorter, C., Regnier, P., 2018. CO2 evasion from boreal lakes: Revised estimate, drivers of spatial variability, and future projections. Glob. Change Biol. https://doi.org/10.1111/gcb.13902

Hedges, J.I., Cowie, G.L., Richey, J.E., Quay, P.D., Benner, R., Strom, M., Forsberg, B.R., 1994. Origins and processing of organic matter in the Amazon River as indicated by carbohydrates and amino acids. Limnol. Oceanogr. https://doi.org/10.4319/lo.1994.39.4.0743

Hedges, J.I., Keil, R.G., Benner, R., 1997. What happens to terrestrial organic matter in the ocean? Presented at the Organic Geochemistry. https://doi.org/10.1016/S0146-6380(97)00066-1

Heikkinen, K., 1994. Organic matter, iron and nutrient transport and nature of dissolved organic matter in the drainage basin of a boreal humic river in northern Finland. Sci. Total Environ. https://doi.org/10.1016/0048-9697(94)90553-3

Heinz, M., Graeber, D., Zak, D., Zwirnmann, E., Gelbrecht, J., Pusch, M.T., 2015. Comparison of organic matter composition in agricultural versus forest affected headwaters with special emphasis on organic nitrogen. Environ. Sci. Technol. https://doi.org/10.1021/es505146h

Heip, C.H.R., Goosen, N.K., Herman, P.M.J., Kromkamp, J., Middelburg, J.J., Soetaert, K., 1995. Production and consumption of biological particles in temperate tidal estuaries. Oceanogr. Mar. Biol. Annu. Rev. Vol 33.

Helms, J.R., Stubbins, A., Ritchie, J.D., Minor, E.C., Kieber, D.J., Mopper, K., 2008. Absorption spectral slopes and slope ratios as indicators of molecular weight, source, and photobleaching of chromophoric dissolved organic matter. Limnol. Oceanogr. https://doi.org/10.4319/lo.2008.53.3.0955

Heyman, W.D., Kjerfve, B., 1999. Hydrological and oceanographic considerations for integrated coastal zone management in Southern Belize. Environ. Manage. https://doi.org/10.1007/s002679900229

Holgerson, M.A., Raymond, P.A., 2016. Large contribution to inland water CO2 and CH4 emissions from very small ponds. Nat. Geosci. https://doi.org/10.1038/ngeo2654

Holt, J., Butenschön, M., Wakelin, S.L., Artioli, Y., Allen, J.I., 2012. Oceanic controls on the primary production of the northwest European continental shelf: Model experiments under recent past conditions and a potential future scenario. Biogeosciences. https://doi.org/10.5194/bg-9-97-2012

Hong, H., Yang, L., Guo, W., Wang, F., Yu, X., 2012. Characterization of dissolved organic matter under contrasting hydrologic regimes in a subtropical watershed using PARAFAC model. Biogeochemistry. https://doi.org/10.1007/s10533-011-9617-8

Hope, D., Billett, M.F., Cresser, M.S., 1994. A review of the export of carbon in river water: Fluxes and processes. Environ. Pollut. https://doi.org/10.1016/0269-7491(94)90142-2

Hotchkiss, E.R., Hall, R.O., 2015. Whole-stream 13C tracer addition reveals distinct fates of newly fixed carbon. Ecology. https://doi.org/10.1890/14-0631.1

Houghton, R.A., 2007. Balancing the Global Carbon Budget. Annu. Rev. Earth Planet. Sci. 35, 313–347. https://doi.org/10.1146/annurev.earth.35.031306.140057

Humphreys, M.P., Matthews, R.S., 2021. Calkulate: total alkalinity from titration data in Python. Zenodo. URL doi:10.5281/zenodo.2634304.

Hunt, R.J., Jardine, T.D., Hamilton, S.K., Bunn, S.E., 2012. Temporal and spatial variation in ecosystem metabolism and food web carbon transfer in a wet-dry tropical river. Freshw. Biol. https://doi.org/10.1111/j.1365-2427.2011.02708.x

Imai, A., Fukushima, T., Matsushige, K., Kim, Y.H., Choi, K., 2002. Characterization of dissolved organic matter in effluents from wastewater treatment plants. Water Res. 36. https://doi.org/10.1016/S0043-1354(01)00283-4

Inamdar, S., Finger, N., Singh, S., Mitchell, M., Levia, D., Bais, H., Scott, D., McHale, P., 2012. Dissolved organic matter (DOM) concentration and quality in a forested mid-Atlantic watershed, USA. Biogeochemistry. https://doi.org/10.1007/s10533-011-9572-4

IPCC, 2013. Working Group I Contribution to the IPCC Fifth Assessment Report - Summary for Policymakers. Clim. Change 2013 Phys. Sci. Basis 1–36. https://doi.org/10.1017/CBO9781107415324.004

Jarde, E., Gruau, G., Mansuy-Huault, L., 2007. Detection of manure-derived organic compounds in rivers drainig agricultural areas of intensive manure spreading. Appl. Geochem. 22, 1814–1824.

Jarvie, H.P., King, S.M., Neal, C., 2017. Inorganic carbon dominates total dissolved carbon concentrations and fluxes in British rivers: Application of the THINCARB model – Thermodynamic modelling of inorganic carbon in freshwaters. Sci. Total Environ. https://doi.org/10.1016/j.scitotenv.2016.08.201

Jeong, J.J., Bartsch, S., Fleckenstein, J.H., Matzner, E., Tenhunen, J.D., Lee, S.D., Park, S.K., Park, J.H., 2012. Differential storm responses of dissolved and particulate organic carbon in a mountainous headwater stream, investigated by high-frequency, in situ optical measurements. J. Geophys. Res. Biogeosciences. https://doi.org/10.1029/2012JG001999

Jones, M.W., Santín, C., van der Werf, G.R., Doerr, S.H., 2019. Global fire emissions buffered by the production of pyrogenic carbon. Nat. Geosci. https://doi.org/10.1038/s41561-019-0403-x

Jones, T.G., Evans, C.D., Freeman, C., 2016. The greenhouse gas (GHG) emissions associated with aquatic carbon removal during drinking water treatment. Aquat. Sci. https://doi.org/10.1007/s00027-015-0458-8

Kalbitz, K., Solinger, S., Park, J.H., Michalzik, B., Matzner, E., 2000. Controls on the dynamics dissolved organic matter in soils: A review. Soil Sci. https://doi.org/10.1097/00010694-200004000-00001

Kamjunke, N., Hertkorn, N., Harir, M., Schmitt-Kopplin, P., Griebler, C., Brauns, M., von Tümpling, W., Weitere, M., Herzsprung, P., 2019. Molecular change of dissolved organic matter and patterns of bacterial activity in a stream along a land-use gradient. Water Res. https://doi.org/10.1016/j.watres.2019.114919

Kandasamy, S., Nagender Nath, B., 2016. Perspectives on the Terrestrial Organic Matter Transport and Burial along the Land-Deep Sea Continuum: Caveats in Our Understanding of Biogeochemical Processes and Future Needs. Front. Mar. Sci. 3, 1–18. https://doi.org/10.3389/fmars.2016.00259

Kaplan, L.A., Cory, R.M., 2016. Chapter 6 - Dissolved Organic Matter in Stream Ecosystems: Forms, Functions, and Fluxes of Watershed Tea, in: Jones, J.B., Stanley, E.H. (Eds.), Stream Ecosystems in a Changing Environment. Academic Press, Boston, pp. 241–320. https://doi.org/10.1016/B978-0-12-405890-3.00006-3

Karanfil, T., Erdogan, I., Schlautman, M.A., 2003. Selecting filter membranes for measuring DOC and UV254. J. Am. Water Works Assoc. https://doi.org/10.1002/j.1551-8833.2003.tb10317.x

Karanfil, T., Schlautman, M.A., Erdogan, I., 2002. Survey of DOC and UV measurement practices with implications for SUVA determination. J. Am. Water Works Assoc. https://doi.org/10.1002/j.1551-8833.2002.tb10250.x

Karper, J., Boles, E., 2004. Human Impact Mapping of the Mopan and Chiquibul Rivers within Guatemala and Belize With Comments on Riparian Forest Ecology , Conservation and Restoration, Access.

Kaushal, N., Sanwlani, N., Tanzil, J.T.I., Cherukuru, N., Sahar, S., Müller, M., Mujahid, A., Lee, J.N., Goodkin, N.F., Martin, P., 2021. Coral Skeletal Luminescence Records Changes in Terrestrial Chromophoric Dissolved Organic Matter in Tropical Coastal Waters. Geophys. Res. Lett. 48, e2020GL092130. https://doi.org/10.1029/2020GL092130

Kellerman, A.M., Kothawala, D.N., Dittmar, T., Tranvik, L.J., 2015. Persistence of dissolved organic matter in lakes related to its molecular characteristics. Nat. Geosci. https://doi.org/10.1038/NGEO2440

Khan, E., Subramania-Pillai, S., 2007. Interferences contributed by leaching from filters on measurements of collective organic constituents. Water Res. https://doi.org/10.1016/j.watres.2006.12.028

Khatiwala, S., Primeau, F., Hall, T., 2009. Reconstruction of the history of anthropogenic CO2 concentrations in the ocean. Nature. https://doi.org/10.1038/nature08526

Kim, S., Kaplan, L.A., Hatcher, P.G., 2006. Biodegradable dissolved organic matter in a temperate and a tropical stream determined from ultra-high resolution mass spectrometry. Limnol. Oceanogr. https://doi.org/10.4319/lo.2006.51.2.1054

King, R.B., Pratt, J.H., Warner, M.P., Zisman, S.A., 1993. Agricultural development prospects in Belize (NRI Bulletin 48) 175–175.

Kirchner, J.W., 2003. A double paradox in catchment hydrology and geochemistry. Hydrol. Process. https://doi.org/10.1002/hyp.5108

Kirschbaum, M.U.F., Zeng, G., Ximenes, F., Giltrap, D.L., Zeldis, J.R., 2019. Towards a more complete quantification of the global carbon cycle. Biogeosciences 16, 831–846. https://doi.org/10.5194/bg-16-831-2019

Kitidis, V., Shutler, J.D., Ashton, I., Warren, M., Brown, I., Findlay, H., Hartman, S.E., Sanders, R., Humphreys, M., Kivimäe, C., Greenwood, N., Hull, T., Pearce, D., McGrath, T., Stewart, B.M., Walsham, P., McGovern, E., Bozec, Y., Gac, J.P., van Heuven, S.M.A.C., Hoppema, M., Schuster, U., Johannessen, T., Omar, A., Lauvset, S.K., Skjelvan, I., Olsen, A., Steinhoff, T., Körtzinger, A., Becker, M., Lefevre, N., Diverrès, D., Gkritzalis, T., Cattrijsse, A., Petersen, W., Voynova, Y.G., Chapron, B., Grouazel, A., Land, P.E., Sharples, J., Nightingale, P.D., 2019. Winter weather controls net influx of atmospheric CO2 on the north-west European shelf. Sci. Rep. https://doi.org/10.1038/s41598-019-56363-5

Kitidis, V., Tizzard, L., Uher, G., Judd, A., Upstill-Goddard, R.C., Head, I.M., Gray, N.D., Taylor, G., Durán, R., Diez, R., Iglesias, J., García-Gil, S., 2007. The biogeochemical cycling of methane in Ria de Vigo, NW Spain: Sediment processing and sea-air exchange. J. Mar. Syst. https://doi.org/10.1016/j.jmarsys.2006.03.022

Klumpp, K., Fontaine, S., Attard, E., Le Roux, X., Gleixner, G., Soussana, J.F., 2009. Grazing triggers soil carbon loss by altering plant roots and their control on soil microbial community. J. Ecol. 97, 876–885. https://doi.org/10.1111/j.1365-2745.2009.01549.x

Koehler, B., Von Wachenfeldt, E., Kothawala, D., Tranvik, L.J., 2012. Reactivity continuum of dissolved organic carbon decomposition in lake water. J. Geophys. Res. Biogeosciences 117, 1–14. https://doi.org/10.1029/2011JG001793

Köhler, S., Buffam, I., Jonsson, A., Bishop, K., 2002. Photochemical and microbial processing of stream and soil water dissolved organic matter in a boreal forested catchment in northern Sweden. Aquat. Sci. https://doi.org/10.1007/s00027-002-8071-z

Kortelainen, P., Pajunen, H., Rantakari, M., Saarnisto, M., 2004. A large carbon pool and small sink in boreal Holocene lake sediments. Glob. Change Biol. https://doi.org/10.1111/j.1365-2486.2004.00848.x

Kothawala, D.N., Kellerman, A.M., Catalán, N., Tranvik, L.J., 2020. Organic Matter Degradation across Ecosystem Boundaries: The Need for a Unified Conceptualization. Trends Ecol. Evol. https://doi.org/10.1016/j.tree.2020.10.006

Kothawala, D.N., Murphy, K.R., Stedmon, C.A., Weyhenmeyer, G.A., Tranvik, L.J., 2013. Inner filter correction of dissolved organic matter fluorescence. Limnol. Oceanogr. Methods. https://doi.org/10.4319/lom.2013.11.616

Kothawala, D.N., Stedmon, C.A., Müller, R.A., Weyhenmeyer, G.A., Köhler, S.J., Tranvik, L.J., 2014. Controls of dissolved organic matter quality: Evidence from a large-scale boreal lake survey. Glob. Change Biol. 20, 1101–1114. https://doi.org/10.1111/gcb.12488

Kritzberg, E.S., Ekström, S.M., 2012. Increasing iron concentrations in surface waters – a factor behind brownification? Biogeosciences 9, 1465–1478. https://doi.org/10.5194/bg-9-1465-2012

Kuhlbusch, T.A.J., Crutzen, P.J., 1995. Toward a global estimate of black carbon in residues of vegetation fires representing a sink of atmospheric CO2 and a source of O2. Glob. Biogeochem. Cycles. https://doi.org/10.1029/95GB02742

Kyung Yoon, T., Jin, H., Oh, N.H., Park, J.H., 2016. Technical note: Assessing gas equilibration systems for continuous pCO2 measurements in inland waters. Biogeosciences. https://doi.org/10.5194/bg-13-3915-2016

Laane, R.W.P.M., Koole, L., 1982a. The relation between fluorescence and dissolved organic carbon in the Ems-Dollart estuary and the western Wadden Sea. Neth. J. Sea Res. 15, 217–227.

Laane, R.W.P.M., Koole, L., 1982b. The relation between fluorescence and dissolved organic carbon in the Ems-Dollart estuary and the western Wadden Sea. Neth. J. Sea Res. 15, 217–227.

Lacis, A.A., Schmidt, G.A., Rind, D., Ruedy, R.A., 2010. Atmospheric CO2: Principal control knob governing earth's temperature. Science 330. https://doi.org/10.1126/science.1190653

Lambert, T., Bouillon, S., Darchambeau, F., Massicotte, P., Borges, A.V., 2016. Shift in the chemical composition of dissolved organic matter in the Congo River network. Biogeosciences Discuss. https://doi.org/10.5194/bg-2016-240

Lambert, T., Darchambeau, F., Bouillon, S., Alhou, B., Mbega, J.D., Teodoru, C.R., Nyoni, F.C., Massicotte, P., Borges, A.V., 2015. Landscape Control on the Spatial and Temporal Variability of Chromophoric Dissolved Organic Matter and Dissolved Organic Carbon in Large African Rivers. Ecosystems. https://doi.org/10.1007/s10021-015-9894-5

Lanza, G., 2019. Chalillo Dam Project , Belize Central America : An Update on the Ecological Health of the Macal River Watershed.

Lapierre, J.-F., Guillemette, F., Berggren, M., del Giorgio, P.A., 2013. Increases in terrestrially derived carbon stimulate organic carbon processing and CO2 emissions in boreal aquatic ecosystems. Nat. Commun. 4. https://doi.org/10.1038/ncomms3972

Lapworth, D.J., Gooddy, D.C., Allen, D., Old, G.H., 2009. Understanding groundwater, surface water, and hyporheic zone biogeochemical process in a Chalk catchment using fluorescence properties of dissolves and colloidal organic matter. J. Geophys. Res. Biogeosciences. https://doi.org/10.1029/2009JG000921

Lapworth, D.J., Zahid, A., Taylor, R.G., Burgess, W.G., Shamsudduha, M., Ahmed, K.M., Mukherjee, A., Gooddy, D.C., Chatterjee, D., MacDonald, A.M., 2018. Security of Deep Groundwater in the Coastal Bengal Basin Revealed by Tracers. Geophys. Res. Lett. https://doi.org/10.1029/2018GL078640

Laudon, H., Sponseller, R.A., 2018. How landscape organization and scale shape catchment hydrology and biogeochemistry: insights from a long-term catchment study. Wiley Interdiscip. Rev. Water. https://doi.org/10.1002/wat2.1265

Lauerwald, R., Hartmann, J., Ludwig, W., Moosdorf, N., 2012. Assessing the nonconservative fluvial fluxes of dissolved organic carbon in North America. J. Geophys. Res. Biogeosciences. https://doi.org/10.1029/2011JG001820

Lavonen, E.E., Gonsior, M., Tranvik, L.J., Schmitt-Kopplin, P., Köhler, S.J., 2013. Selective chlorination of natural organic matter: Identification of previously unknown disinfection byproducts. Environ. Sci. Technol. https://doi.org/10.1021/es304669p

Lee, M.H., Lee, S.Y., Yoo, H.Y., Shin, K.H., Hur, J., 2020. Comparing optical versus chromatographic descriptors of dissolved organic matter (DOM) for tracking the non-point sources in rural watersheds. Ecol. Indic. 117. https://doi.org/10.1016/j.ecolind.2020.106682

Legge, O., Johnson, M., Hicks, N., Jickells, T., Diesing, M., Aldridge, J., Andrews, J., Artioli, Y., Bakker, D.C.E., Burrows, M.T., Carr, N., Cripps, G., Felgate, S.L., Fernand, L., Greenwood, N., Hartman, S., Kröger, S., Lessin, G., Mahaffey, C., Mayor, D.J., Parker, R., Queirós, A.M., Shutler, J.D., Silva, T., Stahl, H., Tinker, J., Underwood, G.J.C., Van Der Molen, J., Wakelin, S., Weston, K., Williamson, P., 2020. Carbon on the Northwest European Shelf: Contemporary Budget and Future Influences. Front. Mar. Sci. https://doi.org/10.3389/fmars.2020.00143

Lehner, B., Verdin, K., Jarvis, A., 2008. New global hydrography derived from spaceborne elevation data. Eos. https://doi.org/10.1029/2008EO100001

Lepistö, A., Futter, M.N., Kortelainen, P., 2014. Almost 50 years of monitoring shows that climate, not forestry, controls long-term organic carbon fluxes in a large boreal watershed. Glob. Change Biol. https://doi.org/10.1111/gcb.12491

Lewis, W.M., Canfield, D., 1977. Dissolved organic carbon in some dark Venezuelan waters and a revised equation for spectrophotometric determination of dissolved organic carbon. Arch. Für Hydrobiol.

Li, M., Peng, C., Zhou, X., Yang, Y., Guo, Y., Shi, G., Zhu, Q., 2019. Modeling Global Riverine DOC Flux Dynamics From 1951 to 2015. J. Adv. Model. Earth Syst. https://doi.org/10.1029/2018MS001363

Lindh, M.V., Lefébure, R., Degerman, R., Lundin, D., Andersson, A., Pinhassi, J., 2015. Consequences of increased terrestrial dissolved organic matter and temperature on bacterioplankton community composition during a Baltic Sea mesocosm experiment. Ambio 44, 402–412. https://doi.org/10.1007/s13280-015-0659-3

Lirman, D., Manzello, D., 2009. Patterns of resistance and resilience of the stress-tolerant coral Siderastrea radians (Pallas) to sub-optimal salinity and sediment burial. J. Exp. Mar. Biol. Ecol. https://doi.org/10.1016/j.jembe.2008.10.024

Liu, Q., Jiang, Y., Tian, Y., Hou, Z., He, K., Fu, L., Xu, H., 2019. Impact of land use on the DOM composition in different seasons in a subtropical river flowing through a region undergoing rapid urbanization. J. Clean. Prod. https://doi.org/10.1016/j.jclepro.2018.12.030

Liu, Y., Shao, M., Lu, S., Chang, C., Wang, J.-L., Chen, G., 2008. Volatile Organic Compound (VOC) measurements in the Pearl River Delta (PRD) region, China. Atmos Chem Phys 15.

Lloyd, C.E.M., Johnes, P.J., Freer, J.E., Carswell, A.M., Jones, J.I., Stirling, M.W., Hodgkinson, R.A., Richmond, C., Collins, A.L., 2019. Determining the sources of nutrient flux to water in headwater catchments: Examining the speciation balance to inform the targeting of mitigation measures. Sci. Total Environ. https://doi.org/10.1016/j.scitotenv.2018.08.190

Lønborg, C., Carreira, C., Jickells, T., Álvarez-Salgado, X.A., 2020. Impacts of Global Change on Ocean Dissolved Organic Carbon (DOC) Cycling. Front. Mar. Sci. https://doi.org/10.3389/fmars.2020.00466

Lovelock, C.E., Evans, C., Barros, N., Prairie, Y., Alm, J., Bastviken, D., Beaulieu, J.J., Garneau, M., Harby, A., Harrison, J., Pare, D., Raadal, H.L., Sherman, B., Zhang, C., Ogle, S.M., Grinham, A., Deemer, B., Aurelio dos Santos, M., Kosten, S., Peacock, M., Li, Z., Stepanenko, V., 2019. 2019 Refinement to the 2006 IPCC Guidelines for National Greenhouse Gas Inventories. Volume 4: Agricultura, forestry and other land use (AFOLU). Chapter 7: Wetlands.

Lucas, N., Bienaime, C., Belloy, C., Queneudec, M., Silvestre, F., Nava-Saucedo, J.-E., 2008. Polymer biodegradation: Mechanisms and estimation techniques – A review. Chemosphere 73, 429–442. https://doi.org/10.1016/j.chemosphere.2008.06.064

Ludwig, W., Probst, J.L., 1996. Predicting the oceanic input of organic carbon by continental erosion. Glob. Biogeochem. Cycles. https://doi.org/10.1029/95GB02925

Ludwig, W., Probst, J.L., Kempe, S., 1996. Predicting the oceanic input of organic carbon by continental erosion. Glob. Biogeochem. Cycles. https://doi.org/10.1029/95GB02925

Luisetti, T., Jackson, E.L., Turner, R.K., 2013. Valuing the European “coastal blue carbon” storage benefit. Mar. Pollut. Bull. 71, 101–6. https://doi.org/10.1016/j.marpolbul.2013.03.029

Luisetti, T., Turner, R.K., Andrews, J.E., Jickells, T.D., Kröger, S., Diesing, M., Paltriguera, L., Johnson, M.T., Parker, E.R., Bakker, D.C.E., Weston, K., 2019. Quantifying and valuing carbon flows and stores

in coastal and shelf ecosystems in the UK. Ecosyst. Serv. https://doi.org/10.1016/j.ecoser.2018.10.013

Lupon, A., Denfeld, B.A., Laudon, H., Leach, J., Karlsson, J., Sponseller, R.A., 2019. Groundwater inflows control patterns and sources of greenhouse gas emissions from streams. Limnol. Oceanogr. https://doi.org/10.1002/lno.11134

Lyard, F., Allain, D., Cancet, M., Carrère, L., Picot, N., 2020. FES2014 global ocean tides atlas: design and performances. Ocean Sci. Discuss. 1–40. https://doi.org/10.5194/os-2020-96

Mallin, M.A., Johnson, V.L., Ensign, S.H., MacPherson, T.A., 2006. Factors contributing to hypoxia in rivers, lakes, and streams. Presented at the Limnology and Oceanography. https://doi.org/10.4319/lo.2006.51.1_part_2.0690

Marescaux, A., Thieu, V., Borges, A.V., Garnier, J., 2018. Seasonal and spatial variability of the partial pressure of carbon dioxide in the human-impacted Seine River in France. Sci. Rep. https://doi.org/10.1038/s41598-018-32332-2

Margat, J., Gun, J. van der, 2013. Groundwater around the World: A Geographic Synopsis. CRC Press.

Marín-Spiotta, E., Gruley, K.E., Crawford, J., Atkinson, E.E., Miesel, J.R., Greene, S., Cardona-Correa, C., Spencer, R.G.M., 2014. Paradigm shifts in soil organic matter research affect interpretations of aquatic carbon cycling: Transcending disciplinary and ecosystem boundaries. Biogeochemistry. https://doi.org/10.1007/s10533-013-9949-7

Massicotte, P., Asmala, E., Stedmon, C., Markager, S., 2017. Global distribution of dissolved organic matter along the aquatic continuum: Across rivers, lakes and oceans. Sci. Total Environ. https://doi.org/10.1016/j.scitotenv.2017.07.076

Mattsson, T., Kortelainen, P., Laubel, A., Evans, D., Pujo-Pay, M., Räike, A., Conan, P., 2009. Export of dissolved organic matter in relation to land use along a European climatic gradient. Sci. Total Environ. https://doi.org/10.1016/j.scitotenv.2008.11.014

Mayor, D.J., Thornton, B., Jenkins, H., Felgate, S.L., 2018. Microbiota: The Living Foundation, in: Mudflat Ecology. https://doi.org/10.1007/978-3-319-99194-8_3

Mayorga, E., Aufdenkampe, A.K., Masiello, C.A., Krusche, A.V., Hedges, J.I., Quay, P.D., Richey, J.E., Brown, T.A., 2005. Young organic matter as a source of carbon dioxide outgassing from Amazonian rivers. Nature. https://doi.org/10.1038/nature03880

Mayorga, E., Seitzinger, S.P., Harrison, J.A., Dumont, E., Beusen, A.H.W., Bouwman, A.F., Fekete, B.M., Kroeze, C., Van Drecht, G., 2010. Global Nutrient Export from WaterSheds 2 (NEWS 2): Model development and implementation. Environ. Model. Softw. https://doi.org/10.1016/j.envsoft.2010.01.007

McDonough, L.K., Santos, I.R., Andersen, M.S., O'Carroll, D.M., Rutlidge, H., Meredith, K., Oudone, P., Bridgeman, J., Gooddy, D.C., Sorensen, J.P.R., Lapworth, D.J., MacDonald, A.M., Ward, J., Baker, A., 2020. Changes in global groundwater organic carbon driven by climate change and urbanization. Nat. Commun. https://doi.org/10.1038/s41467-020-14946-1

McKinley, G.A., Pilcher, D.J., Fay, A.R., Lindsay, K., Long, M.C., Lovenduski, N.S., 2016. Timescales for detection of trends in the ocean carbon sink. Nature. https://doi.org/10.1038/nature16958

McLeod, E., Chmura, G.L., Bouillon, S., Salm, R., Björk, M., Duarte, C.M., Lovelock, C.E., Schlesinger, W.H., Silliman, B.R., 2011. A blueprint for blue carbon: Toward an improved understanding of the role of vegetated coastal habitats in sequestering CO2. Front. Ecol. Environ. 9, 552–560. https://doi.org/10.1890/110004

Meerman, J., 2015. Belize Rivers Shapefile.

Mello, K. de, Valente, R.A., Randhir, T.O., dos Santos, A.C.A., Vettorazzi, C.A., 2018. Effects of land use and land cover on water quality of low-order streams in Southeastern Brazil: Watershed versus riparian zone. Catena 167, 130–138. https://doi.org/10.1016/j.catena.2018.04.027

Mendonça, R., Müller, R.A., Clow, D., Verpoorter, C., Raymond, P., Tranvik, L.J., Sobek, S., 2017. Organic carbon burial in global lakes and reservoirs. Nat. Commun. https://doi.org/10.1038/s41467-017-01789-6

Meybeck, Michel, 1993. Riverine transport of atmospheric carbon: Sources, global typology and budget. Water. Air. Soil Pollut. https://doi.org/10.1007/BF01105015

Meybeck, M., 1993. C, N, P and S in Rivers: From Sources to Global Inputs, in: Interactions of C, N, P and S Biogeochemical Cycles and Global Change. https://doi.org/10.1007/978-3-642-76064-8_6

Meybeck, M., 1982. Carbon. nitrogen, and phosphorus transport by world rivers. Am. J. Sci. 282, 401–450.

Meybeck, M., Ragu, A., 1996. River discharges to the oceans: an assessment of suspended solids, major ions, and nutrients.

Miller, A.E.J., 1999. Seasonal investigations of dissolved organic carbon dynamics in the Tamar Estuary, U.K. Estuar. Coast. Shelf Sci. https://doi.org/10.1006/ecss.1999.0552

Milliman, J.D., Syvitski, J.P.M., 1992. Geomorphic/tectonic control of sediment discharge to the ocean: the importance of small mountainous rivers. J. Geol. https://doi.org/10.1086/629606

Molotoks, A., Stehfest, E., Doelman, J., Albanito, F., Fitton, N., Dawson, T.P., Smith, P., 2018. Global projections of future cropland expansion to 2050 and direct impacts on biodiversity and carbon storage. Glob. Change Biol. https://doi.org/10.1111/gcb.14459

Monteith, D.T., Stoddard, J.L., Evans, C.D., De Wit, H.A., Forsius, M., Høgåsen, T., Wilander, A., Skjelkvåle, B.L., Jeffries, D.S., Vuorenmaa, J., Keller, B., Kopécek, J., Vesely, J., 2007. Dissolved organic carbon trends resulting from changes in atmospheric deposition chemistry. Nature. https://doi.org/10.1038/nature06316

Moody, C.S., Worrall, F., 2017. Modeling rates of DOC degradation using DOM composition and hydroclimatic variables. J. Geophys. Res. Biogeosciences. https://doi.org/10.1002/2016JG003493

Moore, S., Evans, C.D., Page, S.E., Garnett, M.H., Jones, T., Freeman, C., Hooijer, A., Wiltshire, A.J., Limin, S., H., Gauci, V., 2013. Deep instability of deforested tropical peatlands revealed by fluvial organic carbon fluxes. Nature 493, 660–663.

Moore, T.R., 1987. An assessment of a simple spectrophotometric method for the determination of dissolved organic carbon in freshwaters. N. Z. J. Mar. Freshw. Res. https://doi.org/10.1080/00288330.1987.9516262

Moore, T.R., 1985. The Spectrophotometric Determination of Dissolved Organic Carbon in Peat Waters. Soil Sci. Soc. Am. J. https://doi.org/10.2136/sssaj1985.03615995004900060054x

Morris, A.W., Mantoura, R.F.C., Bale, A.J., Howland, R.J.M., 1978. Very low salinity regions of estuaries: important sites for chemical and biological reactions [10]. Nature. https://doi.org/10.1038/274678a0

Mosher, J.J., Kaplan, L.A., Podgorski, D.C., McKenna, A.M., Marshall, A.G., 2015. Longitudinal shifts in dissolved organic matter chemogeography and chemodiversity within headwater streams: a river continuum reprise. Biogeochemistry 124. https://doi.org/10.1007/s10533-015-0103-6

Mostofa, K.M.G., Wu, F., Liu, C.Q., Fang, W.L., Yuan, J., Ying, W.L., Wen, L., Yi, M., 2010. Characterization of Nanming River (southwestern China) sewerage-impacted pollution using an

excitation-emission matrix and PARAFAC. Limnology 11, 217–231. https://doi.org/10.1007/s10201-009-0306-4

Mühlenbruch, M., Grossart, H.P., Eigemann, F., Voss, M., 2018. Mini-review: Phytoplankton-derived polysaccharides in the marine environment and their interactions with heterotrophic bacteria. Environ. Microbiol. https://doi.org/10.1111/1462-2920.14302

Mulholland, P.J., 2003. Large-Scale Patterns in Dissolved Organic Carbon Concentration, Flux, and Sources, in: Aquatic Ecosystems. https://doi.org/10.1016/b978-012256371-3/50007-x

Müller, R.A., Futter, M.N., Sobek, S., Nisell, J., Bishop, K., Weyhenmeyer, G.A., 2013. Water renewal along the aquatic continuum offsets cumulative retention by lakes: Implications for the character of organic carbon in boreal lakes. Aquat. Sci. https://doi.org/10.1007/s00027-013-0298-3

Murphy, K.R., Butler, K.D., Spencer, R.G.M., Stedmon, C.A., Boehme, J.R., Aiken, G.R., 2010. Measurement of dissolved organic matter fluorescence in aquatic environments: An interlaboratory comparison. Environ. Sci. Technol. 44, 9405–9412. https://doi.org/10.1021/es102362t

Murphy, K.R., Stedmon, C.A., Wenig, P., Bro, R., 2014. OpenFluor- An online spectral library of auto-fluorescence by organic compounds in the environment. Anal. Methods 6, 658–661. https://doi.org/10.1039/c3ay41935e

Myhre, G., Shindell, D., Breon, F.-M., Collins, W., Fuglestvedt, J., Huang, J., Koch, D., Lamarque, J.-F., Lee, D., Mendoza, B., Nakajima, T., Robock, A., Stephens, G., Takemura, T., Zhang, H., 2013. Anthropogenic and Natural Radiative Forcing, in: Stocker, T.F., Qin, D., Plattner, G.-K., Tignor, M., Allen, S.K., Boschung, J., Nauels, A., Xia, Y., Bex, V., Midgley, P.M. (Eds.), Climate Change 2013: The Physical Science Basis. Contribution of Working Group I to the Fifth Assessment Report of the Intergovernmental Panel on Climate Change. Cambridge University Press, Cambridge, United Kingdom, and New York, NY, USA, pp. 659–739. https://doi.org/10.1017/CBO9781107415324.018

Nakhavali, M., Friedlingstein, P., Lauerwald, R., Tang, J., Chadburn, S., Camino-Serrano, M., Guenet, B., Harper, A., Walmsley, D., Peichl, M., Gielen, B., 2018. Representation of dissolved organic carbon in the JULES land surface model (vn4.4-JULES-DOCM). Geosci. Model Dev. https://doi.org/10.5194/gmd-11-593-2018

Natchimuthu, S., Sundgren, I., Gålfalk, M., Klemedtsson, L., Crill, P., Danielsson, Å., Bastviken, D., 2016. Spatio-temporal variability of lake CH4 fluxes and its influence on annual whole lake emission estimates. Limnol. Oceanogr. https://doi.org/10.1002/lno.10222

Nebbioso, A., Piccolo, A., 2013a. Molecular characterization of dissolved organic matter (DOM): A critical review. Anal. Bioanal. Chem. 405, 109–124. https://doi.org/10.1007/s00216-012-6363-2

Nebbioso, A., Piccolo, A., 2013b. Molecular characterization of dissolved organic matter (DOM): A critical review. Anal. Bioanal. Chem. 405, 109–124. https://doi.org/10.1007/s00216-012-6363-2

Nellemann, C., Corcoran, E., Duarte, C.M., Valdés, L., De Young, C., Fonseca, L., Grimsditch, G., 2009. Blue Carbon - The Role of Healthy Oceans in Binding Carbon, Environment.

Nydahl, A.C., Wallin, M.B., Weyhenmeyer, G.A., 2017. No long-term trends in pCO2 despite increasing organic carbon concentrations in boreal lakes, streams, and rivers. Glob. Biogeochem. Cycles. https://doi.org/10.1002/2016GB005539

Oksanen, J., Blanchet, F.G., Friendly, M., Kindt, R., Legrendre, O., McGlinn, D., Minchin, P.R., O'Hara, R.B., Simpson, G.L., Solymos, P., Henry, M., Stevens, H., Szoecs, E., Wagner, H., 2019. vegan: Community Ecology Package.

Ollivier, Q.R., Maher, D.T., Pitfield, C., Macreadie, P.I., 2019. Punching above their weight: Large release of greenhouse gases from small agricultural dams. Glob. Change Biol. https://doi.org/10.1111/gcb.14477

Osburn, C.L., Wigdahl, C.R., Fritz, S.C., Saros, J.E., 2011. Dissolved organic matter composition and photoreactivity in prairie lakes of the U.S. Great Plains. Limnol. Oceanogr. https://doi.org/10.4319/lo.2011.56.6.2371

Painter, S.C., Lapworth, D.J., Woodward, E.M.S., Kroeger, S., Evans, C.D., Mayor, D.J., Sanders, R.J., 2018. Terrestrial dissolved organic matter distribution in the North Sea. Sci. Total Environ. 630, 630–647. https://doi.org/10.1016/j.scitotenv.2018.02.237

Panneer Selvam, B., Natchimuthu, S., Arunachalam, L., Bastviken, D., 2014. Methane and carbon dioxide emissions from inland waters in India - implications for large scale greenhouse gas balances. Glob. Change Biol. https://doi.org/10.1111/gcb.12575

Parr, T.B., Cronan, C.S., Ohno, T., Findlay, S.E.G., Smith, S.M.C., Simon, K.S., 2015. Urbanization changes the composition and bioavailability of dissolved organic matter in headwater streams. Limnol. Oceanogr. https://doi.org/10.1002/lno.10060

Parry, M.L., Canziani, O.F., Palutikof, J.P., van der Linden, P.J., Hanson, C.E., 2008. Climate Change 2007: Impacts, Adaptation and Vulnerability. Contribution of Working Group II to the Fourth

Assessment Report of the Intergovernmental Panel on Climate Change. J. Environ. Qual. Chapter 13. https://doi.org/10.2134/jeq2008.0015br

Peacock, M., Audet, J., Jordan, S., Smeds, J., Wallin, M.B., 2019. Greenhouse gas emissions from urban ponds are driven by nutrient status and hydrology. Ecosphere. https://doi.org/10.1002/ecs2.2643

Peacock, M., Evans, C.D., Fenner, N., Freeman, C., Gough, R., Jones, T.G., Lebron, I., 2014. UV-visible absorbance spectroscopy as a proxy for peatland dissolved organic carbon (DOC) quantity and quality: Considerations on wavelength and absorbance degradation. Environ. Sci. Process. Impacts. https://doi.org/10.1039/c4em00108g

Peacock, M., Freeman, C., Gauci, V., Lebron, I., Evans, C.D., 2015. Investigations of freezing and cold storage for the analysis of peatland dissolved organic carbon (DOC) and absorbance properties. Environ. Sci. Process. Impacts. https://doi.org/10.1039/c5em00126a

Pereira, R., Isabella Bovolo, C., Spencer, R.G.M., Hernes, P.J., Tipping, E., Vieth-Hillebrand, A., Pedentchouk, N., Chappell, N.A., Parkin, G., Wagner, T., 2014. Mobilization of optically invisible dissolved organic matter in response to rainstorm events in a tropical forest headwater river. Geophys. Res. Lett. https://doi.org/10.1002/2013GL058658

Prouty, N.G., Hughen, K.A., Carilli, J., 2008. Geochemical signature of land-based activities in Caribbean coral surface samples. Coral Reefs. https://doi.org/10.1007/s00338-008-0413-4

Pucher, M., Graeber, D., Preiner, S., Pinto, R., 2019. staRdom.

Pullin, M.J., Progess, C.A., Maurice, P.A., 2004. Effects of photoirradiation on the adsorption of dissolved organic matter to goethite. Geochim. Cosmochim. Acta 68, 3643–3656. https://doi.org/10.1016/j.gca.2004.03.017

Pumpanen, J., Lindén, A., Miettinen, H., Kolari, P., Ilvesniemi, H., Mammarella, I., Hari, P., Nikinmaa, E., Heinonsalo, J., Bäck, J., Ojala, A., Berninger, F., Vesala, T., 2014. Precipitation and net ecosystem exchange are the most important drivers of DOC flux in upland boreal catchments. J. Geophys. Res. Biogeosciences. https://doi.org/10.1002/2014JG002705

Purdy, E.G., Pusey, W.C., Wantland, K.F., 1975. Continental Shelf of Belize: Regional Shelf Attributes. Presented at the Studies in Geol.

Queimaliños, C., Reissig, M., Pérez, G.L., Soto Cárdenas, C., Gerea, M., Garcia, P.E., García, D., Diéguez, M.C., 2019. Linking landscape heterogeneity with lake dissolved organic matter properties

assessed through absorbance and fluorescence spectroscopy: Spatial and seasonal patterns in temperate lakes of Southern Andes (Patagonia, Argentina). Sci. Total Environ. 686, 223–235. https://doi.org/10.1016/j.scitotenv.2019.05.396

R Core Team, 2019. R: A language and environment for statistical computing. R Foundation for Statistical Computing, Vienna, Austria.

Ramos, M.C., Quinton, J.N., Tyrrel, S.F., 2006. Effects of cattle manure on erosion rates and runoff water pollution by faecal coliforms. J. Environ. Manage. 78, 97–101. https://doi.org/10.1016/j.jenvman.2005.04.010

Ranjan, C., Nahari, V., 2020. nlcor: Nonlinear Correlation.

Rawlins, B.G., O'Donnell, K., Ingham, M., 2003. Geochemical survey of the Tamar Catchment (South-West England). Br. Geol. Surv. Rep.

Rawlins, B.G., Palumbo-Roe, B., Gooddy, D.C., Worrall, F., Smith, H., 2014. A model of potential carbon dioxide efflux from surface water across England and Wales using headwater stream survey data and landscape predictors. Biogeosciences. https://doi.org/10.5194/bg-11-1911-2014

Raymond, P.A., Bauer, J.E., 2001. Use of 14C and 13C natural abundances for evaluating riverine, estuarine, and coastal DOC and POC sources and cycling: A review and synthesis. Org. Geochem. 32, 469–485. https://doi.org/10.1016/S0146-6380(00)00190-X

Raymond, P.A., Hartmann, J., Lauerwald, R., Sobek, S., McDonald, C., Hoover, M., Butman, D., Striegl, R., Mayorga, E., Humborg, C., Kortelainen, P., Dürr, H., Meybeck, M., Ciais, P., Guth, P., 2013. Global carbon dioxide emissions from inland waters. Nature. https://doi.org/10.1038/nature12760

Raymond, P.A., Saiers, J.E., Sobczak, W.V., 2016. Hydrological and biogeochemical controls on watershed dissolved organic matter transport: Pulse- shunt concept. Ecology. https://doi.org/10.1890/14-1684.1

Raymond, P.A., Spencer, R.G.M., 2015. Riverine DOM, in: Biogeochemistry of Marine Dissolved Organic Matter: Second Edition. https://doi.org/10.1016/B978-0-12-405940-5.00011-X

Regan, S., Hynds, P., Flynn, R., 2017. An overview of dissolved organic carbon in groundwater and implications for drinking water safety. Hydrogeol. J. https://doi.org/10.1007/s10040-017-1583-3

Regnier, P., Friedlingstein, P., Ciais, P., Mackenzie, F.T., Gruber, N., Janssens, I.A., Laruelle, G.G., Lauerwald, R., Luyssaert, S., Andersson, A.J., Arndt, S., Arnosti, C., Borges, A.V., Dale, A.W., Gallego-

Sala, A., Goddéris, Y., Goossens, N., Hartmann, J., Heinze, C., Ilyina, T., Joos, F., Larowe, D.E., Leifeld, J., Meysman, F.J.R., Munhoven, G., Raymond, P.A., Spahni, R., Suntharalingam, P., Thullner, M., 2013. Anthropogenic perturbation of the carbon fluxes from land to ocean. Nat. Geosci. 6, 597–607. https://doi.org/10.1038/ngeo1830

Renard, K.G., Laflen, J.M., Foster, G.R., McCool, D.K., 2017. The revised universal soil loss equation, in: Soil Erosion Research Methods. https://doi.org/10.1201/9780203739358

Rodellas, V., Garcia-Orellana, J., Masqué, P., Feldman, M., Weinstein, Y., Boyle, E.A., 2015. Submarine groundwater discharge as a major source of nutrients to the Mediterranean Sea. Proc. Natl. Acad. Sci. U. S. A. https://doi.org/10.1073/pnas.1419049112

Roebuck, J.A., Seidel, M., Dittmar, T., Jaffé, R., 2019. Controls of Land Use and the River Continuum Concept on Dissolved Organic Matter Composition in an Anthropogenically Disturbed Subtropical Watershed. Environ. Sci. Technol. https://doi.org/10.1021/acs.est.9b04605

Rousk, K., Michelsen, A., Rousk, J., 2016. Microbial control of soil organic matter mineralization responses to labile carbon in subarctic climate change treatments. Glob. Change Biol. 22, 4150–4161. https://doi.org/10.1111/gcb.13296

Rowland, C.S., Morton, R.D., Carrasco, L., McShane, G., O'Neill, A.W., Wood, C.M., 2017. Land Cover Map 2015. Cent. Ecol. Hydrol. Wallingford.

Royer, T.V., David, M.B., 2005. Export of dissolved organic carbon from agricultural streams in Illinois, USA. Aquat. Sci. https://doi.org/10.1007/s00027-005-0781-6

Sabine, C.L., Feely, R.A., 2004. The oceanic sink for carbon dioxide. Greenh. Gas Sinks 31–49. https://doi.org/10.1079/9781845931896.0000

Sachse, A., Babenzien, D., Ginzel, G., Gelbrecht, J., Steinberg, C.E.W., 2001. Characterization of dissolved organic carbon (DOC) in a dystrophic lake and an adjacent fen. Biogeochemistry. https://doi.org/10.1023/A:1010649227510

Sachse, A., Henrion, R., Gelbrecht, J., Steinberg, C.E.W., 2005. Classification of dissolved organic carbon (DOC) in river systems: Influence of catchment characteristics and autochthonous processes. Org. Geochem. https://doi.org/10.1016/j.orggeochem.2004.12.008

Sandberg, J., Andersson, A., Johansson, S., Wikner, J., 2004. Pelagic food web structure and carbon budget in the northern Baltic Sea: Potential importance of terrigenous carbon. Mar. Ecol. Prog. Ser. 268, 13–29. https://doi.org/10.3354/meps268013

Santín, C., Doerr, S.H., Preston, C.M., González-Rodríguez, G., 2015. Pyrogenic organic matter production from wildfires: a missing sink in the global carbon cycle. Glob. Change Biol. https://doi.org/10.1111/gcb.12800

Sarmiento, J.L., Sundquist, E. T., 1992. Rvised budget for the oceanic uptake of anthropogenic carbon dioxide. Nature 365, 589–593.

Saunois, M., Stavert, A.R., Poulter, B., Bousquet, P., Canadell, J.G., Jackson, R.B., Raymond, P.A., Dlugokencky, E.J., Houweling, S., Patra, P.K., Ciais, P., Arora, V.K., Bastviken, D., Bergamaschi, P., Blake, D.R., Brailsford, G., Bruhwiler, L., Carlson, K.M., Carrol, M., Castaldi, S., Chandra, N., Crevoisier, C., Crill, P.M., Covey, K., Curry, C.L., Etiope, G., Frankenberg, C., Gedney, N., Hegglin, M.I., Höglund-Isakson, L., Hugelius, G., Ishizawa, M., Ito, A., Janssens-Maenhout, G., Jensen, K.M., Joos, F., Kleinen, T., Krummel, P.B., Langenfelds, R.L., Laruelle, G.G., Liu, L., Machida, T., Maksyutov, S., McDonald, K.C., McNorton, J., Miller, P.A., Melton, J.R., Morino, I., Müller, J., Murgia-Flores, F., Naik, V., Niwa, Y., Noce, S., O'Doherty, S., Parker, R.J., Peng, C., Peng, S., Peters, G.P., Prigent, C., Prinn, R., Ramonet, M., Regnier, P., Riley, W.J., Rosentreter, J.A., Segers, A., Simpson, I.J., Shi, H., Smith, S.J., Steele, P.L., Thornton, B.F., Tian, H., Tohjima, Y., Tubiello, F.N., Tsuruta, A., Viovy, N., Voulgarakis, A., Weber, T.S., van Weele, M., van der Werf, G.R., Weiss, R.F., Worthy, D., Wunch, D., Yin, Y., Yoshida, Y., Zhang, W., Zhang, Z., Zhao, Y., Zheng, B., Zhu, Qing, Zhu, Qiuan, Zhuang, Q., 2019. The Global Methane Budget 2000–2017. Earth Syst. Sci. Data Discuss. https://doi.org/10.5194/essd-2019-128

Sawakuchi, H.O., Neu, V., Ward, N.D., Barros, M. de L.C., Valerio, A.M., Gagne-Maynard, W., Cunha, A.C., Less, D.F.S., Diniz, J.E.M., Brito, D.C., Krusche, A.V., Richey, J.E., 2017. Carbon dioxide emissions along the lower Amazon River. Front. Mar. Sci. 4, 1–12. https://doi.org/10.3389/fmars.2017.00076

Schlesinger, W.H., Melack, J.M., 1981. Transport of organic carbon in the world ' s rivers Transport of organic carbon in the world ' s rivers 2826. https://doi.org/10.3402/tellusa.v33i2.10706

Scully, N.M., Maie, N., Dailey, S.K., Boyer, J.N., Jones, R.D., Jaffé, R., 2004. Early diagenesis of plant-derived dissolved organic matter along a wetland, mangrove, estuary ecotone. Limnol. Oceanogr. 49, 1667–1678. https://doi.org/10.4319/lo.2004.49.5.1667

Sharp, R., Tallis, H.T., Ricketts, T., Guerry, A.D., Wood, S.A., Chaplin-Kramer, R., Nelson, E., Ennaanay, D., Wolny, S., Olwero, N., others, 2014. InVEST user's guide. Nat. Cap. Proj. Stanf.

Sharpless, C.M., Aeschbacher, M., Page, S.E., Wenk, J., Sander, M., McNeill, K., 2014. Photooxidation-induced changes in optical, electrochemical, and photochemical properties of humic substances. Environ. Sci. Technol. https://doi.org/10.1021/es403925g

Shen, Y., Benner, R., 2020. Molecular properties are a primary control on the microbial utilization of dissolved organic matter in the ocean. Limnol. Oceanogr. https://doi.org/10.1002/lno.11369

Shen, Y., Chapelle, F.H., Strom, E.W., Benner, R., 2015. Origins and bioavailability of dissolved organic matter in groundwater. Biogeochemistry. https://doi.org/10.1007/s10533-014-0029-4

Shin, W.J., Chung, G.S., Lee, D., Lee, K.S., 2011. Dissolved inorganic carbon export from carbonate and silicate catchments estimated from carbonate chemistry and δ 13C DIC. Hydrol. Earth Syst. Sci. https://doi.org/10.5194/hess-15-2551-2011

Sholkovitz, E.R., 1976. Flocculation of dissolved organic and inorganic matter during the mixing of river water and seawater. Geochim. Cosmochim. Acta 40, 831–845. https://doi.org/10.1016/0016-7037(76)90035-1

Siebert, S., Burke, J., Faures, J.M., Frenken, K., Hoogeveen, J., Döll, P., Portmann, F.T., 2010. Groundwater use for irrigation - A global inventory. Hydrol. Earth Syst. Sci. https://doi.org/10.5194/hess-14-1863-2010

Singh, S., Dash, P., Silwal, S., Feng, G., Adeli, A., Moorhead, R.J., 2017. Influence of land use and land cover on the spatial variability of dissolved organic matter in multiple aquatic environments. Environ. Sci. Pollut. Res. 24, 14124–14141. https://doi.org/10.1007/s11356-017-8917-5

Škerlep, M., Steiner, E., Axelsson, A., Kritzberg, E.S., 2019. Afforestation driving long-term surface water browning. Glob. Change Biol. https://doi.org/10.1111/gcb.14891

Skoog, D.A., Holler, F.J., Crouch, S.R., 2007. principles of instrumental analysis sixth edition, Principles of Instrumental Analysis.

Slomp, C.P., Van Cappellen, P., 2004. Nutrient inputs to the coastal ocean through submarine groundwater discharge: Controls and potential impact. J. Hydrol. https://doi.org/10.1016/j.jhydrol.2004.02.018

Smeaton, C., Austin, W.E.N., 2017. Sources, Sinks, and Subsidies: Terrestrial Carbon Storage in Mid-latitude Fjords. J. Geophys. Res. Biogeosciences. https://doi.org/10.1002/2017JG003952

Smith, R.M., Kaushal, S.S., 2015. Carbon cycle of an urban watershed: exports, sources, and metabolism. Biogeochemistry 126, 173–195. https://doi.org/10.1007/s10533-015-0151-y

Soares, A.R.A., Berggren, M., 2019. Indirect link between riverine dissolved organic matter and bacterioplankton respiration in a boreal estuary. Mar. Environ. Res. 148, 39–45. https://doi.org/10.1016/j.marenvres.2019.04.009

Sobek, S., Tranvik, L.J., Prairie, Y.T., Kortelainen, P., Cole, J.J., 2007. Patterns and regulation of dissolved organic carbon: An analysis of 7,500 widely distributed lakes. Limnol. Oceanogr. https://doi.org/10.4319/lo.2007.52.3.1208

Sofuoğlu, E., Ay, A., 2020. The relationship between climate change and political instability: the case of MENA countries (1985:01–2016:12). Environ. Sci. Pollut. Res. 27. https://doi.org/10.1007/s11356-020-07937-8

Song, K., Zhao, Y., Wen, Z., Fang, C., Shang, Y., 2017. A systematic examination of the relationships between CDOM and DOC in inland waters in China. Hydrol. Earth Syst. Sci. https://doi.org/10.5194/hess-21-5127-2017

Song, X.P., Hansen, M.C., Stehman, S.V., Potapov, P.V., Tyukavina, A., Vermote, E.F., Townshend, J.R., 2018. Global land change from 1982 to 2016. Nature. https://doi.org/10.1038/s41586-018-0411-9

Sooväli, L., Rõõm, E.I., Kütt, A., Kaljurand, I., Leito, I., 2006. Uncertainty sources in UV-Vis spectrophotometric measurement. Accreditation Qual. Assur. https://doi.org/10.1007/s00769-006-0124-x

Spencer, R.G.M., Ahad, J.M.E., Baker, A., Cowie, G.L., Ganeshram, R., Upstill-Goddard, R.C., Uher, G., 2007. The estuarine mixing behaviour of peatland derived dissolved organic carbon and its relationship to chromophoric dissolved organic matter in two North Sea estuaries (U.K.). Estuar. Coast. Shelf Sci. 74. https://doi.org/10.1016/j.ecss.2007.03.032

Spencer, R.G.M., Butler, K.D., Aiken, G.R., 2012. Dissolved organic carbon and chromophoric dissolved organic matter properties of rivers in the USA. J. Geophys. Res. Biogeosciences. https://doi.org/10.1029/2011JG001928

Spencer, R.G.M., Hernes, P.J., Ruf, R., Baker, A., Dyda, R.Y., Stubbins, A., Six, J., 2010a. Temporal controls on dissolved organic matter and lignin biogeochemistry in a pristine tropical river, Democratic Republic of Congo. J. Geophys. Res. Biogeosciences. https://doi.org/10.1029/2009JG001180

Spitzy, A., Leenheer, J., 1991. Dissolved Organic Carbon in rivers, in: SCOPE 42 - Biogeochemistry of Major World Rivers.

Spray, J.F., Wagner, T., Bischoff, J., Trojahn, S., Norouzi, S., Hill, W., Brasche, J., James, L., Pereira, R., 2021. Unravelling Light and Microbial Activity as Drivers of Organic Matter Transformations in Tropical Headwater Rivers (preprint). Biogeochemistry: Rivers & Streams. https://doi.org/10.5194/bg-2021-92

St. Pierre, K.A., Oliver, A.A., Tank, S.E., Hunt, B.P.V., Giesbrecht, I., Kellogg, C.T.E., Jackson, J.M., Lertzman, K.P., Floyd, W.C., Korver, M.C., 2020. Terrestrial exports of dissolved and particulate organic carbon affect nearshore ecosystems of the Pacific coastal temperate rainforest. Limnol. Oceanogr. https://doi.org/10.1002/lno.11538

Stallard, R.F., 1998. Terrestrial sedimentation and the carbon cycle: Coupling weathering and erosion to carbon burial. Glob. Biogeochem. Cycles. https://doi.org/10.1029/98GB00741

Stanley, E.H., Powers, S.M., Lottig, N.R., Buffam, I., Crawford, J.T., 2012. Contemporary changes in dissolved organic carbon (DOC) in human-dominated rivers: Is there a role for DOC management? Freshw. Biol. https://doi.org/10.1111/j.1365-2427.2011.02613.x

Statistical Institute of Belize, 2019. Percent of Total GDP by Activity (1992 - 2018).

Stedmon, C.A., Bro, R., 2008. Characterizing dissolved organic matter fluorescence with parallel factor analysis: A tutorial. Limnol. Oceanogr. Methods 6, 572–579. https://doi.org/10.4319/lom.2008.6.572

Stedmon, C.A., Markager, S., Bro, R., 2003. Tracing dissolved organic matter in aquatic environments using a new approach to fluorescence spectroscopy. Mar. Chem. 82, 239–254. https://doi.org/10.1016/S0304-4203(03)00072-0

Stedmon, C.A., Thomas, D.N., Granskog, M., Kaartokallio, H., Papadimitriou, S., Kuosa, H., 2007. Characteristics of dissolved organic matter in baltic coastal sea ice: Allochthonous or autochthonous origins? Environ. Sci. Technol. 41, 7273–7279. https://doi.org/10.1021/es071210f

Stocker, T.F., Qin, D., Plattner, G.-K., Tignor, M., Allen, S.K., Boschung, J., Nauels, A., Xia, Y., Bex, V., Midgley, P.M., 2013. IPCC, 2013: Climate Change 2013: The Physical Science Basis. Contribution of Working Group I to the Fifth Assessment Report of the Intergovernmental Panel on Climate Change. IPCC AR5, 1535–1535.

Stubbins, A., Spencer, R.G.M., Chen, H., Hatcher, P.G., Mopper, K., Hernes, P.J., Mwamba, V.L., Mangangu, A.M., Wabakanghanzi, J.N., Six, J., 2010. Illuminated darkness: Molecular signatures of

Congo River dissolved organic matter and its photochemical alteration as revealed by ultrahigh precision mass spectrometry. Limnol. Oceanogr. https://doi.org/10.4319/lo.2010.55.4.1467

Stutter, M.I., Graeber, D., Evans, C.D., Wade, A.J., Withers, P.J.A., 2018. Balancing macronutrient stoichiometry to alleviate eutrophication. Sci. Total Environ. https://doi.org/10.1016/j.scitotenv.2018.03.298

Sugimura, Y., Suzuki, Y., 1988. A high-temperature catalytic oxidation method for the determination of non-volatile dissolved organic carbon in seawater by direct injection of a liquid sample. Mar. Chem. https://doi.org/10.1016/0304-4203(88)90043-6

Sunagawa, S., Coelho, L.P., Chaffron, S., Kultima, J.R., Labadie, K., Salazar, G., Djahanschiri, B., Zeller, G., Mende, D.R., Alberti, A., Cornejo-Castillo, F.M., Costea, P.I., Cruaud, C., D'Ovidio, F., Engelen, S., Ferrera, I., Gasol, J.M., Guidi, L., Hildebrand, F., Kokoszka, F., Lepoivre, C., Lima-Mendez, G., Poulain, J., Poulos, B.T., Royo-Llonch, M., Sarmento, H., Vieira-Silva, S., Dimier, C., Picheral, M., Searson, S., Kandels-Lewis, S., Boss, E., Follows, M., Karp-Boss, L., Krzic, U., Reynaud, E.G., Sardet, C., Sieracki, M., Velayoudon, D., Bowler, C., De Vargas, C., Gorsky, G., Grimsley, N., Hingamp, P., Iudicone, D., Jaillon, O., Not, F., Ogata, H., Pesant, S., Speich, S., Stemmann, L., Sullivan, M.B., Weissenbach, J., Wincker, P., Karsenti, E., Raes, J., Acinas, S.G., Bork, P., 2015. Structure and function of the global ocean microbiome. Science. https://doi.org/10.1126/science.1261359

Sweetman, B.M., Foley, J.R., Steinberg, M.K., 2019. A baseline analysis of coastal water quality of the port Honduras marine reserve, Belize: a critical habitat for sport fisheries. Environ. Biol. Fishes 102, 429–442. https://doi.org/10.1007/s10641-018-0811-6

Tang, W., Llort, J., Weis, J., Perron, M.M.G., Basart, S., Li, Z., Sathyendranath, S., Jackson, T., Sanz Rodriguez, E., Proemse, B.C., Bowie, A.R., Schallenberg, C., Strutton, P.G., Matear, R., Cassar, N., 2021. Widespread phytoplankton blooms triggered by 2019–2020 Australian wildfires. Nature 597, 370–375. https://doi.org/10.1038/s41586-021-03805-8

Taylor, S., Gilbert, P.J., Cooke, D.A., Deary, M.E., Jeffries, M.J., 2019. High carbon burial rates by small ponds in the landscape. Front. Ecol. Environ. https://doi.org/10.1002/fee.1988

Tesi, T., Langone, L., Giani, M., Ravaioli, M., Miserocchi, S., 2013. Source, diagenesis, and fluxes of particulate organic carbon along the western adriatic Sea (mediterranean Sea). Mar. Geol. https://doi.org/10.1016/j.margeo.2013.03.001

Thacker, S.A., Tipping, E., Gondar, D., Baker, A., 2008. Functional properties of DOM in a stream draining blanket peat. Sci. Total Environ. https://doi.org/10.1016/j.scitotenv.2008.09.011

Thorp, J.H., Delong, M.D., 2002. Dominance of autochthonous autotrophic carbon in food webs of heterotrophic rivers. Oikos. https://doi.org/10.1034/j.1600-0706.2002.960315.x

Timperley, M.H., 1985. Dissolved coloured compounds and suspended matter in the waters of the middle Waikato river. N. Z. J. Mar. Freshw. Res. https://doi.org/10.1080/00288330.1985.9516075

Tipping, E., Corbishley, H.T., Koprivnjak, J.F., Lapworth, D.J., Miller, M.P., Vincent, C.D., Hamilton-Taylor, J., 2009a. Quantification of natural DOM from UV absorption at two wavelengths. Environ. Chem. https://doi.org/10.1071/EN09090

Tipping, E., Corbishley, H.T., Koprivnjak, J.F., Lapworth, D.J., Miller, M.P., Vincent, C.D., Hamilton-Taylor, J., 2009b. Quantification of natural DOM from UV absorption at two wavelengths. Environ. Chem. https://doi.org/10.1071/EN09090

Tóth, J., 1963. A theoretical analysis of groundwater flow in small drainage basins. J. Geophys. Res. https://doi.org/10.1029/jz068i016p04795

Tranvik, L.J., Downing, J.A., Cotner, J.B., Loiselle, S.A., Striegl, R.G., Ballatore, T.J., Dillon, P., Finlay, K., Fortino, K., Knoll, L.B., Kortelainen, P.L., Kutser, T., Larsen, S., Laurion, I., Leech, D.M., Leigh McCallister, S., McKnight, D.M., Melack, J.M., Overholt, E., Porter, J.A., Prairie, Y., Renwick, W.H., Roland, F., Sherman, B.S., Schindler, D.W., Sobek, S., Tremblay, A., Vanni, M.J., Verschoor, A.M., Von Wachenfeldt, E., Weyhenmeyer, G.A., 2009. Lakes and reservoirs as regulators of carbon cycling and climate. Limnol. Oceanogr. 54, 2298–2314. https://doi.org/10.4319/lo.2009.54.6_part_2.2298

Trumbore, S.E., 1993. Comparison of carbon dynamics in tropical and temperate soils using radiocarbon measurements. Glob. Biogeochem. Cycles. https://doi.org/10.1029/93GB00468

Tye, A.M., Lapworth, D.J., 2016. Characterising changes in fluorescence properties of dissolved organic matter and links to N cycling in agricultural floodplains. Agric. Ecosyst. Environ. https://doi.org/10.1016/j.agee.2016.01.033

Tzortziou, M., Zeri, C., Dimitriou, E., Ding, Y., Jaffe, R., Anagnostou, E., Pitta, E., Mentzafou, A., 2015. Colored dissolved organic matter dynamics and anthropogenic influences in a major transboundary river and its coastal wetland. Limnol. Oceanogr. https://doi.org/10.1002/lno.10092

Uher, G., Hughes, C., Henry, G., Upstill-Goddard, C., 2001. Non-conservative mixing behavior of colored dissolved organic matter in a humic-rich, turbid estuary. Geophys. Res. Lett. 28. https://doi.org/10.1029/2000GL012509

Urbansky, E.T., 2001. Total organic carbon analyzers as tools for measuring carbonaceous matter in natural waters. Presented at the Journal of Environmental Monitoring. https://doi.org/10.1039/b006564l

Vähätalo, A.V., Wetzel, R.G., 2004. Photochemical and microbial decomposition of chromophoric dissolved organic matter during long (months–years) exposures. Mar. Chem. 89, 313–326. https://doi.org/10.1016/j.marchem.2004.03.010

van Bergen, T.J.H.M., Barros, N., Mendonça, R., Aben, R.C.H., Althuizen, I.H.J., Huszar, V., Lamers, L.P.M., Lürling, M., Roland, F., Kosten, S., 2019. Seasonal and diel variation in greenhouse gas emissions from an urban pond and its major drivers. Limnol. Oceanogr. https://doi.org/10.1002/lno.11173

Verdonschot, R.C.M., Keizer-vlek, H.E., Verdonschot, P.F.M., 2011. Biodiversity value of agricultural drainage ditches: A comparative analysis of the aquatic invertebrate fauna of ditches and small lakes. Aquat. Conserv. Mar. Freshw. Ecosyst. https://doi.org/10.1002/aqc.1220

Vodacek, A., Hogel, F.E., Swift, R.N., Yungel, J.K., Peltzer, E.T., Blough, N.V., 1995. The use of in situ and airborne fluorescence measurements to determine UV absorption coefficients and DOC concentrations in surface waters. Limnol. Oceanogr. https://doi.org/10.4319/lo.1995.40.2.0411

Voight, C., Hernandez-Aguilar, K., Garcia, C., Gutierrez, S., 2019. Predictive modeling of future forest cover change patterns in southern Belize. Remote Sens. 11. https://doi.org/10.3390/rs11070823

von Schiller, D., Bernal, S., Dahm, C.N., Martí, E., 2017. Nutrient and Organic Matter Dynamics in Intermittent Rivers and Ephemeral Streams, in: Intermittent Rivers and Ephemeral Streams: Ecology and Management. https://doi.org/10.1016/B978-0-12-803835-2.00006-1

von Schiller, D., Datry, T., Corti, R., Foulquier, A., Tockner, K., Marcé, R., García-Baquero, G., Odriozola, I., Obrador, B., Elosegi, A., Mendoza-Lera, C., Gessner, M.O., Stubbington, R., Albariño, R., Allen, D.C., Altermatt, F., Arce, M.I., Arnon, S., Banas, D., Banegas-Medina, A., Beller, E., Blanchette, M.L., Blanco-Libreros, J.F., Blessing, J., Boëchat, I.G., Boersma, K.S., Bogan, M.T., Bonada, N., Bond, N.R., Brintrup, K., Bruder, A., Burrows, R.M., Cancellario, T., Carlson, S.M., Cauvy-Fraunié, S., Cid, N., Danger, M., de Freitas Terra, B., Dehedin, A., De Girolamo, A.M., del Campo, R., Díaz-Villanueva, V., Duerdoth, C.P., Dyer, F., Faye, E., Febria, C., Figueroa, R., Four, B., Gafny, S., Gómez, R., Gómez-Gener, L., Graça, M.A.S., Guareschi, S., Gücker, B., Hoppeler, F., Hwan, J.L., Kubheka, S., Laini, A., Langhans, S.D., Leigh, C., Little, C.J., Lorenz, S., Marshall, J., Martín, E.J., McIntosh, A., Meyer, E.I., Miliša, M., Mlambo, M.C., Moleón, M., Morais, M., Negus, P., Niyogi, D., Papatheodoulou, A., Pardo,

I., Pařil, P., Pešić, V., Piscart, C., Polášek, M., Rodríguez-Lozano, P., Rolls, R.J., Sánchez-Montoya, M.M., Savić, A., Shumilova, O., Steward, A., Taleb, A., Uzan, A., Vander Vorste, R., Waltham, N., Woelfle-Erskine, C., Zak, D., Zarfl, C., Zoppini, A., 2019. Sediment Respiration Pulses in Intermittent Rivers and Ephemeral Streams. Glob. Biogeochem. Cycles. https://doi.org/10.1029/2019GB006276

Wagner, S., Schubotz, F., Kaiser, K., Hallmann, C., Waska, H., Rossel, P.E., Hansman, R., Elvert, M., Middelburg, J.J., Engel, A., Blattmann, T.M., Catalá, T.S., Lennartz, S.T., Gomez-Saez, G.V., Pantoja-Gutiérrez, S., Bao, R., Galy, V., 2020. Soothsaying DOM: A Current Perspective on the Future of Oceanic Dissolved Organic Carbon. Front. Mar. Sci. https://doi.org/10.3389/fmars.2020.00341

Wallin, M., Buffam, I., Öquist, M., Laudon, H., Bishop, K., 2010. Temporal and spatial variability of dissolved inorganic carbon in a boreal stream network: Concentrations and downstream fluxes. J. Geophys. Res. Biogeosciences. https://doi.org/10.1029/2009jg001100

Wang, Z.A., Cai, W.J., 2004. Carbon dioxide degassing and inorganic carbon export from a marsh-dominated estuary (the Duplin River): A marsh CO2 pump. Limnol. Oceanogr. https://doi.org/10.4319/lo.2004.49.2.0341

Wangersky, P.J., 1993. Dissolved organic carbon methods: a critical review. Mar. Chem., Measurement of Dissolved Organic Carbon and Nitrogen in Natural Waters 41, 61–74. https://doi.org/10.1016/0304-4203(93)90106-X

Ward, N.D., Keil, R.G., Medeiros, P.M., Brito, D.C., Cunha, A.C., Dittmar, T., Yager, P.L., Krusche, A.V., Richey, J.E., 2013. Degradation of terrestrially derived macromolecules in the Amazon River. Nat. Geosci. https://doi.org/10.1038/ngeo1817

Wassenaara, L.I., Aravena, R., Fritz, P., Barker, J.F., 1991. Controls on the transport and carbon isotopic composition of dissolved organic carbon in a shallow groundwater system, Central Ontario, Canada. Chem. Geol. Isot. Geosci. Sect. https://doi.org/10.1016/0168-9622(91)90032-R

Waterloo, M.J., Oliveira, S.M., Drucker, D.P., Nobre, A.D., Cuartas, L.A., Hodnett, M.G., Langedijk, I., Jans, W.W.P., Tomasella, J., de Araújo, A.C., Pimentel, T.P., Múnera Estrada, J.C., 2006. Export of organic carbon in run-off from an Amazonian rainforest blackwater catchment. Hydrol. Process. https://doi.org/10.1002/hyp.6217

Webb, J.R., Leavitt, P.R., Simpson, G.L., Baulch, H.M., Haig, H.A., Hodder, K.R., Finlay, K., 2019. Regulation of carbon dioxide and methane in small agricultural reservoirs: Optimizing potential for greenhouse gas uptake. Biogeosciences. https://doi.org/10.5194/bg-16-4211-2019

Webster, K.E., Soranno, P.A., Cheruvelil, K.S., Bremigan, M.T., Downing, J.A., Vaux, P.D., Asplund, T.R., Bacon, L.C., Connor, J., 2008. An empirical evaluation of the nutrient-color paradigm for lakes. Limnol. Oceanogr. https://doi.org/10.4319/lo.2008.53.3.1137

Weishaar, J.L., Aiken, G.R., Bergamaschi, B.A., Fram, M.S., Fujii, R., Mopper, K., 2003. Evaluation of specific ultraviolet absorbance as an indicator of the chemical composition and reactivity of dissolved organic carbon. Environ. Sci. Technol. https://doi.org/10.1021/es030360x

West, T.O., Marland, G., King, A.W., Post, W.M., Jain, A.K., Andrasko, K., 2004. Carbon management response curves: Estimates of temporal soil carbon dynamics. Environ. Manage. 33, 507–518. https://doi.org/10.1007/s00267-003-9108-3

Wiegner, T.N., Seitzinger, S.P., 2001. Photochemical and microbial degradation of external dissolved organic matter inputs to rivers. Aquat. Microb. Ecol. https://doi.org/10.3354/ame024027

Williams, C.J., Frost, P.C., Morales-Williams, A.M., Larson, J.H., Richardson, W.B., Chiandet, A.S., Xenopoulos, M.A., 2016. Human activities cause distinct dissolved organic matter composition across freshwater ecosystems. Glob. Change Biol. 22, 613–626. https://doi.org/10.1111/gcb.13094

Williams, C.J., Yamashita, Y., Wilson, H.F., Jaffe, R., Xenopoulos, M.A., 2010. Unraveling the role of land use and microbial activity in shaping dissolved organic matter characteristics in stream ecosystems. Limnol. Oceanogr. https://doi.org/10.4319/lo.2010.55.3.1159

Williamson, J.L., Tye, A., Lapworth, D.J., Monteith, D., Sanders, R., Mayor, D.J., Barry, C., Bowes, Mike, Bowes, Michael, Burden, A., Callaghan, N., Farr, G., Felgate, S., Fitch, A., Gibb, S., Gilbert, P., Hargreaves, G., Keenan, P., Kitidis, V., Juergens, M., Martin, A., Mounteney, I., Nightingale, P.D., Pereira, M.G., Olszewska, J., Pickard, A., Rees, A.P., Spears, B., Stinchcombe, M., White, D., Williams, P., Worrall, F., Evans, C., 2021. Landscape controls on riverine export of dissolved organic carbon from Great Britain. Biogeochemistry 2. https://doi.org/10.1007/s10533-021-00762-2

Wilson, H.F., Xenopoulos, M.A., 2009. Effects of agricultural land use on the composition of fluvial dissolved organic matter. Nat. Geosci. https://doi.org/10.1038/ngeo391

Winemiller, K.O., McIntyre, P.B., Castello, L., Fluet-Chouinard, E., Giarrizzo, T., Nam, S., Baird, I.G., Darwall, W., Lujan, N.K., Harrison, I., Stiassny, M.L.J., Silvano, R.A.M., Fitzgerald, D.B., Pelicice, F.M., Agostinho, A.A., Gomes, L.C., Albert, J.S., Baran, E., Petrere, M., Zarfl, C., Mulligan, M., Sullivan, J.P., Arantes, C.C., Sousa, L.M., Koning, A.A., Hoeinghaus, D.J., Sabaj, M., Lundberg, J.G., Armbruster, J., Thieme, M.L., Petry, P., Zuanon, J., Torrente Vilara, G., Snoeks, J., Ou, C., Rainboth, W., Pavanelli,

C.S., Akama, A., Van Soesbergen, A., Sáenz, L., 2016. Balancing hydropower and biodiversity in the Amazon, Congo, and Mekong. Science. https://doi.org/10.1126/science.aac7082

Winterdahl, M., Wallin, M.B., Karlsen, R.H., Laudon, H., Öquist, M., Lyon, S.W., 2016. Decoupling of carbon dioxide and dissolved organic carbon in boreal headwater streams. J. Geophys. Res. Biogeosciences. https://doi.org/10.1002/2016JG003420

Woodwell, G., Whittaker, R., Reiners, W., Likens, G., Delwiche, C., Botkin, D., 1978. The Biota and the World Carbon Budget. Science 199, 141–6. https://doi.org/10.1126/science.199.4325.141

Worrall, F., Howden, N. J., & Burt, T. P. (2020). The dissolved organic carbon flux from the UK–A new Bayesian approach to flux calculation. *Journal of Hydrology*, *590*, 125511.

Worrall, F., Burt, T.P., Howden, N.J.K., Hancock, G.R., Wainwright, J., 2018. The fate of suspended sediment and particulate organic carbon in transit through the channels of a river catchment. Hydrol. Process. 32, 146–159. https://doi.org/10.1002/hyp.11413

Worrall, F., Davies, H., Bhogal, A., Lilly, A., Evans, M., Turner, K., Burt, T., Barraclough, D., Smith, P., Merrington, G., 2012. The flux of DOC from the UK - Predicting the role of soils, land use and net watershed losses. J. Hydrol. https://doi.org/10.1016/j.jhydrol.2012.04.053

Wu, H., Green, M., Scranton, M.I., 1997. Acetate cycling in the water column and surface sediment of Long Island Sound following a bloom. Limnol. Oceanogr. https://doi.org/10.4319/lo.1997.42.4.0705

Xenopoulos, M.A., Barnes, R.T., Boodoo, K.S., Butman, D., Catalán, N., D'Amario, S.C., Fasching, C., Kothawala, D.N., Pisani, O., Solomon, C.T., Spencer, R.G.M., Williams, C.J., Wilson, H.F., 2021. How humans alter dissolved organic matter composition in freshwater: relevance for the Earth's biogeochemistry. Biogeochemistry 3. https://doi.org/10.1007/s10533-021-00753-3

Xenopoulos, M.A., Downing, J.A., Kumar, M.D., Menden-Deuer, S., Voss, M., 2017. Headwaters to oceans: Ecological and biogeochemical contrasts across the aquatic continuum. Limnol. Oceanogr. https://doi.org/10.1002/lno.10721

Yamashita, Y., Maie, N., Briceño, H., Jaffé, R., 2010a. Optical characterization of dissolved organic matter in tropical rivers of the Guayana Shield, Venezuela. J. Geophys. Res. Biogeosciences. https://doi.org/10.1029/2009JG000987

Yamashita, Y., Scinto, L.J., Maie, N., Jaffé, R., 2010b. Dissolved Organic Matter Characteristics Across a Subtropical Wetland's Landscape: Application of Optical Properties in the Assessment of Environmental Dynamics. Ecosystems 13, 1006–1019. https://doi.org/10.1007/s10021-010-9370-1

Yan, J., Manelski, R., Vasilas, B., Jin, Y., 2018. Mobile colloidal organic carbon: An underestimated carbon pool in global carbon cycles? Front. Environ. Sci. https://doi.org/10.3389/fenvs.2018.00148

Yang, H., Graham, N. J., Wang, W., Liu, M., & Yu, W. (2021). Evaluating and improving the reliability of the UV-persulfate method for the determination of TOC/DOC in surface waters. *Water Research*, *196*, 116918Yool, A., Popova, E.E., Anderson, T.R., 2013. MEDUSA-2.0: An intermediate complexity biogeochemical model of the marine carbon cycle for climate change and ocean acidification studies. Geosci. Model Dev. https://doi.org/10.5194/gmd-6-1767-2013

Yang, L., Hong, H., Guo, W., Huang, J., Li, Q., Yu, X., 2012. Effects of changing land use on dissolved organic matter in a subtropical river watershed, southeast China. Reg. Environ. Change 12, 145–151. https://doi.org/10.1007/s10113-011-0250-9

Young, C.A., 2008. Belize's Ecosystems: Threats and Challenges to Conservation in Belize. Trop. Conserv. Sci. 1, 18–33. https://doi.org/10.1177/194008290800100102

Zhang, Y., Zhou, L., Zhou, Y., Zhang, L., Yao, X., Shi, K., Jeppesen, E., Yu, Q., Zhu, W., 2021. Chromophoric dissolved organic matter in inland waters: Present knowledge and future challenges. Sci. Total Environ. https://doi.org/10.1016/j.scitotenv.2020.143550